

LOAN COPY ONLY

PROCEEDINGS  
of the **CIRCULATING COPY**  
**Sea Grant Depository**

SYMPOSIUM ON REMOTE SENSING IN MARINE BIOLOGY AND FISHERY RESOURCES

January 25-26, 1971

College Station, Texas

Sponsored by

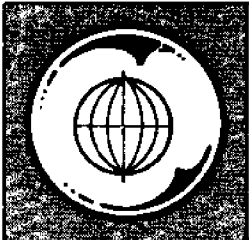
REMOTE SENSING CENTER and SEA GRANT PROGRAM OFFICE

TEXAS A&M UNIVERSITY

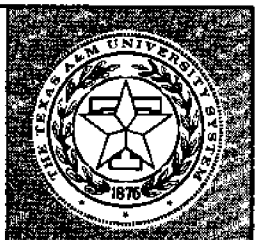
TAMU-SG-71-106

March 1971

With the support of the Food and Agriculture Organization  
(FAO) and Intergovernmental Oceanographic Commission (IOC).



**TEXAS A&M UNIVERSITY**  
**REMOTE SENSING CENTER**  
COLLEGE STATION, TEXAS



LOAN COPY ONLY

**CIRCULATING COPY**  
**Sea Grant Depository**

PROCEEDINGS  
of the  
SYMPOSIUM ON REMOTE SENSING IN MARINE BIOLOGY AND FISHERY RESOURCES

January 25-26, 1971  
College Station, Texas

Sponsored by  
REMOTE SENSING CENTER and SEA GRANT PROGRAM OFFICE  
TEXAS A&M UNIVERSITY

*TAMU-SG-71-106*

*March 1971*

With the support of the Food and Agriculture Organization  
(FAO) and Intergovernmental Oceanographic Commission (IOC).

NATIONAL SEA GRANT DEPOSITORY  
PELL LIBRARY BUILDING  
URI, NARRAGANSETT BAY CAMPUS  
NARRAGANSETT, RI 02882

## AGENDA

Monday - January 25, 1971

- 8:00 Registration in lobby of Ramada Inn
- 9:00 Welcome and Introduction - J. W. Rouse, Jr., Director, Remote Sensing Center, Texas A&M University
- 9:15 Welcome and Introduction - Richard A. Geyer, Head, Department of Oceanography, Texas A&M University
- 9:30 Welcome - John C. Calhoun, Jr., Vice President for Programs, Dean of College of Geosciences, and Director of Sea Grant Program at Texas A&M University
- Introduction - J. W. Rouse, Jr.

### SESSION 1 - 9:45 - 12:30

Chairman: John W. Sherman, Project Manager, Spacecraft Oceanography Project, U. S. Naval Oceanographic Office, Washington, D. C.

*Remote Sensing in the National Marine Fisheries Service* - William H. Stevenson, Chief of Program at National Marine Fisheries Service, MTF, Bay Saint Louis, Mississippi

*Operational Use of Remote Sensors in Commercial Fishing* - Paul M. Maughan and Allan D. Marmelstein, Earth Satellite Corporation, Washington, D. C.

*Some Potential Applications of Remote Sensing in Fisheries* - Kirby L. Drennan, Head, Zapata Remote Sensing, Ocean Protein, Inc., Lafayette, Louisiana

### SESSION 2 - 1:30 - 5:00

Chairman: Willis E. Pequegnat, Biological Oceanographer, Department of Oceanography, Texas A&M University

*Remote Spectrography of Ocean Color as an Index of Biological Activity* - Gifford C. Ewing, Woods Hole Oceanographic Institution, Woods Hole, Massachusetts

*The Absorption and Fluorescence Characteristics of Biochemical Substances in Natural Waters* - Charles S. Yentsch, University of Massachusetts, Gloucester, Massachusetts

*The Remote Sensing of Vapours of Marine Organic Origin* - A. J. Moffat, Barringer Research Ltd., Ontario, Canada

*Remote Sensing of Marine and Fisheries Resources by Fluorescence Methods* - Arthur W. Hornig, Baird-Atomic, Inc., Bedford, Massachusetts

*Remote Sensing of the Pelagic Fisheries Environment off Oregon* - William Percy, Department of Oceanography, Oregon State University, Corvallis, Oregon

### Monday Evening

- 6:30 - 8:15 Social Hour and Banquet in Rooms B, C & D
- 8:15 *Man's Effect on the Estuarine Environment* - Leo F. Childs, Special Assistant, Earth Observations Division, NASA/MSC, Houston

## AGENDA

Tuesday - January 26, 1971

### SESSION 3 - 9:00 - 12:00

Chairman: Jack F. Paris, Meteorologist, Department of Meteorology, Texas A&M University

*GAP Color Films for Special Remote Sensing Applications* - Ira B. Current, Manager, Reversal Color Products, General Aniline and Film Corporation, Binghamton, New York

*Applications of Multispectral Sensing* - Fabian C. Polcyn, Infrared and Optical Sensors Group, Willow Run Laboratories, University of Michigan, Ann Arbor, Michigan

*Acoustic Methods for Estimation of Fish Abundance* - Lars Midttun, Food and Agriculture Organization (FAO) of the United Nations, Bergen, Norway

*Studies of Benthic Cover in Near-shore Temperate Waters Using Aerial Photography* - Mahlon G. Kelly, Department of Environmental Science, University of Virginia, Charlottesville, Virginia

### SESSION 4 - 1:00 - 3:00

Chairman: G. Tomczak, Chief, Marine Environment Section, Food and Agriculture Organization (FAO) of the United Nations, Rome, Italy

*An Application of the Theory of Games toward Improving the Efficiency of Certain Pelagic Fishing Operations* - Saul Salla, FAO, Paris, France

*Upwelling Studies with Satellites* - Karl-Heinz Szekiela, Goddard Space Flight Center, Greenbelt, Maryland

Closing Remarks - Jack F. Paris, Department of Meteorology, Texas A&M University



## FOREWORD

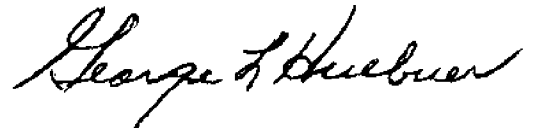
These Proceedings contain papers presented at the Symposium on Remote Sensing in Marine Biology and Fishery Resources, held on the 25th and 26th of January 1971, at Texas A&M University in College Station, Texas.

The symposium was sponsored by the Remote Sensing Center and the Sea Grant Program of Texas A&M University. In addition, support was given by the Fisheries Biology Branch of the Food and Agriculture Organization (FAO) and the Intergovernmental Oceanographic Commission (IOC).

The objectives of this Symposium were two-fold: (1) to bring together the investigators active in the utilization of remote sensing in marine biology and fisheries; and (2) to provide for discussions leading to improved harvest and management of these resources. The agenda for this symposium was arranged to satisfy or compliment the objectives and provide an overall review of the expertise in this particular application of remote sensing. This symposium is one of a continuing series by one or both of the sponsoring organizations and is devoted to the many diverse disciplines.

The success of this symposium can be attributed to the excellent cooperation by the participating scientists, the interest of those in attendance, and especially to the ability of the conference coordinator, Mrs. Rosemary E. Boykin.

George L. Huebner



Note - Copies of these Proceedings are available for \$4.00 per copy from the Office of Sea Grant Program, Texas A&M University, College Station, Texas 77843.



## TABLE OF CONTENTS

<i>Remote Sensing in the National Marine Fisheries Service</i> by William H. Stevenson . . . . .	1
<i>Operational Use of Remote Sensors in Commercial Fishing</i> by Paul M. Maughan and Allan D. Marmelstein . . . . .	8
<i>Some Potential Applications of Remote Sensing in Fisheries</i> by Kirby L. Drennan . . . . .	25
<i>Remote Spectrography of Ocean Color as an Index of Biological Activity</i> by Gifford C. Ewing. . . . .	66
<i>The Absorption and Fluorescence Characteristics of Biochemical Substances in Natural Waters</i> by Charles S. Yentsch. . . . .	75
<i>The Remote Sensing of Vapours of Marine Organic Origin</i> by A. J. Moffat . . . . .	98
<i>Remote Sensing of Marine and Fisheries Resources by Fluorescence Methods</i> by Arthur W. Hornig . . . . .	127
<i>Remote Sensing of the Pelagic Fisheries Environment off Oregon</i> by William Percy . . . . .	158
<i>Man's Effect on the Estuarine Environment</i> by Leo Childs . . . . .	172
<i>GAF Color Films for Special Remote Sensing Applications</i> by Ira B. Current . . . . .	173
<i>Applications of Multispectral Sensing to Marine Resources Surveys</i> by Fabian Polcyn. . . . .	194
<i>Acoustic Methods for Estimation of Fish Abundance</i> by Lars Midttun . . . . .	218
<i>Studies of Benthic Cover in Near-shore Temperate Waters Using Aerial Photography</i> by Mahlon G. Kelly . . . . .	227
<i>An Application of the Theory of Games toward Improving the Efficiency of Certain Pelagic Fishing Operations</i> by Saul Salla . . . . .	249
<i>The Use of Fish in Biological Situations</i> by George W. Klontz . . . . .	266
<i>Upwelling Studies with Satellites</i> by Karl-Heinz Szekiolda . . . . .	271
<i>List of Attendees</i> . . . . .	294

## REMOTE SENSING IN THE NATIONAL MARINE FISHERIES SERVICE

by

W. H. Stevenson  
NMFS Bay, St. Louis Missouri

Before presenting my remarks concerning the role of remote sensing in the National Marine Fisheries Service, I thought it might be appropriate to identify the National Marine Fisheries Service, or NMFS, nowafter referred to as "NYMPHS" -- the connotation being somewhat vague.

NMFS is a part of the new agency called "NOAA". NOAA, the National Oceanic and Atmospheric Administration, was created within the U. S. Department of Commerce on October 3, 1970, by Presedential Reorganization Plan Number 4 of 1970.

Its formation brought together the functions of the Commerce Department's Environmental Science Services Administration (including its major elements: the Weather Bureau, Coast and Geodetic Survey, Environmental Data Service, National Environmental Satellite Center, and Research Laboratories); the Interior Department's Bureau of Commercial Fisheries, Marine Game Fish Research Program, and Marine Minerals Technology Center; the Navy-Administered National Oceanographic Data Center and National Oceanographic Instrumentation Center; the Coast Guard's National Data Buoy Development Project; the National Science Foundation's National Sea Grant Program; and elements of the Army Corps of Engineers' U. S. Lake Survey.

NOAA will explore, map, and chart the global oceans, their geological cradles, their geophysical forces and fields, and thier mineral and living resources. New physical and biological knowledge will be translated into systems capable of assessing the sea'a potential yield, and into techniques which the nation and its industries can employ to manage, use, and conserve these animal and mineral resources.

NOAA will exercise leadership in developing a National Oceanic and Atmospheric Program of Research and Development. It will coordinate its own scientific and technical resources with the technical and operational capabilities of other government agencies and private institutions.

As important, NOAA will continue to provide those services to other agencies of government, industry, and to private individuals which have become essential to the efficient operation of our transportation systems, our agriculture, our fisheries and our national security.

This morning I am not going to try to explain the NOAA organization. However, I would like to give you a brief outline of the objectives of the NMFS, -- and particularly those having a bearing in this symposium.

The NMFS seeks to discover, describe, develop, and conserve the living resources of the global sea, especially as these affect the American economy and diet.

The Fisheries Service conducts biological research on economically important species, analyzes economic aspects of fisheries operations and rates, develops methods for improving catches, and, in cooperation with the U. S. Department of State, is active in international fisheries affairs. With the U. S. Coast Guard, the National Marine Fisheries Service conducts enforcement and surveillance operations on the high seas and in territorial waters. It also studies game fish behavior and resources, seeks to describe the ecological relationships between game fish and other marine and estuarine organisms, and investigates the effects on game fish of thermal and chemical pollution.

The National Marine Fisheries Service conducts a voluntary grading and inspection program under which fishery products that meet established quality standards and product specifications can bear a special shield that is the shopper's guarantee that the product was of high quality when it left the processor. A staff of marketing specialists and home economists provide

services to Federal and State Governments, industry, and consumer organizations in the use of fish and fishery products. The Service also maintains a national program of fishery statistics and market news.

#### NMFS REMOTE SENSING

The role of remote sensing in this new organization has made a significant shift over the past 12 months. The shift puts more emphasis upon the need to assess, monitor and predict the status of living marine resources than has heretofore been identified. It also emphasizes that the NMFS will focus on the living marine resources, their development and management, and look to elements in NOAA and other agencies to provide the bulk of non-biological information necessary to understand the resource fluctuations. These will include physical oceanographic and meteorological data and preliminary data reduction.

As indicates, a major effort of the NMFS is to monitor and assess living marine resources of the United States on a continuing basis. To make this effort effective, we must apply new technology to obtain data on the distribution, abundance, and availability of fish stocks for use by resource managers, developers, and entrepreneurs. One area in which the applications of new technology are particularly obvious is remote sensing of resources. Remote sensing offers two distinct opportunities to obtain data on the status of oceanic resources: (1) the direct sensing of living resources; (2) the measurement of broad physical, chemical, and biological conditions of the ocean which have an inter-related effect upon the resources themselves.

The objective of the new NMFS remote sensing program is to recruit new tools to locate, survey, and monitor living marine resources. As specific instruments are shown to be applicable, they will be incorporated into ongoing operational surveys or commercial harvesting procedures. Operational

instruments will be upgraded as required. In airborne sensor systems emphasis will be placed on acquiring information not readily obtainable from ships, satellites, or other sources.

#### PROGRAM ORGANIZATION

The focal point for NMFS remote sensing role was relocated at MTF in September 1970. Formal agreements between USDI/BCF and NASA were signed in August 1970 establishing a working relationship to apply advanced technology to fishery problems at MTF. The MTF program has three organizational components - program management, project evaluation, and operations (SEE FIGURE I).

Activities in the program will be conducted in remote sensing, data management, biological sample handling, and technical development. The immediate program established the remote sensing element of the program. Limited efforts in the other three activities are being initiated this year to establish the project criteria and to take advantage of existing NASA/MTF technical support.

#### ACTIVITIES

The current major activities of the remote sensing role at MTF are to locate, develop, and test new resource-sensing tools, and to facilitate the incorporation of these tools into ongoing survey and harvesting procedures. The tools presently under consideration are spectrophotometers, low light level image intensifiers, lasers, acoustic imaging, micro-infrared detectors and photography. Several other sensing modes, not presently used for fish detection, are also being considered: bat sonar, oil-film detection, and detection of airborne iodine particles. Some of these activities are continuations of the efforts of many people in this audience and are being continued when practical.

Fig. 1 THE NMFS REMOTE SENSING PROGRAM AT MTF IS ORGANIZED INTO THREE COMPONENTS: MANAGEMENT, EVALUATION AND OPERATIONS.

I. MANAGEMENT GROUP RESPONSIBILITIES

- PROGRAM DEVELOPMENT
- MANAGEMENT
- ADMINISTRATION

II. EVALUATION GROUP

A. RESPONSIBILITIES

- ESTABLISH INTERFACES WITH USERS
- EVALUATE PROJECT PROPOSALS
- ESTABLISH TECHNICAL REQUIREMENTS
- ASSIGN REQUIREMENTS
- REEVALUATE RESULTS
- ESTABLISH AND ASSIST IN CARRY OUT DEMONSTRATION PROCEDURES

B. STRUCTURE

- REMOTE SENSING
- DATA MANAGEMENT
- BIOLOGICAL SAMPLE HANDLING
- TECHNICAL DEVELOPMENT CAPABILITY

III. OPERATIONS GROUP

A. RESPONSIBILITIES

- DEVELOP AND TEST ESTABLISHED SYSTEMS OR COMPONENTS
- DIRECT INTERFACE WITH TECHNICAL SUPPORT AND CONTRACTED EFFORTS
- REVIEW TEST SERIES RESULTS
- ESTABLISHMENT OF DEMONSTRATION PROCEDURES

B. STRUCTURE

- ENGINEERING
- DATA HANDLING AND PROCESSING
- BIOLOGICAL
- SYSTEM OR COMPONENT OPERATING CAPABILITY



Activities in the remote sensing program in FY-71:

(1) Test and evaluate an airborne image intensifier to detect bioluminescence stimulated by fish schools, and develop a compatible television monitor whose output can be digitized.

(2) Test and evaluate a portable imaging infrared detector for monitoring fish schools swimming near the surface.

(3) Continue studying the reflectance spectra of fish schools in impoundments and in their natural environment as a means for detecting and identifying pelagic fish stocks.

(4) Re-evaluate the feasibility of using a fluorescence spectrophotometer to detect and identify fish oil slicks on the sea surface.

(5) Investigate the feasibility of using advanced acoustical systems and techniques for fishery application. Concepts under consideration include airborne "dunking" sonar, airborne underwater listening devices, acoustical imaging, and the type of sonar used by fishing bats. In addition, the program will provide service and support functions to the regional laboratories undertaking acoustical research.

(6) Coordinate and conduct programs in support of the NMFS participation in the application of high flying aircraft and satellites with EROS, NASA, NESS, and SPOC. Through program personnel at MTF establish support from EROS and NASA through NESS as the NOAA Space Applications Coordinator.

(7) A fully instrumented impoundment system consisting of a series of laboratory aquaria, portable tanks, permanent ponds, and at sea controlled areas is under design by NMFS at MTF. This facility will be unique in that the biological and physical characteristics of the fish and the environment will be fully recorded in computer compatible language. With this system the NMFS will be able to test any instrument system against established constant. New and improved techniques of documenting animal behavior can also be expected to evolve from this system.

#### BENEFITS

The impact of remote sensing systems upon the Marine Resource Monitoring and Assessment Program (MARMAP) and other programs of the NMFS is expected

to be dramatic. Significant increases in the information acquisition rate of MARMAP are anticipated from the improved performance of existing sensors and from the development of completely new ones. Because the sensor improvement/development program will be undertaken via a systems approach, with appropriate attention to data management, we can further anticipate a much greater reliability of the data. Where the sensors can be used commercially we also anticipate significant increases in vessel efficiency and in the profit margin. The development of remote sensing technology to exploit and expand the usage of underutilized coastal fish stocks will provide accurate fisheries intelligence as a basis for new investment and will also narrow the gap between imports and domestic production of fishery products.

The Federal Government must assume an active leadership role in developing the technology needed for conserving, managing, and exploiting our marine resources, since it alone has the necessary resources and authority to coordinate a program of this complexity. NOAA has a unique opportunity to expand the industrial, academic, and state partnership currently under development in conserving and utilizing our marine environment for the benefit of the American people. Assumption of the lead agency role in remote sensing of marine resources in an integral part of the NMFS responsibility to the public to assess, monitor, and assist in managing the United States living resources.

## OPERATIONAL USE OF REMOTE SENSORS IN COMMERCIAL FISHING

by

Paul M. Maughan and Allan D. Marmelstein

Earth Satellite Corporation

Washington, D.C.

INTRODUCTION

A commercial fisherman, in attempting to sense the presence of fish, is limited to what he can see, hear or smell. His eyes respond to light in a very narrow part of the electromagnetic spectrum, between 400 and 700 nanometers; his ears to sound between 16 and 20,000 Hertz and his nose to vapors with minimum concentrations of one part per million parts air (1). Energy and gases beyond these ranges go undetected.

For many years, the difference between success and failure for the fisherman depended on these senses; success in many cases came to those with a keener development of these senses.

With the advent of electronic sensors, fishermen are no longer limited to the relatively narrow ranges of the human senses. However, to date only the fisherman's sense of hearing has been electronically extended in the operational fishing industry. SONAR (SOUND Navigation And Ranging) has become the operational example of a large number of devices called remote sensors, devices which have the capability of acquiring information about an object or phenomena without physically touching it. In the broadest sense then, these devices must include the fisherman's eyes, ears, and nose.

The task of finding fish by sound has been under intensive study for many years. Because it deals strictly with underwater remote sensing, we would like to dismiss this aspect by referring the reader to the Proceedings - BCF Acoustical Workshop (2), one of a large number of summary volumes on fish finding by sound.

The location of fish by smell is an art that has been used for centuries. Many fish emit a characteristic odor which can be picked up down-wind from any large concentration of the fish. For example, swordfish fishermen are quite successful at locating their catch, solely on the ability to smell the animal. In this case the fishermen are smelling the remains of the material regurgitated by the swordfish, material which has a distinctive rich, sweet, oily odor (3).

Whereas the location of fish by smell contributes to the ultimate success of a fish finding operation, the principal use of this technique is in support of visual sightings. Frequently, the fisherman will make a simultaneous identification of both an odor and a surface phenomena associated with a school of fish. Such is often the case with oil slicks (3).

Because the eye is the fisherman's most important remote sensor, this paper will focus on the use of sight, and the electronic extension of human vision in commercial fishing.

#### DEVELOPMENT OF AERIAL FISH SPOTTING

There is evidence that primitive man could catch fish by quietly standing on the shore of streams and lakes until a fish swam close enough to spear. This fishing technique was improved by adding an additional man; the one with the better eyes would provide what is presently known as "fish spotting" while the other one would provide the fishing labor. Eventually, one man became better at spotting fish, others became better at catching fish. The logical pregression was then for the fish spotter to service a larger number of fishermen. This arrangement apparently produced a competitive advantage and was soon

incorporated into fishing efforts for most near surface species of fish.

As fishing fleets were developed, the role of the fish spotter played an important part in providing the competitive edge of the successful boat. It wasn't long before the fish spotter found that by climbing the mast head he could see greater distances and could get a more accurate picture of the potential harvest within his range of sight. The first crow's nest was an attempt to make the fish spotter safer and more comfortable.

Fish spotters were restricted to mast-head heights for many years; we see occasional reference to the fact that they were aware of the limitations of being confined to an elevation only a few feet above the sea surface. One early attempt at solving this problem involved the use of blimps (4); another technique involved the use of hot air balloons tethered to the fishing vessel (5). <sup>1/</sup> Both platforms were not entirely satisfactory and have been used very little.

Aircraft opened a whole new dimension of capabilities to the fish spotter. At aircraft altitudes and speeds, he was able to see broader areas with each glance and to cover the potential fishing grounds more rapidly and more frequently. One of the earliest records of successful aerial fish spotting was in December, 1919 by the Naval Air Station Fish Patrol in southern California. An agreement drawn up between the Naval Air Station at San Diego and the Fish and Game Commission of California provided sea planes to survey potential fishing grounds.

---

<sup>1/</sup> During 1965, scientists of the Bureau of Commercial Fisheries Tuna Resources Laboratory at LaJolla, California did extensive experimentation with hot air balloons for tuna fish spotting under varying wind and sea conditions. They concluded that the difficulty of handling a balloon during non-ideal weather conditions precluded the extensive use of such platforms for fish spotting.

Upon sighting a school of fish, their location was radioed to the Naval Air Station, which would then telephone the information to the San Diego office of the Fish and Game Commission. The Commission would in turn immediately notify all fishermen and processors. This service was applauded by the fishing industry inasmuch as the Tuna canners of southern California had been closed for four months due to the lack of an adequate fish supply (6

Following on this early example, aerial fish spotters have been used extensively in a number of fisheries. However, the art of aerial fish spotting is still dependent upon the ability of the fish spotter to properly interpret visual observations of surface or near surface phenomena (Fig. 1). Although an aerial fish spotter is primarily interested in directly locating schools of fish, he frequently sees surface phenomena which indirectly lead him to an area of interest. For example, he may see an individual large fish, an oil slick, a color front, or flocks of birds, all of which yield information to the trained spotter. He may also indirectly locate schools of fish at night by observing the bioluminescence organisms (plankton) stimulated by the fish (7). Although he cannot sense it with his eyes, the trained aerial fish spotter is aware that there are temperatures gradients which control the movement and location of certain fish populations (8). Finally, he is intimately aware of the weather in the vicinity of his operations; many times certain weather characteristics indicate the presence or lack of fish.

Scant information exists in the literature about commercial applications of aerial fish spotting, particularly that segment which is dependent upon the use of privately owned single engine aircraft, the aircraft most widely used today. However, several government agencies have provided aerial support to certain commercial fisheries.

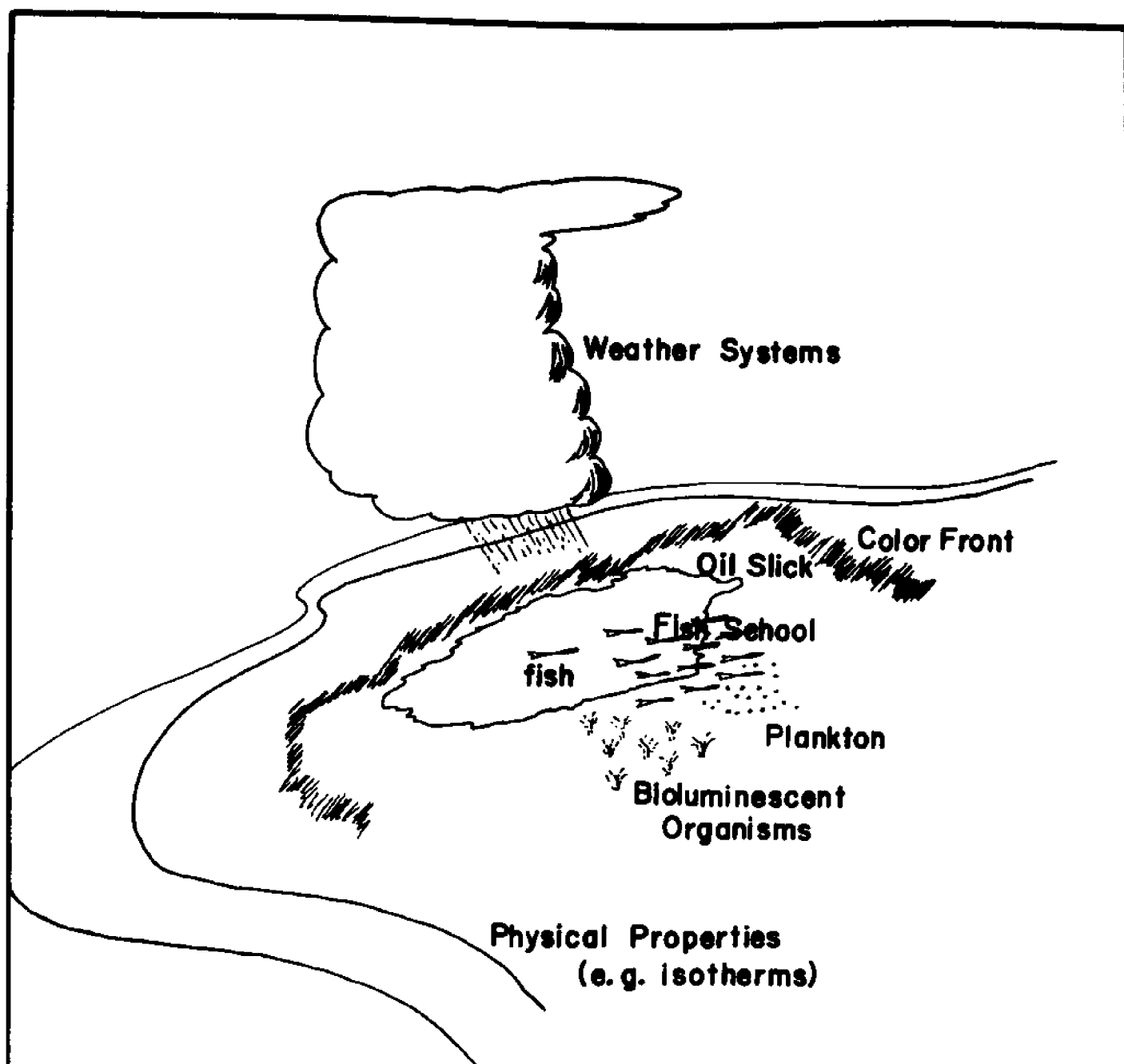


Figure 1. Bio-environmental factors of interest to commercial fishermen.

The National Marine Fisheries Service (NMFS) laboratory at Pascagoula, Mississippi, flew a series of aerial surveys between 1963 and 1966 to determine the occurrence of adult menhaden during the off-season (November to April) (9). Another NMFS laboratory at Miami, Florida used a light aircraft to survey the surface schooling tuna in the Lesser Antilles (10). The Bureau of Sports Fisheries and Wildlife for several years scheduled monthly flights using Coast Guard aircraft off the east and west coasts of the United States. During these flights, which are now operationally under the Coast Guard, marine life visible from the air was recorded (11). The State of California has provided annual aerial censuses of marine mammals including sea otter (12), grey whale (13), and sea lion (14). These counts have been made from a single-engine aircraft and have proved to be the only way to get an accurate census.

Aerial fish spotting is not restricted to the United States. For at least the last sixteen years, the Japanese have been carrying out aerial fish surveys off the northeastern coast of Japan (15). The Australian Commonwealth Scientific Industrial Research Organization flew a single-engine aircraft off the southeast coast of Australia in support of the Australian tuna fishermen. The Australian Fishermen's Cooperative estimated the cost of the operation to be about \$7,000. However, an estimated 700 additional tons of tuna valued in excess of \$100,000 were caught as a result of the program (16).

Aerial fish spotting operations are generally executed at altitudes of 500 to 1,000 feet. At this altitude and under ideal weather conditions, fish schools can be seen at distances from five to eight miles (10).



### CURRENT FISH SPOTTING OPERATIONS

There are currently from 66 to 73 aerial spotter aircraft in operation in the near-shore areas of the Pacific, Atlantic, and Gulf of Mexico (Table 1). Several fisheries use the aircraft only as incidental support, others are directly tied to aircraft support as a key element of fishing operations. The latter are characterized by the Atlantic and Gulf of Mexico Menhaden Fisheries; we will discuss these fisheries as an example of current fish spotting operations.

Menhaden is a herring-like fish. The Atlantic menhaden (Brevoortia tyrannus) is found from New England to Florida and the Gulf of Mexico menhaden (B. patronus) are found from Florida to Texas. Menhaden are not normally used for human consumption; their value lies principally as a processed product: fish meal, fish oil, and condensed solubles. Fish cakes from menhaden have been found to be a valuable high protein source used as a feed supplement for livestock. The oil is used in paints, soaps and lubricants.

U. S. fishermen catch more menhaden each year than any other species. Menhaden accounted for 36% by weight of the total domestic catch of all species in 1969. Landings of 1.5 billion pounds were recorded in 1969; a record 2.3 billion pounds was taken in 1962 (17).

Spawning of menhaden takes place at various times of the year over the continental shelf. Newly hatched larvae probably spend about a month in the open ocean and then enter estuarine environments for their post larval development. The larvae gradually move into the upper estuary as they grow. By the time they reach fresh water, they have transformed into juveniles. Menhaden generally winter in the estuaries and then move out into the open ocean in early spring. Beyond these

Table 1. SPOTTER AIRCRAFT OPERATING WITH THE U. S.  
FISHING INDUSTRY DURING 1969-70

<u>FISHERIES</u>		<u>NUMBER OF SPOTTER AIRCRAFT</u>
Atlantic	Mackeral, Herring	1*
	Tuna	2*
	Swordfish	3-4*
	Menhaden	18-20**
Pacific	Mackeral, Anchovy, Bonita	5-6*
	Tuna	5*+
Gulf	Menhaden	32-35**

\* Sund, Paul, Staff Assistant for Marine Resources. National Marine Fisheries Service, National Oceanic and Atmospheric Administration, Department of Commerce. Washington, D. C. November 18, 1970, Personal Communication.

\*\* Angelovic, Joseph, Program Chief, Menhaden Investigations, National Marine Fisheries Service Biological Laboratory, National Oceanic and Atmospheric Administration, Department of Commerce. Beaufort, North Carolina. January 6, 1971, Personal Communication.

+ Not included are an unknown number of helicopters operating with the Pacific Tuna fleet.

broad aspects, very little is known about the spawning and early life of the menhaden (18). The estuaries are of critical importance in the life history of the menhaden; over the last several years, pollution and environmental changes in estuaries have probably contributed to the decreased availability of this species of fish.

Harvesting of menhaden is a very complex undertaking requiring the time and effort of many men and much equipment. Before dawn, the large menhaden boats ("mother" boats), each carrying two smaller boats ("purse" boats) set off for the fishing grounds. Simultaneously, an aerial fish spotter flies reconnaissance searching for a reddish-brown colored area or a large abrasion on the surface of the water, both of which are common indicators of a menhaden school feeding on plankton (Figure 2.).

A radio man in the mother boat listens for communications from the aircraft. As the spotter radios that a school has been sighted, the lookout in the crow's nest aboard the mother boat pinpoints the exact location of the school. The two purse boats are lowered, each carrying half of the 60 by 1200 foot purse seine net that is used to entrap the school. Working in close communication with the aerial fish spotter, the purse boats separate to surround the school with the net. The purse boats swiftly close in on each other forming a circle with the net after which the bottom of the net is drawn together (Fig. 3). If this operation (called a "set") is successful, the mother boat closes in and the catch is pumped aboard into large refrigerated holds. Numerous sets are made before the mother boat is fully loaded and returns to its home base.

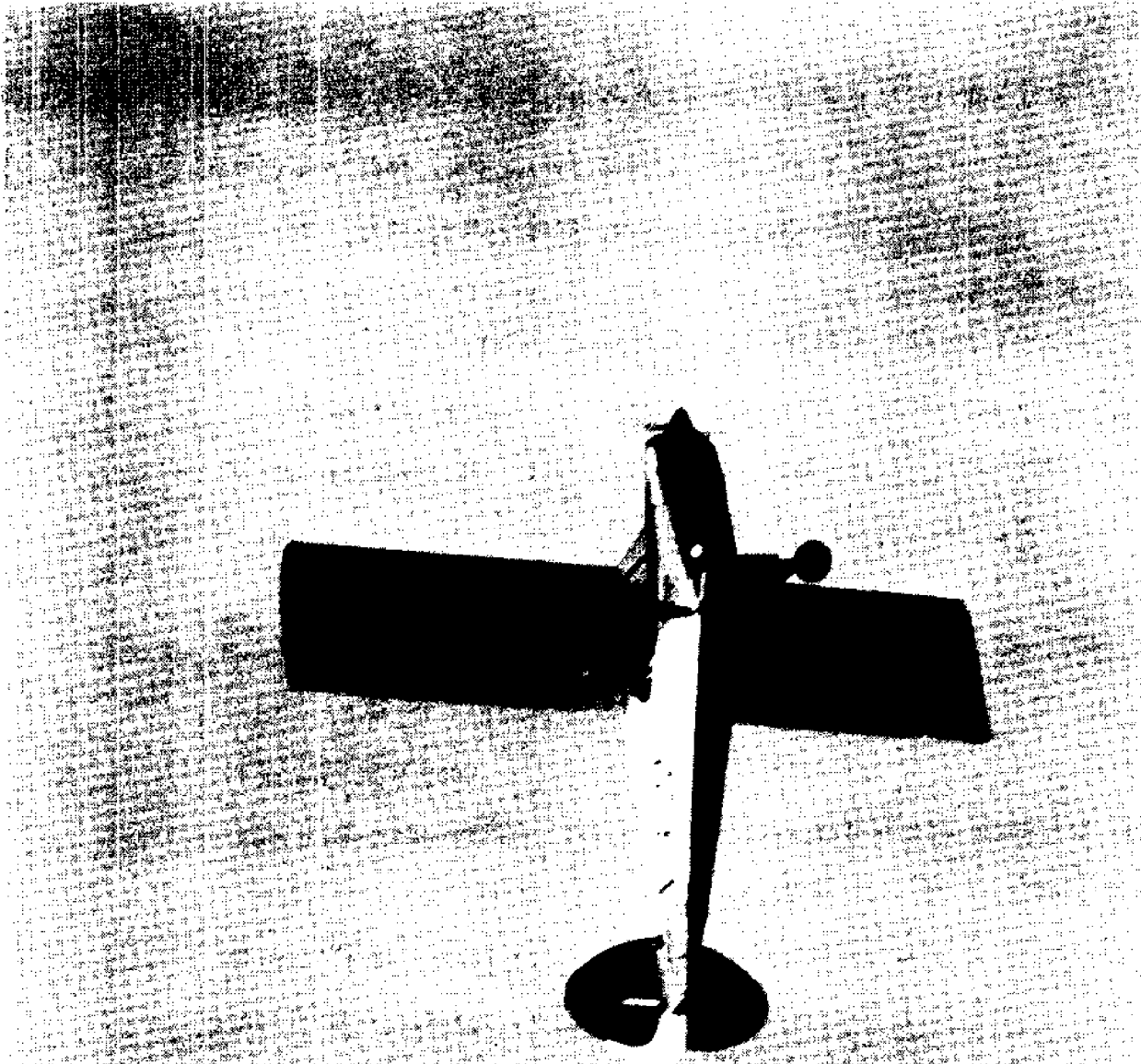


Figure 2. Menhaden spotter aircraft. To enable the aircraft to remain airborne for long periods of time, the rear seat is usually replaced with a gasoline tank. For better visibility during actual fish spotting operations the side windows are lowered. (Photo by Bob Williams)

It is obvious that the aerial fish spotter has a very important role in the harvesting of menhaden. Not only do they locate the fish, but they also assist in setting the purse seine net on the school. This close coordination becomes essential when the net is drifting in heavy currents to prevent the loss of much of the school.

The number of spotter aircraft operating in the Gulf Menhaden fishery has remained fairly constant since 1965. However, as shown in Table 2 there has been a marked decrease in the number of spotter aircraft operating in the Atlantic Menhaden fishery.

In 1969, 32 to 35 aerial fish spotters worked in the Gulf menhaden fishery and 18 to 20 worked in the Atlantic menhaden fishery. Single-engine aircraft (i.e., Cessna 180; Aeronca; Super Cub) are the most popular. One twin-engined aircraft has occasionally been used for search, but not in the net setting operation.

Norton (19) estimates the average annual costs associated with aerial fish spotting in the menhaden industry at about 1.4 million dollars. This is roughly nine percent of the costs associated with catching menhaden, and is apparently justified, as one of the major menhaden companies indicated that aerial assistance in setting nets had cut the unsuccessful sets down to less than one percent.

As in many industries where the human factor is a consideration in the efficiency of the operation, some spotter pilots are noted for their ability to locate schools of fish; others are noted for their capabilities in helping the purse boats set the nets. In all cases when the aerial fish spotter is viewing the sea surface he interprets what he sees largely from experience rather than from prescribed procedures.



Figure 3. Menhaden purse boats. The purse seine net has been closed around a school of fish and the bottom of the net drawn together. The purse boat on the right has begun to haul the net into the boat to compact the fish in preparation for the mother ship to come along side and empty the net into refrigerated holds.

Table 2. SPOTTER AIRCRAFT OPERATING WITH THE U.S. MENHADEN FISHERY\*

<u>Year</u>	<u>Atlantic</u>	<u>Gulf</u>
1954	23	
1955	29	
1956	33	
1957	37	
1958	41	
1959	40	
1960	32	
1961	34	
1962	34	
1963	35	
1964	39	
1965	31	32-35
1966	27	32-35
1967	22	32-35
1968	23	32-35
1969	18-20	32-35

\* Angelovic, Joseph, Program Chief, Menhaden Investigations, National Marine Fisheries Service Biological Laboratory, National Oceanic and Atmospheric Administration, Department of Commerce. Beaufort, North Carolina. January 6, 1971, Personal Communication.

Several of the companies currently engaged in the menhaden fishery are leaders in the integration of surface environmental data with aerial observations. One company has recorded environmental information on IBM punch cards for correlation and comparison with aerial observations. This information will be an immense help in long range plans to provide an operational forecasting model for incorporating observations from aircraft and satellite platforms.

Currently, no electronic remote sensors are carried on any of the spotter aircraft, and the spotter pilot is usually the only observer. There are plans, however, to incorporate the airborne radiation thermometer (ART) into the search operation as a first step into the use of electronic remote sensors in the industry. If this proves of value, more sophisticated instrumentation can be put to operational use.

#### FUTURE USE OF REMOTE SENSORS IN FISH SPOTTING

The primary thrust of environmental information gathered through remote sensors should, in our opinion, be towards resource management. By this we are referring to both strict conservation applications wherein the continuity of the resource is guaranteed, and commercial applications wherein the resource is harvested by the most economical means. We can envision a number of ramifications resulting from remotely sensed data leading to improved techniques and efficiencies in the conservation of the resource and in the operational aspects of commercial fishing.

The previous discussion of the menhaden industry provides the background for the development of future concepts in the application of remote sensors to fish spotting. Menhaden fishing is limited to daylight hours because it depends largely on the ability of aerial fish spotters



in low flying aircraft to see schools of fish. Being a planktonic feeder, menhaden frequently associate with bioluminescent planktonic organisms. It is therefore probable that schools of menhaden could be detected at night as a result of bioluminescence generated in the water by the feeding behavior of the animal. An operational system incorporating a low-light level sensor, a doppler laser and a computer could be employed to harvest menhaden at night. This system would function as follows. Both purse boats would have a computer readout which would allow the monitoring of the output of the computer. The low-light level sensor would detect a concentration of menhaden based on bioluminescence of the associated planktonic organisms and delineate the exact boundaries and depth of the school on the basis of relative light flux. A doppler laser would simultaneously measure the movement of the fish school and the surface and near surface currents. This information would be analyzed by the computer which would be programmed to direct the purse boats to an optimal set.

A low-light level sensor/doppler laser/ computer system would extend the fishery into a 24-hour operation. It would also provide better information on the behavior of menhaden during darkness. Such a system would allow for easier estimation of the total population size in an area and hence provide better information for management of the resource. When sufficiently refined, the system could operate from the light aircraft presently employed in the menhaden industry as well as from aircraft flying at higher altitudes. These larger aircraft could manage the activities of more than one mother ship at a time.

# REFERENCES

1. Beadle, G. W. Smell. The World Book Encyclopedia - Volume S. Field Enterprises Educational Corp., Chicago. pp 423. 1970.
2. Pereyra, W. T. (ed.). Proceedings - BCF Acoustical Workshop, Nov. 25-27, 1968. Exploratory Fishing and Gear Research Base, Bureau of Commercial Fisheries, Seattle, Washington. 1969.
3. Smelling fish schools. Sea Secrets. 12(6):5. 1968.
4. Ripley, W. E. K. W. Cox and J. L. Baxter. California sea lion census for 1958, 1960, and 1961. California Fish and Game. 48(4):228-231. 1962.
5. Bureau of Commercial Fisheries sends up trial balloon. Bureau of Commercial Fisheries, internal report. March, 1965.
6. Naval Air Station fish patrol opens idle canneries. California Fish and Game. 6(1):71. 1920.
7. New techniques for locating and assessing unutilized stocks. Exploratory Fish and Gear Research Base, Bureau of Commercial Fisheries. Circular 351. November, 1970.
8. ASWEPS oceanographers help Icelandic fishermen. Naval Oceanographic Newsletter. 7(4):1-2. 1968.
9. Bullis, H. R., Jr. Flight reports 1-15. Gulf explorations for off-season adult menhaden. U. S. Dept. of Interior, Fish and Wildlife Service, Bureau of Commercial Fisheries - Region II. 1963-65.
10. Jones, A. C. and P. N. Sund. An aircraft and vessel survey of surface tuna schools in the Lesser Antilles. Commercial Fisheries Review. 29(3):41-45. 1967.
11. Aerial survey of waters between Cape Cod and Cape Hatteras. Commercial Fisheries Review. 28(9):32.
12. Carlisle, J. G., Jr. Aerial census of California sea otters in 1964 and 1965. California Fish and Game. 54(4):300-302. 1966.
13. Hubbs, C. L. and L. C. Hubbs. Gray whale censuses by airplane in Mexico. California Fish and Game. 53(1):23-27. 1967.
14. Frey, H. W. and J. A. Aplin. Sea lion census for 1969, including counts of other California pinnepeds. California Fish and Game. 56(2):130-133. 1970.
15. Aircraft to be used for fish spotting and hydrographic observations. Commercial Fisheries Review. 6(27):63. 1965.

16. More science means more fish. Australian Science Newsletter. August, 1968.
17. Fisheries of the United States. . .1969. U. S. Dept. of the Interior. U. S. Fish and Wildlife Service, Bureau of Commercial Fisheries, C.F.S. No. 5300. pg. xii. 1970.
18. Reintjis, J. W. Menhaden life history program. Exploratory Fish and Gear Research Base, Bureau of Commercial Fisheries. Circular 350. pp 11-41. 1970.
19. Norton, V. J. Some potential benefits to commercial fishing through increased search efficiency. A case study -- the tuna industry. Final analysis report to Geological Survey, U. S. Dept. of Interior. January, 1969.

SOME POTENTIAL APPLICATIONS OF REMOTE SENSING  
IN FISHERIES

Kirby L. Drennan\*  
Zapata Remote Sensing Division  
Ocean Protein, Inc.  
Lafayette, Louisiana

ABSTRACT

Present techniques utilized by industry and Government to locate harvestable fish stocks and survey the resources of large oceanic areas, are inadequate.

Remote sensing from aerospace platforms appears to offer a more effective and economical means for assessing present resources and providing the information needed to predict the future abundance and distribution of fishery resources.

A number of significant characteristics of fish and their environment, which may be observed through the use of remote sensors, are presented. Those sensors which have been shown to have potential application, as well as the environmental factors which contribute to and limit their usefulness, are also discussed.

---

INTRODUCTION

In recent months much has been published concerning the decline of the United States Fishing Industry. It has been stated that in a period of eight years this nation has dropped from second to fifth place in world fishery production. This

\*This paper is based on research supported by the Spacecraft Oceanography Project, U. S. Naval Oceanographic Office, Washington, D. C. and conducted by the National Marine Fisheries Service, Exploratory Fishing and Gear Research Base, Pascagoula, Mississippi, where the author was employed as Chief, Fisheries Intelligence Systems Program.

decline has occurred despite a steady increase in per capita use of fish and shellfish products. The United States, with only 6% of the world's population, used in excess of 12% of the world's production of fish and shellfish in 1967. More than 70% of these fishery products are now supplied by foreign fishing fleets. There are many factors; social, political, and technological, which have contributed to this condition. However, in order to reverse this trend, and meet future demands for food for an exploding population, we must find more effective and efficient means of locating and harvesting our fishery resources.

A recent study (Norton, 1969) of the search activities of the California-based tuna purse seine fleet, has shown that 75% of the time spent on the fishing grounds is spent in search activities. This results in a direct cost of almost 13 million dollars annually, and represents over 1/3 of the total cost per pound of tuna landed by this fleet. It was also shown that a 50% reduction in search time, combined with a 25% increase in catch, could result in elimination of over 1/3 of the vessels required to maintain present catch rates. This would represent an annual cost reduction of almost 11.94 million, and a decrease in investment of 6.4 million.

This study points out one of the major inefficiencies related to tuna harvesting. However, search inefficiency is a problem which is not unique to the tuna fishery. Search time for trawlers fishing the most dense fish concentrations accounts

for approximately 50% of the total time at sea.

It may be concluded, therefore, that any technological improvement in the ability to locate fish would have considerable impact on harvesting costs, thereby resulting in substantial increased economic benefits to the fisheries and nations involved. This fact has been demonstrated by several foreign nations, e.g., Iceland, Japan, and the U.S.S.R., which provide mapping and forecasting services for their fishing fleets. United States fishermen, however, are at a disadvantage, since they do not receive comparable assistance in defining the resources. In order to place United States fishermen in a more competitive position, comparable assistance must be provided.

This assistance should include:

- (1) An assessment of the resources, i.e., intelligence on the location, identity and quantity of fish in a given region.

- (2) Assistance in the deployment and tactical direction of fishing fleets.

- (3) Forecasts of the temporal and spatial abundance and distribution of harvestable fish stocks.

The application of recent technological advances in the field of "Remote Sensing" appear to offer a more effective and economical means of assessing new and underutilized resources, as well as providing data which could result in large-scale reductions in the time spent by many vessels in searching for fish.

### SENSOR APPLICATIONS

Those characteristics of the marine environment, which are considered significant and may possibly be observed through the use of remote sensors, are given in Figure 1. These observations could, if obtained with sufficient frequency and accuracy, provide the data required to estimate oceanic productivity and determine the temporal and spatial abundance and distribution of fish stocks.

Some of the sensors which appear to have potential application in fisheries and the phenomena or activities which may be observed with each sensor, are shown in Figure 2. Those remotely sensed data of significance to fisheries may be divided into two major categories--environmental data from which estimates of biological productivity and distributions of fish stocks may be determined and--direct observations of fish which are needed to assess the resources of a given area. Direct observations are also needed to determine the reliability and accuracy of fisheries forecasts based on environmental data.

Remote sensing from aerospace platforms will most likely be limited to the use of pure electromagnetic sensors as opposed to magnetometers, gamma ray spectrometers, etc. The sensing devices may be either active, such as laser systems which illuminate the target with a coherent beam of monochromatic light and determine target distance from the time required for the light to travel to the target and return; or passive, such as film cameras which



Figure 1- OBSERVABLES OF SIGNIFICANCE TO FISHERIES



OBSERVABLES	SENSOR							
	MULTI-SPECTRAL CAMERA	METRIC CAMERA	LASER	SPECTRO PHOTOMETER	RADIATION THERMOMETER	THERMAL MAPPER	LOW LIGHT LEVEL TV	MICRO WAVE RADIO-LEVEL METER
SCHOOLS	●	●	●	●			●	
FISH COLOR	●			●				
WATER COLOR	●	●		●				
SURFACE ANOMALIES	●	●		●			●	●
UPWELLING	●	●		●	●	●		●
BIOLUMINESCENCE							●	
PLANKTON			●				●	
CURRENTS	●	●		●	●	●		●
SURFACE TEMPERATURE					●	●		●
SEA STATE		●	●					●
FISHING ACTIVITY	●	●		●			●	

Figure 2- REMOTE SENSORS AND THEIR POTENTIAL APPLICATION IN FISHERIES

record reflected sunlight through a process wherein the photons incident on the film, interact with halide grains in the film's emulsion.

Examination of the electromagnetic spectrum (Figure 3) suggests that we should be able to "look" at radiation reflected or re-emitted by the sea in any number of wavelength bands we choose over a spectrum which covers more than twenty orders of magnitude. However, atmospheric absorption and scattering limit the transmission of radiation to certain wavelengths or "windows" (Figure 4).

The strong attenuation of electromagnetic radiation by the water medium further limits direct detection to a narrow band of frequencies in the visible portion of the spectrum (Figure 5).

The transmission of electromagnetic radiation in clearest oceanic water peaks at a wavelength of approximately 470 nanometers, with a shift to longer wavelengths in coastal waters which have greater concentrations of particulate matter. Therefore, only those sensors operating in this narrow "oceanic window" in the visible portion of the electro-magnetic spectrum have potential application in the direct detection of fish.

## ENVIRONMENTAL SENSING

### Surface Temperature

Hela and Laevastu (1970) report that fish search for and select a certain optimum combination of physical and biological conditions in the environment. According to these investigators,

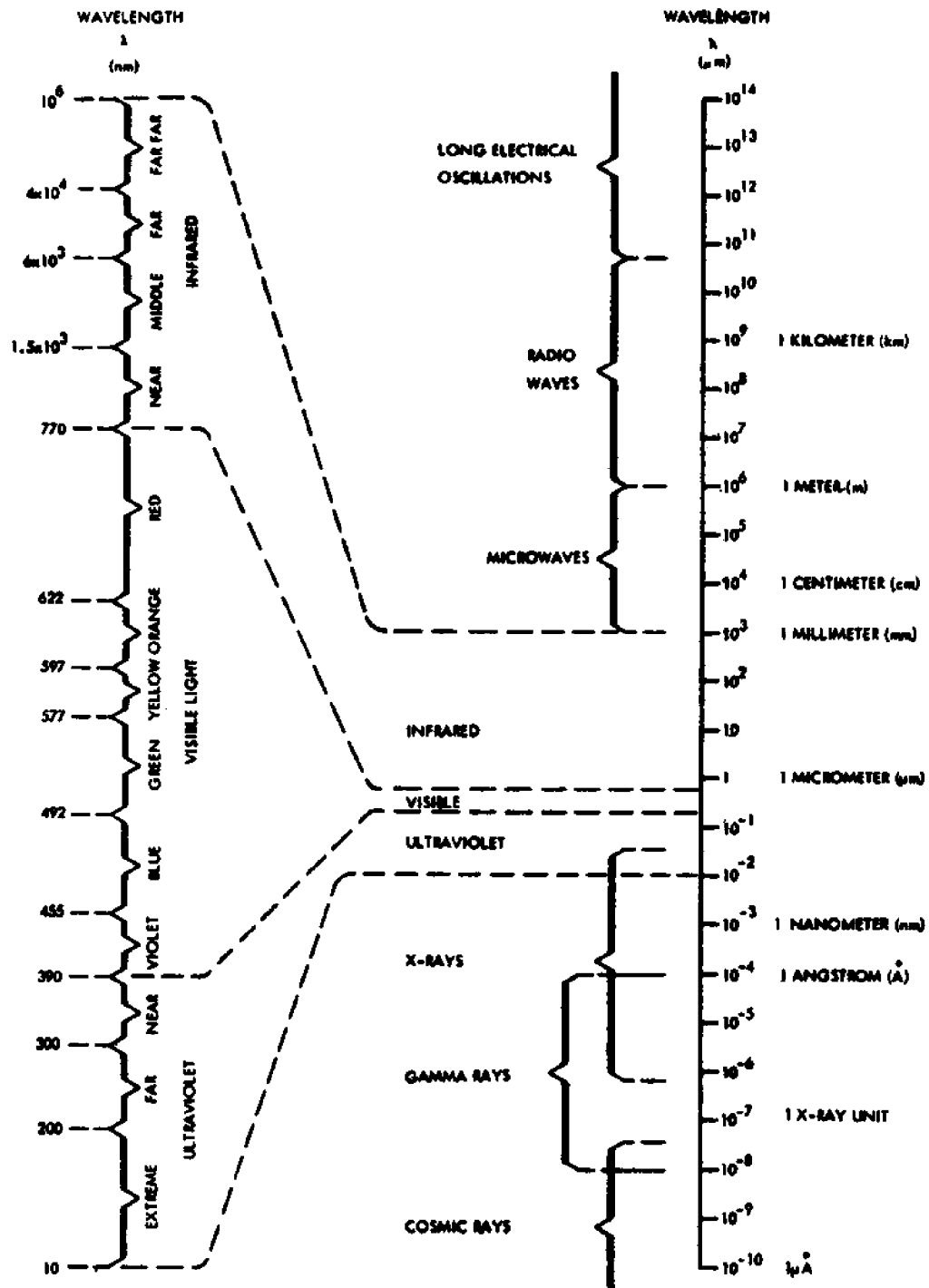


Figure 3- ELECTROMAGNETIC SPECTRUM (From RCA Electro-Optics handbook, 1968)

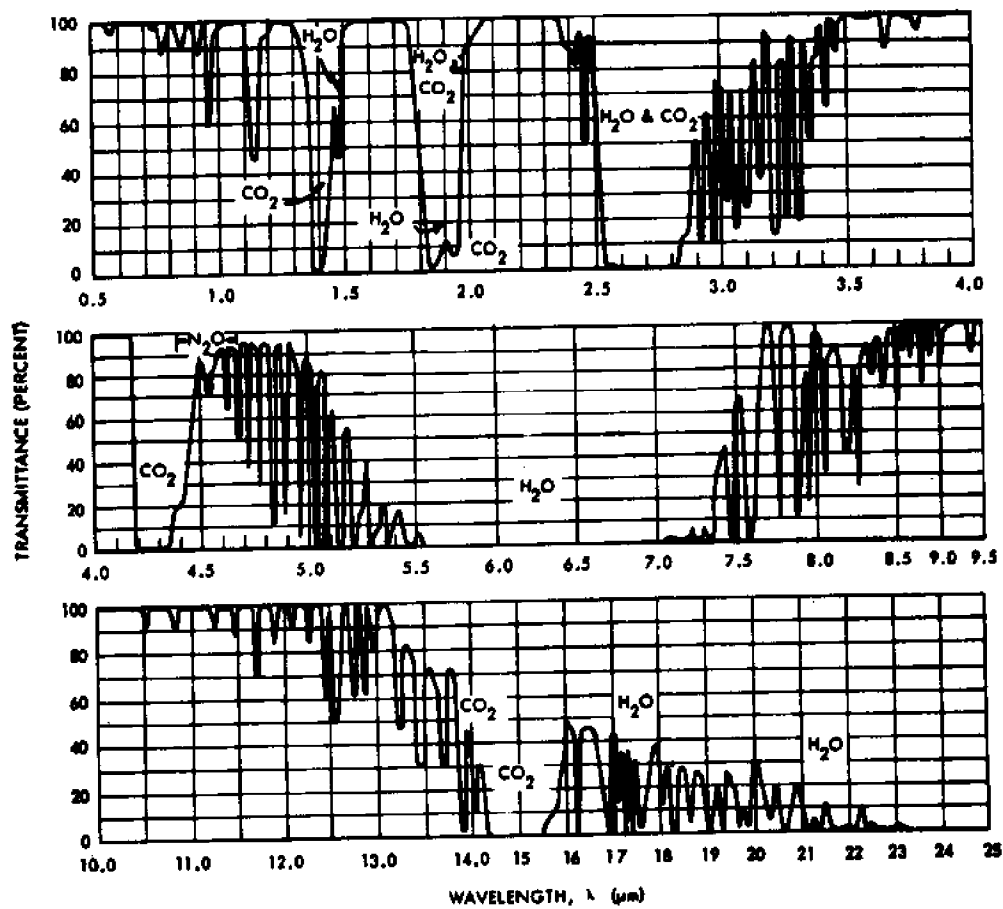


Figure 4- TRANSMISSION OF 1000FT HORIZONTAL AIR PATH AT SEA LEVEL  
5.7 MM PRECIPITABLE WATER 79° F TEMP (SBRC Chart 3 M 67)

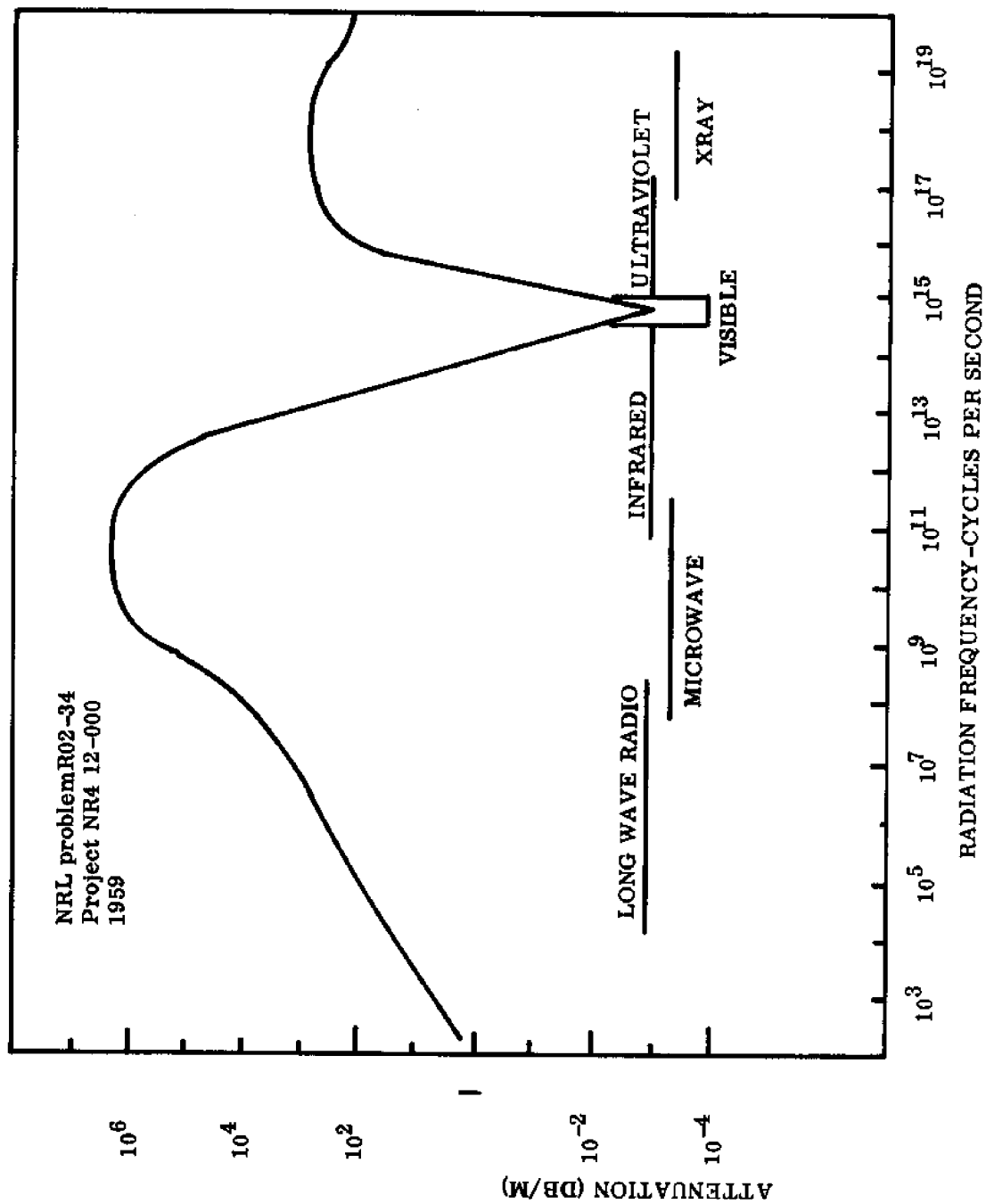


Figure 5- ATTENUATION OF ELECTROMAGNETIC RADIATION BY SEA WATER  
(From Lankes, L.R. 1969)

nearly all fish stocks have optimum temperatures which may be used in predictions of their seasonal abundance and distribution. The relationship between catches of albacore tuna and sea surface temperature is given in Figure 6. This parameter can be measured remotely from aerospace platforms, through the use of thermal scanners or infrared radiometers.

The basic equations governing the emission of infrared radiation from the sea, are:

The Stefan-Boltzman Law,  $W = \epsilon \sigma T^4$ ;

The Wien Displacement Law,  $\lambda_{\max} T = 2898 \mu(\text{OK})$ ;

and Planck's Law,  $u_{\lambda} = C_1 \lambda^{-5} (e^{C_2/\lambda T} - 1)^{-1}$

where -

$W$  = radiant power in watts

$\epsilon$  = emissivity of sea water = 0.98

$\sigma = (0.56687 \pm 0.00010) \times 10^{-8}$  watt cm<sup>-2</sup> degrees<sup>-4</sup>

$T$  = absolute temperature in ° Kelvin

$\lambda$  = wavelength in microns

$u$  = radiant energy density

$C_1$  = constant

$C_2$  = constant

The radiant energy distribution at the extreme temperatures, - 2° C to + 35° C, encountered over the oceans can be determined from these equations. The maximum emission at these temperatures will occur around 10 microns (1000 nm), in accordance with Wiens Displacement Law. The radiant energy available for detection

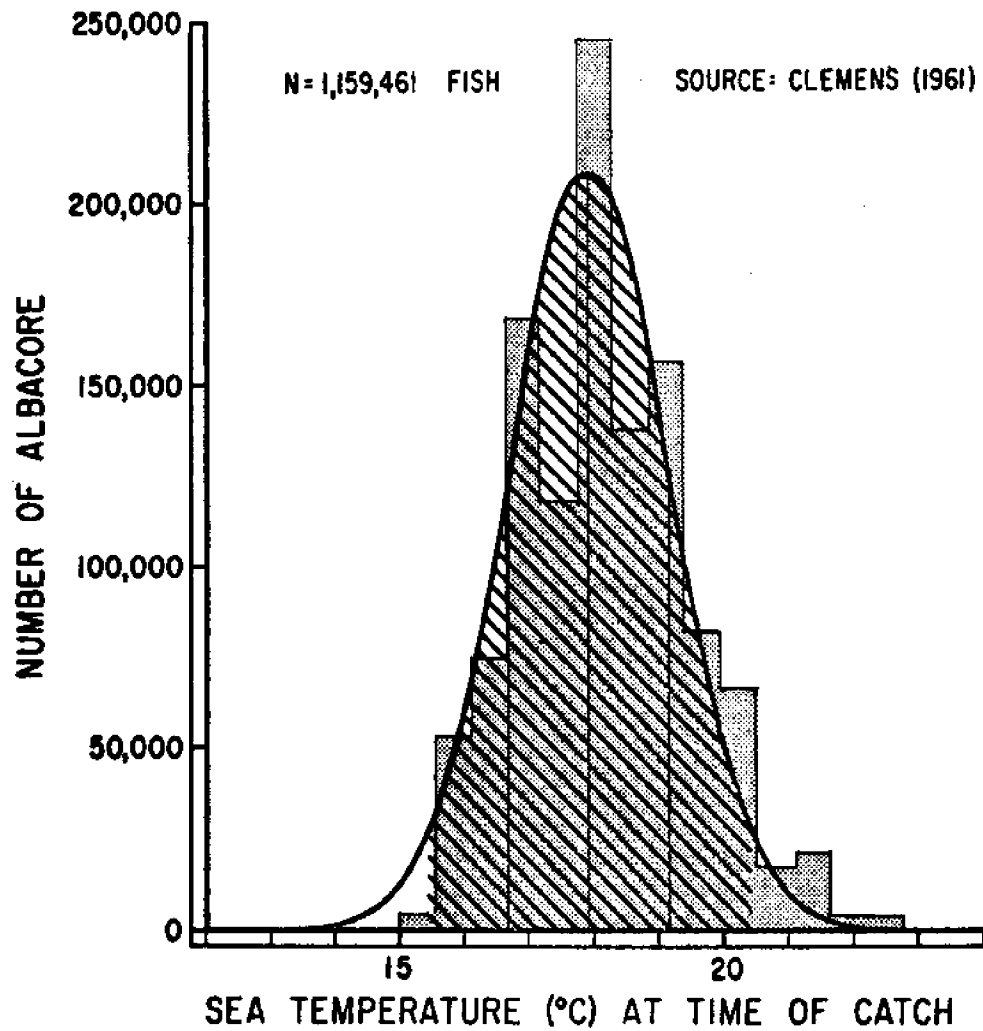


**Figure 6- THE RELATION BETWEEN THE SEA SURFACE TEMPERATURE AND THE ALBACORE CATCH. HATCHED AREA INCLUDES 95 PERCENT OF TOTAL CATCH. (From Hela and Laevastu, 1970)**

from the sea surface, is given by the Stefan-Boltzman Law.

Investigations by Dorsey (1940) and Defant (1961) have shown that the sea is opaque to radiation in the 4 to 100  $\mu$  region of the electro-magnetic spectrum. Its transmissivity is such that a layer of sea water approximately 0.02 mm thick, will absorb virtually all incident radiation within this wavelength band. Therefore, the emission from the sea must come from a layer of the same thickness.

Drennan (1967) showed, from a comparative analysis of sea-surface temperature patterns based on direct measurements and those based on remote measurements from aircraft, that reliable measurements of this parameter can be determined remotely. It was also shown that the horizontal gradients of surface temperature, observed in the Gulf of Mexico, are identified with the major current systems and areas of upwelling.

Airborne measurements of surface temperature (Drennan 1966) have been used to delineate Mississippi River outflow patterns and the major surface features of the circulation in the northern Gulf of Mexico. The significance of these phenomena to fisheries has been recognized by fishermen and fishery scientists alike. The convergence "sinking" of water along current boundaries, brings about a "mechanical" aggregation of forage organisms and small fish as well, which serve as a source of food for larger commercially important species, such as tuna, saury, etc. (Hela and Laevastu, 1970).



Upwelling of cold, nutrient-rich water and river runoff contribute to the food supply and productivity of the oceans. However, the positions and intensities of currents and areas of upwelling change seasonally and in response to meteorological conditions. Since these phenomena exhibit anomalous temperatures and color characteristics, their movements can be determined, and predictions of future position made through the use of remote sensors from aerospace platforms.

#### Ocean Color

Recent research has been conducted by Clarke, et al (1969) in an effort to relate biological productivity to changes in the ratio of upwelling light in the green (540 nm) to blue (460 nm) portions of the spectrum. The feasibility and significance of this approach is based upon the knowledge that photosynthesis, which initiates the food chain in the sea, is carried out by chlorophyll-bearing algae known as phytoplankton. Spectral analysis of these organisms have shown that they exhibit two absorption bands at approximately 460 nm and 670 nm. In clear "biologically poor" oceanic waters, absorption is minimal at a wavelength of approximately 470 nm. With increased concentration of chlorophyll, the wavelength band of minimum absorption approaches the wavelength of minimum absorption for chlorophyll at 540 nm. Therefore, highly productive oceanic areas are characterized by a greenish color which is indicative of high concentrations of chlorophyll and other biochromes.

The significance of chlorophyll measurements in identifying and delineating fertile fishing grounds has been established (Summer Study on Space Applications, 1969). The relationships between chlorophyll, tuna food, and presence of tuna, have been studied off the California Coast. It has been shown from these studies, that areas of high surface chlorophyll and high standing crop of tuna food tend to be congruent at a given time. The presence of these properties in waters within the limited temperature range of tuna provide the largest commercial catches of this resource. It is expected that knowledge of the distribution of chlorophyll would be of even greater importance in determining the distribution of animals at lower trophic levels.

Therefore, the studies of Clarke, et al (1969) which have shown the feasibility of distinguishing areas containing low to moderate concentrations of chlorophyll from altitudes up to 10,000 feet, with an experimental airborne spectro-photometer, are a significant step toward the development of a capability to measure the productivity of the oceans.

The color of the ocean, and other surface features of significance to fisheries, can also be observed through the use of photography (Stevenson 1967, 1969, Lindner and Bailey, 1968). Although the spectral resolution of present films is not sufficient to resolve the subtle color differentials associated with small changes in chlorophyll concentration, the more pronounced color differences and surface features which serve to identify the boundaries of major current systems, areas of upwelling, and sediment distribution in coastal areas can be delineated.

## DIRECT SENSING OF FISH STOCKS

### Spectro-Photometric Studies

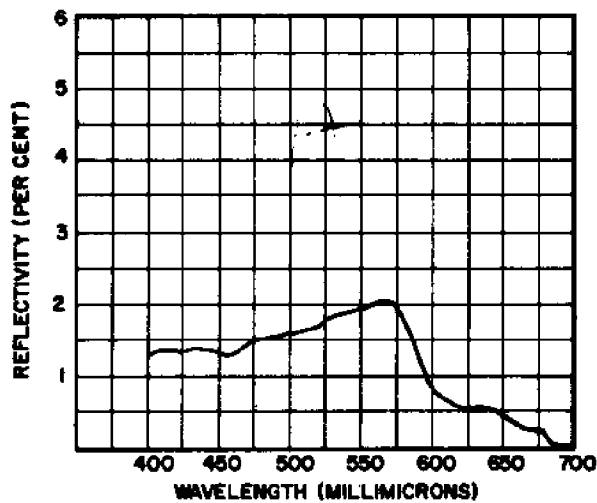
It has been demonstrated by spotter pilots of the commercial fishing industry that certain species of pelagic fish can be differentiated by color. These spotters also use other features, such as schooling patterns, fish behavior, surface roughness, and diving birds to locate, identify, and quantify commercial fish stocks. Although the color differentials are in some cases subtle, they are distinct, which suggests that spectro-photometric techniques might be applied to determine unique spectral signatures of commercially important species.

During September 1968, the National Marine Fisheries Service (NMFS, formerly BCF) and TRW Systems, Redondo Beach, California, under contract to NMFS, obtained spectral reflectance measurements of 15 schooling species in the northern Gulf of Mexico. Observations were made of single fish, fish in small groups, and fish in schools inside an impoundment using a recently developed TRW water color spectrometer. Individual fish were anesthetized and placed in a small water-filled container with a black background. Observations were made, with the fish held just under the water surface during the 1.2 seconds required for observation. Observations were also made of fish in the water inside a net. For these observations, the spectrometer was set up on an oceanographic platform at a height of 80 feet above the water surface.

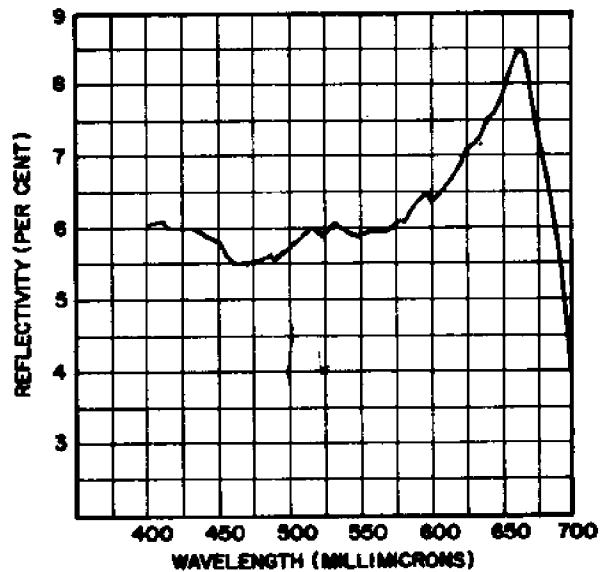
Thirty-three of approximately 120 spectra obtained during this period were analyzed by TRW. Examination of the data indicate

that, in general, the reflectances are separable on a species basis and are different from sea water reflectance. Examples of the reflectance curves obtained during this period are shown in Figure 7. The curve on lower right shows the spectral reflectivity of Spanish mackerel (Scomberomorus maculatus). This is a very bright fish which exhibits high reflectance and a very distinctive shape with a high hump in the green portion of the spectrum (500-600 nm). Cigar fish (Decapterus punctatus) observed in a net, exhibit a very distinctive reflectance curve. The major characteristics being high reflectance and a peak in the red portion of the spectrum (600-700 nm). An examination of the reflectance curves obtained reveals a number of peaks and valleys. The set of wavelengths at which these occur form what appears to be special identification codes which may be referred to as spectral signatures.

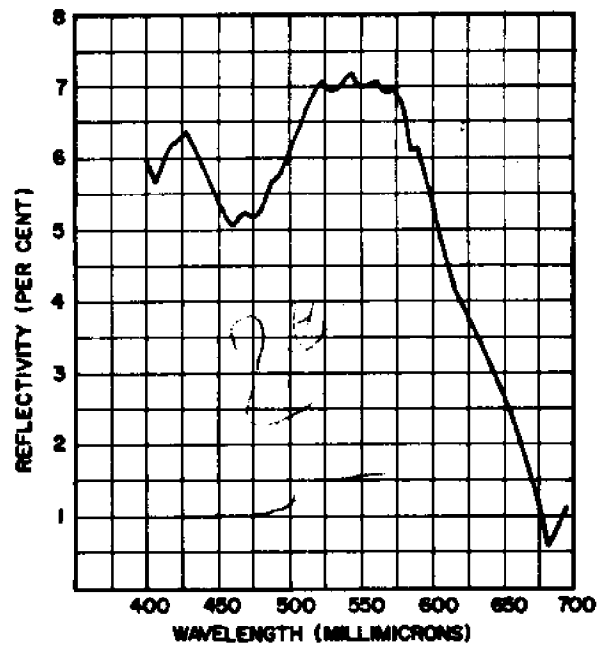
The problem of detection and identification of fish schools of varying densities was considered for three commercially important species. One of these species was Spanish mackerel. The calculated reflectance curves are shown in Figure 8. These calculations are based on observations which would be obtained from a low flying aircraft, 1,000 feet, on a clear day 45° sun angle, over a typical body of water, i.e., water with a concentration of one milligram per cubic meter of chlorophyll "a", with the fish at a depth of 50 centimeters. Curve "A" shows the predicted instrument reading for sea water on that day. Curve "B"



**SPECTRAL REFLECTIVITY OF SHALLOW, TURBID OCEAN WATER (24 SEP 1968 AT 1256)**



**SPECTRAL REFLECTIVITY OF CIGAR FISH (*DECAPTERUS PUNCTATUS*) IN A NET IN THE OCEAN (28 SEP 1968 AT 0935)**



**SPECTRAL REFLECTIVITY OF SPANISH MACKEREL (*SCOMBEROMORUS MACULATUS*) SUBMERGED IN A BLACK TRAY OF WATER (2 OCT 1968 AT 0940)**

**Figure 7 - SPECTRAL REFLECTANCE CURVES**

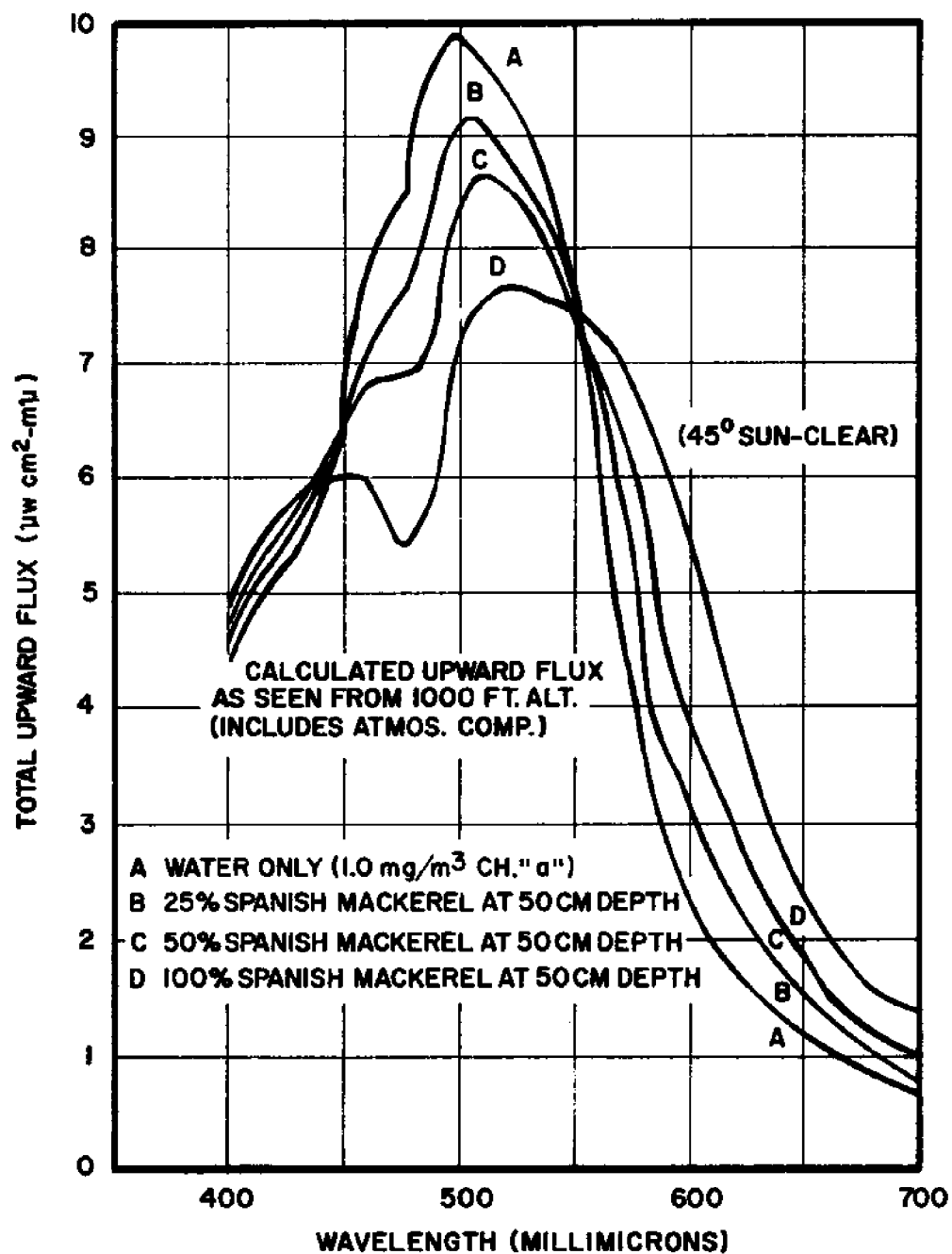


Figure 8- COMPARISON OF UPWARD RADIATION FROM OCEAN WATER WITH VARIOUS DENSITIES OF SPANISH MACKEREL

shows the data if 25% of the area under the surface is covered with Spanish mackerel. "C" and "D" are the 50% and 100% coverage curves. From these data, it was computed that the minimum density in which fish could be detected under these conditions is 10%.

The results obtained suggest the feasibility of species identification through spectral analysis of reflected radiation. However, these data were acquired under near ideal conditions, and it is yet to be determined whether these techniques will achieve similar results when applied to schools of fish in their natural environment.

#### Bioluminescence

Preliminary results of the first known efforts to use low-light-level sensors to detect fish stimulated bioluminescence, were reported by Drennan (1969). The following is a discussion and evaluation of some of the major environmental and physical factors which contribute to and limit the detection of bioluminescence with these devices.

#### Distribution, Intensity, and Spectral Characteristics of Bioluminescence

The phenomenon of bioluminescence has been used by fishermen for centuries and has undoubtedly attracted the attention of seafarers of all oceans since prehistoric time. However, appreciation of the truly ubiquitous nature of the phenomenon has come about only recently.

Bioluminescence can be induced through mechanical, thermal, chemical, electrical and light stimulation means. Bioluminescence associated with fish or other moving objects beneath the surface,

results primarily from mechanical stimulation caused by the object as it moves through the water. Staples (1966) refers to three types of bioluminescent displays: "sheet-like", "spark-type" and glowing ball or "globe-type". The sheet-like displays are created by large numbers of luminescent bacteria, euphausiids and copepods - a kind of luminescence which often occurs in colder waters and only when the waters are disturbed. The spark-like displays are attributed to dinoflagellates. The glowing ball or globe-like displays are seen most frequently in the warmer waters of the world. This type of display is caused primarily by ctenophores. Staples (1966) used approximately three thousand reports, on file at the United States Naval Oceanographic Office, to prepare a series of charts showing the seasonal distribution of bioluminescence over most of the world's oceans. These charts do not give a complete representation of the geographic distribution of bioluminescence since the majority of the reports were from frequently traveled shipping lanes. However, the report firmly suggests that many of the planktonic forms of luminescing organisms are world-wide in their distribution. The report also points out the seasonal and geographical variations in the intensity of bioluminescence.

The major concentrations of luminescing organisms appear to be in the upper layers of the ocean, usually within the euphotic zone, or above the thermocline (Figure 9). However, Clarke and Hubbard (1959); Clarke and Brestlau (1960); Clarke and Kelly (1965),



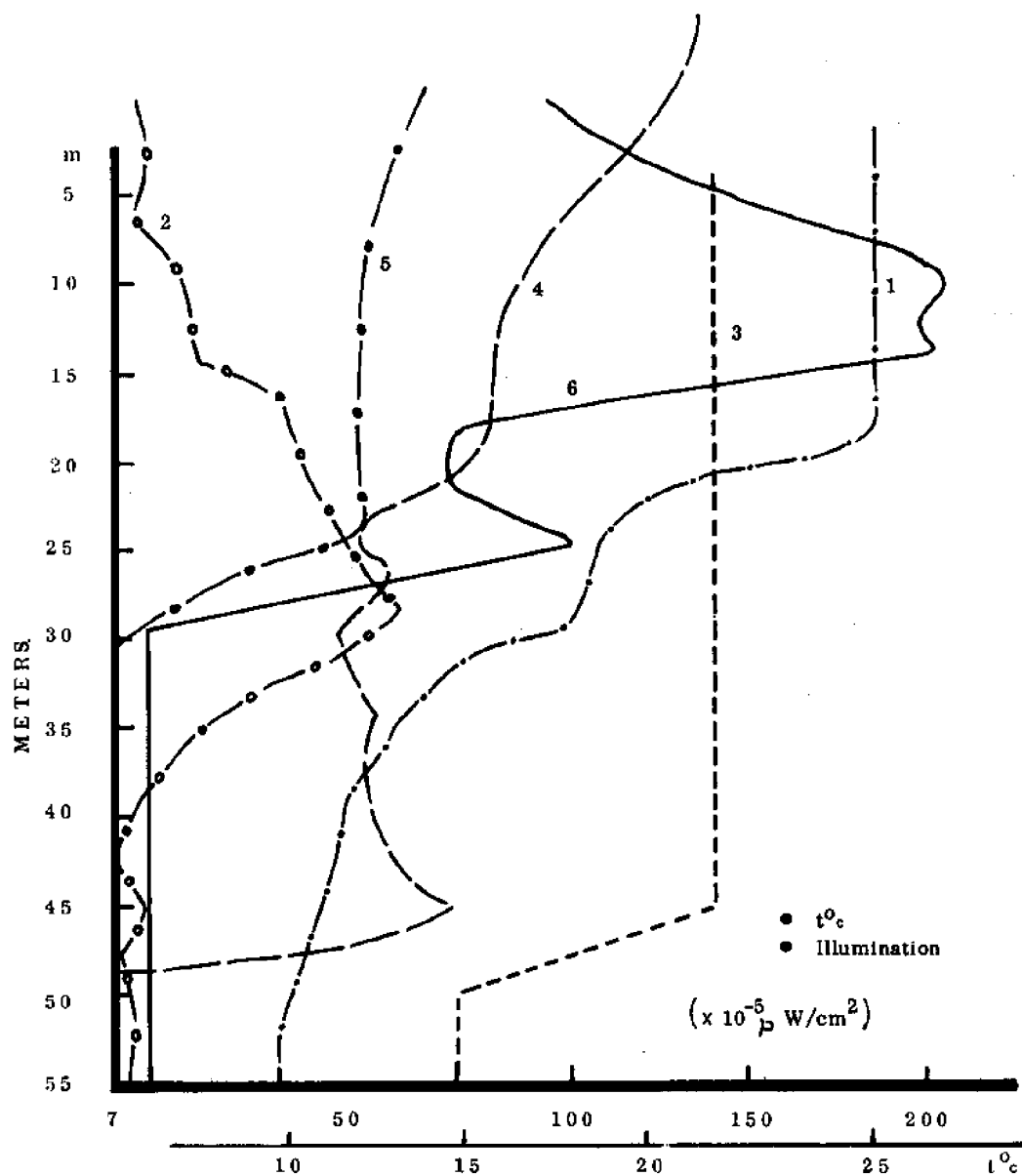
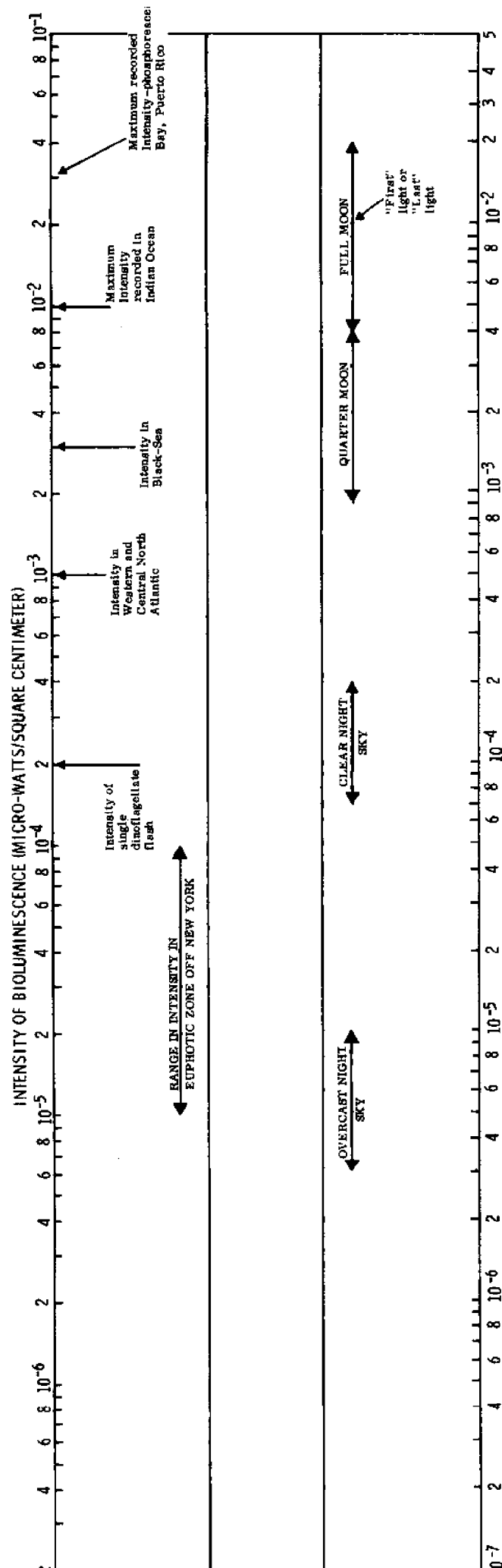


Figure 9- RECORD OF INTENSITY OF BIOLUMINESCENCE WHILE THE INSTRUMENT WAS RAISED FROM 55 m TO THE SURFACE AND TEMPERATURE CURVE FOR 13 AUGUST 1966 (2 and 1 respectively), FOR 3 OCTOBER 1966 (4 and 3) AND FOR 11 NOVEMBER 1965 (6 and 5) (From Bityoukov et al, 1967)

have obtained vertical profiles of the intensity, frequency and duration of bioluminescence flashes at many stations in the Atlantic and Indian Oceans and Mediterranean Sea. These observations suggest that luminescing organisms are present in varying concentration throughout the entire water column.

Clarke and Backus (1956) documented a transition in the nature of bioluminescence occurring below the euphotic zone, which they attributed to a change in the type of organism responsible for the bioluminescence. Netting placed over the agitation intake of a bioluminescence photometer showed that most of the luminescent organisms in the upper few hundred meters were smaller than 0.24 mm. Larger animals apparently account for much of the bioluminescence at greater depths. The recent work of Kelly (1969) has implicated dinoflagellates as most likely responsible for the bulk of near surface luminescence.

The intensity and spectral distribution of bioluminescence is of primary importance due to the strong attenuation of certain wavelengths by the water medium. The intensity of bioluminescence has been measured at a number of locations in the open ocean and in certain areas where it is most intense (Figure 10). The intensity of these values relative to the ambient illumination incident at the sea surface from the night sky is also given. A scotopic luminosity coefficient of .713 was assumed for these calculations. Intensities above  $10^{-3}$   $\mu$  w/cm<sup>2</sup>, or about  $10^{-7}$  times surface light with bright sun, were recorded in the slope waters southeast of New York by Clarke and Denton (1962). The flashes



RELATIVE INTENSITY OF ILLUMINATION FROM NIGHT SKY (FOOTCANDLES)

Figure 10- SOME RECORDED OBSERVATIONS OF BIOLUMINESCENCE AND ITS INTENSITY RELATIVE TO ILLUMINATION FROM NIGHT SKY

ranged from less than two-tenth second to more than one second in duration with light from overlapping flashes lasting sometime for more than ten seconds. Measurements in the Mediterranean revealed a large number of the brightest flashes, some were  $10^{-2} \mu\text{w}/\text{cm}^2$ . However, the frequency of flashing was generally less than in the Atlantic. Sustained light levels of about  $3 \times 10^{-2} \mu\text{w}/\text{cm}^2$  were produced by continuous agitation of the water in Phosphorescent Bay, Puerto Rico, which contained large populations of dinoflagellates (Clarke and Brestlau 1960). An annual variation in the intensity of bioluminescence in the Black Sea, off the Crimean Coast, has been observed by Bitjukov, et al 1967, (Figure 11). Values on vertical scale are times  $10^{-3} \mu\text{w}/\text{cm}^2$ . These data show a marked seasonal change in the intensity of the bioluminescence, with peaks occurring in Spring and Autumn. A review of the literature suggests a cyclic variation in the intensity of the bioluminescence in temperate and arctic waters.

The emission spectra of four diverse species of dinoflagellates have been measured and are shown in Figure 12. All have a spectral peak between 470 and 480 nanometers. This factor contributes to the transmission of luminescent energy in the sea and the ability of the scotopic (dark adapted) eye to detect it. The transmissivity of clear oceanic water is at a maximum in the wavelength region 470 to 480 nanometers and approximates the spectral sensitivity curve of the scotopic eye. An example of the sensitivity of the

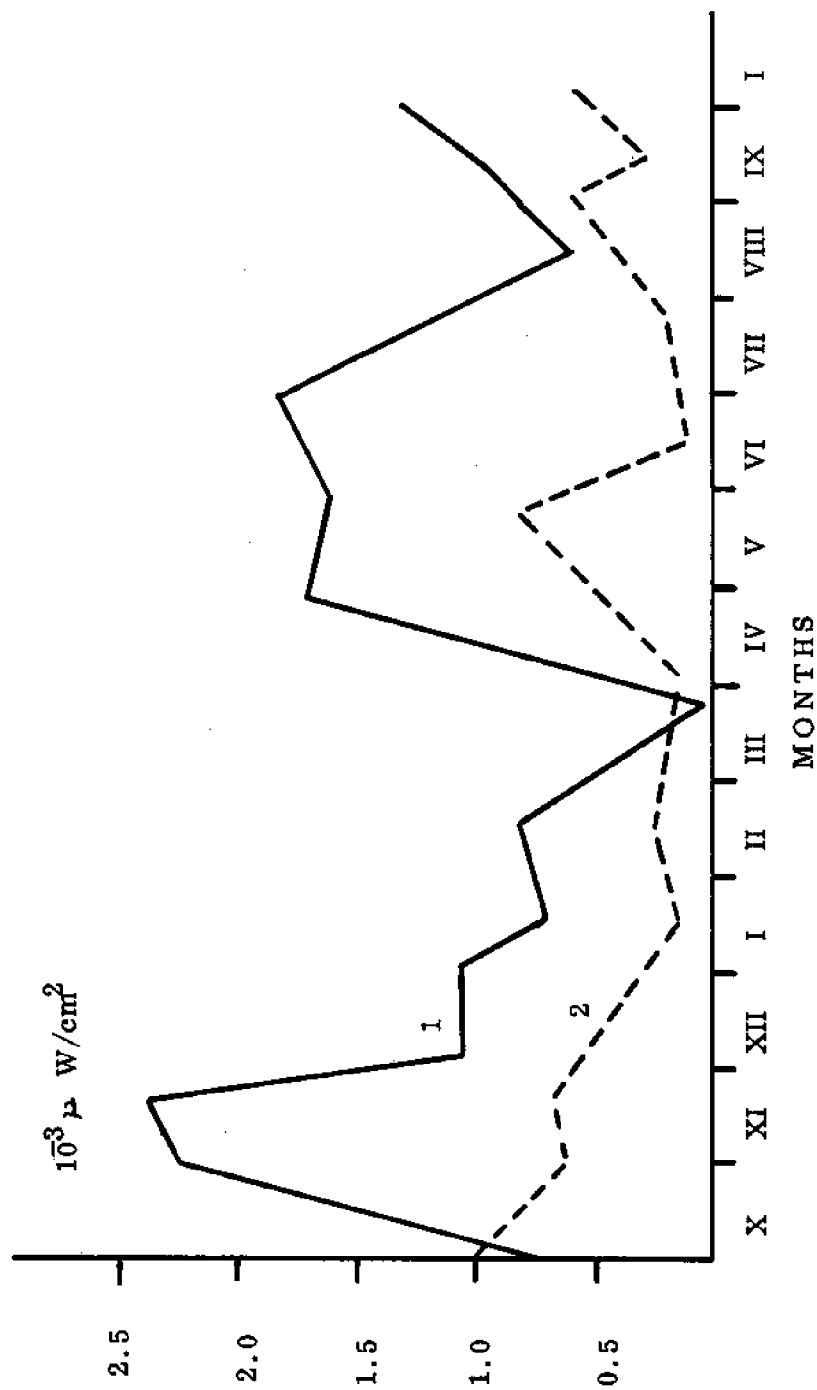
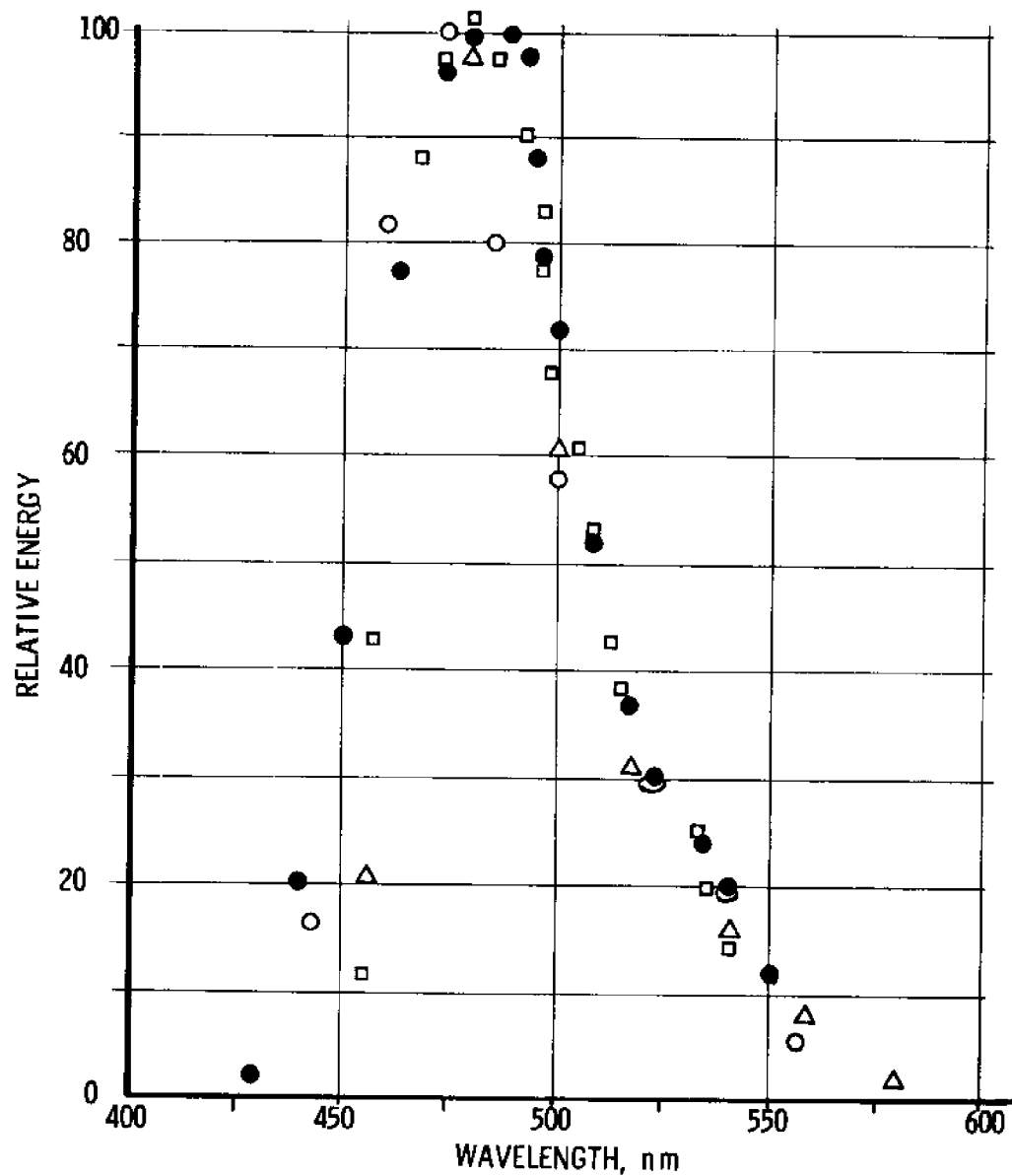


Figure 11- MEAN INTENSITY OF THE BIOLUMINESCENCE FIELD OFF THE CRIMEAN COAST WHEN THE BATHYPHOTOMETER WAS TOWED AT A DEPTH OF 10 m (1) AND RAISED FROM 55 m TO THE SURFACE (2). (From Bityukov et al 1967)



○ Noctiluca Scintillans (Nicol, 1958); □ Pyrodinium Bahamense (Taylor et al., 1966);  
 ● Gonyaulax Polyedra acetone extract (Hastings and Sweeney, 1957);  
 △ Pyrocystis Lunula "cysts" (Swift and Taylor, 1967).  
 (From Kelly, M. G., 1968)

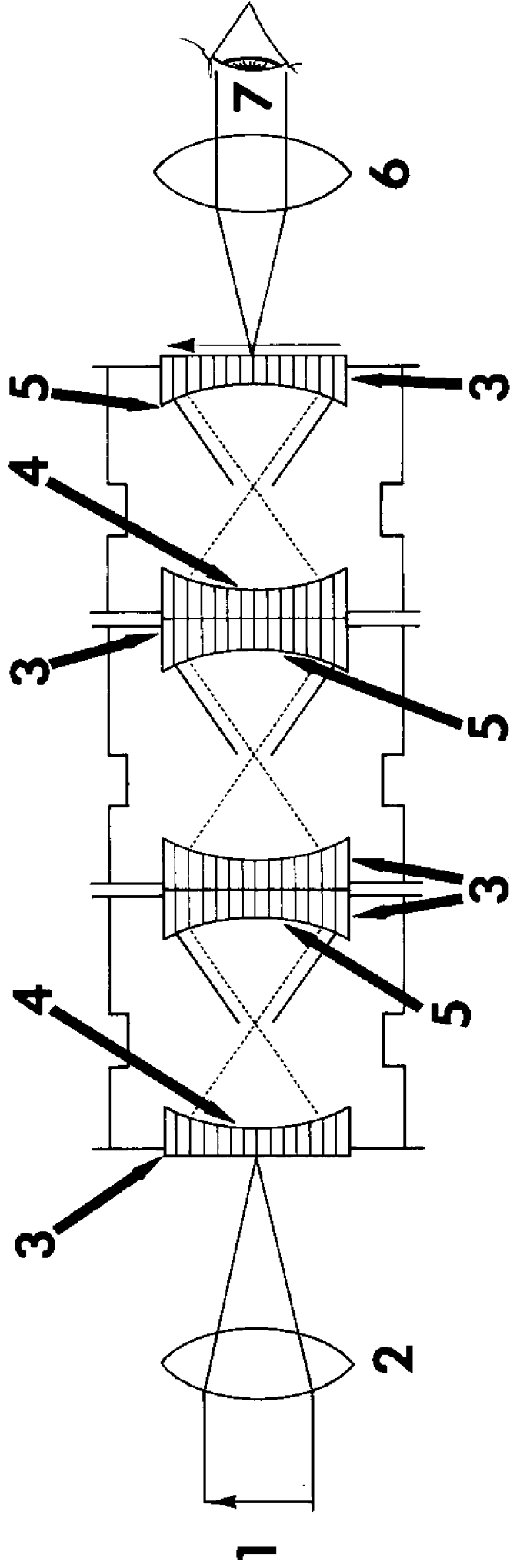
Figure 12- EMISSION SPECTRA OF FOUR SPECIES OF DINOFLAGELLATES

eye is given as follows: the fully dark adapted human eye with a pupil of about 0.5 centimeters square, can detect about  $10^{-8}$   $\mu\text{w}/\text{cm}^2$  of retina (510 nm) when looking at five-second flashes of a uniform circular field subtending  $47^\circ$  at the eye (Clarke and Denton 1960). Therefore, the recorded intensities of bioluminescence  $3 \times 10^{-2}$   $\mu\text{w}/\text{cm}^2$ , are well above the visual threshold of the human eye.

An examination of Figure 10 provides some indication of the range in intensity of bioluminescence which may be encountered throughout the world's ocean. It also shows that the illumination incident from the night sky with a full moon exceeds the maximum recorded intensity of bioluminescence. The energy reflected, however, varies from 4% at angles of  $0^\circ$  to approximately 20% at  $70^\circ$  off the vertical. This is a factor which limits the usefulness of bioluminescence as a means for detecting fish, or other submerged targets.

#### Light Amplification Through the Use of Image Intensifiers

The United States Department of Defense has recently declassified a number of tactical night vision devices which are being used by our forces in Vietnam. These devices consist basically of three components; an input optical objective, an image tube at the focus of this objective, and an eyepiece or ocular, each optically coupled as shown in Figure 13. When light, however faint, enters the forward end of the device, the image input lens focuses it onto the photocathode of the first stage of the image tube which



KEY: 1 - target image input, 2 - lens, 3 - fiber optics, 4 - photocathode, 5 - phosphor screen, 6 - lens, 7 - intensified image output to observer's eye.

Figure 13- DIAGRAM OF IMAGE INTENSIFIER



produces a beam of electrons directed toward the phosphor screen. On leaving the cathode, the electrons are accelerated by an electrostatic field, 15,000 volts, and focused on the phosphor screen which transforms the kinetic energy of the electron beam into visible light energy. This falls onto the photocathode of the next stage and this process is repeated. Each stage is linked by fiber optics and the final greatly intensified image is formed on the third phosphor screen, converted to visible light, and viewed through the eyepiece.

The brightness gain achievable with present low-light-level sensors, is in excess of 75,000. System brightness gain is defined as the ratio of the apparent brightness when looking through the system to the actual brightness of the scene when viewed by the eye. The principal advantages afforded by the use of image intensifiers are as follows:

(Soule 1968)

1. They permit the use of optical objectives that are much larger than the dark adapted eye without reduction of the angular field of view.
2. The best photocathode materials have quantum efficiencies (i.e., capability of converting photons into visible information) of about 0.20 for white light and thus improve on the eye which has a quantum efficiency of approximately 0.05.
3. Present photocathodes are sensitive to ultraviolet, visible, and near infrared radiation (i.e., radiation

in the wavelength band 300 to 1,000 nanometers).

4. Light output of the image tube is of sufficient intensity that when used with a TV pickup tube, such as the image orthicon, SEC vidicon, etc., high resolution video imagery can be obtained at low-scene illumination levels.

The performance of a low-light-level sensor is commonly expressed in terms of its dynamic or static resolution (i.e., minimum detail which can be detected or resolved) under given light-levels for a specified target contrast and reflectance. Sensor performance is governed or limited by the signal-to-noise, modulation transfer and gain. In addition to noise produced internally, statistical variations in the rate of arrival of photons at the photocathode produce a noisiness of the image which limits sensor performance (provided sufficient system gain is available) at the lowest light levels.

#### Bioluminescence Detection

Although no observations have been made to determine the intensity of the luminescence associated with a fish school or individual fish, the major factors affecting the intensity of the luminescence available at the surface for detection are known. These are: concentration of luminescing organisms, degree of agitation imparted by the fish to the water, transmission properties of the water and atmosphere, and reflection at the water/air interface. Detection of bioluminescence will

further depend upon its contrast or brightness relative to the ambient light reflected from the sea surface, which serves as a source of noise. It appears, therefore, that contrast and photon noise will be the major factors which limit the detection of fish-stimulated bioluminescence.

The limiting resolution of a low-light-level sensor due to the quantum nature of light, with given component performance characteristics, viewing a luminescent target of  $10^{-4} \mu\text{W}/\text{cm}^2$  intensity, at a depth of 5 meters in coastal oceanic waters, from an altitude of 1 km. under clear moonless sky conditions, may be determined from the following equations (Electro-Optics Handbook 1968):

$$\text{Equation (1)} \quad \frac{\text{line pairs}}{\text{picture width}} = \frac{3.1 w}{k} \sqrt{\frac{\beta t}{e}} \sqrt{\frac{|H_t - H_b|}{H_t + H_b}}$$

where:

w - picture width on photocathode, 80% of 80 mm

photocathode = 0.064 m

k - signal/noise factor = 5

$\beta$  - sensitivity of S-20 photocathode

t - integration time of eye = 0.2 second

e - charge on electron =  $1.6 \times 10^{-19}$  coulombs

$H_t$  - irradiance of target image on photocathode =

$3.02 \times 10^{-8} \text{ Wm}^{-2}$

$H_b$  - irradiance of background image on photocathode =

$3.3 \times 10^{-9} \text{ Wm}^{-2}$

The irradiance of target and background images on the photocathode is given by:

Equations (2a) 
$$H_b = \frac{H_s \rho_a T_a}{4 (T/no)^2 (m + 1)^2}$$

(2b) 
$$H_t = \frac{N T_a T_w (1 - \rho_w)}{4 (T/no)^2 (m + 1)^2}$$

where:

N - radiant emittance of target, assuming lambertian  
distribution =  $\frac{W}{\pi}$

m - size of image/size of object = 0 for distant objects

W - radiance of luminescent target =  $10^{-6} \text{ Wm}^{-2}$

$H_s$  - scene incident irradiance =  $10^{-6} \text{ Wm}^{-2} =$   
 $10^{-4} \text{ } \mu\text{W cm}^{-2} = 5 \times 10^{-5} \text{ ft. cd.}$

$\rho_a$  - radiant reflectance of sea surface = .04

$T/no = f/no / \sqrt{Tr} = 1.5$

$\rho_w$  - water to air reflectance coefficient = 0.02

$T_a$  - transmittance of atmosphere,

$e^{-\sigma h}$  where  $\sigma$  is attenuation coefficient  $\text{km}^{-1}$  and

h is altitude =  $e^{-(.3)(1)} = .75$

$T_w$  - transmittance of water =  $e^{-KD} = 0.37$

K - diffuse attenuation coefficient =  $0.20 \text{ m}^{-1}$  for coastal  
oceanic water

D - depth in meters = 5

Substituting in equations 2a and 2b gives:

$$H_b = \frac{(10^{-6} \text{ Wm}^{-2}) (0.04) (.75)}{4 (1.5)^2 (0 + 1)^2} = 3.3 \times 10^{-9} \text{ Wm}^{-2}$$

$$H_t = \frac{(10^{-6} \text{ Wm}^{-2}) (0.75) (.37) (0.98)}{4 (1.5)^2 (0 + 1)^2} = 3.02 \times 10^{-8} \text{ Wm}^{-2}$$

Substituting the values obtained for radiation incident on the photocathode from target and background into equation (1):

$$\begin{aligned} \frac{\text{line pairs}}{\text{picture width}} &= \frac{(3.1)(0.064)}{5} \sqrt{\frac{(0.05)(0.2)}{1.6 \times 10^{-19}}} \sqrt{\frac{3.02 \times 10^{-8} - 3.3 \times 10^{-9}}{3.02 \times 10^{-8} + 3.3 \times 10^{-9}}} \\ &= (3.97 \times 10^2) (2.5 \times 10^8) (1.47 \times 10^{-4}) \\ &= 1,459 \end{aligned}$$

This is equivalent to approximately 4,000 TV lines resolution assuming 1 line pair =  $2/\sqrt{2}$  TV lines (Jensen 1968).

In present day low-light-level sensors, particularly low-light-level TV, the resolution obtainable at the light level considered is an order of magnitude or more less than the theoretical photon noise limit. This is due primarily to noise produced within the system and loss of contrast due to aberrations in the optical components of the system. It is significant, however, that photon-noise does not appear to be a factor which will seriously limit the detection of bioluminescence under these assumed conditions.

However, sufficient contrast must exist between the target (luminescent school) and background (water) in order for the target to be detectable. If it is assumed that a target with an intensity equal to that of the background can be detected, i.e., the intensities are additive and produce a signal/noise ratio of two, then the depth beyond which the luminescent signal would be attenuated to a level which would render it undetectable may be calculated as follows:

$$H_s \rho_a = W T_w$$

substituting the assumed values into the above equation:

$$(10^{-6}) (.04) = (10^{-6}) (e^{-.2D})$$

and solving for depth gives:

$D = 16.07$  meters; maximum depth at which the luminescent school could be detected from the background. It would appear, therefore, that the use of low-light-level sensors to detect fish stimulated bioluminescence has some potential application in fisheries. It should be pointed out, however, that present knowledge of the concentration and abundance of luminescent plankton is extremely limited. Also, data relating the intensity of the luminescence associated with a fish or fish school to the concentration of luminescent organisms, are not available. These data are needed however, to determine the potential of this method.

### LASERS

The preceding discussion has dealt with some of the sensors which have been shown, from previous research, to have potential application in fisheries. There are also other sensors which appear to have application, although no fisheries research has been conducted to date to investigate their potential.

One of the most promising is the laser. In recent months, neon and frequency doubled Yttrium Aluminum Garnet (Double YAG) lasers have been used as airborne bathymetric sensors in water depths greater than 250 feet (Hickman, et al, 1969, and Cunningham, 1970). Lasers have also been employed to measure wave-height (Kirk, 1967; Ross, et al, 1968) with accuracies on the order of inches.

Lasers may be divided into two major categories according to their mode of operation: 1) pulsed and 2) continuous wave. Only pulsed lasers have been used in the bathymetry and wave-height studies conducted to date. Aircraft altitude and wave-height information is obtained by measuring the time difference between transmission of the laser pulse and its reflection, back into the receiver by the surface. Water depth is obtained by measuring the time difference between the energy reflected from the surface and the sea floor.

The neon and Double YAG Lasers operate in the "oceanic window" at wavelengths of 540.1 nm and 530 nm, respectively. This and other characteristics of these sensors, such as: 1) peak pulse power of up to 30 kw; 2) narrow, three nanosecond, pulse width; and 3) pulse rates up to 1,000 pulses per second (Hickman et al, 1969), make these lasers well suited for application in fisheries and oceanography.

Some of the major parameters affecting the performance of a laser system, are: 1) power output; 2) transmission of the intervening medium (water and atmosphere); 3) surface reflectivity; 4) target reflectivity; and 5) sensitivity of the receiver to the reflected energy. The output of the neon laser, up to 30 kw, should provide sufficient power to penetrate that portion of the water column, i.e., euphotic zone, wherein the greatest concentration of fish occur. Surface reflections which tend to saturate the receiver, can be overcome through the use of spatial filters,

or gating techniques. The reflectance of those species measured in the spectro-photometric study referred to above, ranged from 3 - 9% in the wavelength band of interest, whereas the reflectance of sea water varies from approximately .3 to 3%. This difference in reflectivity, and the other factors considered, contribute to the potential of pulsed lasers as fish detection devices.

There are also other techniques which, to the author's knowledge, have not been applied but appear to offer considerable potential in fishery and subsurface target detection problems. One approach is the use of a continuous wave laser with an optical system designed to provide a raster scan of a large area along the aircraft track. Elimination of surface reflection and maximum depth penetration, could be achieved by employing certain polarization and "look" angle techniques. Another approach to consider is the use of a laser operating at the wavelength of a Fraunhofer line in the "oceanic window". This should provide maximum signal/noise ratio, and thus the greatest depth penetration during day or night operations, with minimum power output.

Although present lasers are limited due to their optical inefficiency, short operating life, and high costs, it is anticipated that these devices will be used extensively in the future. It is expected that future laser systems will provide near synoptic information on sea state, coastal bathymetry, plankton concentration, and abundance and distribution of harvestable fish stocks over large oceanic areas.



### CONCLUSIONS

The present state-of-the-art in sensor technology is such that only those sensors which operate in the visible and infrared portions of the spectrum have been used successfully from space; however, satellite generated thermal, and visual imagery of the sea surface can provide valuable information on large scale phenomena of significance to fisheries. This information can serve to delineate areas of upwelling, major current boundaries and other surface features which could then be "looked" at in greater detail with instrumented aircraft. Aircraft could provide operational information to the fleet on the abundance and distribution of the resources in a given area. Such data would also serve to validate fishery models developed to provide forecasts of the future abundance and distribution of fish stocks.

It can be stated that remote sensing from aerospace platforms will play a significant role in the future exploration, utilization and management of the living resources of the sea.

# REFERENCES

- AEROSPACE SYSTEMS DIVISION, RCA, Burlington, Massachusetts -  
Electro-Optics Handbook (1968)
- BITYUKOV, E. P., RYBASOV, V. P. and SHAIDA, V. G. -  
 "Annual Variations of the Bioluminescence Field Intensity in the  
 Neritic Zone of the Black Sea"  
 Institute of Oceanography, USSR Academy of Sciences (1967)
- CLARKE and BRESTLAU  
 "Studies of Luminescent Flashing in Phosphorescent Bay, Puerto  
 Rico, and in the Gulf of Naples using a Portable Bathyphotometer"  
 Bull. Inst. Oceanogr., Monaco, No. 1171, 4 Mars 1960
- CLARKE, G. L. and BACKUS, R. H.  
 "Measurements of Light Penetration in Relation to Vertical Migration  
 and Records of Luminescence of Deep Sea Animals"  
 Deep-Sea Res., 4, Pages 1-14 (1956)
- CLARKE, G. L. and DENTON, E. J.  
 "Light and Animal Life"  
 The Sea, Vol. 1, Editor M. N. Hill, Wiley & Sons, Inc. New York
- CLARKE, G. L., EWING, G. C. and LORENZEN, C. J.  
 "Remote Measurement of Ocean Color as an Index of Biological  
 Productivity"  
 Proceedings of the 6th International Symposium on Remote Sensing  
 of Environment, Vol. 11, Willow Run Laboratories, University of  
 Michigan (1969)
- CLARKE, G. L. and HUBBARD, C. J.  
 "Quantitative Records of Luminescent Flashing of Oceanic Animals at  
 Great Depths"  
 Limnology and Oceanography, 4, Pages 163-180 (1959)
- CLARKE, G. L. and KELLY, M. G.  
 "Measurements of Diurnal Changes in Bioluminescence from the Sea  
 Surface to 2000 Meters Using a New Photometric Device"  
 Limnol. Oceanog., 10 (Suppl.); R54-R-66 (1965)
- CUNNINGHAM, L. L.  
 Personal Communication (1970)
- DEFANT, A.  
Physical Oceanography, Vol. 1, Pergamon Press, London, England (1961)
- DORSEY, N. E.  
Properties of Ordinary Water-Substance  
 Reinhold Publishing Corporation, New York, N. Y. (1940)

DRENNAN, K. L.

"An Investigation of Sea Surface Temperature Patterns in the Gulf of Mexico as Determined by an Airborne Infrared Sensor"

Reference 67-0-1, Gulf South Research Institute, New Iberia, Louisiana, Unpublished (1967)

DRENNAN, K. L.

"Airborne Measurements of Infrared Sea Temperature in the Northern Gulf of Mexico"

Technical Report #2, Gulf Coast Research Laboratory, Ocean Springs, Mississippi, Unpublished (1966)

DRENNAN, K. L.

"Fishery Oceanography from Space"

Proceedings 6th Space Congress, Cocoa Beach, Florida, March 17-19, 1969. Edited by L. E. Jones III, printed by Brevard Printing Co., Cocoa Beach, Florida

HELA, I. and LAEVASTU, T. (Editors)

Fisheries Oceanography Fishing News (Books) Ltd.

London, E. C. 4, England (1970)

HICKMAN, G. D., HOGG, J. E., SPADARO, A. R. and FELSCHER, M.

"The Airborne Pulsed Neon Blue-Green Laser: A New Oceanographic Remote Sensing Device"

Proceedings of 6th International Symposium on Remote Sensing of Environment, Vol. II, University of Michigan, Ann Arbor, Michigan (1969)

JENSEN, N.

Optical and Photographic Reconnaissance Systems

John Wiley and Sons, Inc., New York (1968)

KELLY, M. G.

"The Occurrence of Dinoflagellates at Woods Hole"

The Biological Bulletin, Vol. 135 No. 2, Pages 279-295, Oct. (1968)

KIRK, R. L.

"Ocean Surface Environmental Definition Utilizing Laser Techniques"

IEEE Intern. Conv. Record Part A, Mar. 20-23 (1967)

LANKES, L. R.

Optics and the Physical Parameters of the Sea. Optical Spectra.

Volume II (1969)

LINDNER, M. J. and BAILEY, J. S.

"Distribution of Brown Shrimp (*Penaeus aztecus*

*aztecus* IVES) as Related to Turbid Water Photographed from Space"

Fishery Bulletin, Vol. 67 No. 2 (1968)

NORTON, V. J.

"Some Potential Benefits to Commercial Fishing Through Increased Search Efficiency - A Case Study: The Tuna Industry"  
University of Rhode Island, Kingston, Rhode Island (1969)

PANEL 5 of SUMMER STUDY ON SPACE APPLICATIONS

"Useful Applications of Earth-Oriented Satellites"  
National Academy of Sciences (1969)

ROSS, D. B., JR., PELOQUIN, R. A. and SHIEL, R. J.

"Observing Ocean Waves with a Helium-Neon Laser"  
5th U. S. Navy Symp. Mil. Oceanog., May 1-3 (1968)

SANTA BARBARA RESEARCH CENTER, Goleta, California

SBRC Wall Chart 3M 67 (1967)

SOULE, H. V.

Electro-Optical Photography at Low Illumination Levels  
John Wiley and Sons, Inc., New York (1968)

STAPLES, R. F.

"The Distribution and Characteristics of Surface Bioluminescence in the Oceans"  
Technical Report, U. S. Naval Oceanographic Office, Washington, D. C.  
Tr. - 184 (1966)

STEVENSON, R. E.

"A Real-Time Fisheries Satellite System"  
Proceedings 6th Space Congress, Cocoa Beach, Florida March 17-19, 1969  
Volume II edited by L. E. Jones III, printed by Brevard Printing Co.,  
Cocoa Beach, Florida

STEVENSON, R. E.

"The Oceans, an Overview Regarding the Commercial Utilization of Space, in Commercial Utilization of Space"  
Edited by J. R. Gilmer, A. M. Mayo, R. C. Peavey  
American Astronautical Society, Washington (Advances in Astronautical Sciences, Volume 23) Abstract Pages 196-197 (1967)

# REMOTE SPECTROGRAPHY OF OCEAN COLOR AS AN

## INDEX OF BIOLOGICAL ACTIVITY

Gifford C. Ewing

Woods Hole Oceanographic Institution

Woods Hole, Massachusetts

### ABSTRACT

Over 3,000 ocean spectra of sunlight backscattered from the upper layers of the sea have been obtained at flight altitudes to 10,000 feet together with detailed ground truth. The backscattered light in each part of the visible spectrum has been calculated as a percentage of the incident downwelling irradiance at the sea surface. The spectrum thus obtained reveals the action of the water itself and of materials (living and non-living) suspended and dissolved in the water. The relationship between light extinction and biological productivity has been studied by Dr. Carl J. Lorenzen. Certain important materials such as chlorophyll have recognizable spectral signatures; thus the shape of the spectrum can be used to measure the kinds and amounts of substances present. Although the shape of the spectra changed characteristically with altitudes, the differences between members of each pair and their contrast ratio remained nearly the same and clearly showed the location of the transition. It is expected that further analyses of curves of this type will enable us to recognize changes in the spectra due to other important materials in the water, including pollutants.

Except for local disturbances, the upper layers of the open ocean are thermally stratified. As a consequence, nutrients become exhausted biologically, leaving the water sterile and blue in color. Where the stratification is overturned by currents or storms, nutrients and cold water are returned to the euphotic layers where photosynthesis renews biological activity, producing an accumulation of chlorophyll and related biochromes. Such accumulations can conveniently be qualitatively assessed by measurement of chlorophyll a concentration although quantitative inferences as to the relative amounts of biochemicals present may be unwarranted. In highly productive areas, freshly upwelled water is initially cold and clear, gradually warming and turning greenish with increased surface age. Thus young surface water is characterized by cold and blueness; water of intermediate age is greenish; and aged surface water is blue without noticeable thermal contrast with surrounding water. As the thermal contrast fades out, color contrast increases for a time and then gradually disappears. Thus simultaneous remote sensing of ocean color and relative surface temperature is a convenient index of the surface age of water and hence of its biological state. In some areas typified by Georges Bank off the coast of Massachusetts, the upwelling is caused by local mixing, and the three processes occur simultaneously and nearly indistinguishably. In other areas, notably along the Peruvian coast, these processes are separated in space by the action of the Peru Current so that the three stages of the upwelling cycle are readily distinguishable. In such regions, young water shows positive correlation between color and chlorophyll whereas older stages show negative correlation.

Equipment for measuring meaningful thermal anomalies of the sea surface temperature is readily available and has been used extensively over the last two

decades from low-flying aircraft. Extensive programs of airborne thermal reconnaissance have been conducted on both coasts of the United States notably by the U.S. Naval Oceanographic Office, the Bureau of Sports Fishing and Wild Life and, more recently, by the U.S. Coast Guard. Attempts to apply this technique to satellite surveillance have met with considerable success in viewing such phenomena as the Gulf Stream and other boundary currents. In other areas where the temperature contrasts are less pronounced, this method is subject to uncertainties caused by clouds and haze. This type of environmental "noise" can, to a certain extent, be dealt with by repetitive sampling although such methods always lose acuity both in regard to space and time variation (LaViolette and Chabot) (Ref. 1).

The color of the ocean associated with thermal changes has been measured by instruments of various degrees of sophistication. Where the chlorophyll concentrations are high (of the order of tens of mgs. per cubic meter) color effects are sufficiently strong to be readily observed by eye, giving rise to such common names as the Yellow Sea and the Red Sea. Attempts to monitor ocean water masses and their biological condition by direct color observation from the air have been made since the early advent of aircraft. A well documented correlation between ocean water color and the comparative distribution of two species of *Sagitta* was carried out by Alister Hardy in 1923 (Ref. 2).

In subsequent years the color of the sea has been remotely sensed by means of more elaborate methods of which spectrometry yields the most easily quantified results. In 1961 Strickland conducted airborne observations in Georgia Strait using a tri-color, hand-held photoelectric device (Strickland) (Ref. 3).

During the summers of 1967 and '68, measurements of water color were made from the Woods Hole research aircraft by Prof. George L. Clarke and the author simultaneously with shipboard measurements of chlorophyll concentrations made by Carl J. Lorenzen (Ref. 4). These measurements were made at flight levels from 500 ft. to 10,000 ft. using a spectrometer designed by Peter White of TRW Systems, Inc. and described by L. A. Gore (Ref. 5). R. C. Ramsey of TRW operated the instrument and took part in the reduction of the data and in the interpretation of the results.

The TRW spectrometer is an electroptical sensor of the off-plane Ebert type with an RCA 7265 (S-20 response) photomultiplier. The spectral range is 400 to 700 nm with a spectral resolution of 5 to 7.5 nm, a scan time of 1.2 seconds, and a field of view of  $3^\circ$  by  $0.5^\circ$ . A continuous curve of the spectrum is provided by a Sanborn recorder for each scan. The spectrum of the incident light from the sun and sky was determined before and after each series of measurements by recording the light reflected from a horizontally placed Eastman Kodak "gray card" with a nonselective reflectivity of 18 percent. The ratio of light scattered by the sea was compared to that from the gray card to determine their relative reflectance. A series of tests made to detect changes in the spectral distribution of incident light during the three hours before and after noon due to changes in the sun's altitude and to changes in sky conditions from clear to light cloudiness showed that the changes found were not great enough to affect significantly our investigation of the differences in backscattered light from the ocean.

This work showed that large differences in the spectral characteristic of the upward scattered light of the sea surface are easily detected from low-flying aircraft and are associated with chlorophyll distribution in such a way that the blueness of the light (as shown by the mean square slope of the reflectance spectrum) is strongly correlated with the absence of chlorophyll in the water. This effect is illustrated in Figure 1 which shows that with increasing concentrations of chlorophyll the energy in the blue region of the spectrum decreased markedly whereas the energy at longer wavelengths tended to increase. These effects can be explained by the well-known absorption of chlorophyll a which is particularly high in the blue (Yentsch) (Ref. 6).

During the summer of 1969 we concentrated our investigations on a region close to Georges Bank where a sharp temperature and color front persisted for several weeks (Figure 2). The warm side of this front in the slope water had an average temperature of  $25.3^\circ\text{C}$  and a chlorophyll content of  $0.07\text{ mg/m}^3$ . The warm inshore side of the front had an average temperature of  $19.5^\circ\text{C}$ , and a chlorophyll content of  $0.21\text{ mg/m}^3$ . Twenty pairs of spectra were taken on either side of this front from August 21-27 at flight altitudes of from 500 to 10,000 ft. In every case the spectra unambiguously differentiated the two water masses. Examples are shown in

Figures 3 and 4. Comparison of the two figures shows that with increased altitude, the percentage of blue light increased markedly relative to red light. However, Figure 5 shows that the difference in radiance was relatively insensitive to increased altitude.

It is concluded from this work that the spectral characteristics of light scattered upward from underneath the ocean surface is strongly affected by the presence of biochromes such as are found in the upper sea and that these differences are easily detectable under clear sky conditions at altitudes up to 10,000 ft. Since the layer below 10,000 ft. represents approximately  $1/4$  of the total atmosphere in terms of mass, and since this layer is the most variable in composition, it seems probable that color differences, even for these small concentration differences, will be detectable at satellite altitudes. For larger concentrations it is well established by numerous photographs taken by GEMINI and APOLLO astronauts that color differences are readily observable (Ref. 7).

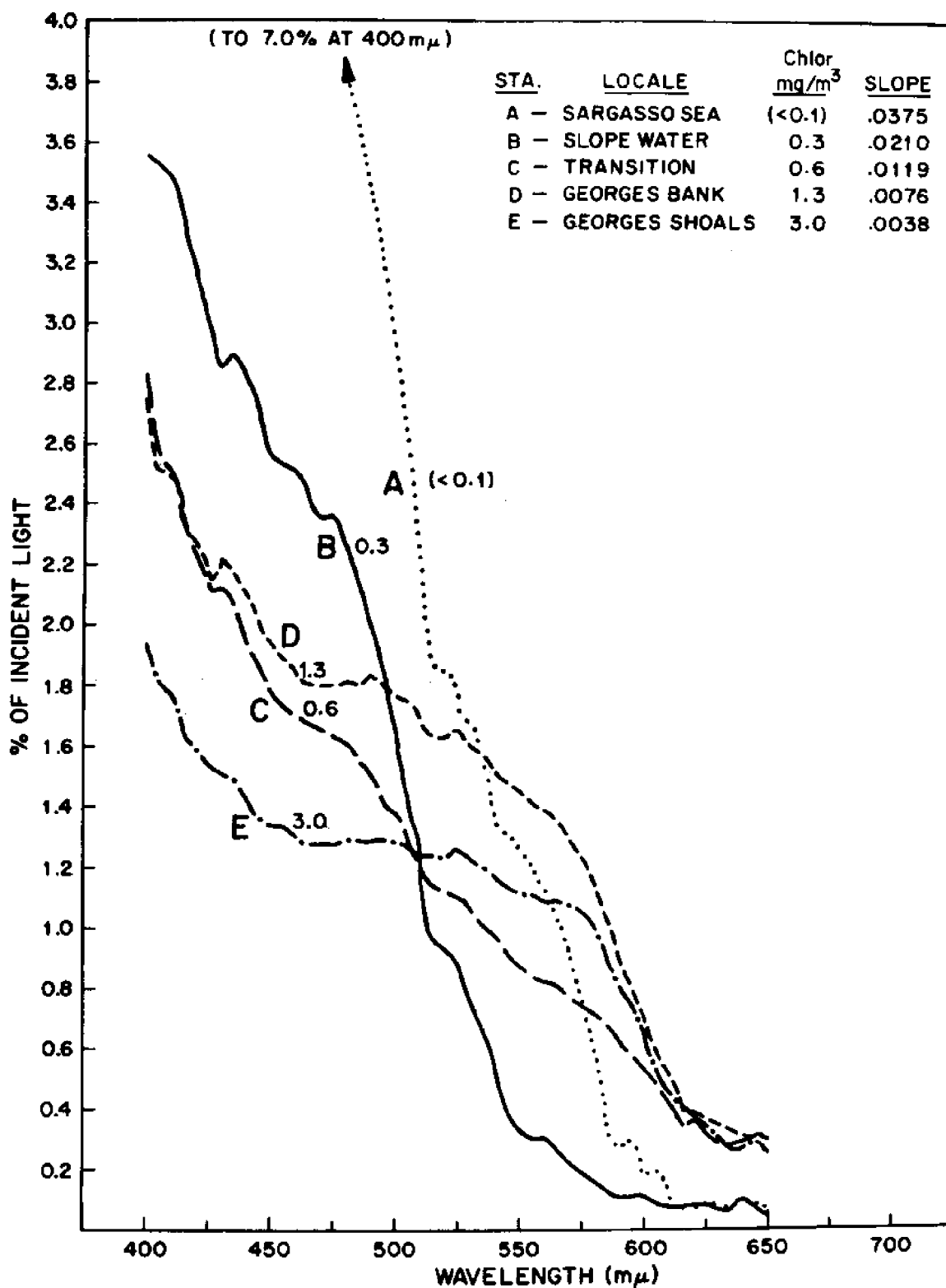


FIGURE 1. Spectra of backscattered light measured from the aircraft at 305 m on 27 Aug. 1968 at the following stations (Fig. 2) and times (all E.D.T.): Station A, 1238 hours; Station B, 1421 hours; Station C, 1428.5 hours; Station D, 1445 hours; Station E, 1315 hours. The spectrometer with polarizing filter was mounted at 53° tilt and directed away from the sun. Concentrations of chlorophyll a were measured from shipboard as follows: on 27 Aug., Station A, 1238 hours; on 28 Aug., Station B, 0600 hours; Station C, 0730 hours; Station D, 1230 hours.



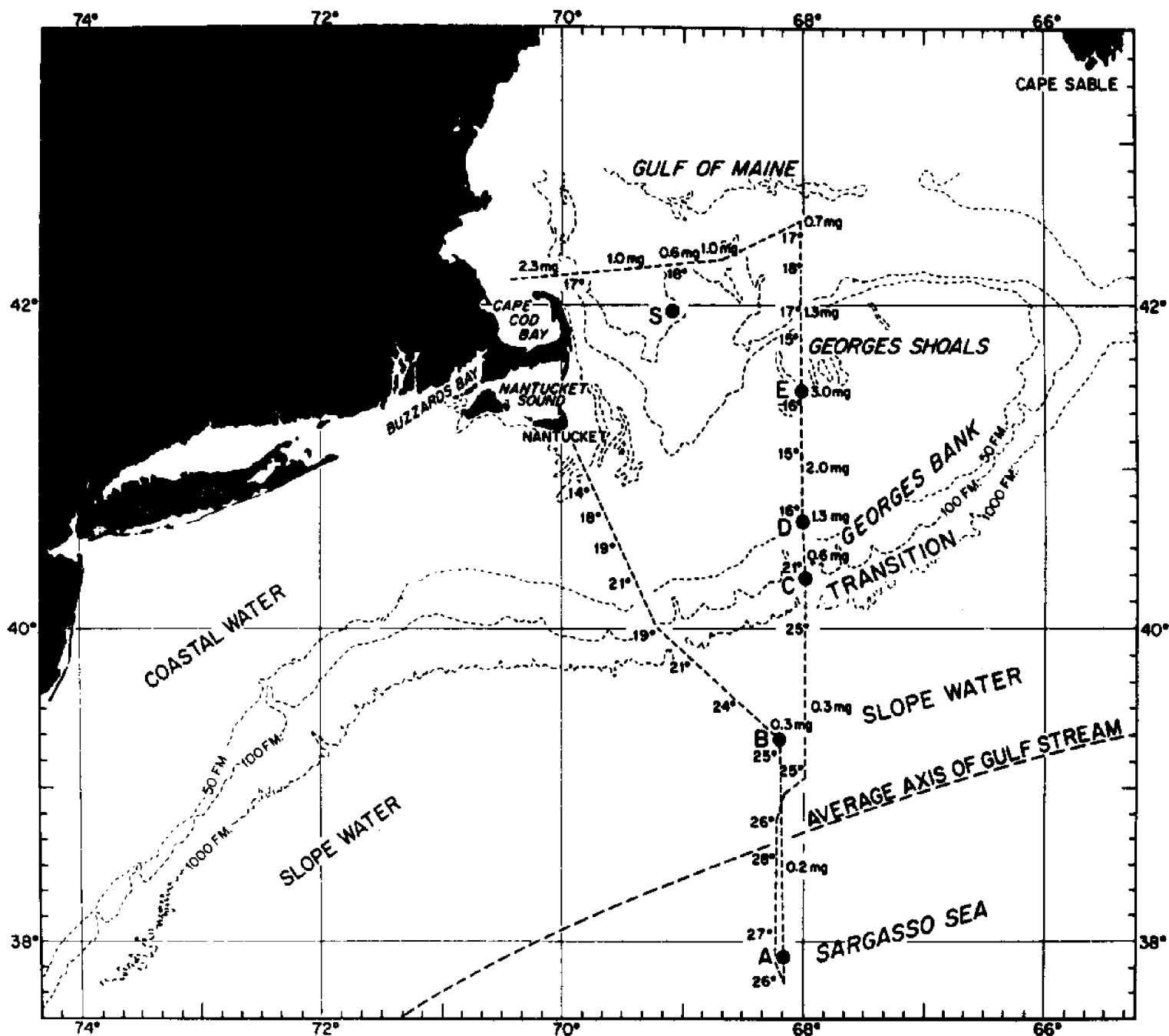


FIGURE 2. The flight of the aircraft after leaving Nantucket on 27 Aug. 1968 and the location of Stations A to E. Station S was occupied on 26 Aug. Representative temperatures measured from the aircraft flying at 305 m are shown to the left or below the flight path; representative chlorophyll concentrations in milligrams per cubic meter measured from the surface ship are shown to the right or above the flight path.

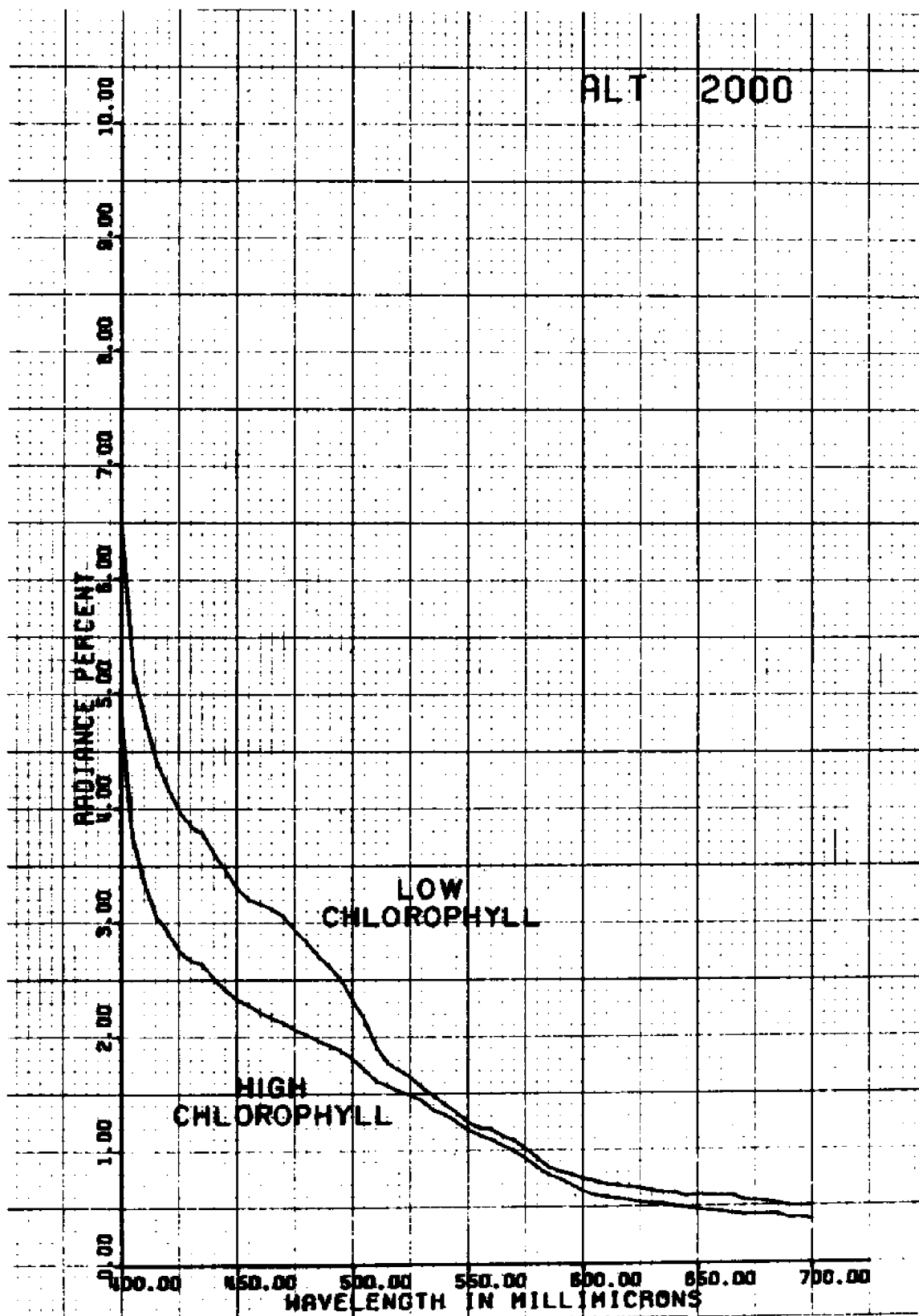


FIGURE 3. Spectra of sunlight backscattered from chlorophyll-rich and chlorophyll-poor areas at 2,000 feet flight altitude.

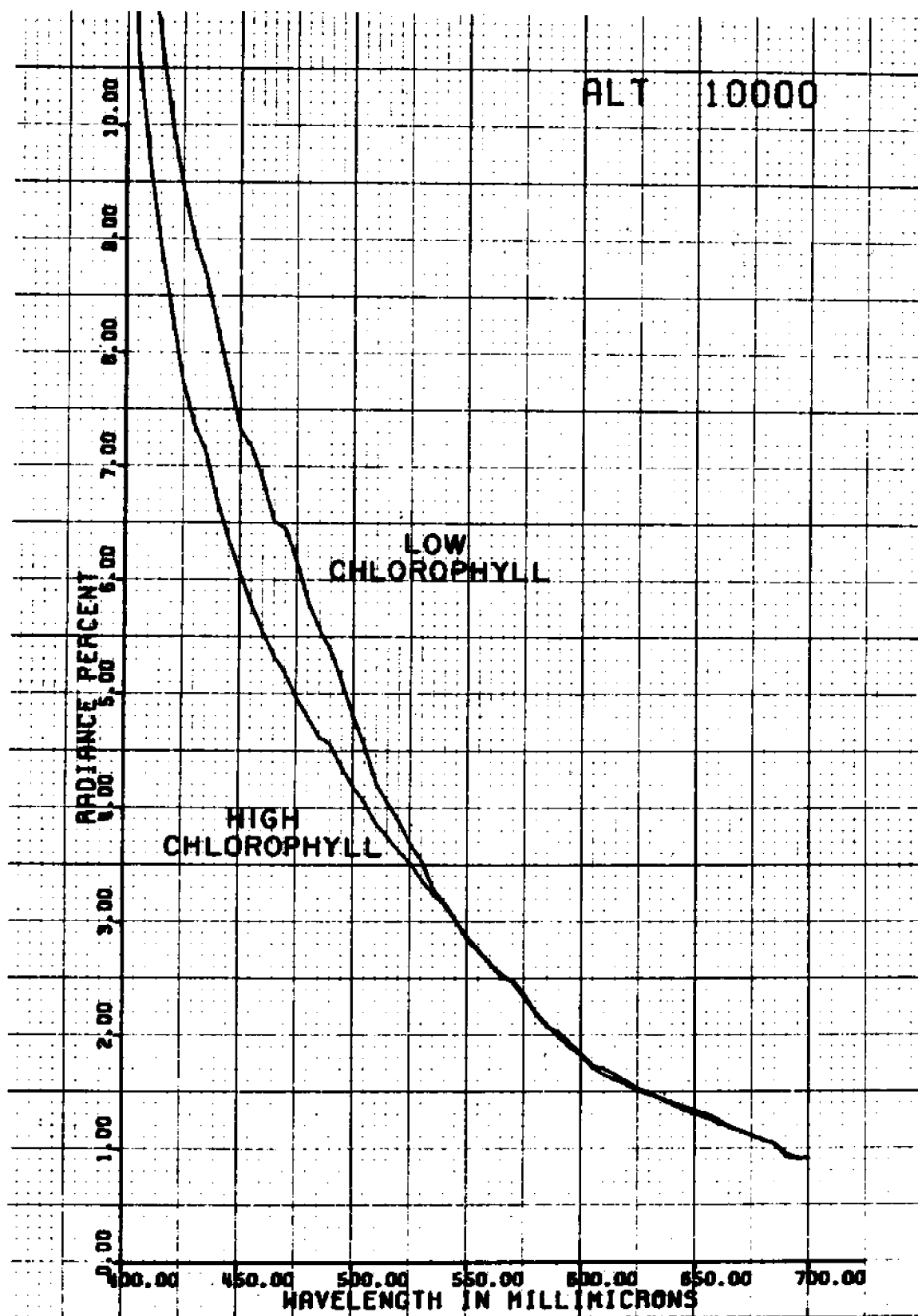


FIGURE 4. Spectra of sunlight backscattered from chlorophyll-rich and chlorophyll-poor areas at 10,000 feet flight altitude.

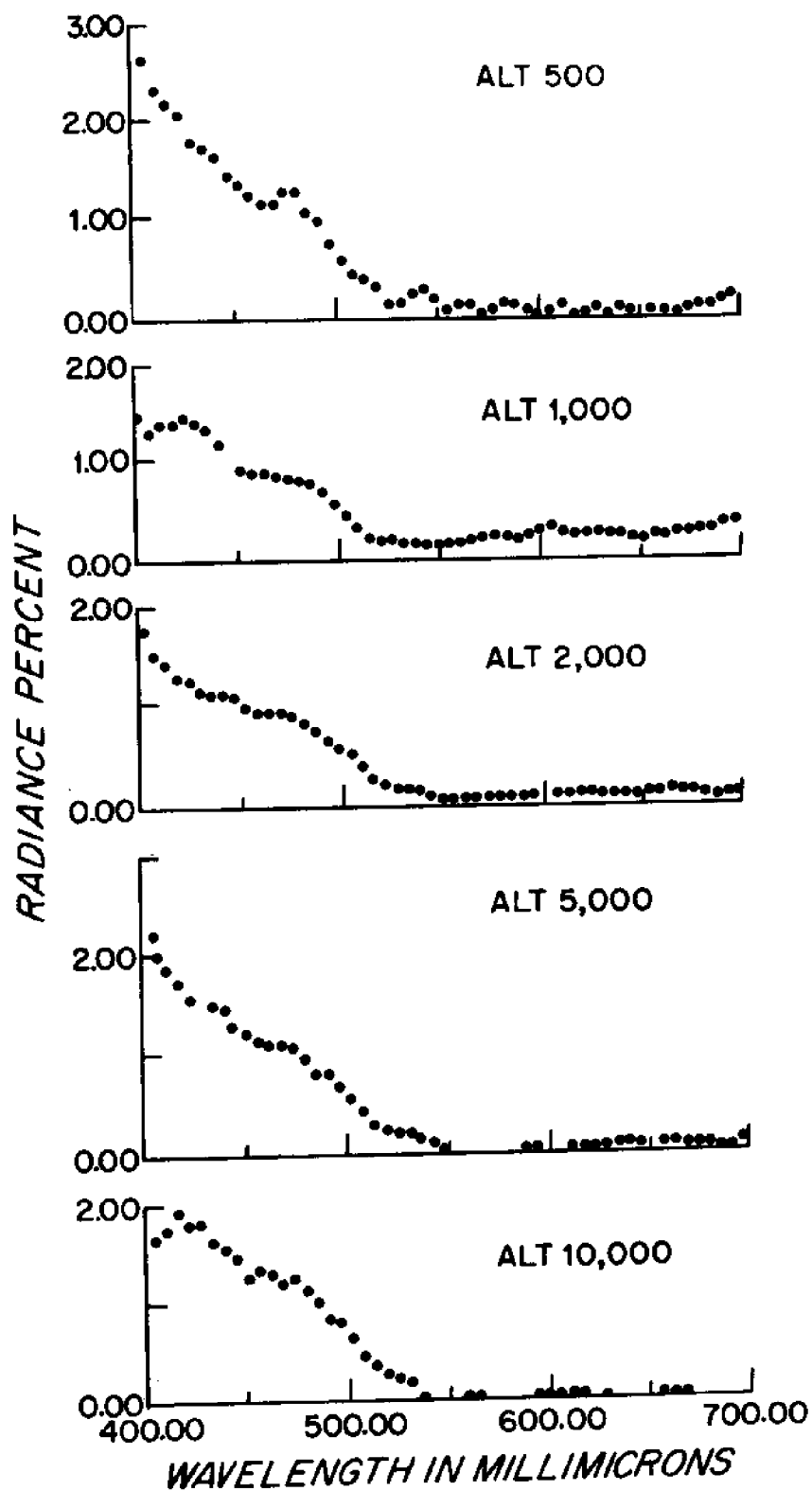


FIGURE 5. Differences in radiance percent between spectra taken at various altitudes over areas of low and high chlorophyll concentration.

## References

1. LaViolette, Paul E. and Paul L. Chabot. A Method of Eliminating Cloud Interference in Satellite Studies of Sea Surface Temperatures. Deep Sea Research, Vol. 16, November 1969.
2. Hardy, Alister C. The Open Sea--Its Natural History: The World of Plankton. Collins, London, England, 1956.
3. Strickland, J. D. H. The Estimation of Suspended Matter in Sea Water from the Air. In Ms. Rep. Ser. (Oceanogr. Limnol.) No. 88 (Fisheries Research Board of Canada, 1967).
4. Clarke, George L., Gifford C. Ewing and Carl J. Lorenzen. Spectra of Back-scattered Light from the Sea Obtained from Aircraft as a Measure of Chlorophyll Concentration. Science, Vol. 167, No. 3921, pp. 1119-1121, 20 Feb. 1970.
5. Gore, L. A. Unpublished report (Electronic Systems Division, TRW Systems, Inc., 1968).
6. Yentsch, C. S. The Influence of phytoplankton pigments on the colour of sea water. Deep Sea Research, Vol. 7, pp. 1-9, 1960.
7. Ewing, G. C. et al. The Color of the Sea, in Oceans from Space, edited by P. C. Badgley, L. Miloy and L. Childs, Gulf Pub. Co., Houston, Tex., pp. 46-49, 1969.
8. The Color of the Ocean, report of conference sponsored by NASA, held at Woods Hole, Ma., Aug. 5-6, 1969.
9. Jerlov, N. G. Optical Oceanography. Elsevier Pub. Co., Amsterdam, the Netherlands, 1968.

THE ABSORPTION AND FLUORESCENCE CHARACTERISTICS  
OF BIOCHEMICAL SUBSTANCES IN NATURAL WATERS

By

Charles S. Yentsch  
University of Massachusetts  
MARINE STATION  
Gloucester, Massachusetts

INTRODUCTION

One aspect of the studies in oceanography has concentrated on the distribution, chemical characteristics and biochemical cycling of particulate organic matter. It is natural that these interests would feed back into the area of remote sensing of the oceans since much of the research has concentrated on light absorption and fluorescence of particulate and dissolved organic matter.

This report reviews the major factors known to selectively transmit or remove wavelengths of visible light in ocean waters. It discusses the prime substances affecting light absorption and fluorescence, and what environmental factors alter their distribution and abundance. The report suggests problems where remote sensing would be invaluable.

FACTORS AFFECTING THE SPECTRAL DEFINITION OF LIGHT IN  
NATURAL WATERS

I shall confine the discussion mostly to the type of remote measurement where visual daylight returning from

the water column is viewed by an airborne detector, and light scattered from the surface of the water is excluded from detection. The light returning from the water column is frequently termed backscattered ( $I_B$ ) and is mostly a small component, that is, the backward component ( $I_S'$ ), of the total volume scattered. The detector would also see light produced by the emission from fluorescence and bioluminescence. Therefore in daylight,

$$(1) \quad I_B = I_S' + E$$

In daylight the measurement of  $I_B$  must take into account the amount of light ( $I_O$ ) entering the water.  $I_B$  as a percentage of the total light or any wavelength can be expressed

$$(2) \quad I_B\% = \frac{I_S' + E}{I_O} (100)$$

In most cases the magnitude of  $E$  is much smaller than  $I_S'$ . The scattered light  $I_S'$  is equal to the incident incoming light minus that absorbed  $I_a$ ,

$$(3) \quad I_S' = I_O - I_a$$

This then allows us to look empirically at the absorption factors modifying the wavelength characteristics of  $I_S'$ .

The absorption factors are,

$$(4) \quad I_a = I_{a,w} + I_{a,p} + I_{a,c}$$

where,  $I_{a,w}$  is light absorbed by water,  $I_{a,p}$  is light absorbed by particles and  $I_{a,c}$  is light absorbed by dissolved yellow materials (Gelbstoff).

In the open ocean the dominant absorber is the water, the other two terms are small by comparison. But, the situation changes in coastal waters. They are generally more productive, hence absorption by photosynthetic pigments and dissolved organics more abundant.

If spectral definition  $\frac{d_B}{d_\lambda}$  is defined as the rate of change in  $I_B$  for wavelengths throughout the visible region, then the rate is proportional upon the ratio of scattered to absorbed light,

$$(5) \quad \frac{d_B}{d_\lambda} \approx \frac{I_{a,w} + I_{a,p} + I_{a,c}}{I_s}$$

Since scattering is not wavelength selective because the particles are too large, spectral definitions will be small when the ratio approaches or is slightly less than one. Since  $(I_{a,w})$  is a constant for all waters, it is  $I_{a,p} + I_{a,c}$  that will greatly influence spectral definition. Spectral definition would be expected to be high, i.e. a low ratio in productive coastal waters. Spectral definition will be low, i.e. high ratios in open ocean situations.



# INFLUENCE OF REFLECTION FROM THE BOTTOM IN SHALLOW WATER

Many of the observations made remotely from the air will be in shallow waters where the bottom reflection of the light will constitute a sizeable signal. There is no easy means of predicting, primarily because of the wide variety of bottom absorbing materials associated with shallow waters. If the bottom has no absorptive characteristics, then the overall influence is to increase the term  $I_S'$  in Equation 4.

If we take the simplest case where incident light entering the water and reflecting from the bottom is treated as parallel light, then  $I_B$  becomes equal to

$$(6) \quad I_O - (A_{\uparrow w} + A_b + A_{\downarrow w})$$

where  $(A_{\uparrow w})$  represents the attenuation\* of light in the water column, and  $A_b$  is the attenuation by the bottom.

Since the length of the light path is the depth of the water column (L) then,

$$(7) \quad I_B = I_O - \{L(\ln I_O - \ln I_L) + A_b + L(\ln I_R - \ln I_B)\}$$

The attenuation of the light striking the bottom ( $I_L$ ) is equal to  $I_L - I_R$ , the latter is the portion of the incident light reflected from the bottom, thus

---

\* attenuation = absorption + scattering

$$(8) \quad I_B = I_O - \{L(\ln I_O - \ln I_L) + (I_L - I_R) + \\ L(\ln I_R - \ln I_B)\}$$

This equation points out that the percentage of back-scattered light from the bottom will decrease linearly with depth. The rate of decrease will be dependent upon the attenuation coefficient of the water column. The attenuation due to the bottom does not affect the rate of decrease of  $I_B$  with depth. It does, however, influence the total amount of light reflected.

To test this model we have made measurements of  $I_B$  at different water depths over white, highly reflecting calcium carbonate sands off Bimini in the Bahamas. At specific depths the photometer (visual spectral sensitivity) first measured  $I_O$  then  $I_S' + E$ .  $I_B(\%)$  plotted against water depth is shown in Figure 1. Also included in the figure is the theoretical relationship between  $I_B$  and depth using Equation 8. The observations agree with the theoretical model for shallow depths. One can say that treating the situation in terms of parallel light parameters is justified. However, at depths of 20 meters it becomes obvious that the returning light, now mostly  $I_S'$ , does not fit the parallel theory. Or in other words,  $I_S'$  is a phenomenon of multiple scattering. Also included in Figure 1 are percentages of  $I_B$  measured at different depths over

bottom covered with coral and algae. Differences between the reflectance is apparent.

In remote sensing, bottom reflection in clear water is a factor to be reckoned with. It argues that when information on suspended particulate matter is desired, some sort of reference point is needed to cancel out the bottom reflection.

#### SUBSTANCES WHICH ABSORB LIGHT IN NATURAL WATERS

The foregoing discussion was confined to an empirical discussion of factors which alter the attenuation of visible light in natural waters. It was demonstrated that spectral definition, that is, a change in signal per unit wavelength would be dependent upon the absorbing factors in waters. Let us now examine the specific absorbers. Figure 2 summarizes these. In addition to the spectrum for water absorption, the figure includes spectra for different members of phytoplankton commonly found in natural waters. The absorption is due to the photosynthetic pigments. In the red region of the spectrum peaking around 675 nanometers, the prominent absorber is chlorophyll a. This pigment is found in all photosynthetic algae and plants. The spectra of brown and green algae are similar with the exception that the brown algae tend to absorb light at longer wavelengths in the middle portion of the spectrum. This is because of the carotenoid fucoxanthin, which is another

photosynthetic pigment. Red and blue-green algae also have pigments that absorb in the middle portion of the spectrum. These pigments are called phycobilins and are used as the taxonomic distinction for algae into these groups. At times it is these pigments that are responsible for "red water".

The visible absorption of Gelbstoff is due to a strong absorption in the ultraviolet which tails into the visible portion of the spectrum. The distinction between this absorber and the phytoplankton is that Gelbstoff is mostly in the dissolved state. Varying concentrations of Gelbstoff can greatly change water color, its "tail" absorption is in the window of maximum transmission of water. Increasing concentrations of Gelbstoff shifts the peak transmission (minimum absorption) from short to long wavelengths.

There have been very few measurements of the transmission and absorption characteristics of naturally occurring particulate matter collected from oceans and lakes. However, in the case of the measurements made in the oceans, the attenuation spectrum clearly reveals the strong absorption band of chlorophyll a. In general one can say that the spectra tend to reflect that of brown algae in general (Yentsch, 1960). This is due to the fact that the principal members of the phytoplankton community are diatoms and dinoflagellates which in a general sense are classified

as brown algae. In summary, the principal absorbers are the pigments of the photosynthetic algae and the yellow dissolved organic material called Gelbstoff. Both of these substances strongly absorb in the region where light is transmitted most readily. Hence increasing or decreasing concentration greatly influences the color of natural waters.

#### SPECTRAL CHARACTERISTICS OF EMISSIONS FROM NATURAL WATER

In an earlier section of this report it was emphasized that emissions from fluorescence and bioluminescence were much weaker than daylight scattered out of the water column. This however, does not mean that these emitted radiations cannot be useful for remote sensing. Indeed they have an advantage. For example, in the case of fluorescence if the proper excitation wavelength is used, the emission can be quite specific for individual compounds.

Figure 3 shows the excitation and emission characteristics for substances. Most of the phytoplankton algae have a fluorescence emission at 685 nanometers which is close to the red in vivo absorption by chlorophyll a. This fluorescence is excited by light absorbed in the region of 450 nanometers in the case of the brown, green and blue-green algae. However, brown algae can also be excited at 530 nanometers. This is due to light energy which is trapped by the fucoxanthin. The red and blue-green algae have different

excitations and emissions due to the presence of the phycobilin pigments. Absorption of light in the region around 470 nanometers produces emission from phycobilins and chlorophylls throughout the region between 520 to 750 nanometers.

Gelbstoff also has a weak fluorescence. When excited around 360 millimicrons a broad band of fluorescence occurs in the region of 460 to 470 then gradually tails off into the longer wavelengths of the visible spectrum. One of the surprising features of the excitation and fluorescence spectra of the Gelbstoff is that the absorption spectrum of the Gelbstoff shows no correspondence with the excitation spectrum. This is undoubtedly due to some factor which tends to mask the substance responsible for the fluorescence. However, we have demonstrated in the laboratory that removal of all the Gelbstoff essentially removes all of this fluorescence.

Bioluminescence of course is not fluorescence. It is generated by a series of chemical reactions which produce light. Most of the bioluminescence seen in the oceans is termed "stimulatable" bioluminescence, that means that the light is given up after agitation of the organism. The bioluminescence spectrum shown in this figure is that for dinoflagellates which are the most common source of flashing in the oceans. The characteristics of fluorescence from naturally occurring particulate matter has not been

extensively studied. Figure 4 shows characteristics of excitation and emission of particulate matter collected in the tropical waters of the Straits of Florida. The curves for excitation and emission are characteristic of a mixture of brown and green algae. This suggests that the dominant fluorescing material in the particulate matter is the algae.

#### SUGGESTED APPLICATIONS IN REMOTE SENSING

In this report I have emphasized that the prime factors involved in wavelength characterization of light and/or water color are absorbing properties. Therefore, some of the principal efforts of remote studies should concern measurement of Gelbstoff and phytoplankton algae.

The importance of measuring Gelbstoff is related to its origin. One is land run-off and the other associated with compounds liberated mainly by an algae. The chemistry of these compounds is badly known. However, absorption and fluorescence characteristics are similar. Evidence suggests that they are quite resistant to biochemical decomposition. Near shore most of the Gelbstoff is associated with run-off. Or to put it another way, the amounts contributed by algae are small. Figure 5 shows the concentration of Gelbstoff flowing out of the Amazon River along the Eastern Coast of Brazil. Now imagine yourself as the observer or detector flying over this area. The

features of interest would be the high concentration of Gelbstoff (yellow water) adjacent to the coast. Generally the yellow color decreases as one moves away from the coast. However, patches of high concentrations are found as much as 150 miles off the coast. The picture that one sees could be comparable to what would occur in a yellow dye experiment. The dye coming out of the Amazon moves in a northwesterly direction. It encounters a current moving in the opposite direction which pinches off segments of the yellow water. Gelbstoff is a tracer of the Amazon freshwater outflow. This is demonstrated by relating the optical density of Gelbstoff to the salinity, Figure 6. The range of salinity covered is basically the range encountered at the mouth of the Amazon going to salinities as high as 36 o/oo which is near the maximum observed in these waters. The implication here is obvious, remote detection of Gelbstoff would be valuable in tracing water masses.

Throughout this symposium there has been considerable discussion regarding the measurement of chlorophyll as to productivity. The discussion is largely centered around the area of fisheries biology where the work of Blackburn<sup>\*</sup> has shown a strong correlation between the concentration of chlorophyll and abundance of tuna. What Blackburn has suggested is that in certain areas of the Pacific the food-

---

\*Dr. Maurice Blackburn, Scripps Institution, La Jolla, Calif.



chain is simplified with the intermediate step between the phytoplankton and the tuna being a crustacean. Blackburn has stated that the scouting efficiency of the tuna fisherman would be greatly increased if chlorophyll and temperature could be remotely measured. There are other uses where surveillance of chlorophyll over large areas of the oceans would be of value. The complications leading to eutrophication\* are frequently difficult to ascertain unless one has a large aerial coverage. Outbreaks of certain organisms such as "red tide" at times could be traced back to the source. The general concept of the distribution of blooms, their size, how related to physical processes such as upwelling, are not well understood by biological oceanographers.

I have been especially interested in the onset of phytoplankton blooming in the North Atlantic Ocean. The onset of this bloom is regulated by the interrelationship of vertical and solar radiation. During winter months the growth of phytoplankton is arrested by low light intensity and deep vertical mixing in the water column. With increasing solar radiation (winter → summer) however, the depth of vertical mixing is reduced and a bloom occurs. As the sun changes latitude from spring to summer, one should almost see a wave of primary production moving across the North Atlantic Ocean. In shallow coastal waters

---

\* over-fertilization of natural waters

this process is complexed by the bottom. For example, the blooms start in shallow water. Here the depth of vertical mixing is limited by the bottom and phytoplankton are not light limited. Moving into deeper waters, population becomes light limited since the maximum depth (hence mixing depth) becomes deeper, thus light limiting population growth. This condition can be seen in the section shown in Figure 7. The high chlorophyll values in the water column are associated with depths of around 70 meters and as soon as these depths increase, the chlorophyll values decrease. Thus gradations in bottom depth strongly influence the population size and these situations are difficult to find or are frequently missed and/or misinterpreted for shipboard observations.

#### CONCLUSIONS

It has been repeatedly stated that the value of remote sensing lies in the ability to survey large areas in a synoptic fashion. The cost per unit data can be much lower than any other method.

There are many problems in aquatic biology where remote sensing is the easiest, most accurate and cheapest means of obtaining this information. Yet much of the difficulty in developing remote sensing devices appears to be stymied by hardware development. I cannot imagine this difficulty

lasting very long. What is needed is a coordinated program where detectors are flown at low altitudes with ground truth measurements. These would be the precursor to satellite systems.

It can be argued that the real reason for going into space is to get a whole view of the earth. Therefore, develop earth sensors. The other argument however, is to develop these sensors for future planetary exploration. The detection of life on other planets is one of the goals; earth sensors for living substances is a necessity.

#### ACKNOWLEDGEMENTS

Portions of the research reported were supported by the National Science Foundation GA-27082 and the Atomic Energy Commission AT(30-1)4241.

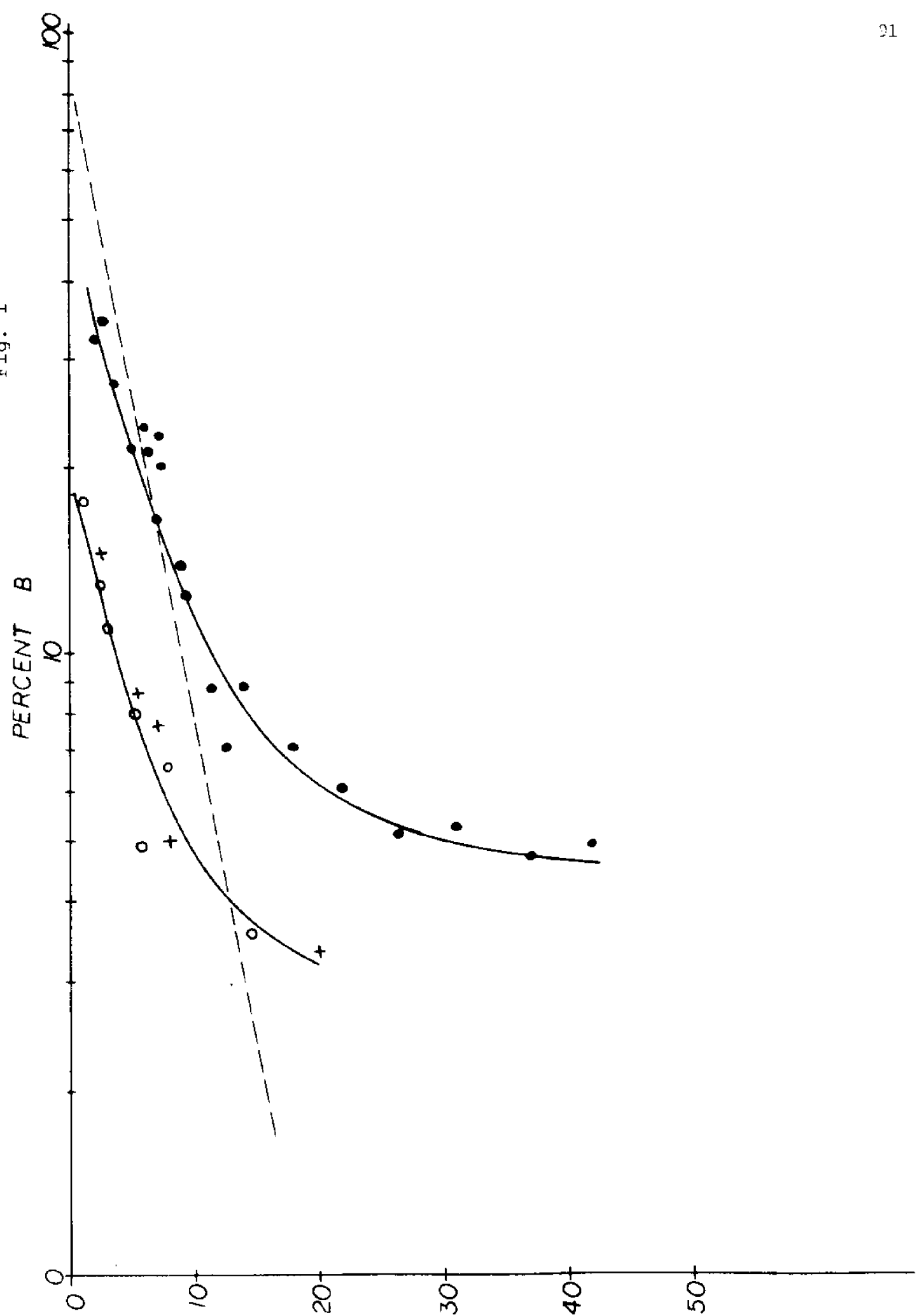
## REFERENCES

- YENTSCH, C.S. The influence of phytoplankton pigments on the colour of sea water. Deep-Sea Research, vol. 7 pp. 1-9, 1960.

## FIGURES

1. The percentage of backscattered light as a function of water depth. Off Bimini Island in the Bahamas. The black dots represent measurements over white sand bottom. The crosses over coral reefs; the open circles over grass areas. The slashed line represents a theoretical parallel light computation, Eq. 8 in the text.
2. Principal substances absorbing light in natural waters.
3. Principal sources of light emission in natural waters. Dotted lines indicate area of maximum light transmission.
4. Fluorescence excitation and emission from particulate matter collected in the Straits of Florida off Fort Lauderdale.
5. Distribution of Gelbstoff off Brazil. Values are percentage of light absorbed in a 20 cm cuvette at 270 nm.
6. Relationship between Gelbstoff and salinity. Fig. 5 values changed to absorbence.
7. Chlorophyll fluorescence transect in the Gulf of Maine. Heavy line is bottom contour.

Fig. 1



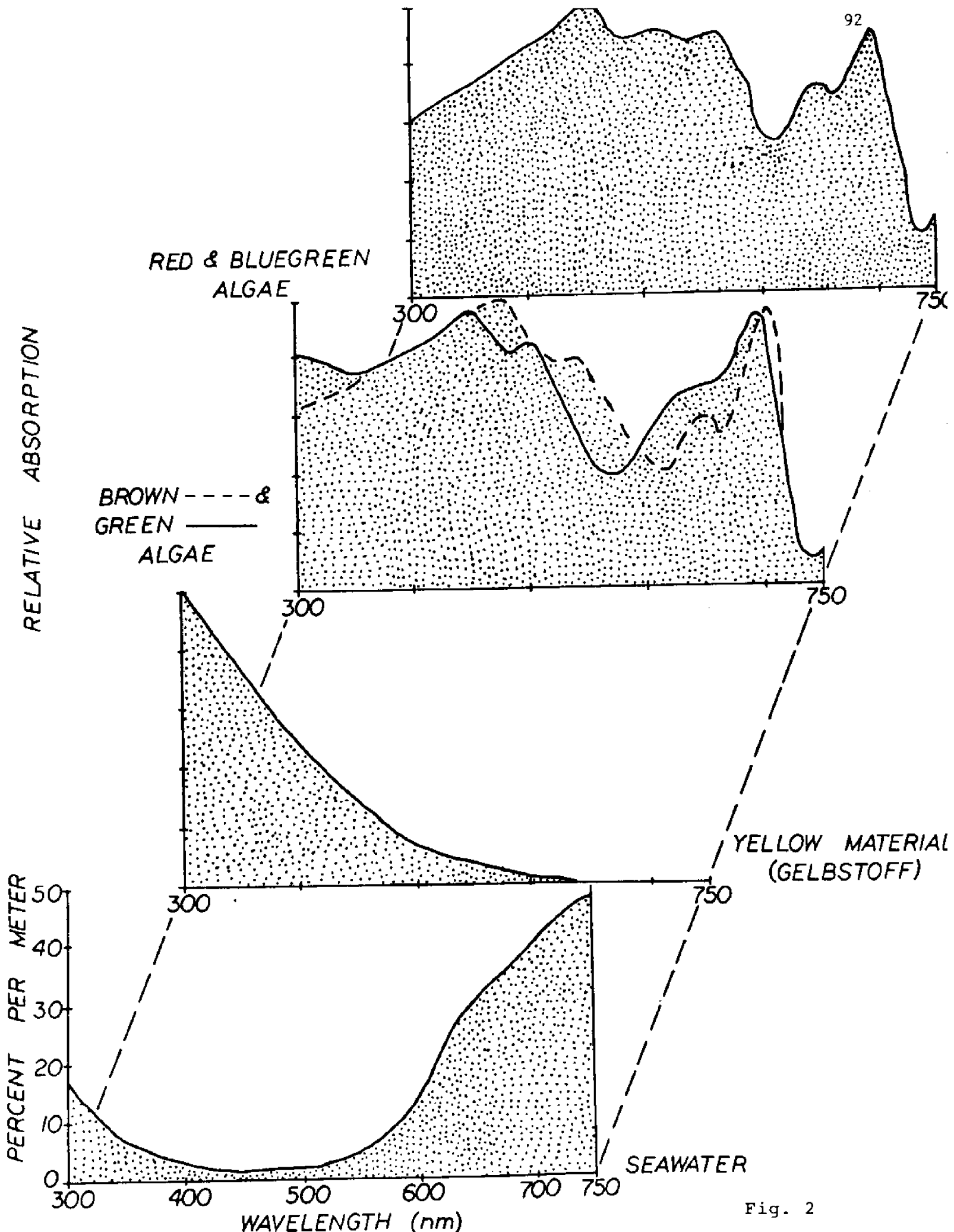


Fig. 2

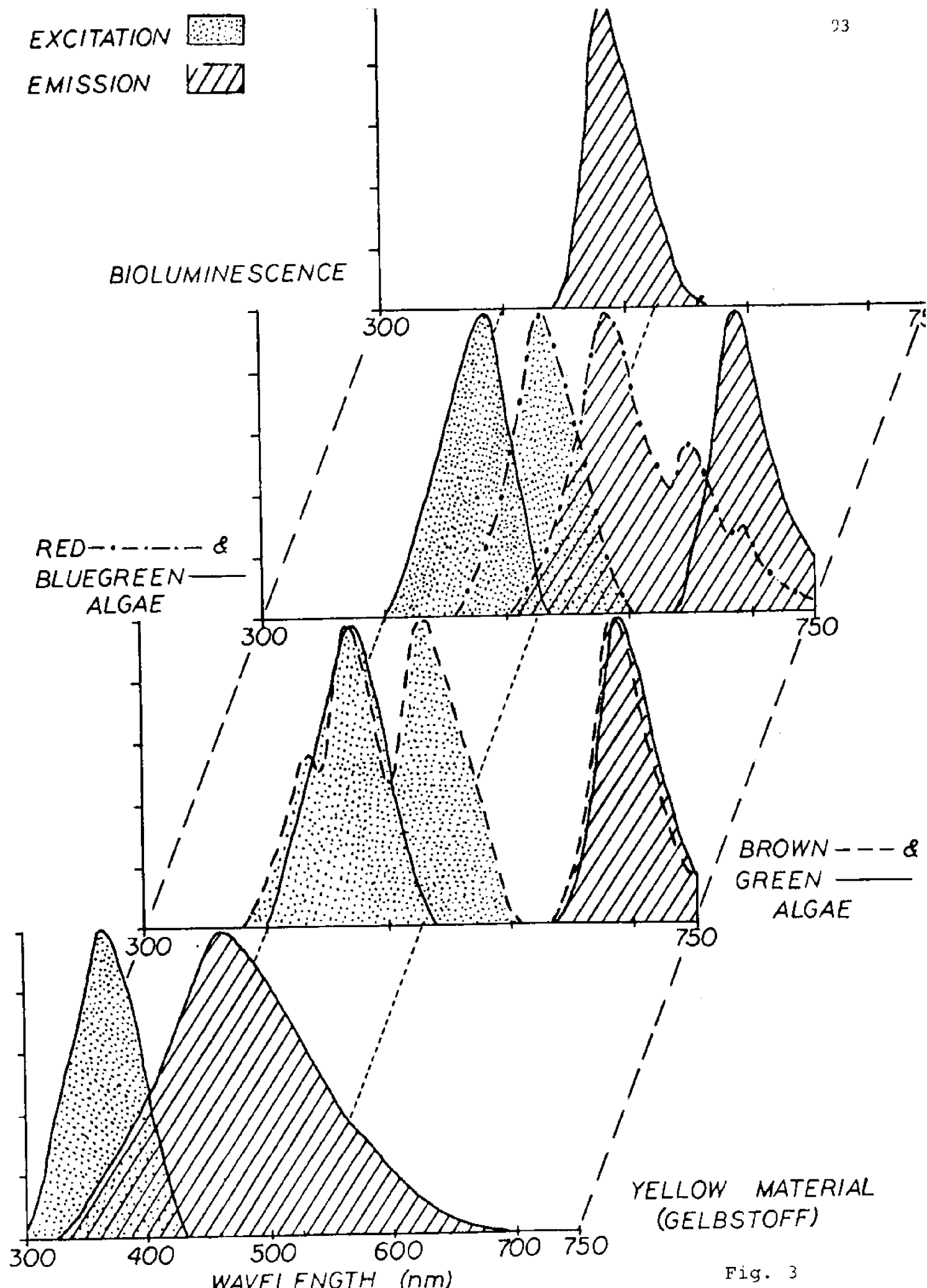


Fig. 3



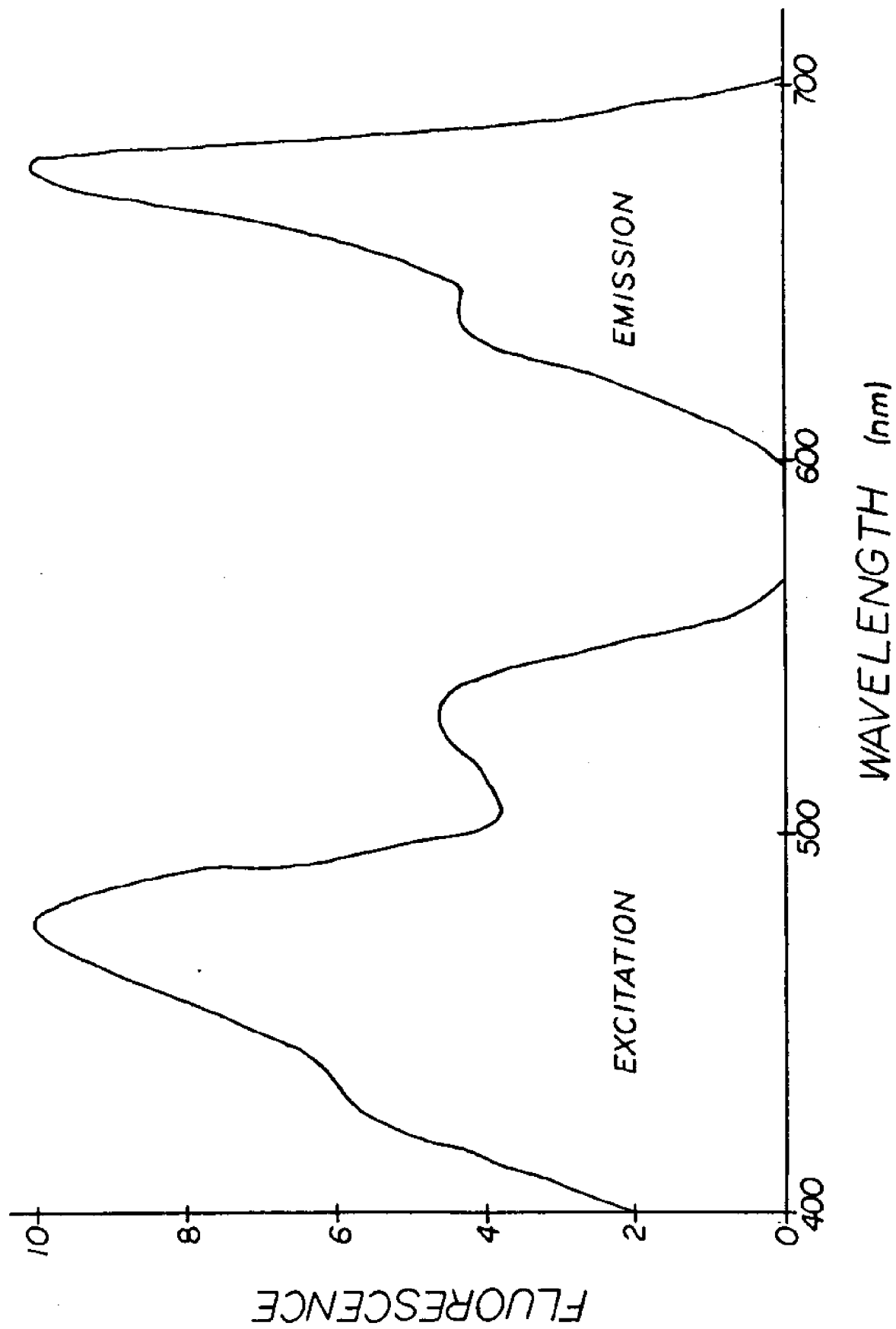


Fig. 4

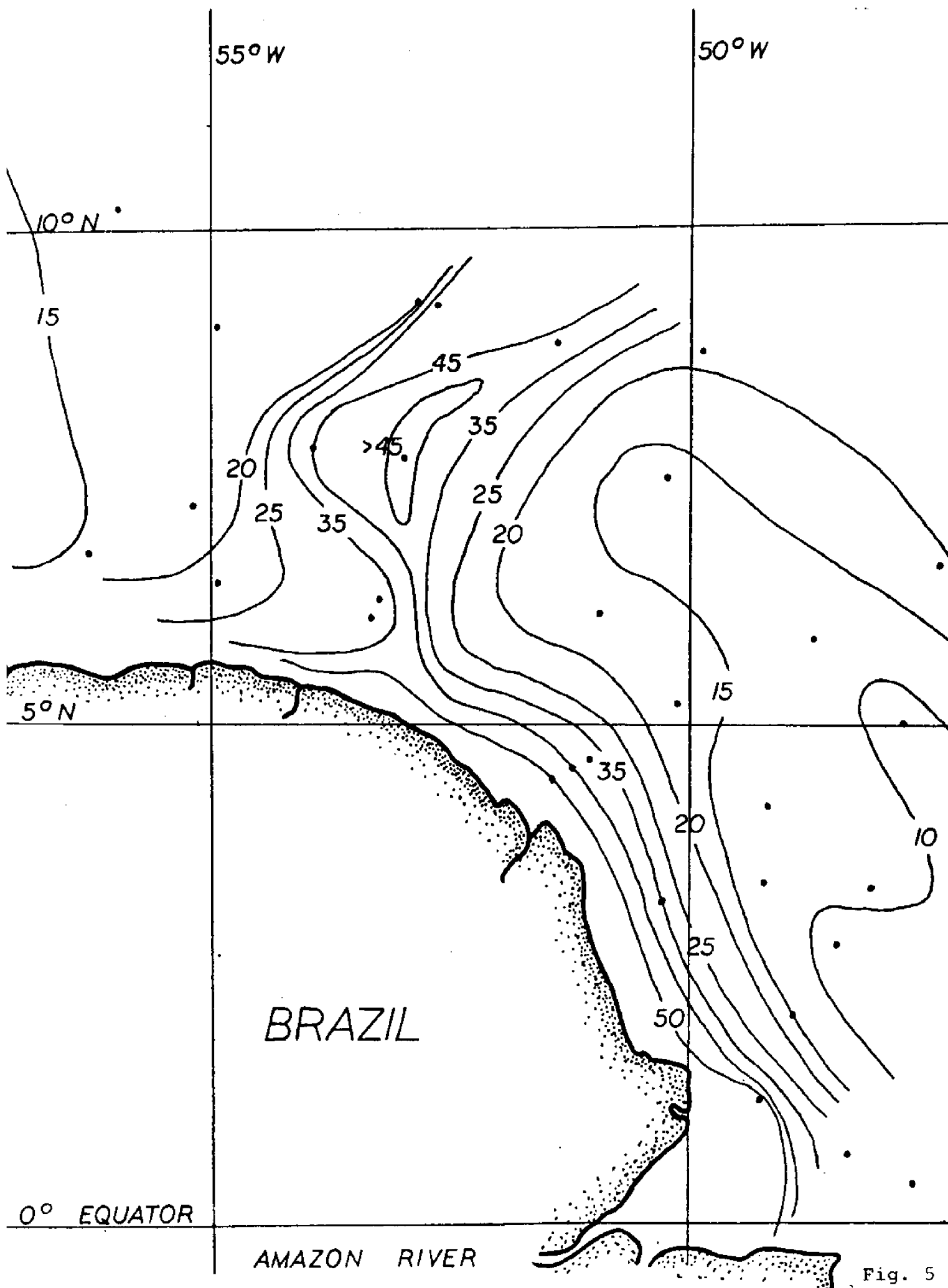


Fig. 5

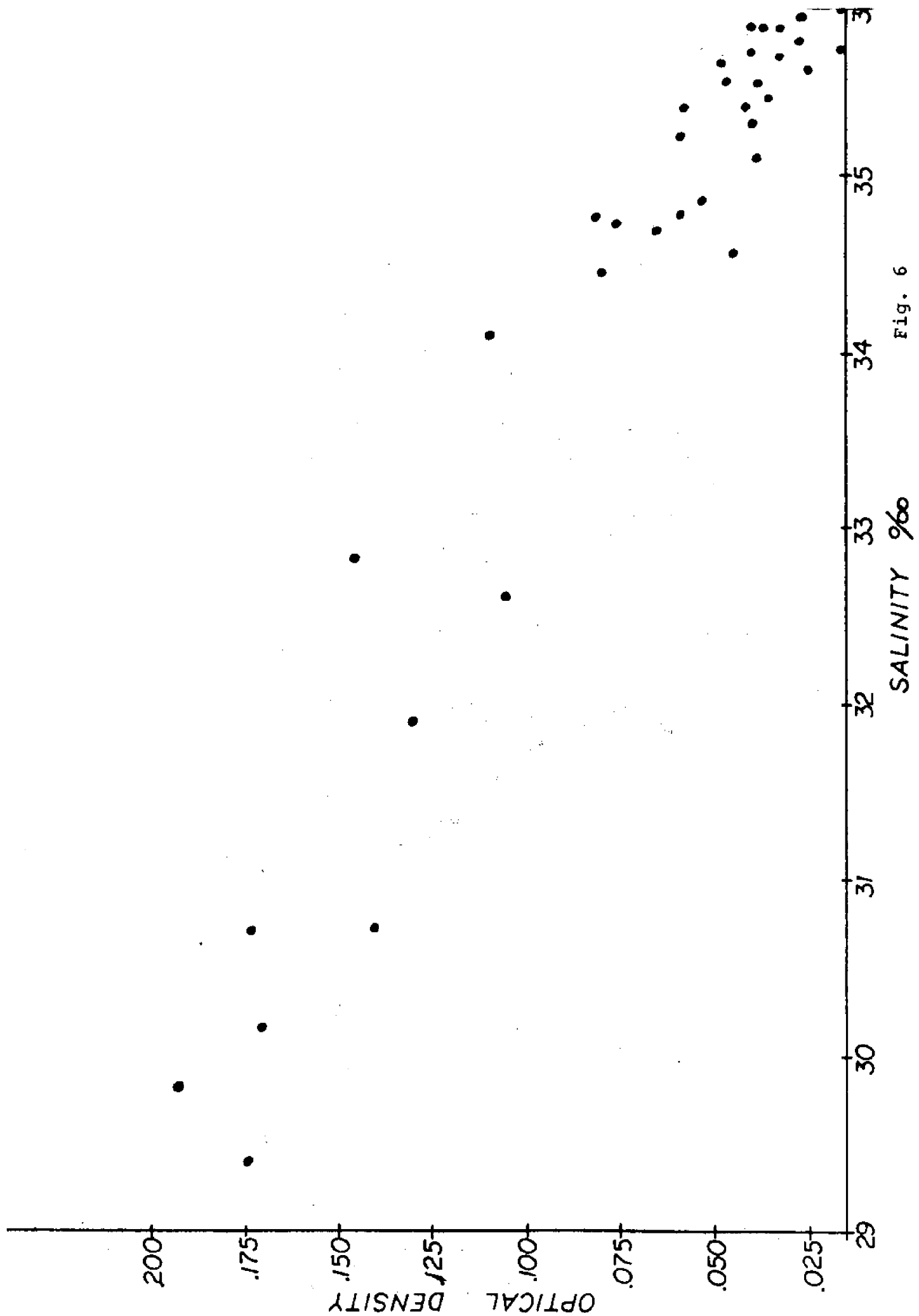


Fig. 6

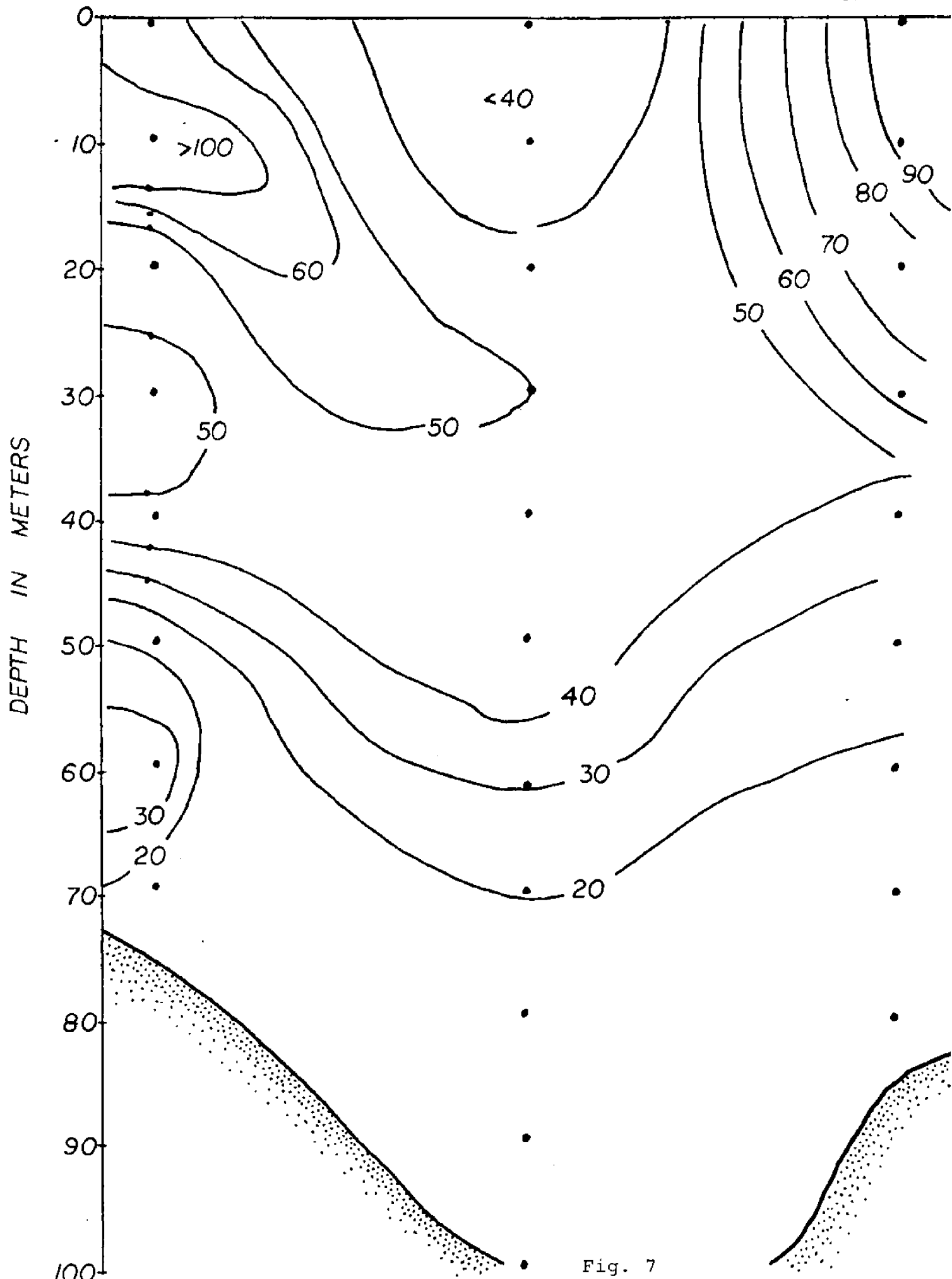


Fig. 7



## THE REMOTE SENSING OF VAPOURS OF MARINE ORGANIC ORIGIN

## ABSTRACT

By

A. J. Moffat, A. R. Barringer

Barringer Research Limited

Three types of remote sensing of vapours are possible, one of which is suitable for use from high altitude aircraft and spacecraft and the other two from low altitude aircraft and ships. In the case of high altitude remote sensing, optical methods can be employed in vertical incidence for detecting spectral characteristics of emitted or reflected optical radiation. Experiments have been carried out with a technique known as correlation spectroscopy in which incoming radiation in the visible spectrum has been matched in real time against a stored replica of the iodine spectrum in order to monitor the vertical burden of free iodine over the ocean. Iodine is considered to be of interest as a potential indicator of biological productivity and region of primary fish food. Preliminary tests of the use of correlation spectroscopy for iodine detection have indicated the feasibility of this approach and have shown that anomalous iodine concentrations can be measured over kelp beds. Greater sensitivity can be achieved, however, with these techniques used in horizontal scanning modes from low flying aircraft, ships and truck-mounted monitors on the coastline. There has been some evidence that increased concentrations of free iodine vapour can be measured over plankton areas using the latter technique. Theoretical calculations indicate that instruments can be optimized for iodine detection to provide adequate sensitivity for satellite monitoring.

Limited work on the detection of fish oil slicks by infrared methods used in vertical incidence has not been encouraging and there is considerable doubt regarding the feasibility of identifying specific characteristics of fish oil slicks from high altitude. The measurement of fish oil vapours using optical correlation methods in horizon scanning mode offers more promise, but has not been investigated in any detail.

## INTRODUCTION

Remote sensing spectroscopy offers considerable potential as a means for monitoring sea surface phenomenon and properties of the near surface zones of the ocean. Since the sun-lit upper layers of the ocean support the growth of photo synthetic plankton, which is fundamental in the food chain of marine biology, methods of remotely sensing phenomenon relating to biological activity in the surface layers would be of far reaching importance not only to the marine biologist but to the commercial fisheries as well.

A promising method of monitoring biological activity in the ocean is the remote monitoring of vapours of biological origin which are dispersed into the atmosphere at the ocean surface. Trace amounts of organic and inorganic material produced by various phases of marine plant and animal life cycles are dissolved or suspended in the sea and eventually pass through the air/sea interface into the atmosphere in the form of an organic or inorganic aerosol through the mechanism of wave and spray or as a vapour by photochemical action and/or evaporation.

The purpose of this paper is to present various aspects of the remote sensing of sea surface vapours from spacecraft, aircraft and surface vessels and to discuss these aspects in relation to initial results of airborne and ground based measurements of atmospheric iodine and preliminary investigations into the remote sensing of fish oil vapours.

## SIGNIFICANCE OF MARINE IODINE

Iodine vapour of marine origin is considered to be potentially useful as an atmospheric tracer in delineating areas of high biological activity because iodine is highly concentrated in plants and animals and appears to transfer readily from the sea surface to the atmosphere. Table 1 shows examples of iodine concentration found in various species of plants, animals, and media in the marine environment. Note that the iodine content of brown algae can be as much as 400,000 times that of sea water.

	<u>PPM-BY WT.</u>
River Water	0.0018
Coastal Water	0.02
Sea Water (average)	0.05
Brown Algae	1,000 - 4,000
Red Algae	10 - 1,000
Green Algae	10 - 1,500
Diatoms	up to 20
Sponges	1,000 - 20,000
Fish (dry basis)	1 - 30
Sea Mollus	11 - 310
Coral	210 - 7,800
Non Marine Atmosphere	0.0001 - 0.0015
Marine Atmosphere	0.012

(From Goldschmidt, Vinogradov & Fallenburg)

#### MARINE $I_2$ CONCENTRATIONS

TABLE 1



Iodine is present in ocean water as iodide and iodate ions. Iodide is unstable when exposed to sunlight and escapes readily into the atmosphere as free iodine after photochemical oxidation. (Mijake and Tsunogai, 1963). In spite of losses through the surface, iodide is most highly concentrated in the surface layers where it is apparently produced by conversion of the more stable iodate by biological activity. (Tsunoda and Sase, 1969). It appears highly probable that characteristically high iodine levels in the marine atmosphere are closely associated with marine surface life such as sea weeds and plankton. Since plankton is fundamental to all biological life in the ocean the ability to detect and monitor the occurrence of phytoplankton blooms in the world's oceans would be of considerable importance to marine biology and fisheries research.

#### REMOTE SENSING OF VAPOURS & GASES

The principles of remote sensing by correlation spectroscopy have been discussed in detail previously (Millan et al, 1970). In brief, the technique relies basically on matching a selected portion of the spectrum of radiance received by the sensor with a stored replica of the spectrum of the target gas. Since most gases or vapours have unique molecular absorption or emission spectra and the sensor functions in real time the method is highly specific and the data rate is very high. The output of the sensor is conventionally calibrated in ppm-meters i.e. the average concentration of the vapour x the total effective path length through the cloud.

Under conditions of similar irradiance of the background scene, the highest probability of detection of a cloud of vapour in the atmosphere is realized when the angle of viewing is such as to result in the greatest burden or optical depth (ppm-meters). Figure 1 depicts three different concepts for the remote sensing of spectral information at or near the ocean surface.

An obvious difference between surface craft, aircraft and spacecraft sensing systems is the difference in scale, i.e. the area of sea surface scanned in a given unit of time.

For example, in the case of a ship-borne remote sensor with a  $180^\circ$  forward scan pattern and assuming a maximum detection range along a horizontal path of say 8,000 meters for large vapour clouds, then for a ship speed of 15 knots a search area of approximately 0.6 square miles (nautical) could be scanned per minute. This compares with  $8.0 \text{ (nm)}^2 \text{ min}^{-1}$  for an aircraft flying at 200 knots (at low altitude) under similar scan conditions. For a satellite system in low earth orbit the ground track velocity would be of the order of  $4 \text{ nm sec}^{-1}$  and with a scan swath width of 100 nm a sea surface coverage of some  $3,400 \text{ (nm)}^2 \text{ min}^{-1}$  would be obtained. These figures are of course only crude comparisons but they serve to indicate the scale of things. It is also worthwhile noting that the detectability of a gas cloud depends on the search time available. On this basis alone the satellite system would be suitable for only large scale surface phenomena whereas the ship sensor with its relatively slow scan and long integration time would have the best detection capability.

In the case of vapour detection, basic factors in determining detectability are optical depth (ppm-meters) of the target cloud and the signal-equivalent noise level of the satellite measurement. Sources of noise will include wavelength selective absorption and scattering by background gases and aerosols in the atmosphere and varying spectral characteristics of the surface of the ocean and its upper layers. Radiant energy which is backscattered from the atmosphere and which contains no gas signature (air light) tends to dilute the energy which is reflected from the ocean's surface. In the detection of surface vapors therefore a remote sensor at satellite altitudes will suffer a greater loss in sensitivity due to air light dilutions than would be the case from either aircraft or surface-based sensors.

#### IODINE DETECTION

Considerable improvement in vapour detection sensitivity is obtained by observing the vapour cloud at shallow oblique or grazing angles as depicted by the aircraft sensor in Figure 1. This mode permits much longer optical paths through the cloud particularly when viewing upwind or downwind of the source. This method of iodine detection was evaluated using an experimental correlation spectrometer over the New England coast (Barringer Research 1969). Figure 2 shows the aircraft and Figure 3 the console arrangement.

Special windows were inserted in pods in the side of the fuselage and the aircraft was flown at 2,500 feet to 3,500 feet with the spectrometer pointed out of the right side of the aircraft at approximately  $10^{\circ}$  below the horizontal. This not only maximized the pathlength in the lower atmosphere but also minimized background noise. The technique was satisfactory in establishing the presence of variable iodine backgrounds. Figure 4 shows the build-up of iodine that occurs in the vicinity of Matinicus Island off the coast of Maine which is apparently associated with a strong build-up of kelp lying in the vicinity of this island. Figure 5 shows a larger portion of the Maine Coast in which repeated flights confirmed the build-up of iodine along the kelp rich coastline. These results are qualitative since they cannot be referred to a specific pathlength, and calibration between flights was subject to certain errors connected with changes in ambient lighting conditions. Nevertheless, the records obtained repeatedly established that atmospheric iodine concentrations do increase over the coastline and in particular, over kelp-rich areas.

The third method of vapour detection illustrated in Figure 1, that is scanning of the horizon sky from a surface vessel, will provide the best S/N ratio of all three methods (in the ultra-violet and visible) because of the combined effects of long horizontal or slant paths through the first 100 meters or so of atmosphere and the relative brightness and spectral uniformity of the day sky.

In April 1970 a series of ground based measurements were made of atmospheric  $I_2$  over the Midway-Sunset oil field near Bakersfield California. These tests were part of a larger NASA supported program of geochemical  $I_2$  measurements (Barringer Research 1970) and some results of this project are included here because of the marine organic origin of oil accumulations. Oil field brines which are closely associated with oil accumulations are generally rich in iodine. Figure 6 shows a typical ground-based set-up for measuring  $I_2$  over Midway-Sunset. Figure 7 shows a polar plot of the data obtained from the top of a mountain peak to the west of the oil field. These readings, which were all taken with the sensor scanning in a horizontal plane, were done in clockwise fashion beginning at  $0^\circ$  and progressing clockwise through  $360^\circ$ . The time required to complete the full circle was 60 minutes and during this time the wind shifted direction from S.E. at the start to due East and occasionally northerly at the finish, and increased in speed from 15 m.p.h. to 25 m.p.h. in the same period. This may account for the much smaller burden recorded at  $350^\circ$  than at  $10^\circ$ .

Note also that the values shown are all relative to the minimum value which was set equal to zero. The minimum value was obtained with the sensor on "bearing"  $310^\circ$ . At a bearing of  $160^\circ$  the sensor recorded a burden of 4,900 ppb-meter greater than that recorded at  $310^\circ$ . The S/N ratio at  $310^\circ$  was 16. In terms of  $\mu\text{gms}/\text{m}^3$  the equivalent peak value of the anomaly was  $5.1 \times 10^4 \mu\text{gms}/\text{m}^3$  referred to a 1000 meter path length.

The much greater response from the S.E. direction is considered to be due to the fact that wind-born  $I_2$  emissions from the region of Midway-Sunset south of Midway Peak would be substantially greater than regions of the field north of the peak. The Elk Hill oil field is a Naval reserve and is non-productive. Little is known about Buena Vista area, but its production rate and hence its  $I_2$  emission is certainly substantially less than the Midway-Sunset field.

Subsequent to the oil field measurements a series of tests were performed over phytoplankton blooms along the California coast. Figure 8 shows the sensor observation sites. The method of measurement here was similar to that used in the oil fields, namely stepping the sensor around in the horizontal plane and recording the response at each position. The sites shown in Figure 8 were chosen to provide a maximum breadth of scan over the sea surface where red tide plankton blooms were visible in the water. Although the red tide was distributed over much of the coastal waters there were areas of dense patches of plankton.

Barringer Research is indebted to TRW for assistance in locating the primary red tide concentrations. (At the time of the Barringer measurements TRW was performing initial airborne flights of a chlorophyll remote sensing system coupled with "ground truth" sampling of the surface waters using a small surface vessel.)

Figure 9 shows the results obtained from a set-up on the Hermosa Beach pier. The circled points were taken in rapid sequence to minimize time effects. The value of 3.3 ppm-m at  $255^{\circ}$  compares with 2.3 ppm-m obtained along the coast to the north, 1.3 ppm-m inland and 1.2 ppm-m directly overhead.

The counter-clockwise scan in the south west sector shows a particularly strong anomaly of about 0.7 ppm-m at  $210^{\circ}$ . The wind over the period of observation was 14 knots at  $230^{\circ}$  (southwesterly). The total amount of  $I_2$  vapor was clearly fluctuating with time and the polar plots contain time variations. The plankton blooms were too widespread to obtain discrete anomalies but certainly there was much more  $I_2$  present over the ocean than over the land and the peak values appeared to coincide with the most visible plankton concentrations.

Figure 10 shows similar results for the following day taken at the Palos Verdes swimming pool some four miles due south of the Hermosa Beach Pier.

A distinct iodine anomaly was detected to the northwest over Santa Monica Bay probably due to the same bloom which produced the southwest anomaly on the previous day. The conditions were similar for the two days.

The results of a third experiment are shown in Figure 11. This set up was made following reports from the TRW aircraft that a plankton bloom was growing inside the breakwater. Readings of 2.2 ppm-meter over the bloom in San Pedro Bay were in fact somewhat higher than readings obtained directly north but the strongest anomaly was at  $210^{\circ}$ . This could be due to one or more unreported blooms or possibly to kelp in the coastal waters to the south east.

Figure 12 shows data taken a day later at Santa Barbara approx. 95 miles northwest of San Pedro. A comparison of Figure 12 with the previous three figures shows the iodine levels to be generally much higher in the Hormosa Beach/San Pedro area. A strong anomaly is evident in Figure 12. This may have been related to the local offshore oil field or to a kelp bed since there was no plankton bloom visible from the sensor station.

A final data plot is shown in Figure 13. This shows a comparison of readings obtained with the sensor looking at the zenith sky for basically three widely separated locations. The data are normalized to the Morro Bay readings which were assigned a zero value because the horizontal readings were consistently very close to the vertical readings.

Although the results of the ground based iodine measurements along the California coast do not conclusively relate the high iodine concentrations to the red tide plankton, the association of high readings with obviously very intense plankton growth appears to be strong. The likelihood that the anomalies observed were simply the result of an on-shore wind of marine origin seems to be discounted since the high iodine concentrations were not present further north. It is possible of course that much of the iodine vapor was produced by kelp beds which are numerous along the southern California coast. A more extensive program is obviously required to clearly establish the relationship between marine iodine emanations and plankton blooms.

Experience todate with the prototype  $I_2$  sensor shows that greater sensitivity can be realized with further optimization of the correlation mask and the method of correlating with the incoming spectrum.

Theoretical studies of an improved instrument design suitable for a satellite indicates that a photon limited noise level of  $1.3 \times 10^{-1} \mu\text{gms}/\text{m}^3$  referred to 1,000 meters is feasible. (Barringer Research 1970.) Ignoring atmospheric and sea surface reflectance noise sources this represents, for a spacecraft sensor, a noise level equivalent to the minimum background iodine 0.1 ppb or  $0.13 \mu\text{gms}/\text{m}^3$  (Table 1) assuming the background to be a homogeneous layer of some 1,000 meters in depth and all the iodine to be in the free vapour phase. If the above mentioned noise sources are assumed to degrade this performance by a factor of 10, the threshold sensitivity (1:1 S/N) would still be lower than the maximum terrestrial atmospheric background and substantially lower than coastal marine atmospheric backgrounds (Table 1,  $0.012 \text{ ppm} = 15.5 \mu\text{gm}/\text{m}^3$ ).

## FISH OIL DETECTION

Investigations of the feasibility of detecting fish oil slicks by virtue of their spectral absorption characteristics in vertical incidence have not been encouraging (Barringer Research 1968). There is considerable doubt whether specific characteristics of oil slicks can be identified from high altitudes. The study of fish oil vapors may, on the other hand, prove more rewarding. Some preliminary work at Barringer Research indicates that fish oil vapors have useful spectra if the pathlength-concentration product is adequate. For example Figure 14 shows the absorption spectra of cod liver oil. The mineral oil spectra is included to demonstrate the potential capability of specific identification.

Figure 15 shows spectra of Menhaden oil and its vapor in transmission.

Although much remains to be done to prove or disprove the feasibility of detecting fish oil vapors over the oceans surface using spectroscopy, the preliminary work is encouraging.

## 2-GAS SENSOR

Based on the experience gained with the prototype correlation spectrometer a new instrument design has evolved at Barringer Research which has considerably greater potential in terms of sensitivity and versatility as a multi-gas sensor. Figure 16 shows the instrument layout. Two turret-mounted cassegrain telescopes provide a choice of one degree or one milliradian field of view. An Ebert-Fastie configuration and two separate gratings are used to superimpose two selected spectral intervals in the exit focal plane. The correlation mask containing arrays of curved slits are photo-etched on a rotating quartz disc in the exit plane (Figure 17). The spectral intervals are then separated by a dichroic mirror and directed to two separate photomultiplier tubes. The slit arrays in the spinning disc are arranged to correlate sequentially in an in-phase and anti-phase fashion



with the spectra to be detected and the modulations produced at each photomultiplier are individually processed in separate channels. Additional slits are etched on the disc for switching logic and synchronous detection. Fused silica reference cells are included for calibration purposes. This design is now in limited production as a remote sensor of  $\text{SO}_2$  in the ultraviolet and  $\text{NO}_2$  in the blue visible. By making rudimentary changes e.g. gratings, correlation disc and reference cells, the sensor can be used as a remote sensor of any two alternative spectra such as iodine, fish vapours, water color, fluorescence, etc.

#### CONCLUDING OBSERVATIONS

The presence of atmospheric iodine in anomalous concentrations in certain marine environments has been demonstrated but the relationships of iodine emissions to specific marine biological activity has yet to be resolved.

The application of spectroscopic methods to the remote sensing of vapours of marine origin obviously requires a detailed knowledge of the spectra sought. The volatile components of fish oils for example, must be identified and their spectral characteristics related, where possible, to specific fish species, their feeding habits, metabolic activity etc. Further work is also required to determine the significance of fish oil vapours in a quantitative sense and their potential as indicators of marine animal life.

Finally, the application of spectroscopy to other materials of interest to the marine biologist should not be ignored. The presence of dimethyl-B-propiethetin in planktonic marine organisms is well documented as are its natural degradation products, acrylic acid and dimethyl sulfide which are liberated spontaneously through enzymic action upon death. (Ackman, and Tocher, 1966) Little information is presently available on the spectral characteristics of these materials or on their potential as indicators of marine biological activity. It is probable also that some of these substances are released at the sea surface as aerosols or as vapours which tend to polarize readily into

aerosols, in which case air sampling techniques on surface vessels and/or low flying aircraft may be appropriate. At Barringer Research spectroscopic methods are presently being developed for the detection of trace elements and inorganic compounds as well as organic vapours using the air sampling approach. The results of this work will be reported on elsewhere.

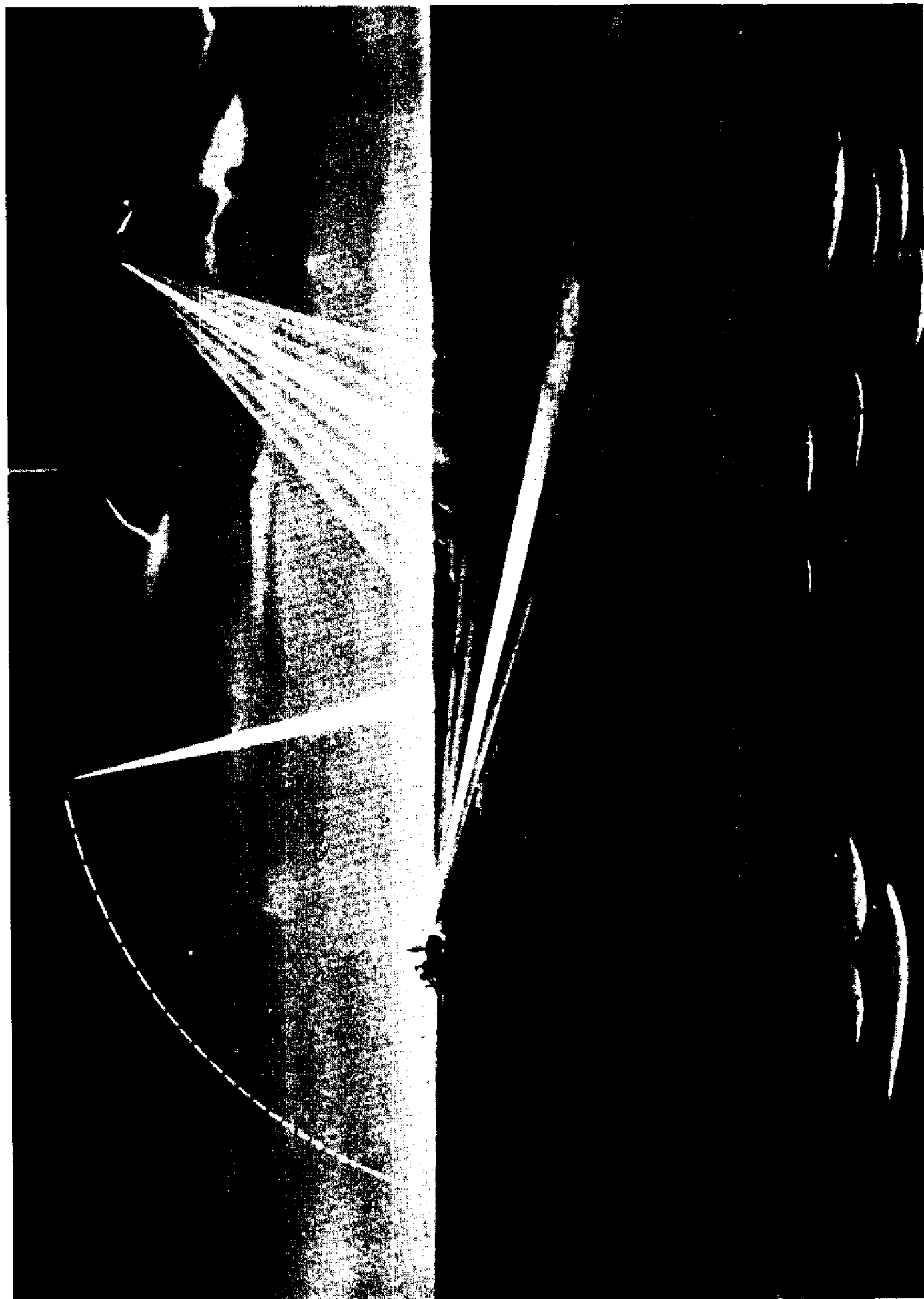
It is fair to conclude that the technology of remote sensing spectroscopy for the detection and measurement of atmospheric gases is advancing rapidly. Experimental verification in the marine environment is as yet only cursory but the indications to date are very promising and the high sensitivity and versatility of the technique auger well for its application as a useful tool in promoting man's understanding of biological life in the oceans.

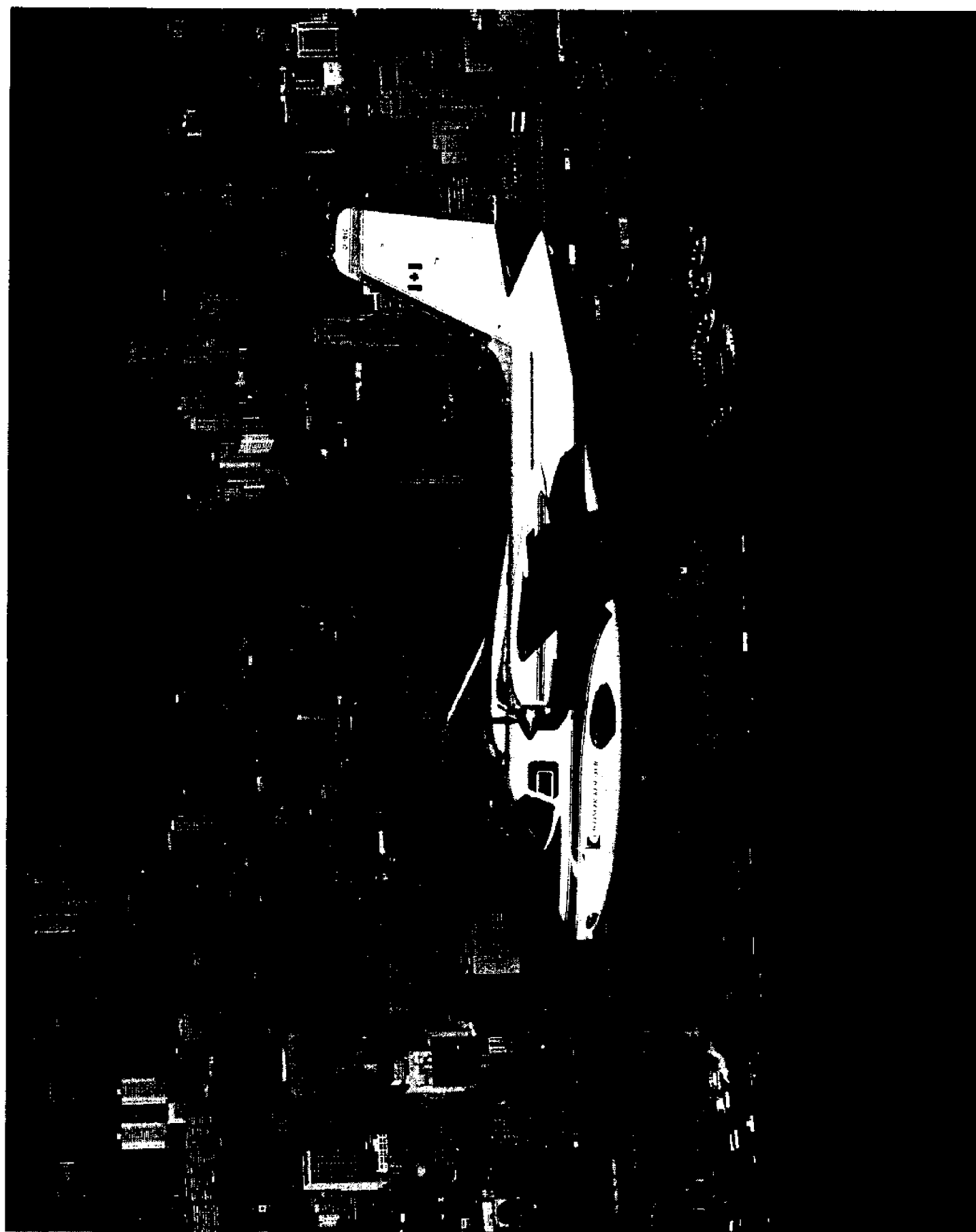
#### ACKNOWLEDGEMENTS

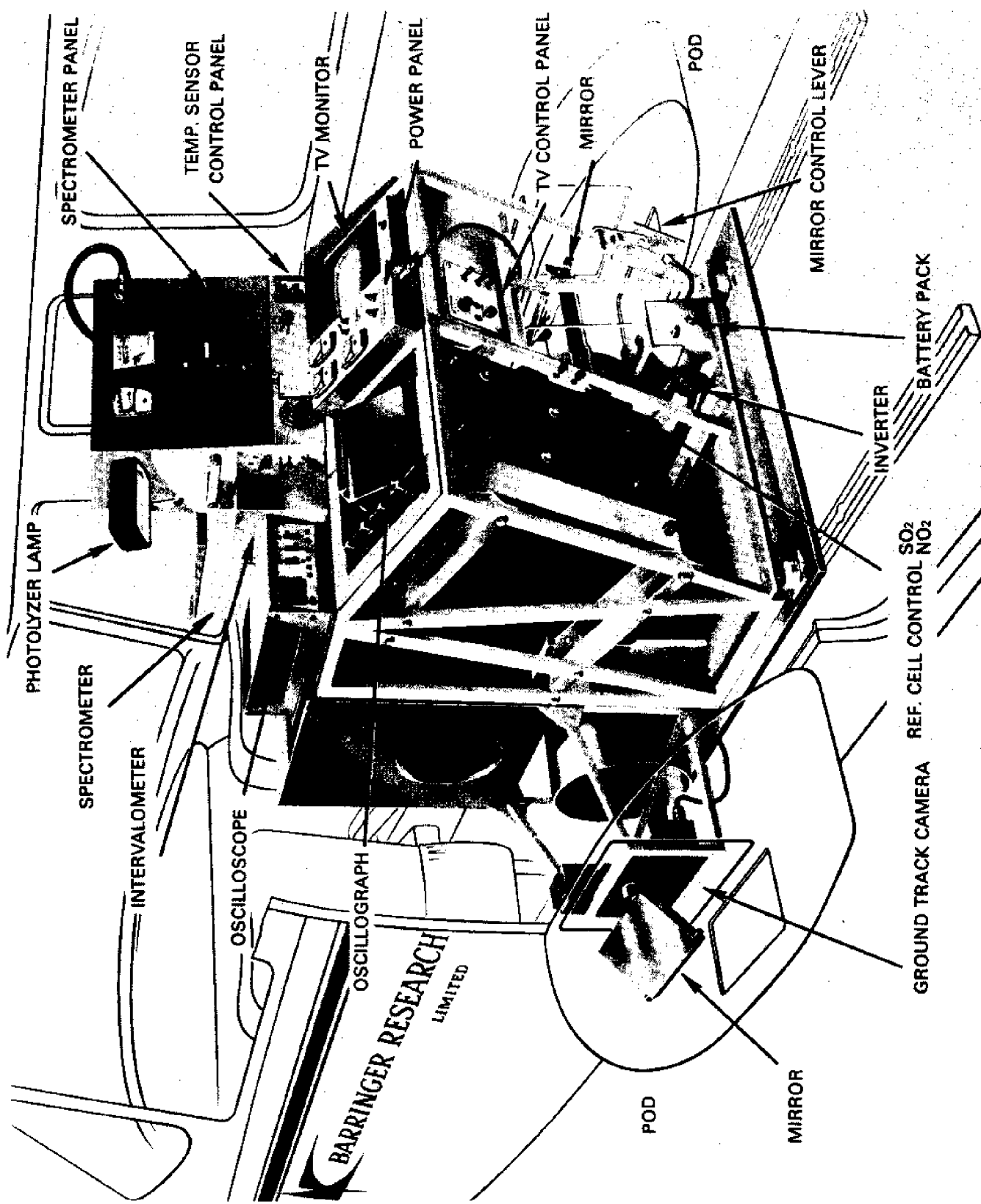
The generous support of the National Aeronautics and Space Administration (MSC) for the airborne work and oil field experiments is gratefully acknowledged as is the assistance provided by Environmental Measurements Inc. of San Francisco in performing the California coastal measurements on behalf of Barringer Research.

REFERENCES

1. Miyake, Y., and Tsunogai, S., (1968) "Evaporation of Iodine From the Ocean". Journal of Geophysical Research, Vol. 68, No. 1, July 1968, pp. 3989-3993.
2. Tsunogai, S., and Sase, T., (1969). "Formation of Iodide-Iodine in the Ocean". Deep-Sea Research, 1969, Vol. 16, pp. 489-496.
3. Millan, M. M., Stanley, J., and Davies, J., (1970). "Study of the Barringer Refractor Plate Correlation Spectrometer as a Remote Sensing Instrument". Institute for Aerospace Studies, University of Toronto, Report No. 146, August, 1970.
4. Barringer Research (1969) "Final Report Absorption Spectrometer Modifications and Flight Testing" NASA Contract NAS 9-7958 Jan. 1969 BR6 Report TR69-79.
5. Barringer Research (1970) "Final Report Absorption Spectrometer Balloon Flight and Iodine Investigations, NASA Contract NAS9-9492, BRL Report TR70-148.
6. Barringer Research (1968) "Final Report, "The Feasibility of Detection and Classification of Fish Oil Slicks by Remote Sensing" NASA Contract NASW-1642 BRL Report TR68-54.
7. Ackman R.G., and Tocher C.S., "Occurrence of Dimethyl-B-Propiothetin in Marine Phytoplankton" J. Fish, Res. Bd. Canada 23(3) 1966.







**BARRINGER RESEARCH**  
LIMITED

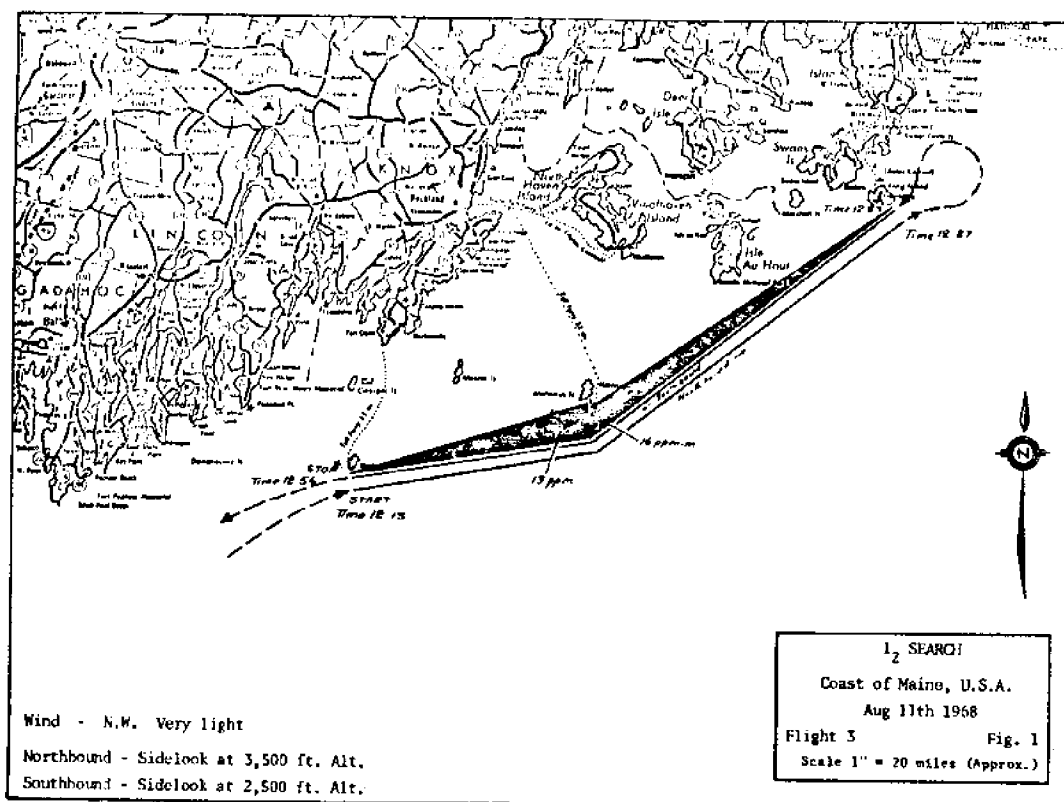


FIGURE 4

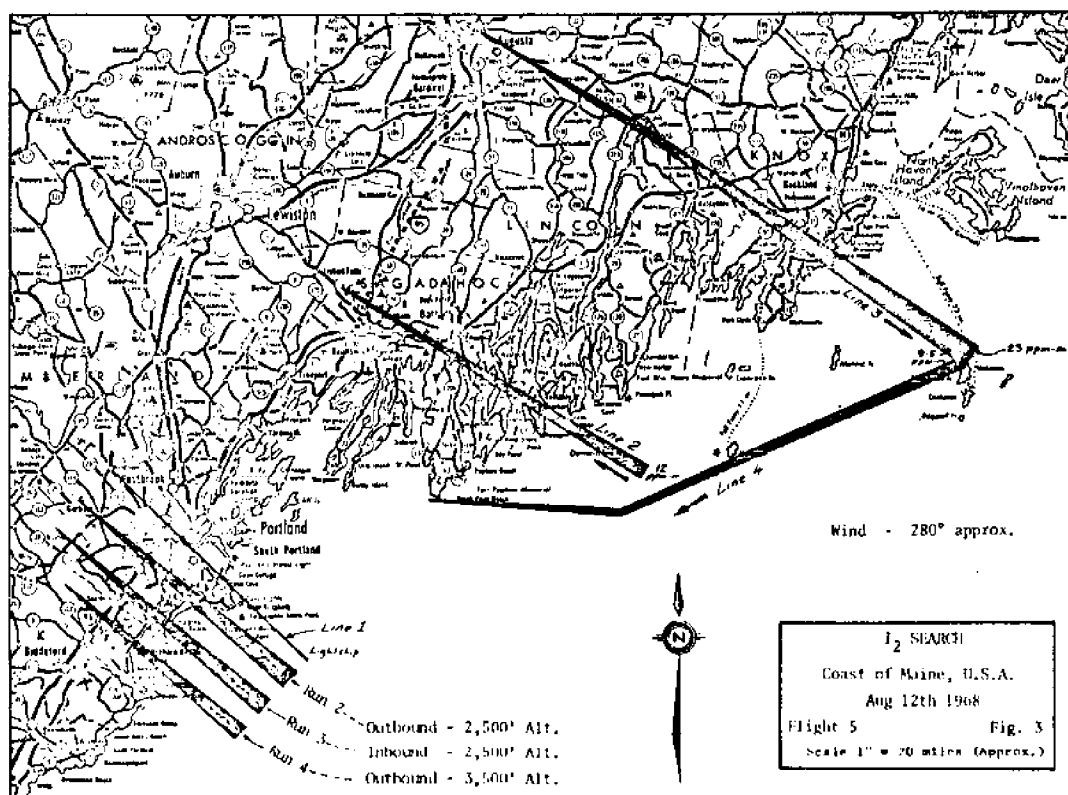


FIGURE 5

THE UNITED STATES OF AMERICA  
DOES hereby certify that  
the following is a true and  
correct copy of the  
original as the same appears  
in the records of the  
Department of the Interior  
at Washington, D. C.  
this 1st day of January  
1901.

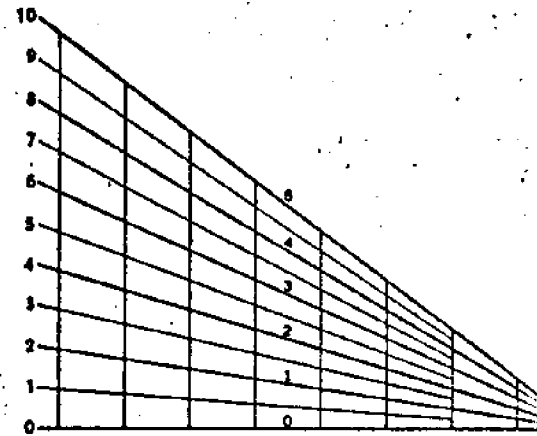






The numerical  
skywave correction indi-  
cates to which it applies.

EXAMPLE: +79°



LORAN LINEAR INTERPOLATOR  
**SITES**

⊙  
AERO  
Rot W&G

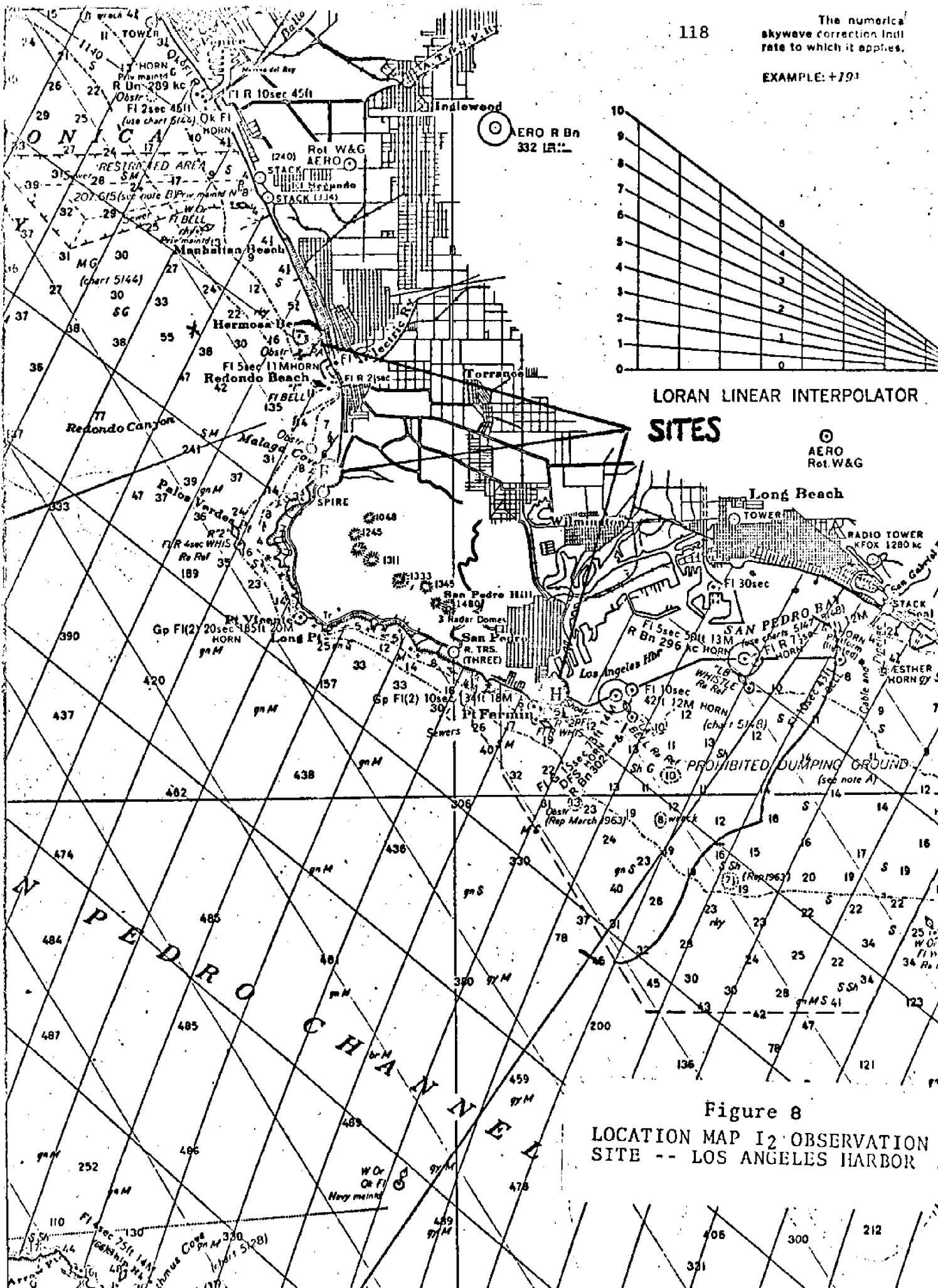
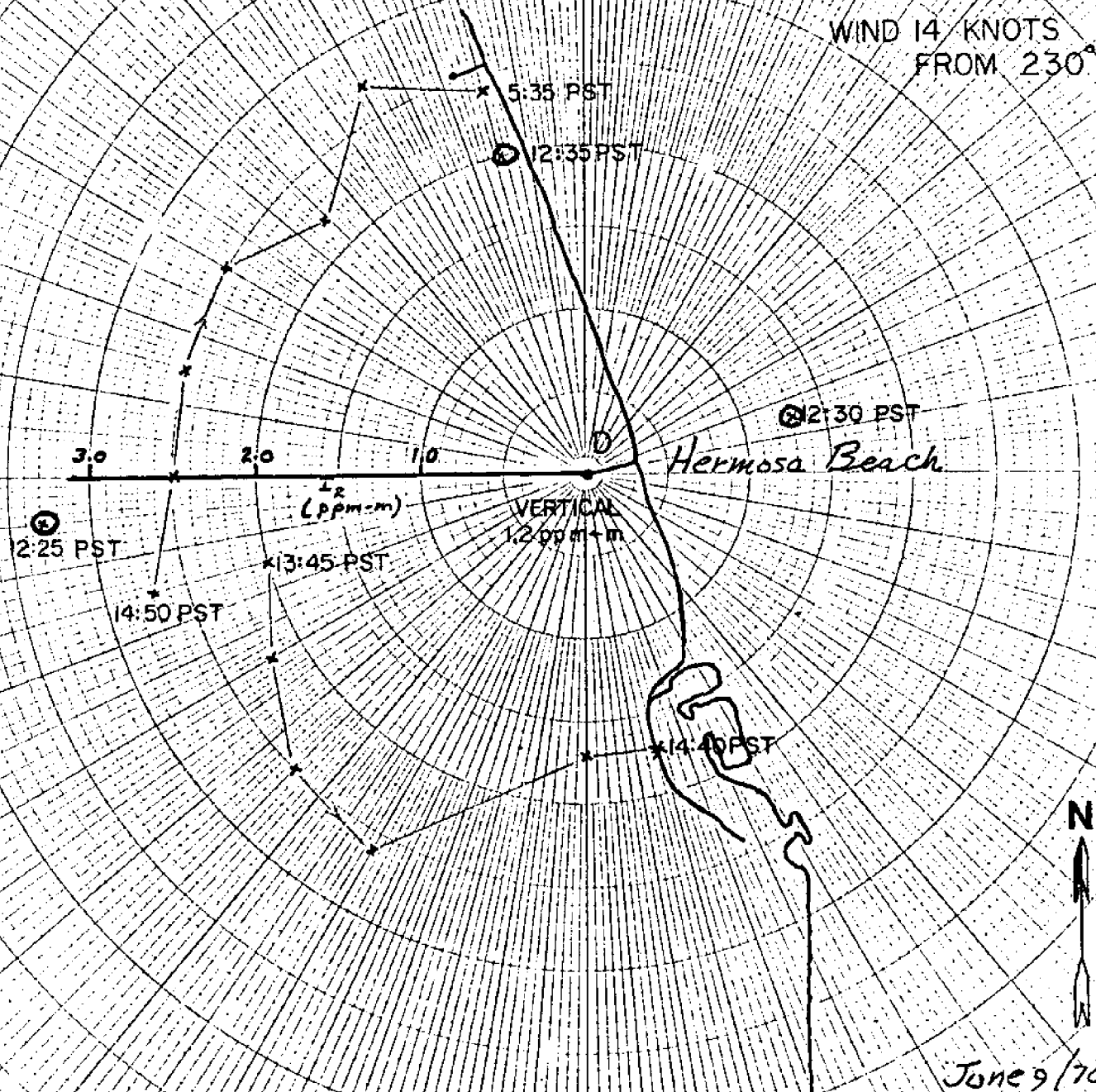


Figure 8  
LOCATION MAP I2 OBSERVATION  
SITE -- LOS ANGELES HARBOR

Figure 9  
IODINE LEVELS OFFSHORE FROM  
HERMOSA BEACH PIER



30°  
350°

20°  
300°

10°  
350°

0

350°  
10°

340°  
20°

330°  
30°

120°  
53

Figure 10  
IODINE LEVEL MEASURED FROM  
PALOS VERDES SWIMMING POOL

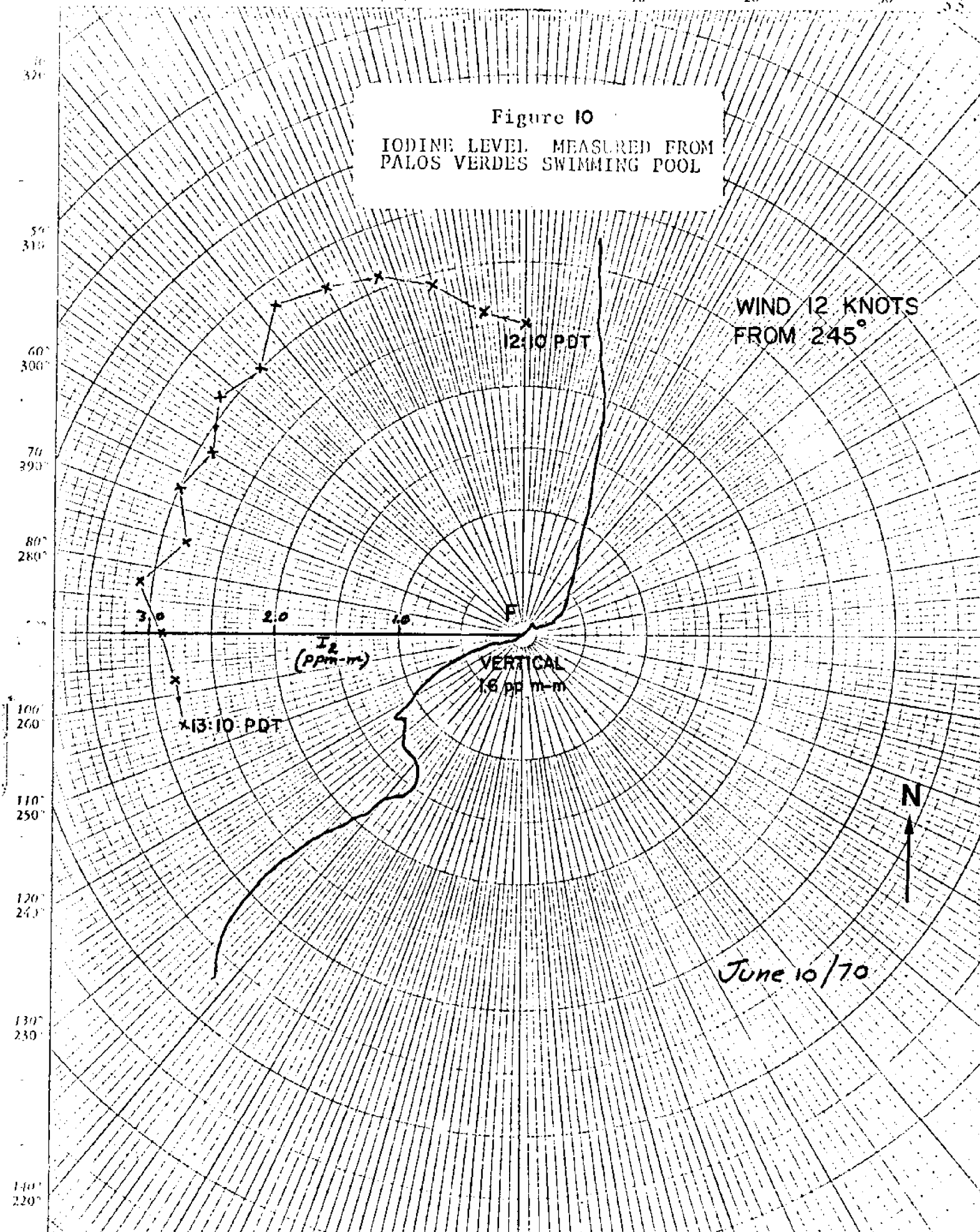


Figure 11  
IODINE LEVELS MEASURED FROM  
CABRILLO FISHING PIER  
L.A. HARBOR

WIND 6-11 KNOTS  
FROM 225°

14:05 PDT

$I_2$   
(ppm·m)

VERTICAL  
16.22 ppm·m

3.0

2.0

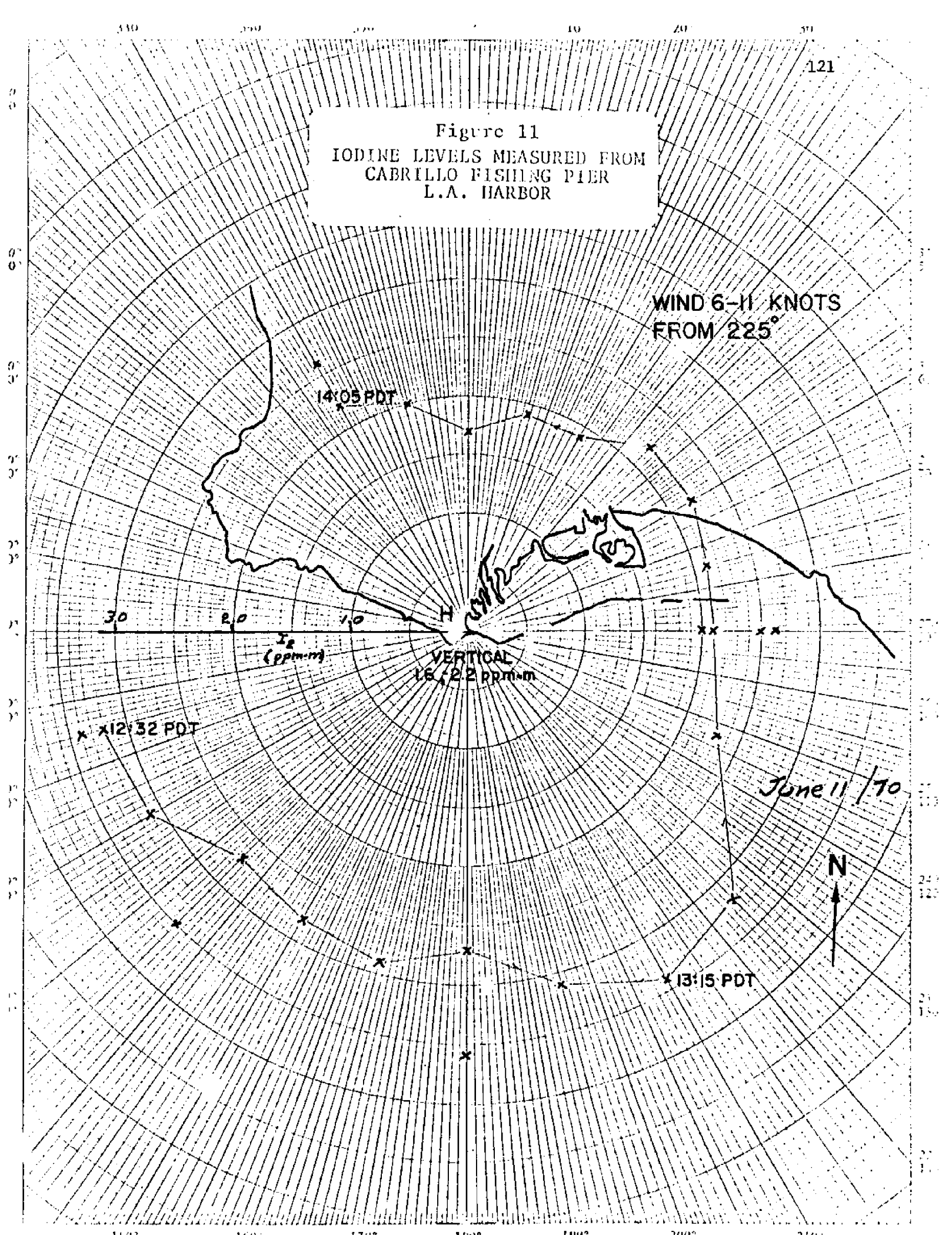
1.0

12:32 PDT

June 11 / 70

N

13:15 PDT





340°

330°

320°

310°

300°

290°

280°

122

Figure 12  
IODINE LEVELS MEASURED FROM  
SHORELINE PARK  
SANTA BARBARA

WIND 6 KNOTS  
FROM 270°

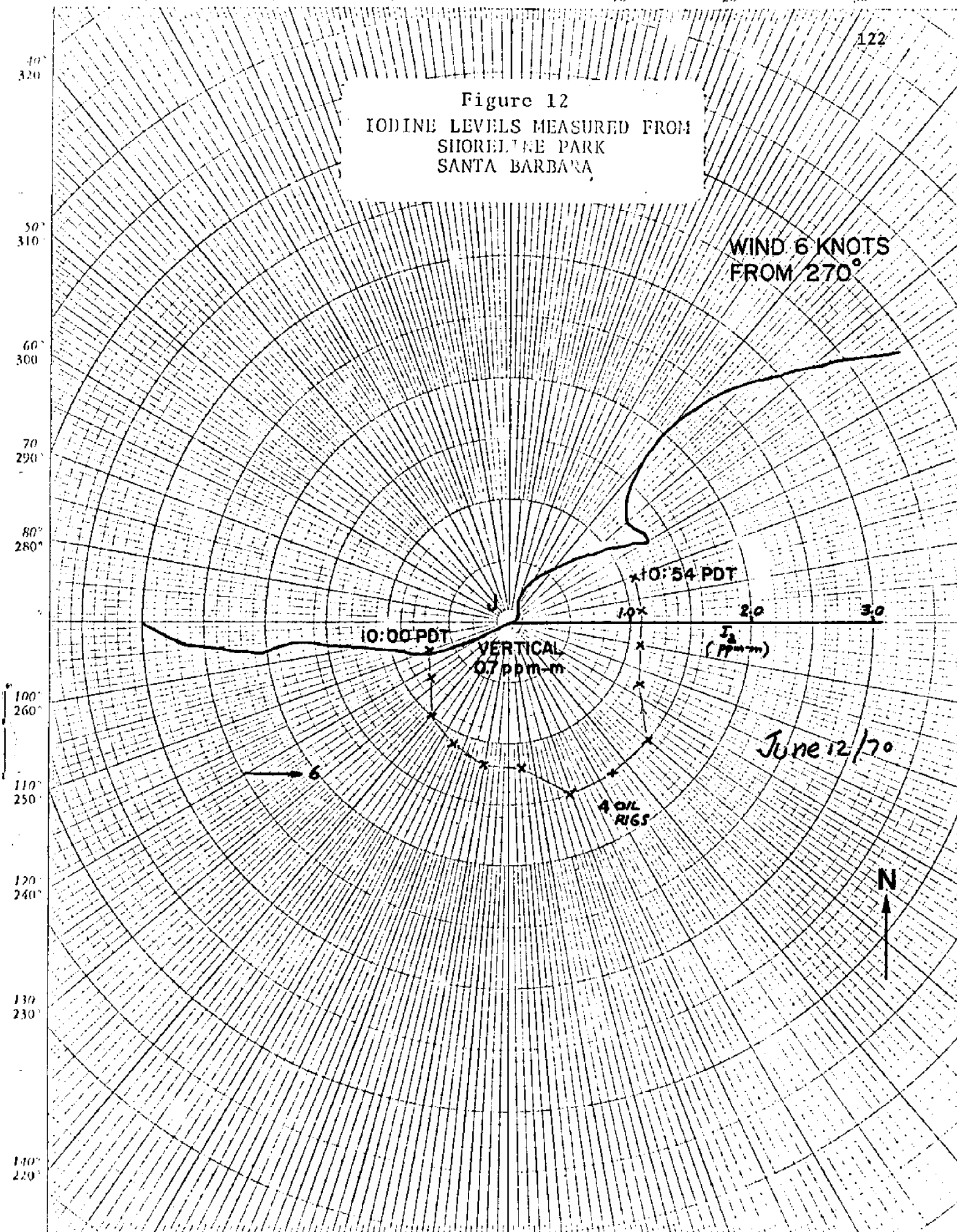
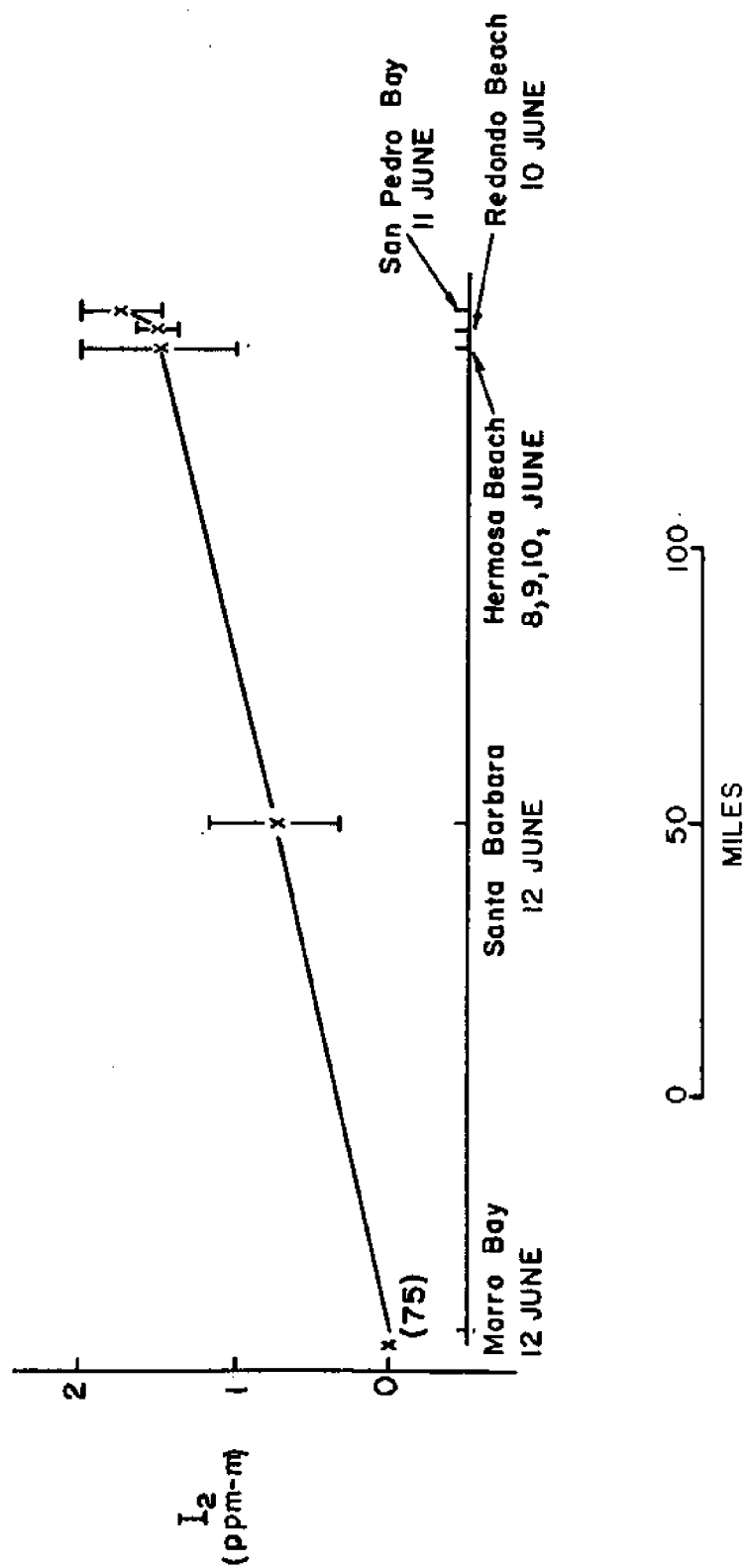


FIGURE 13  
UPWARD LOOKING IODINE LEVELS  
SECTION NW-SE  
MORRO BAY-LONG BEACH



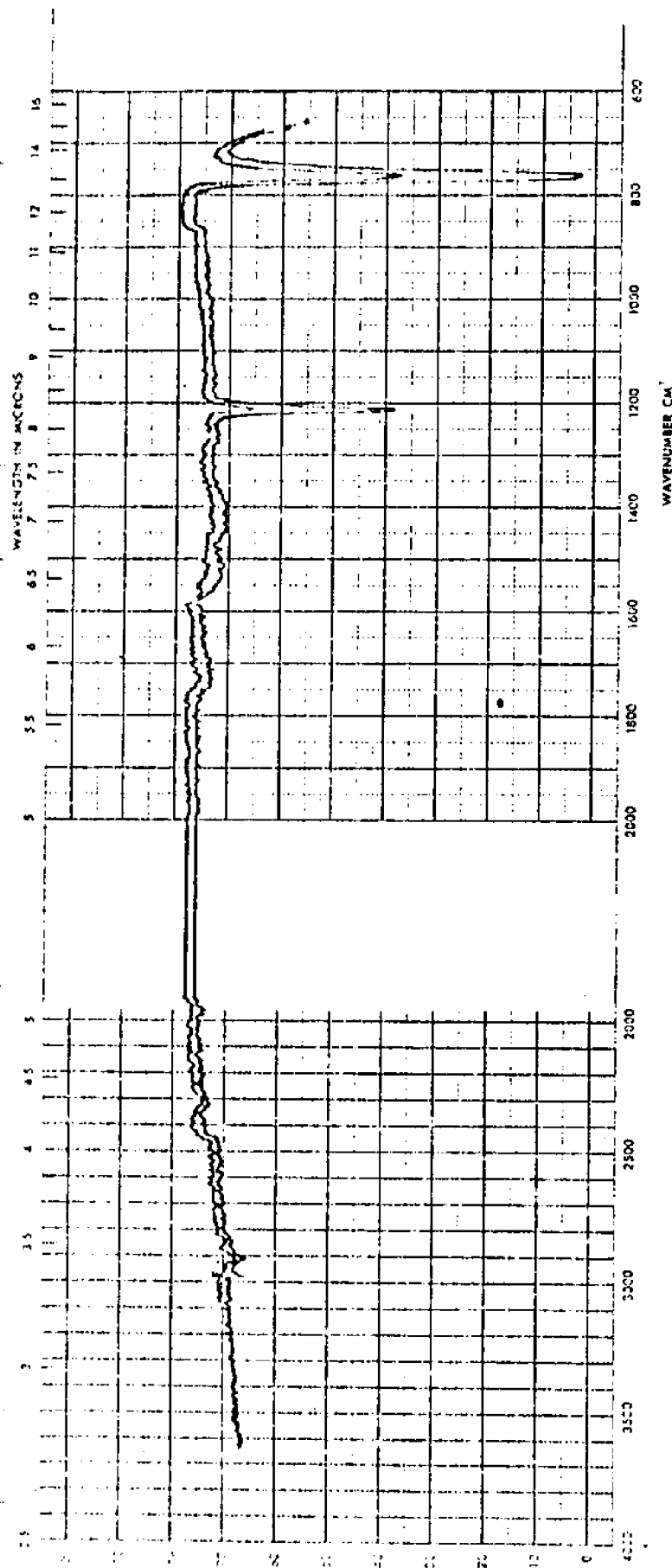
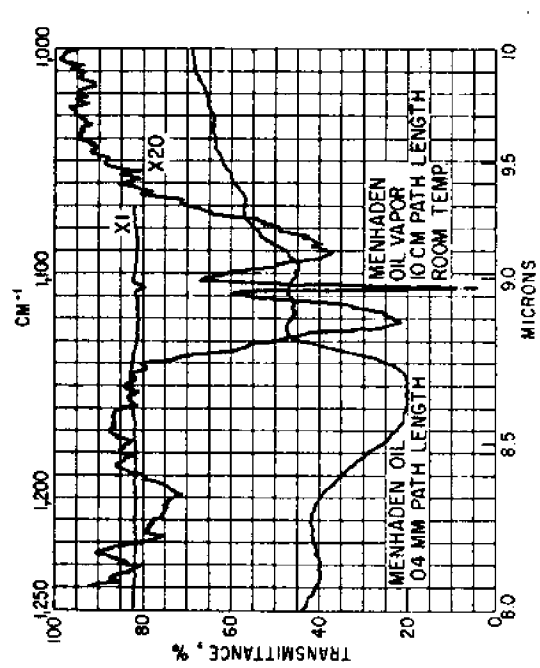


FIGURE 14 COD LIVER OIL VAPOUR



-Film of menhaden oil compared with 10 cm path-length.

FIGURE 15



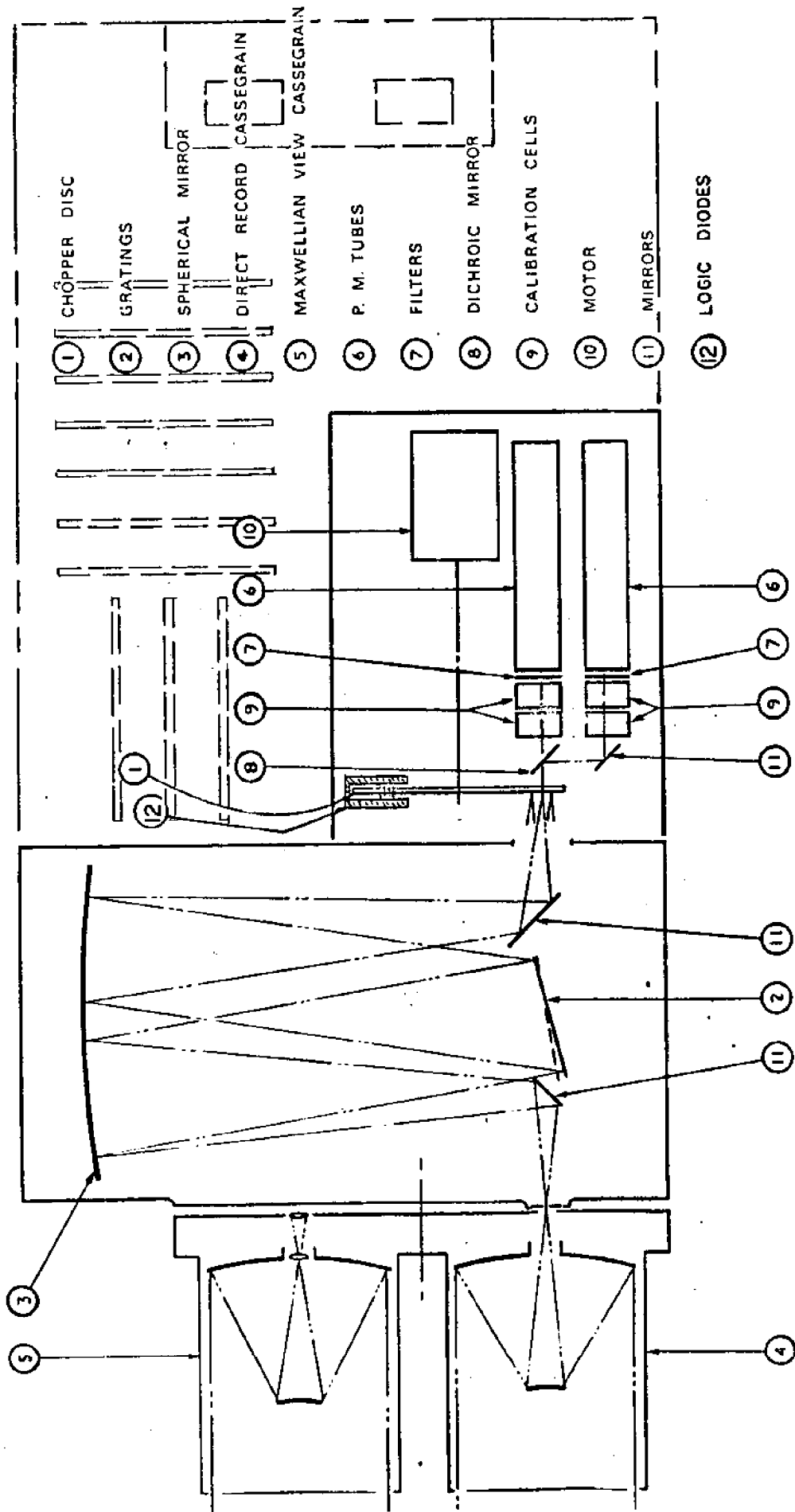
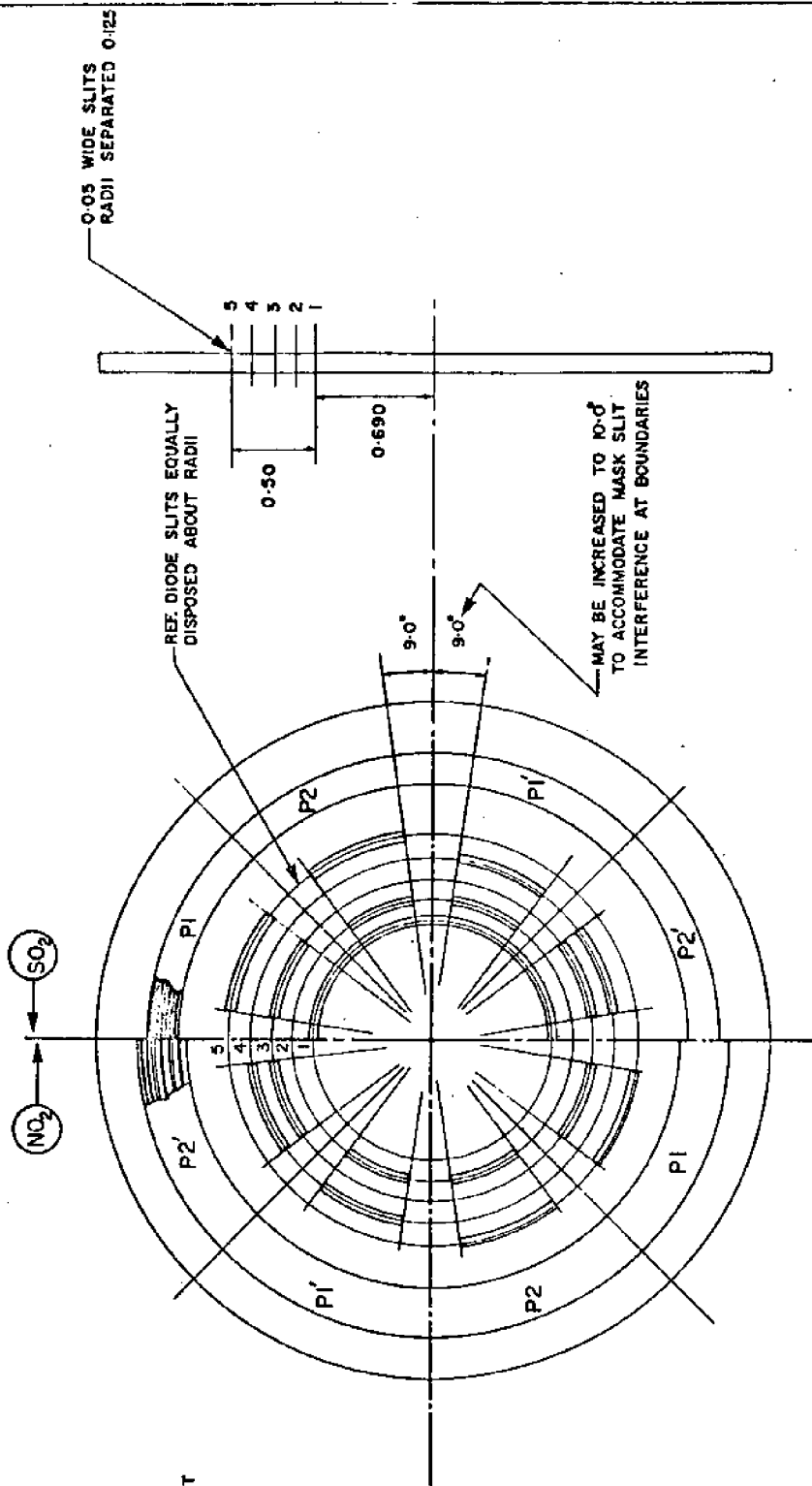


FIGURE 16

DO NOT SCALE DRAWING

DATE	BY	CHKD	APP'D



ORG N°	OP	DISC POS N°
SO <sub>2</sub>		
P1	MAX	1
P2	MIN	2
P1'	MAX	3
P2'	MIN	4
NO <sub>2</sub>		
P1	MAX	5
P2	MIN	6
P1'	MAX	7
P2'	MIN	8

ITEM		REQD		PART NO.		DESCRIPTION	
1		1		BARRINGER RESEARCH		CHOPPER DISC OPTICAL PATTERN	
2		2		H-6-70		2 GAS CORRELATION SPECTROMETER	
3		3		SCT		H-6-70	
4		4		SCT		H-6-70	
5		5		SCT		H-6-70	
6		6		SCT		H-6-70	
7		7		SCT		H-6-70	
8		8		SCT		H-6-70	
9		9		SCT		H-6-70	
10		10		SCT		H-6-70	
11		11		SCT		H-6-70	
12		12		SCT		H-6-70	
13		13		SCT		H-6-70	
14		14		SCT		H-6-70	
15		15		SCT		H-6-70	
16		16		SCT		H-6-70	
17		17		SCT		H-6-70	
18		18		SCT		H-6-70	
19		19		SCT		H-6-70	
20		20		SCT		H-6-70	
21		21		SCT		H-6-70	
22		22		SCT		H-6-70	
23		23		SCT		H-6-70	
24		24		SCT		H-6-70	
25		25		SCT		H-6-70	
26		26		SCT		H-6-70	
27		27		SCT		H-6-70	
28		28		SCT		H-6-70	
29		29		SCT		H-6-70	
30		30		SCT		H-6-70	
31		31		SCT		H-6-70	
32		32		SCT		H-6-70	
33		33		SCT		H-6-70	
34		34		SCT		H-6-70	
35		35		SCT		H-6-70	
36		36		SCT		H-6-70	
37		37		SCT		H-6-70	
38		38		SCT		H-6-70	
39		39		SCT		H-6-70	
40		40		SCT		H-6-70	
41		41		SCT		H-6-70	
42		42		SCT		H-6-70	
43		43		SCT		H-6-70	
44		44		SCT		H-6-70	
45		45		SCT		H-6-70	
46		46		SCT		H-6-70	
47		47		SCT		H-6-70	
48		48		SCT		H-6-70	
49		49		SCT		H-6-70	
50		50		SCT		H-6-70	
51		51		SCT		H-6-70	
52		52		SCT		H-6-70	
53		53		SCT		H-6-70	
54		54		SCT		H-6-70	
55		55		SCT		H-6-70	
56		56		SCT		H-6-70	
57		57		SCT		H-6-70	
58		58		SCT		H-6-70	
59		59		SCT		H-6-70	
60		60		SCT		H-6-70	
61		61		SCT		H-6-70	
62		62		SCT		H-6-70	
63		63		SCT		H-6-70	
64		64		SCT		H-6-70	
65		65		SCT		H-6-70	
66		66		SCT		H-6-70	
67		67		SCT		H-6-70	
68		68		SCT		H-6-70	
69		69		SCT		H-6-70	
70		70		SCT		H-6-70	
71		71		SCT		H-6-70	
72		72		SCT		H-6-70	
73		73		SCT		H-6-70	
74		74		SCT		H-6-70	
75		75		SCT		H-6-70	
76		76		SCT		H-6-70	
77		77		SCT		H-6-70	
78		78		SCT		H-6-70	
79		79		SCT		H-6-70	
80		80		SCT		H-6-70	
81		81		SCT		H-6-70	
82		82		SCT		H-6-70	
83		83		SCT		H-6-70	
84		84		SCT		H-6-70	
85		85		SCT		H-6-70	
86		86		SCT		H-6-70	
87		87		SCT		H-6-70	
88		88		SCT		H-6-70	
89		89		SCT		H-6-70	
90		90		SCT		H-6-70	
91		91		SCT		H-6-70	
92		92		SCT		H-6-70	
93		93		SCT		H-6-70	
94		94		SCT		H-6-70	
95		95		SCT		H-6-70	
96		96		SCT		H-6-70	
97		97		SCT		H-6-70	
98		98		SCT		H-6-70	
99		99		SCT		H-6-70	
100		100		SCT		H-6-70	

FIGURE 17

1. REMOVE BURRS & BREAK ALL SHARP EDGES.

## REMOTE SENSING OF MARINE AND FISHERIES RESOURCES BY FLOURESCENCE METHODS\*

by

A. W. Hornig  
Baird-Atomic, Inc.  
Bedford, Massachusetts

## INTRODUCTION

Detection and identification of marine biota and pollutants must be accomplished remotely if large ocean areas are to be surveyed rapidly and economically. Optical remote sensing usually involves the sun as a source and depends on selective absorption and scattering. While the sun is powerful, broad-band and free, aircraft and satellite sensors suffer a large decrease in sensitivity on cloudy or overcast days and are useless at night.

An attractive alternative and supplement to sensing the color of sun-illuminated scenes involves active stimulation of fluorescence. This technique is best used at night and, hence, complements color measurements during the day. The particular advantage of the technique involves the double specificity of excitation and luminescence wavelengths, and a high inherent sensitivity for certain materials of marine interest.

The success of active-stimulation luminescence techniques depends on the existence of powerful light sources which can produce a surface irradiance approaching that of the sun (over limited areas for short times). Future improvement in such sources will result in continual upgrading of the technique, resulting in increased aircraft altitude, spatial resolution and spectral resolution.

For eventual satellite applications laser sources must be employed. Used in aircraft, lasers will allow daylight application of the technique,

---

This paper describes work supported, in part, by the Spacecraft Oceanography of the U. S. Naval Oceanographic Office, Washington, D. C.

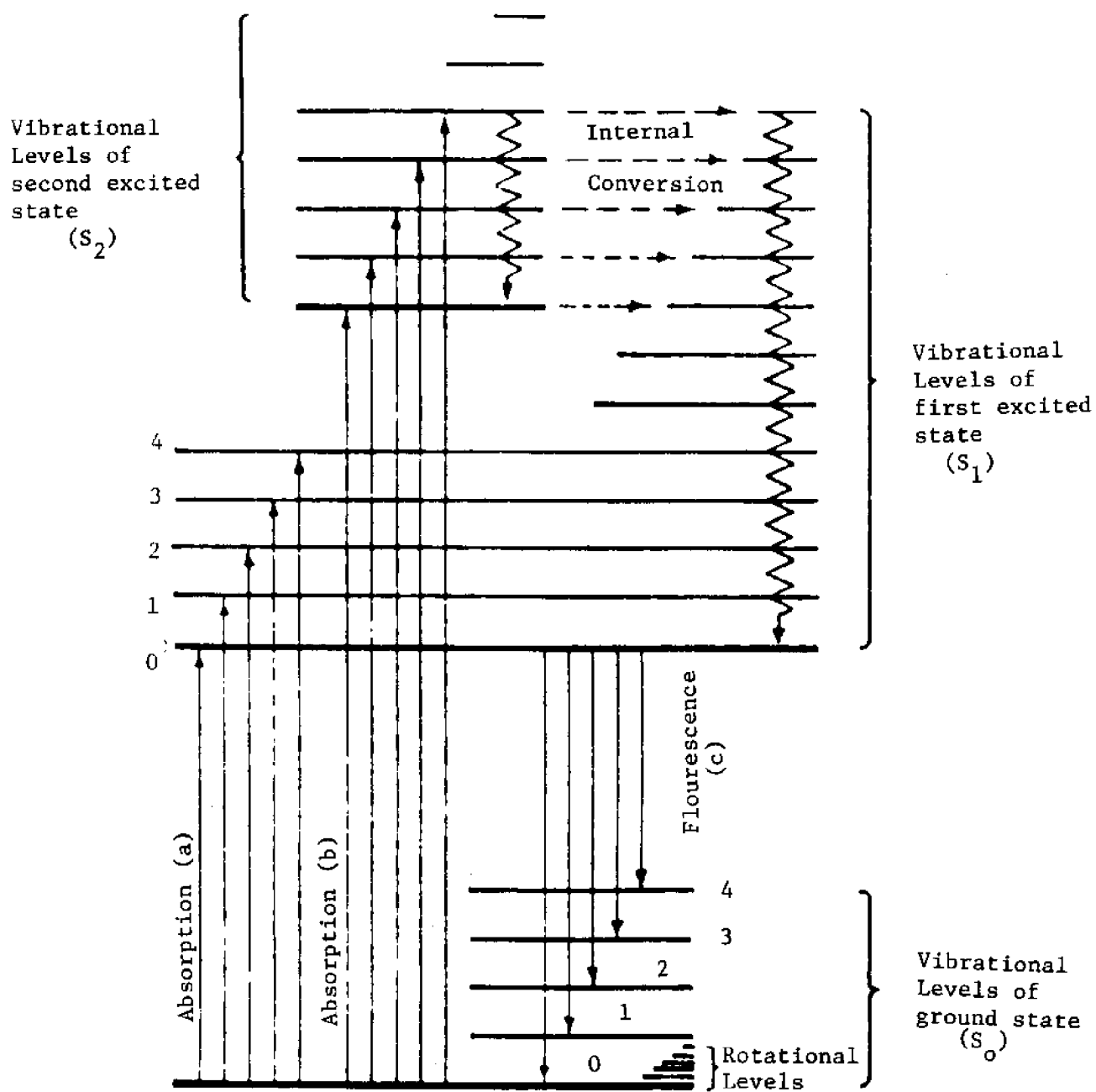
but with loss of excitation specificity.

Calculations indicate that with non-laser sources now available, good optics and standard detectors, materials of marine interest may be sensed at altitudes exceeding 1000 meters with good spectral definition of both excitation and luminescence wavelengths.

#### FLOURESCENCE METHODS

The most common optical methods of remote sensing involve the selective absorption and scattering of radiation. In multi-spectral photography, for example, the target acquires a color because of selective absorption of solar radiation. Further contrast results from a difference in scattering and reflection between the target and the surrounding background. While this technique has already proven to be very valuable, it has several drawbacks. Since the "color" depends on the subtraction of certain wavelengths from the essentially white light of the sun, it is difficult to gain great specificity. Thus, in some of the remarkable photographs of the earth from satellites there is often a color difference in waters; however, there is also much disagreement as to the interpretation and identification of the phenomena responsible.

In Slide 1 we relate and define absorption and flourescence by means of a generalized energy level diagram which would apply to a typical organic material. Light is absorbed by the molecule in its ground state--usually a singlet--here designated  $S_0$ . The absorption of energy raises it to one of a number of higher electronic singlet levels, designated  $S_1$ ,  $S_2$ , etc. These levels are further split by small vibrational differences into sub-levels, indicated by fine lines in the diagram. Further rotational splitting is usually masked by the broadening caused by molecular collisions in the matrix which may be solid or liquid.



SLIDE 1 Transitions giving rise to absorption and fluorescence emission spectra.

The vibrational spacing in organic molecules is typically  $700\text{ cm}^{-1}$ , whereas the thermal energy at room temperature ( $300^\circ\text{K}$ ) is only about  $210\text{ cm}^{-1}$ . As a result, the major  $S_0$  population is in the zero vibrational state. Absorption then occurs to the various vibrational sub-levels of the higher singlets. This selective absorption is the basis of identification by absorption spectroscopy.

Once excited, a molecule may return to the ground state by radiating light or by radiationless transitions (aided by molecular collisions) which result in dissipation of energy in the form of heat. It is almost universally true that aromatic organic molecules excited to higher states will decay, stepwise, to the zero-vibrational level of the first excited singlet,  $S_1$ , by radiationless processes. These are indicated on the slide by zig-zag lines. In fluorescent molecules the radiative decay from  $S_1$  to ground is much more probable than the radiationless, and this is termed fluorescence.

Fluorescence, originating in the zero-vibrational level of  $S_1$ , may terminate at any of the ground-vibrational states. Thus, fluorescence may also have vibrational structure very similar to absorption.

Comparison of possible absorption and fluorescence transitions reveals that the transition between zero-vibrational levels, the so-called 0-0 transition, is common to absorption and fluorescence, resulting in self-absorption at the common wavelength. All other fluorescence transitions occur at lower energies (and longer wavelengths) than the corresponding absorption. As a result, fluorescence is found to occur at wavelengths just greater than the longest wavelength absorption. In actuality not even the 0-0 transitions coincide because of possible adjustment of inter-atomic distances occurring in the excited state.

A third possibility exists for a molecule in the  $S_1$  state-- and this is not depicted on the slide. It may undergo a radiationless intersystem crossing to an excited triplet level,  $T_1$ , lying slightly below  $S_1$ . Such a triplet may also radiate, resulting in phosphorescence at even longer wavelengths. Because the radiative lifetime of the triplet is so much longer than the singlets (typically one second compared to  $10^{-8}$  seconds), non-radiative processes usually dominate at room temperature and phosphorescence is not observed. Since we are interested in room-temperature luminescence, we shall disregard triplets except as further non-radiative paths for deexcitation from  $S_1$ .

To continue our contrast of absorption and emission processes, note that in an absorption experiment one measures an incident intensity and a transmitted intensity, both at the same wavelength, which are almost equal in magnitude. The small intensity difference is the desired information about the sample. In a fluorescence experiment the incident (exciting) light is at one wavelength and the emitted light (fluorescence) is at another wavelength. Since the incident light can be made monochromatic, its contribution to background at the fluorescence wavelength can be made very small. As a result, the fluorescence, which contains the desired information, is measured against an almost zero background. It is this difference which makes fluorescence methods so much more sensitive than absorption for materials which fluoresce with reasonable efficiency. Standard laboratory instrumentation, such as the Baird-Atomic "Fluorispec" Fluorescence Spectrophotometer shown in Slide 2, allows measurement of sub-nanogram quantities of material corresponding to concentrations of less than one part per billion.

Fluorescence spectroscopy has another advantage, in addition to great sensitivity. This results from the double specificity of excitation and emission wavelengths. In absorption spectroscopy the sum of the absorbances





of all components is measured. In fluorescence spectroscopy it is often possible to excite selectively emission from each of several components in a mixture. This will be illustrated later for cases of marine interest.

Before concluding this physical description of fluorescence, I would like to mention a fluorescence technique which does not require a separate source of excitation and which works during the day. This involves sun-induced fluorescence. Since the sun is a broad-band source of radiation spanning the infrared, visible and near-ultraviolet, it will also excite fluorescence. The basic problem with sun-excitation is that the sun also illuminates at the fluorescence wavelength, thus making it difficult to measure a weak fluorescence against a strong sun-scatter background. This difficulty can be ameliorated by restricting detection to Fraunhofer lines--narrow spectral regions where the sun's intensity is much reduced due to absorption in gases surrounding the sun. An instrument based on this principle has been built by the Perkin-Elmer Corporation for the U. S. Geological Survey and is called a Fraunhofer Line Discriminator (FLD). Initial tests, using a single Fraunhofer line at 589 nm, have demonstrated utility for the monitoring of river currents by the fluorescence of the dye Rhodamine WT. A second-generation prototype, operating at 486.1 nm, is currently under test and may be useful for a variety of materials of marine interest.

Unfortunately the specificity of such an instrument is limited both because of the limited choice of detection wavelengths and because the sun will excite all fluorescent materials present, lowering the selective excitation possible with an external source at night.

#### FLOURESCENCE OF MARINE BIOTA AND POLLUTANTS

We next consider what materials of marine interest may be expected to

fluoresce usefully. The advantages claimed for fluorescence spectroscopy are somewhat circumscribed by the limited number of materials which fluoresce strongly. Thus, saturated aliphatics fluoresce not at all or very weakly. However, the greater part of aromatic and conjugated unsaturated compounds are fluorescent, and non-fluorescence is rather an exception. Fortunately it is just these materials which often occur in low concentration in marine biota and which can serve for identification. Fortunately also water itself does not fluoresce, nor do the common inorganic salts occurring in sea-water.

In Slide 3 we list some of the materials in the marine environment which may be usefully detected and identified by fluorescence. We next illustrate the excitation/emission spectra of several marine pollutants and biota from laboratory measurements, many of them taken against a sea-water background. In Slide 4 we see the excitation and emission spectra of a Number 2 mineral oil. This is just the most prominent fluorescence. Other crude oil samples will have slightly different signatures which will often allow identification of the oil. In Slide 5 we see spectra for an industrial pollutant associated with the paper pulp industry, lignin sulfonate. In this slide you will note two excitation and two emission spectra, illustrating selective excitation of different fluorescing components of the complex lignin system.

Turning to marine biota, Slide 6 illustrated multiple fluorescence excitation/emission spectra from the scales of a fresh smelt (from the local grocery store). Preliminary examination of several other species makes us believe that the native fluorescence of fish scales may allow remote detection and identification of schooling fish at or near the water surface. In Slides 7 and 8 we illustrate the multiple excitation/emission spectra of pure body oil extracted from Spanish Sardine. The long wavelength emission at 670 nm has been identified as due to a type of chlorophyll, presumably originating

SLIDE 3 LUMINESCENT MATERIALS ASSOCIATED WITH  
THE MARINE ENVIRONMENT

MARINE PLANTS:

ALGAE, PHYTOPLANKTON

MARINE ANIMALS:

FISH (SCALES), BACTERIA,  
ZOO PLANKTON

MARINE DECAY:

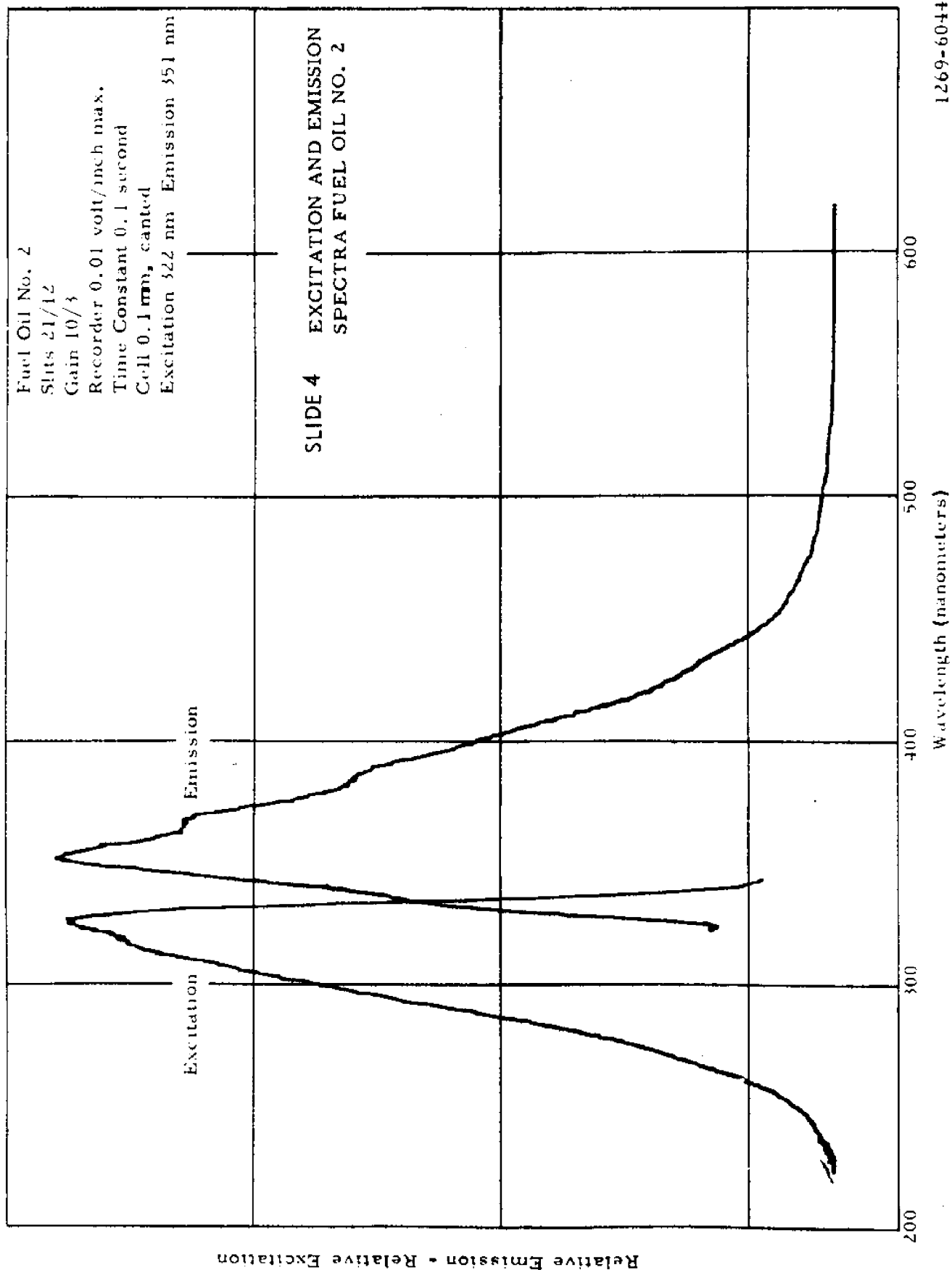
FISH OILS, HUMUS, GELBSTOFF,  
CAROTENOIDS, CHLOROPHYLL,  
PTERINS

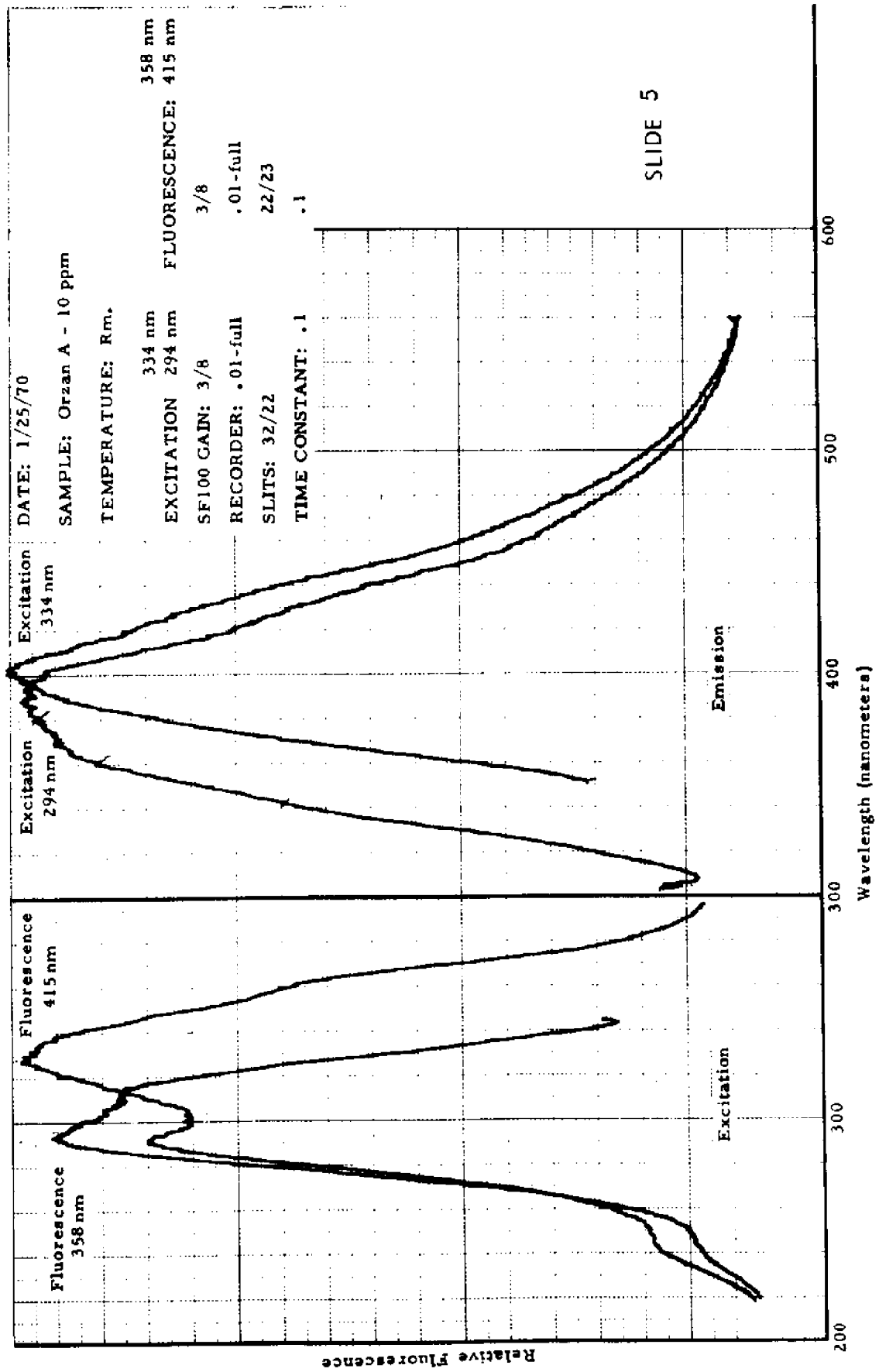
MARINE POLLUTANTS:

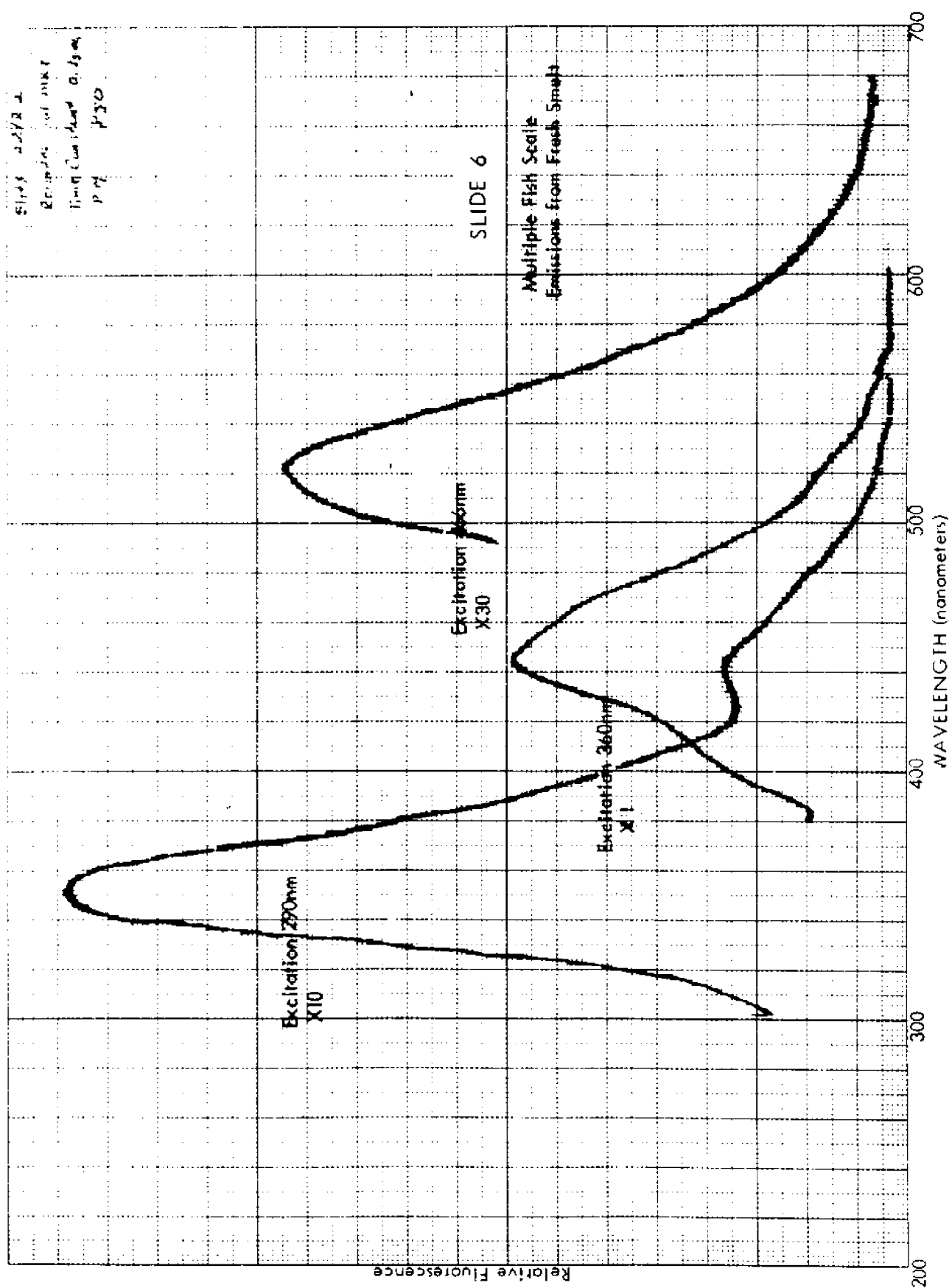
CRUDE OIL, LIGNIN SULFONATES  
(SPECIAL INDUSTRIAL)

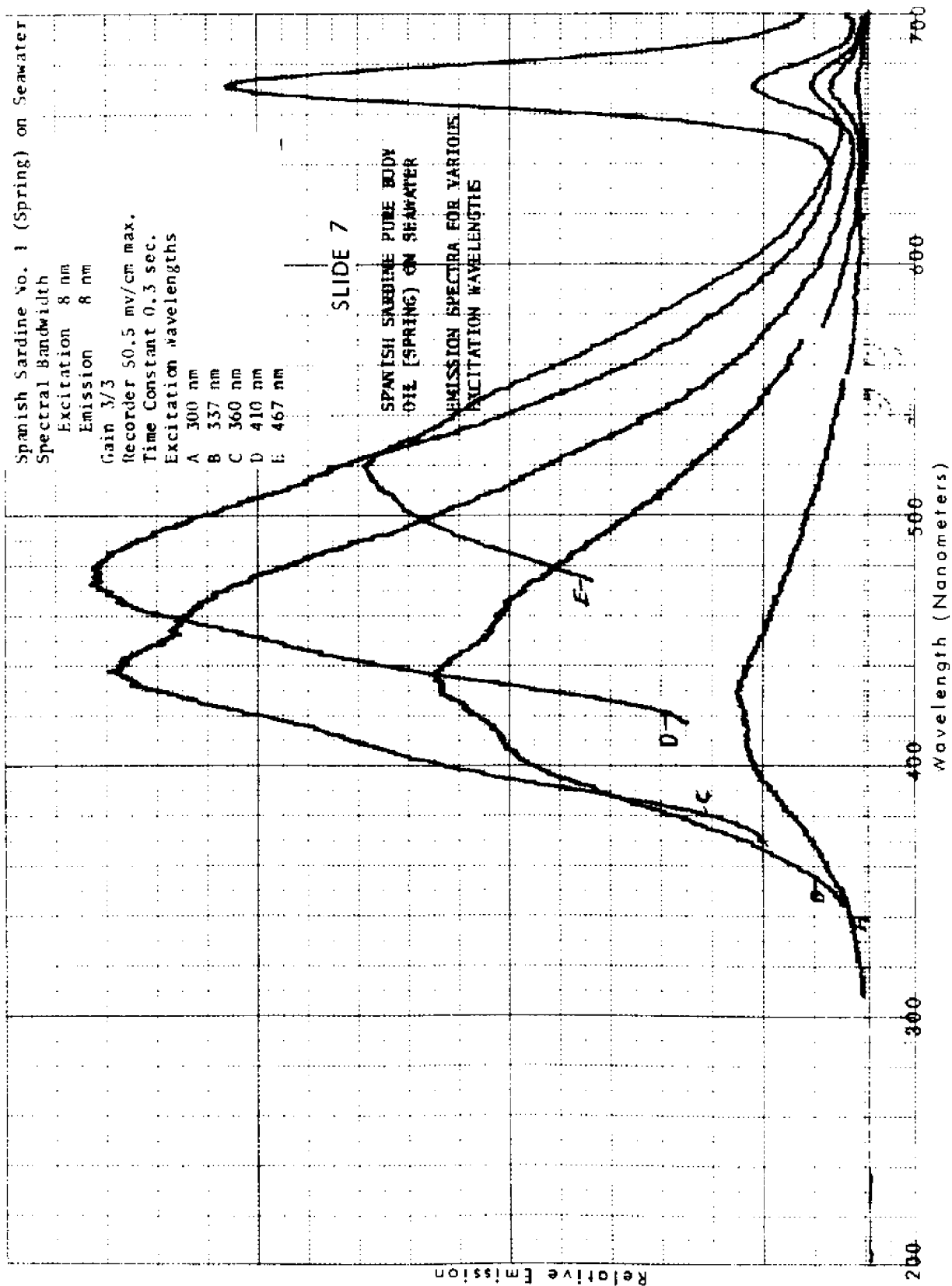
BIOLUMINESCENT ANIMALS:

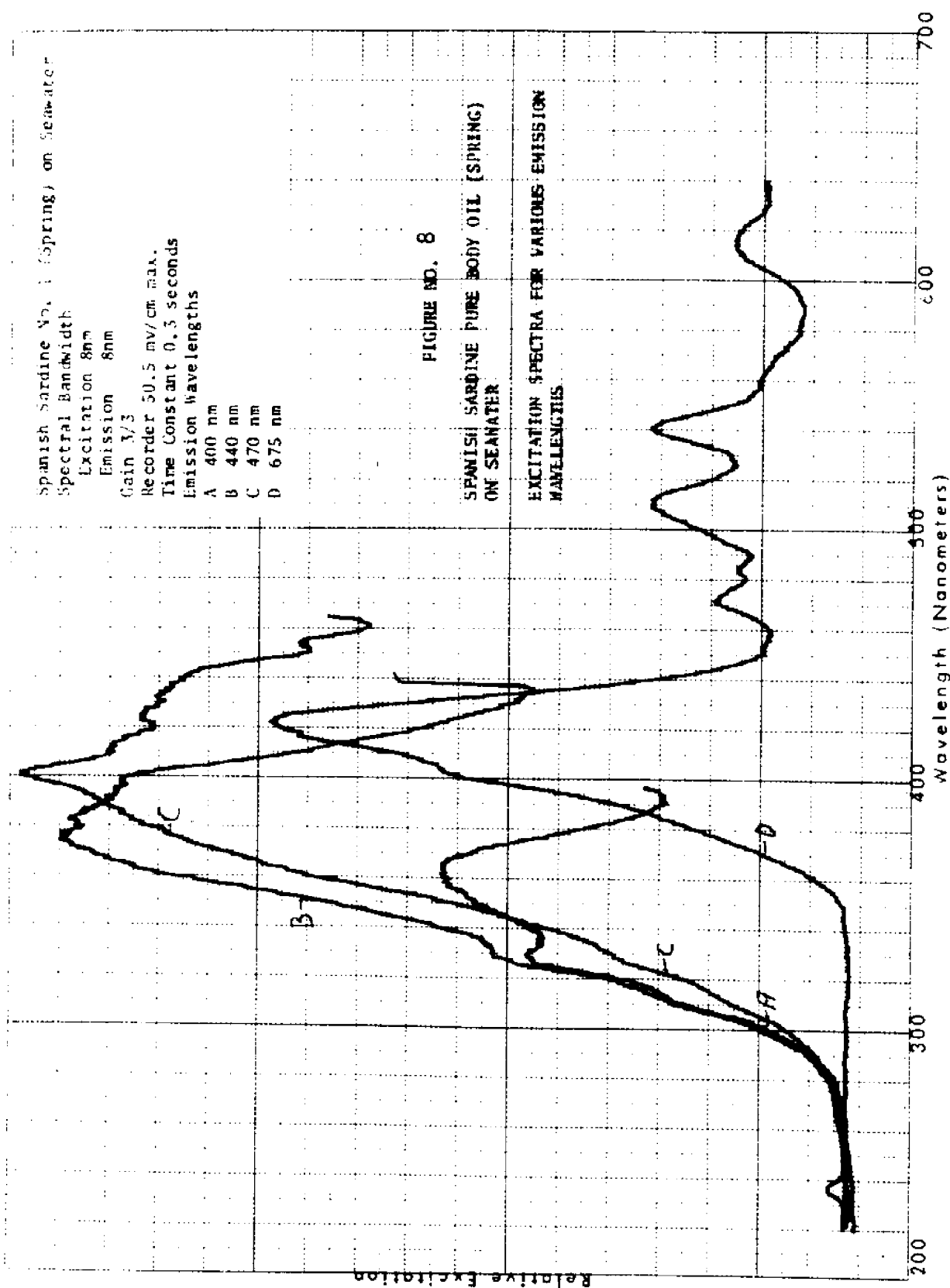
DINOFLAGELLATES











SLIDE 8



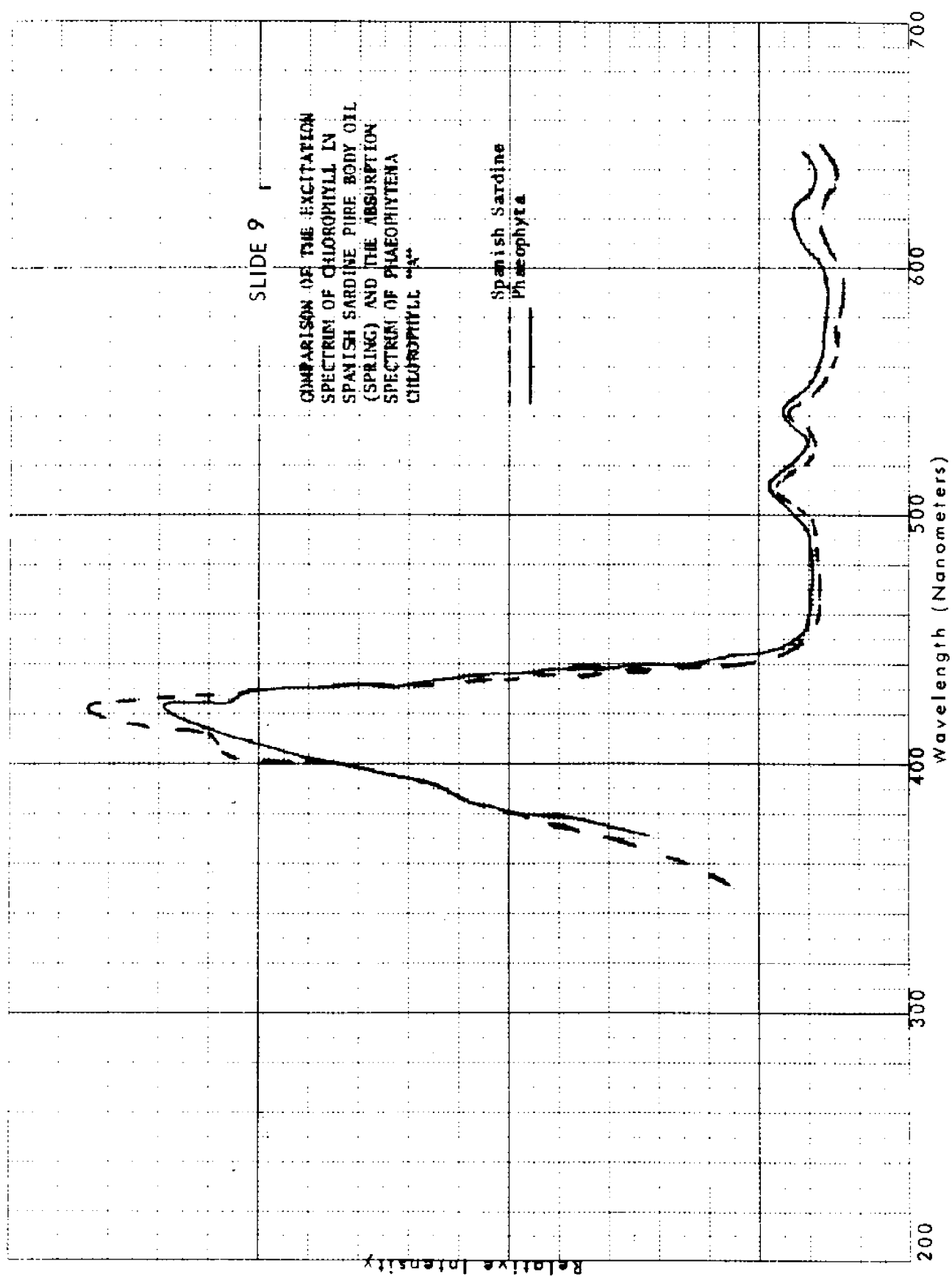
from recently ingested plankton. This identification is made from the rarity of emission at such long wavelengths and the similarity of excitation with that of a known sample. In Slide 9 we have superposed excitation data from Slide 7 with absorption data for chlorophyll a in phaeophytina\* (supplied by Dr. Lorenzen of WHOI).

To complete our sampling we shown in Slide 10 the excitation/emission spectra of *Anacharis*, freshly removed from our aquarium. In this case the leaves were placed flat in a demountable cuvette and examined front-surface. The emission resembles that of chlorophyll a but falls at longer wavelengths.

#### FISH OIL FLOURESCENCE

To illustrate the potential of remote sensing by flourescence I shall next summarize some of the results of a study of the luminescence of fish oils, performed by the Spacecraft Oceanography Project of the U. S. Naval Oceanographic Office, under direction of the Bureau of Commercial Fisheries. The intent of the study was to establish excitation/luminescence signatures of fish oils and determine whether remote detection and identification was possible, employing arc-stimulated flourescence. Such sensing would serve as an indirect method of locating, identifying and possibly quantitating schooling fish.

Because of the difficulty of collecting actual fish oil slicks of known identity and freshness, initial studies were performed in oils extracted from freshly caught fish as outlined in Slide 11. The variants were prepared in order to determine whether the extracted pure body oils were representative of actual fish slicks which would be mixed with sea water and subjected to oxidation from the air. Samples were supplied in the Fall and Spring to determine whether signatures changed during spawning.



DATE: 1/18/71

SAMPLE: Anacharis

EXCITATION: 470 nm FLOURESCENCE: 680 nm

SF 1 GAIN: 1/1

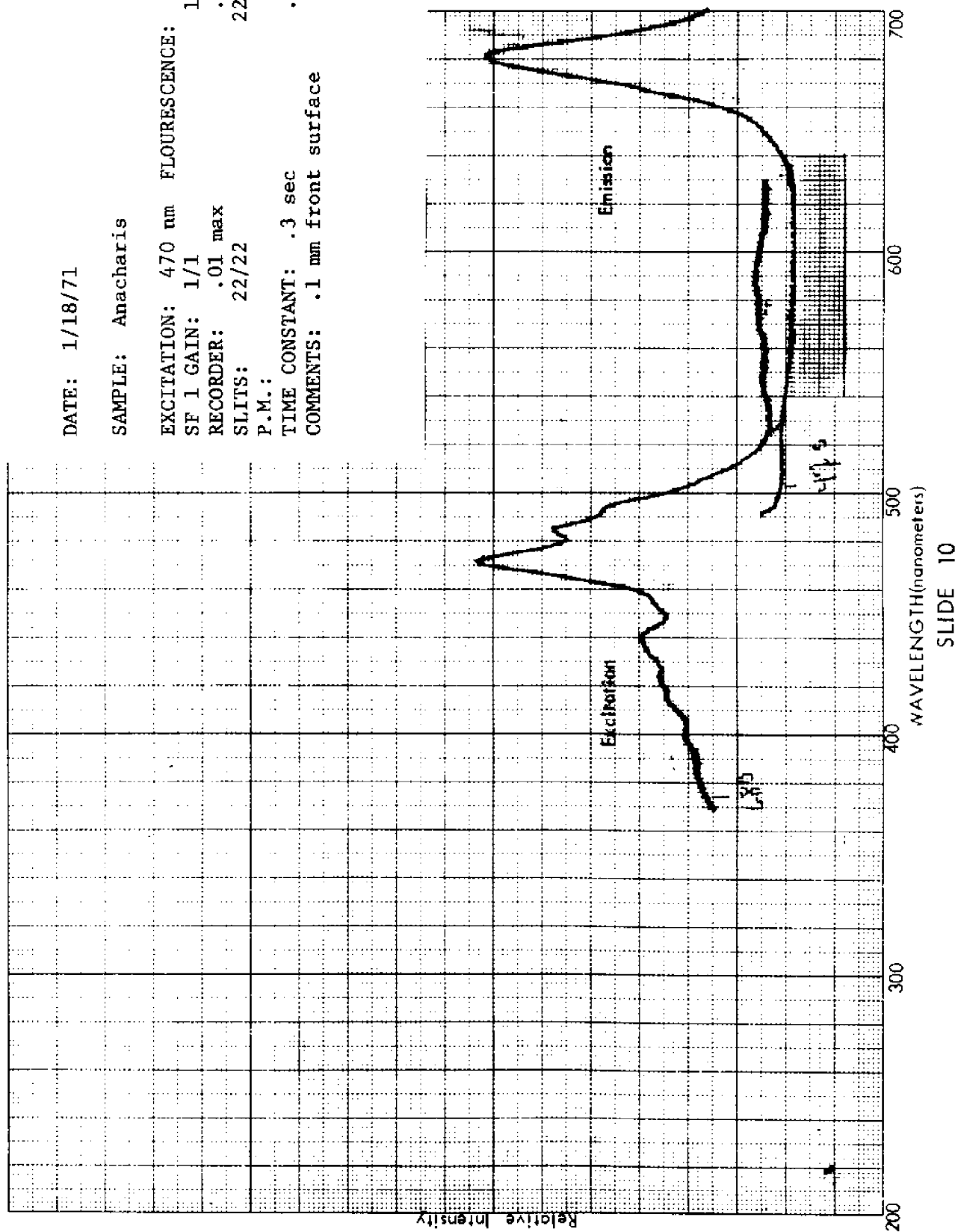
RECORDER: .01 max

SLITS: 22/22

P.M.:

TIME CONSTANT: .3 sec

COMMENTS: .1 mm front surface



SLIDE 11

PREPARATION OF PURE BODY FISH OIL

- 1) WHOLE FISH HOMOGENIZED AND EXTRACTED WITH ACETONE
- 2) ACETONE FRACTION EXTRACTED WITH 1:1 ETHYL ETHER:  
PETROLEUM ETHER
- 3) WATER REMOVED BY FILTRATION THROUGH ANHYDROUS  $\text{Na}_2\text{SO}_4$

VARIANTS PREPARED BY

- a) ADDITION OF B.H.A. ANTI-OXIDANT (250 PPM)
- b) STIRRED WITH SEAWATER
- c) BOTH a) AND b)

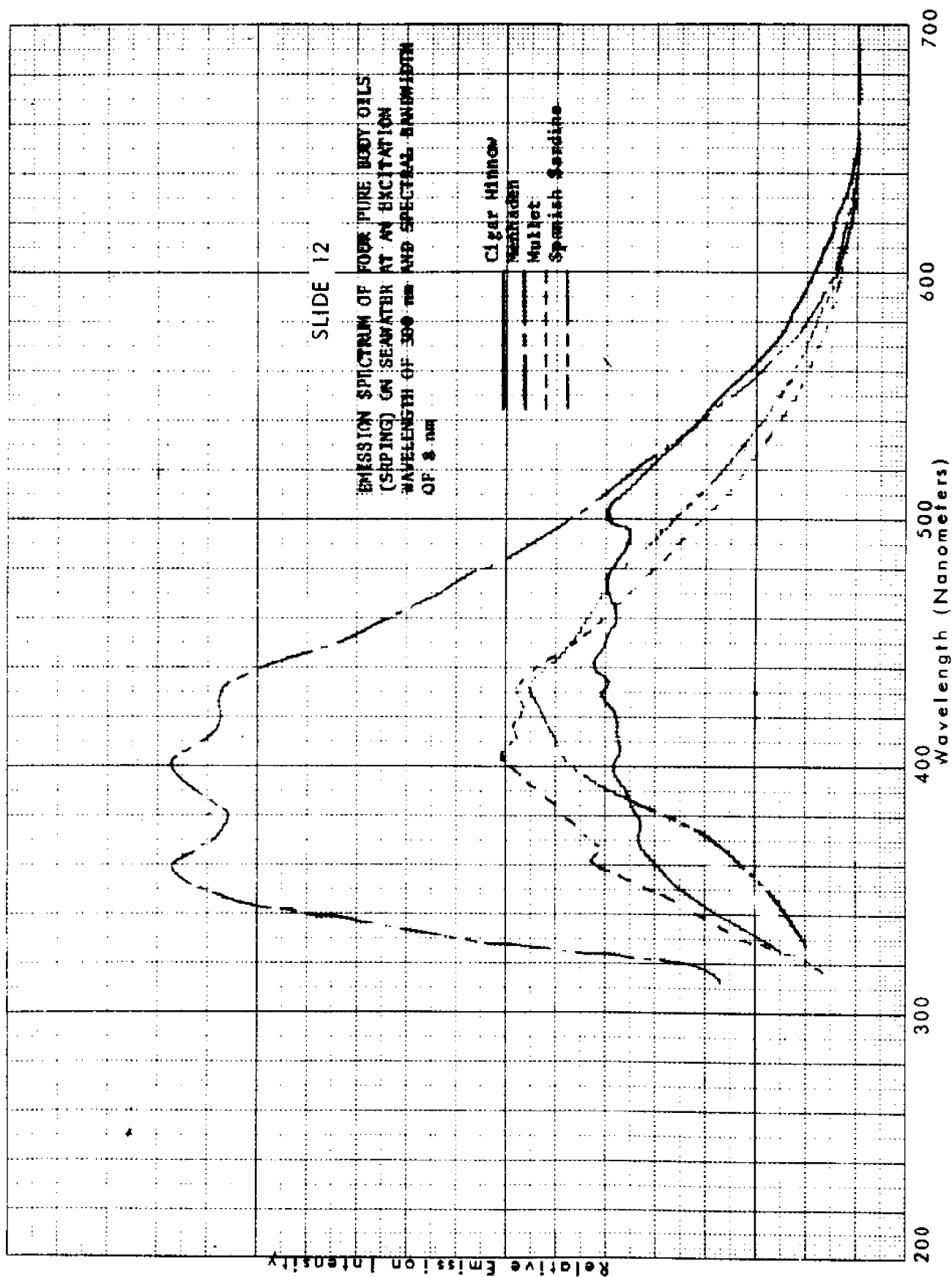
The species studies included Thread Herring, Gulf Menhaden, Black Mullet, Cigar Minnow (Round Scad), Spanish Sardine and Razorbelly (Scaled Sardine). Spectra obtained were similar to those shown for Spanish Sardine in Slides 7 and 8. In general, multiple emissions were observed for all oils, with peaks near 375, 400, 440, 470, and 520 nm. Differences were largely in the proportion of the various emissions present. The emission at 470 nm excited at 400 nm was characteristic of all fish oils examined and might be the basis of a generic identification of fish slicks as opposed to other slicks. For identification among species the distribution of emission in the various centers must be utilized.

In general, it is desirable to make multiple emission measurements at one wavelength of excitation rather than the reverse. This is true first because of the greater specificity of emission as compared to excitation, and second because it is easier to tune a detector than a high intensity source.

In Slide 12 we compare the emission of four fish oils on sea-water when excited at 300 nm. Excitation and emission bandwidths are both 8 nm. Instrument gain is the same for the four traces, indicated relative efficiencies of emission at this excitation. The curves are uncorrected for instrumental factors, but this has no bearing on the logic of the following discussion.

Consider emission at 360 nm and 420 nm. Menhaden shows stronger emission at 360 than at 420. The other three species show less emission at 360 than 420. Therefore, this serves to identify Menhaden from the other three.

Next, consider emission at 430 nm and 500 nm. Cigar Minnow has about equal emission intensities while all the other species show considerably less emission at 500 than at 430. This may serve to distinguish Cigar Minnow from all the other species.



The remaining species are Mullet and Spanish Sardine. Mullet emission is shifted to shorter wavelengths than Spanish Sardine. Thus, if we compare emissions at 360 nm and 530 nm we note that Spanish Sardine emission is about equal at these two wavelengths, while Mullet emission is almost three times greater at 360 than at 530. This may serve to distinguish between these species.

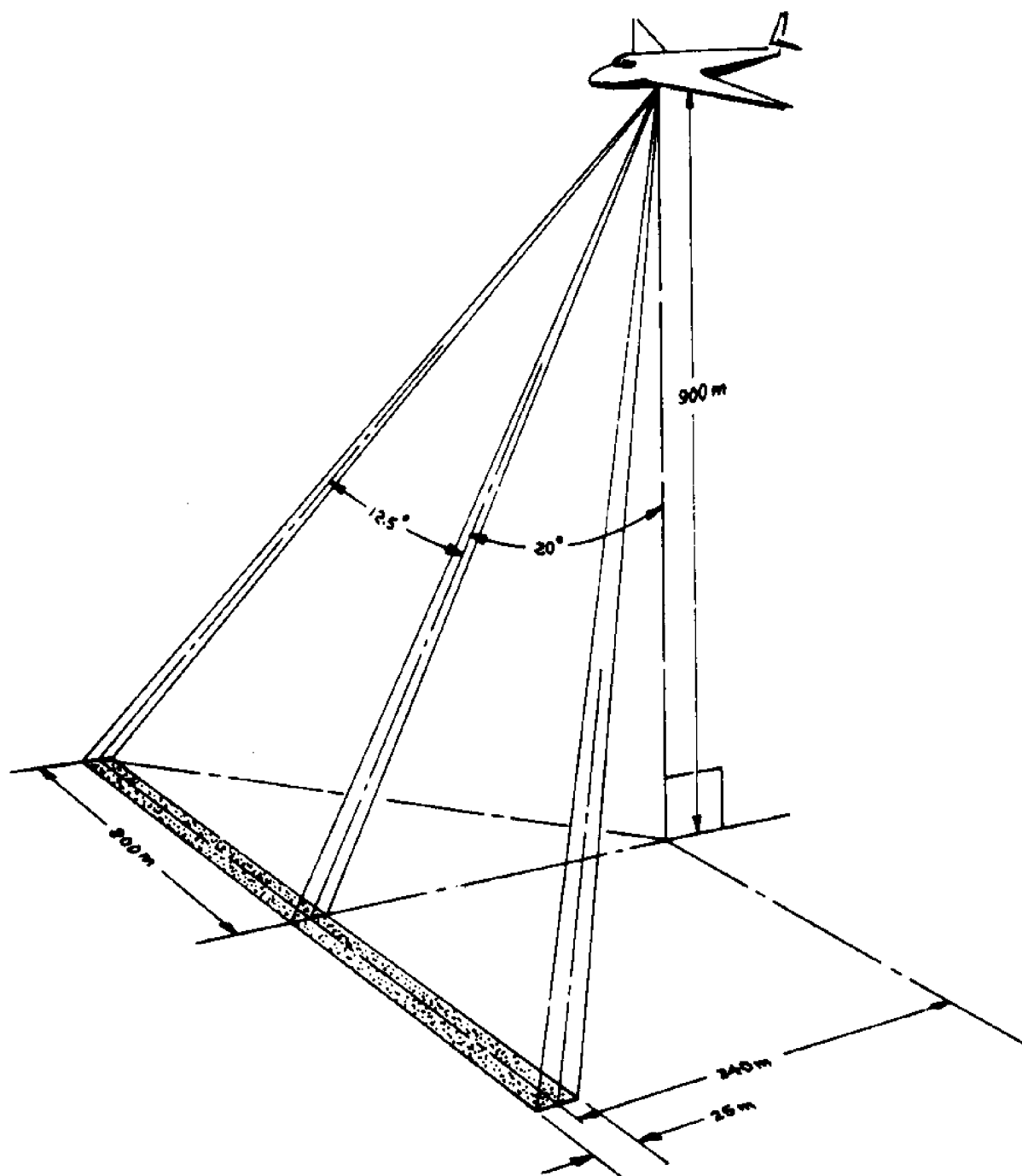
The preceding heuristic argument is based on emission data from a single excitation. For more species, the excitation may also have to be changed. Finally, it might be necessary to scan spectra and perform correlations with a computer. In most practical situations, only a few species are included.

For highest sensitivity, it is desirable to utilize the greatest spectral bandwidths consistent with the needed specificity. Measurements at 32 nm bandpass revealed sufficient specificity but required slight changes in choice of monitoring wavelengths. We believe the bandwidth can be extended to 50 nm without losing sufficient specificity.

#### INSTRUMENTAL DESIGN

These measurements indicate sufficient specificity for laboratory determination between the species. I would now like to indicate results of a calculation to demonstrate the feasibility of remote sensing. The model chosen for this calculation, illustrated in Slide 13, was configured not only to demonstrate feasibility but as an operational search system for an aircraft flying systematic patterns at potentially high ground speeds.

The transmitter/detector system is assumed to be located in an aircraft flying at an altitude of 900 m. The transmitter (light source) and detector are positioned as far apart from each other as possible. To minimize transmitter backscatter from the sea surface, the system looks forward at an angle of  $20^\circ$  from the vertical.



SLIDE 13 Model System Receiver Field of View Dimensions  
for 900 Meters Altitude



The water-cooled arc lamp used in our calculations is a developmental lamp produced under another contract with the following characteristics:

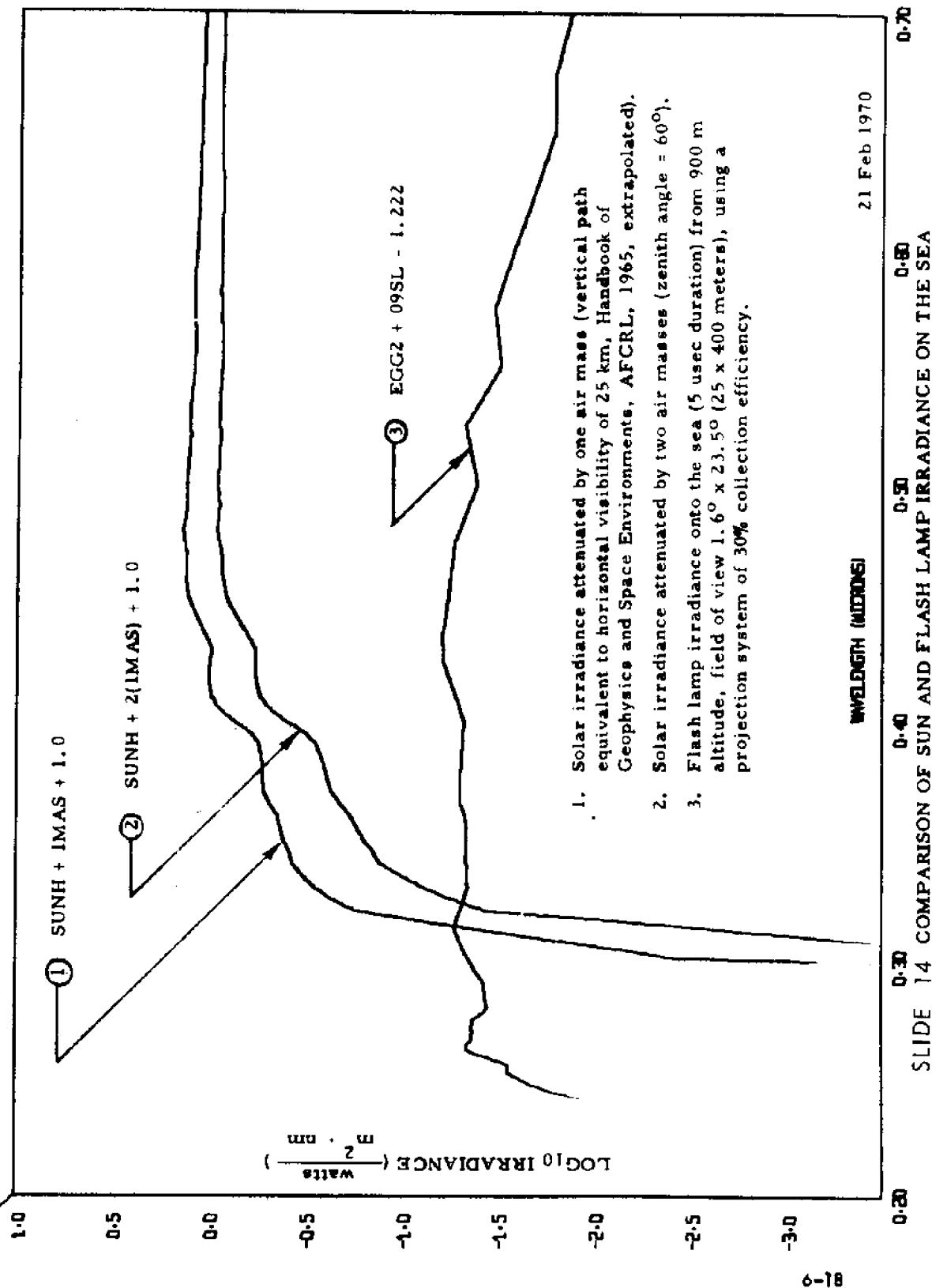
Flash Duration	5 microseconds
Repetition Rate	20 pulses per second
Input Energy Per Flash	32 joules
Arc Size	5 mm x 75 mm

The optical projection system assumed was developed under an Air Force contract. This system has a collection efficiency of  $1/3$  and will image the 5 mm x 75 mm arc onto 25 m x 400 m of sea corresponding to  $1.6^\circ \times 23.5^\circ$ . This is reasonable for the problem since minimum slick size is assumed to be about 25 m.

As the plane flies in a horizontal path, the projector system "sweeps" an area 400 m wide and 25 m in the direction of travel. (At the forward angle of  $20^\circ$ , this area would be somewhat larger; however, calculations are based on the 25 m x 400 m area). For a pulse repetition rate of 20 pulses per second and an aircraft speed of 300 mph (135 m/sec), the irradiated swath would be displaced 6.7 m between pulses, or approximately  $1/4$  of the short dimension of the swath. This is more overlap than is needed for simple measurements, but might be useful if alternate pulses were synchronized with a filter wheel or monochromator timed to take successive measurements at various wavelengths. Alternately the airplace could be flown faster.

In Slide 14 we produce the irradiance of EGG2 in such a projection system at 900 m (lowest curve). For comparison we show also the irradiance due to the sun through 1 and 2 model atmospheres. It will be observed that at short wavelengths the irradiance of EGG2 is actually greater than that of the sun, while at 400 nm it is about an order of magnitude less.

A sophisticated versatile source would employ a monochromator in the



source. For simplicity and sensitivity, we assume the source has a fixed filter.

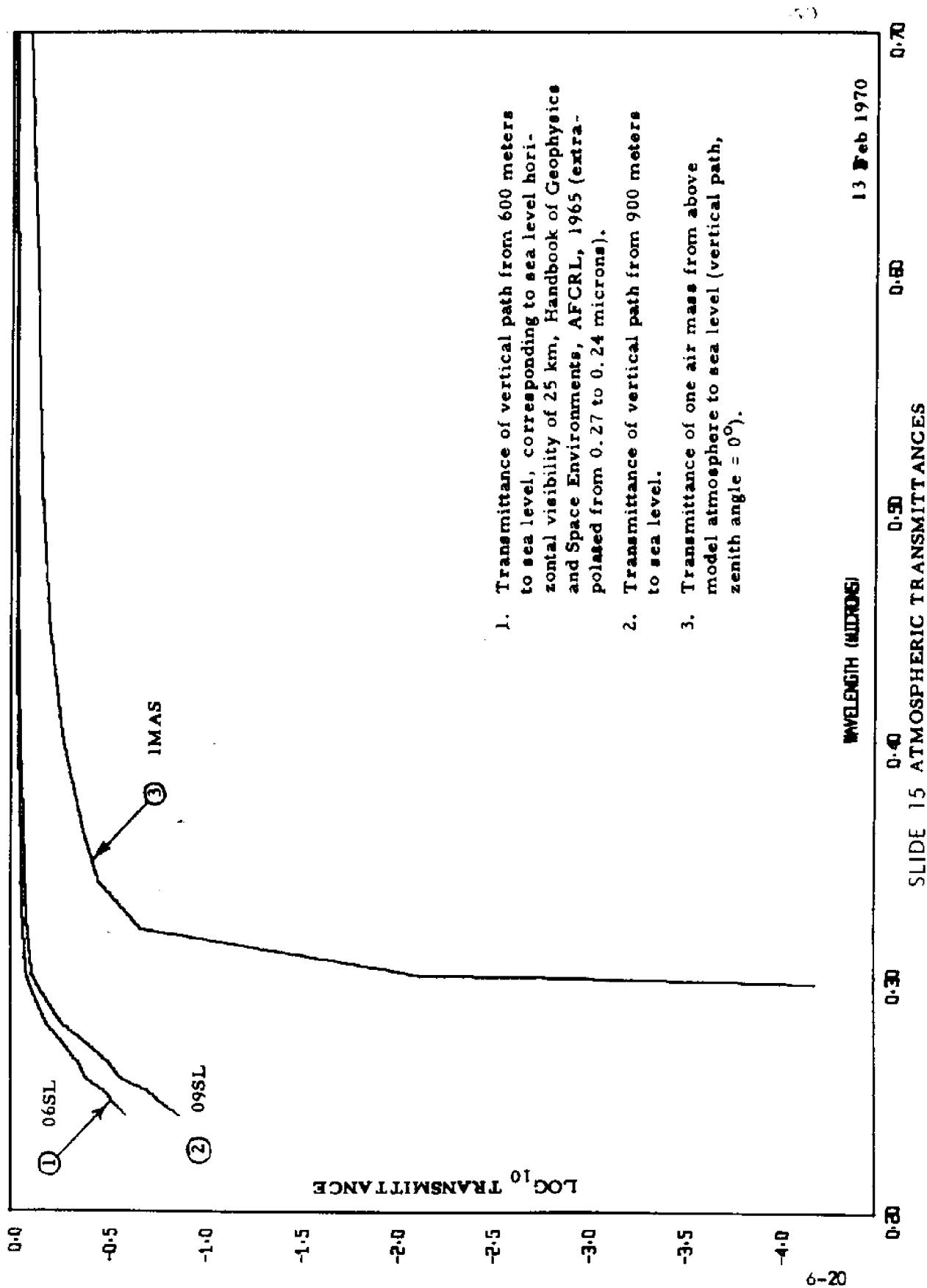
The geometry of the detection system is assumed to be much like that of the projection system. The collector dish is assumed to be 0.4 m in diameter which subtends  $\pi/2 \times 10^{-7}$  steradians at 900 m. Again, a sophisticated instrument might employ a monochromator. We assume a fixed filter for this calculation. Photometric detection will employ standard photomultipliers and electronics, since limiting noise is expected to be scatter and other background, rather than electronic noise.

In the simple system used for our calculation signals from the illuminated area are integrated over the entire field of view. Where greater sensitivity is available (i.e. at lower altitudes or with improved light sources or smaller fields of view) direct imaging of the scene may be possible, using image intensifiers developed for night-vision technology.

For our model calculations we have chosen an excitation band centered at 350 nm with a bandwidth of 50 nm and emission band centered at 440 nm with a bandwidth of 50 nm. The band centers were chosen to lie in the approximate centers of the range of excitation and emission wavelengths encountered in fish oil films; at an excitation of 350 nm almost every fish oil will exhibit significant emission at 440 nm.

Slide 15 contains data on the transmission of the atmosphere as a function of wavelength in the region 0.2 micron to 0.7 micron. The lowest curve is the transmission of one model atmosphere (vertical path, zenith angle =  $0^\circ$ ). The upper curves are the transmission through the atmosphere from sea level to 900 m and 600 m, corresponding to useful airplane altitudes. Transmission of 0.76 at the 350 nm excitation is included in the irradiance data of Slide 12. Transmission at the emission wavelength of 440 nm is 0.89.

For the source filter we use two standard thicknesses of Corning 7-54 which will have a transmission of 0.65 at 350 nm and an average transmission



of  $4 \times 10^{-6}$  in the receiver band from 415-465 nm.

For the receiver we use a 3 mm thickness of Schott CG 400 plus a Corning 4-76 to suppress a red-leak. The transmission of this pair at 440 nm is about 0.76 while its transmission throughout the transmitter band is less than  $10^{-5}$ .

Because the identity and concentration of specific emitting moieties in the fish oils are unknown, it is impossible to state quantum yields. Nevertheless it is necessary to have some measure of the relative optical emission efficiency of each oil. The Relative Emission Efficiency is defined as the probability of emission of a fluorescence quantum per incident excitation quantum.

As defined, the REE is dependent on choice of excitation wavelength and on the thickness of the oil film, becoming constant once the film is totally absorbing. The absorbance of 0.1 mm of the fish oils varies from about 0.2 to 1.4 at 350 nm, corresponding to 37% and 96% absorption respectively. Actual absorption will depend on the film thickness, the fraction of the slick actually covered with oil and the presence of other absorbing materials. Since the major components of fish oils are fatty acids, the fish oil matrix should be quite clear at 350 nm.

Experimental values for the REE's of fish oils were obtained by comparison with a sodium salicylate standard. For excitation at 320 nm, the REE's ranged from 0.004 to 0.016. We assume an average value of 0.01 for the model calculations.

The fluorescence power at the detector is determined according to the following formula:

$$P_F = H_{xe} \times \Delta\lambda_{350} F_{350} \text{ REE } f F_{440} T_{440} \Omega/4\pi S \lambda_{ex}/\lambda_{em}$$

where the factors have the following definitions and values:

$P_F$  = Fluorescence power at the detector (watts during 5 microseconds)

$H_{xe}$  = Irradiance from EGG2 at 900 m and 350 nm, taken from Slide 14  
 $= 4.68 \times 10^{-2} \text{ watts/m}^2/\text{nm}$

$\Delta\lambda_{350}$  = Source filter spectral bandwidth = 50 nm

$F_{350}$  = Average transmission of source filter in excitation band = 0.65

REE = Relative Emission Efficiency of Fish Oils = 0.01

f = Fraction of fluorescence in detector bandwidth = 0.3

$F_{440}$  = Average transmission of detector filter in emission band = 0.76

$T_{440}$  = Transmission of atmosphere to 900 m at 440 nm = 0.89

$\Omega$  = Solid angle subtended by detector at 900 m =  $1/2 \times 10^{-7}$  sterad.

S = Area of minimum fish slick = 25 m x 25 m = 625 m<sup>2</sup>

$\lambda_{ex}/\lambda_{em}$  = Wavelength ratio of excitation and emission = 350/440 = 0.8

Substituting these values, we find for the fluorescence power at the detector:

$$P_F = 1.92 \times 10^{-8} \text{ watts}$$

The resulting background powers and the corresponding Signal/Background ratios are given in the following table: in each case we have assumed it is possible to subtract the average background.

<u>Source</u>	<u>Power (Watts)</u>	<u>Signal/Background</u>
Flourescence	$1.9 \times 10^{-8}$	_____
Moonlight--glassy sea-- direct reflection	$2.1 \times 10^{-7}$	55
Atmospheric Backscatter	$2.4 \times 10^{-8}$	160
Transmitter--Beaufort 4 Sea-- off glitter	$3.1 \times 10^{-9}$	4500
Moonlight--Beaufort 4 Sea-- off glitter	$1.6 \times 10^{-9}$	6300
Transmitter--Underwater Scattering	$1.3 \times 10^{-10}$	
Moonlight--Night skylight reflection	$5 \times 10^{-12}$	
Moonlight--underwater scattering	$4 \times 10^{-12}$	

## SLIDE 16

The fluorescence power at the detector is determined according to the following formula:

$$P_F = H_{xe} \cdot \Delta\lambda_{350} \cdot F_{350} \cdot REE \cdot f \cdot F_{440} \cdot T_{440} \cdot \Omega / 4\pi \cdot S \cdot \lambda_{ex} / \lambda_{em}$$

where the factors have the following definitions and values:

$P_F$	=	Fluorescence power at the detector (watts during 5 microseconds)
$H_{xe}$	=	Irradiance from EGG2 at 900m and 350nm, taken from Figure 6-2 = $4.68 \times 10^{-2}$ watts/m <sup>2</sup> /nm
$\Delta\lambda_{350}$	=	Source filter spectral bandwidth = 50 nm
$F_{350}$	=	Average transmission of source filter in excitation band = 0.65
REE	=	Relative Emission Efficiency of Fish Oils = 0.01
f	=	Fraction of fluorescence in detector bandwidth = 0.3
$F_{440}$	=	Average transmission of detector filter in emission band = 0.76
$T_{440}$	=	Transmission of atmosphere to 900m at 440nm = 0.89
$\Omega$	=	Solid angle subtended by detector at 900m = $1/2 \times 10^{-7}$ sterad
S	=	Area of minimum fish slick = 25m x 25m = 625m <sup>2</sup>
$\lambda_{ex} / \lambda_{em}$	=	Wavelength ratio of excitation and emission = 350/440 = 0.8

Substituting these values, we find for the fluorescence power at the detector:

$$P_F = 1.92 \times 10^{-8} \text{ watts}$$

## SLIDE 17

<u>Source</u>	<u>Power (watts)</u>	<u>Signal/Background</u>
Fluorescence	$1.9 \times 10^{-8}$	
Moonlight--glassy sea--direct reflection	$2.1 \times 10^{-7}$	55
Atmospheric Backscatter	$2.4 \times 10^{-8}$	160
Transmitter--Beaufort 4 sea--off glitter	$3.1 \times 10^{-9}$	4500
Moonlight--Beaufort 4 sea--off glitter	$1.6 \times 10^{-9}$	6300
Transmitter--underwater scattering	$1.3 \times 10^{-10}$	
Moonlight--night skylight reflection	$5 \times 10^{-12}$	
Moonlight--underwater scattering	$4 \times 10^{-12}$	



The greatest background, due to reflection of moonlight from a glassy sea, is not relevant since one would never choose to look directly into the moon reflection. The atmospheric backscatter is the limiting background, and this could be reduced further by choice of more elaborate filters, or a monochromator.

#### CONCLUSIONS

Many materials of importance to marine and fisheries resources fluoresce with sufficient efficiency to be detectable at reasonable aircraft altitudes when excited at night with existing light sources. Further, the specificity of the excitation and emission spectra is great enough to allow discrimination between many materials. Arc or laser stimulated fluorescence promises to provide a new and useful method for remote sensing which supplements multispectral and color photography.

Remote Sensing and the Pelagic  
Fisheries Environment off Oregon

William G. Percy  
Department of Oceanography  
Oregon State University  
Corvallis, Oregon

INTRODUCTION

One of the biggest advantages of remote sensing is that large areas of the earth's surface can be surveyed in short periods of time, providing near-synoptic "pictures." Repeated surveys of one area, like time-lapse photography, can be interpreted as a movie to illustrate the dynamics of detectable features. These attributes of remote sensing from aircraft or spacecraft are especially important in coastal and upwelling regions of the oceans, where oceanographic conditions change rapidly. The world's largest fisheries are also located in these dynamic areas.

In general, oceanographic variables, measured by remote (or non-remote) sensors can be used in two ways to increase the efficiency of exploited fisheries. They differ in the time lag between collection and use of data, but both endeavor to predict fish concentrations in time and space.

First, measured variables such as temperature can be compared with fish catches in hopes of discovering good correlations between ocean factors and the distribution of species so that scientists can provide fishermen with new indicators or methods for locating fish stocks. This approach, in my opinion, has not been especially fruitful in the past. One reason is the difficulty in obtaining environmental data and catch statistics from the same area at the same time and on the same geographical scale.

Obtaining catch data from fishermen and correlating them with oceanographic data takes time. One reason for this is that remote sensing data are extensive and are often recorded on magnetic tapes. Therefore, correlation studies seldom have application during the same fishing season the data were collected.

Even if a positive relationship exists between high catches and an oceanographic feature, predicting availability may be based on the assumption that this feature is relatively static and will persist for days or weeks. In coastal waters influenced by upwelling, however, temperature and oceanographic features fluctuate rapidly and are difficult to predict (Lane, 1965).

These considerations argue for the second approach: to disseminate information in realtime; i.e., make it rapidly available to fishermen so they can use it to plan their day-to-day fishing tactics. In this way, the fisherman relies on his past experience to interpret data. Timely information is vital to improved scouting for motile pelagic species whose distributions change constantly in a dynamic medium.

## A Pelagic Environment Study

Both of these approaches have been used in our research at Oregon State University during 1969 and 1970. Our objectives were (1) to learn more about the ocean conditions off Oregon during the summer and how they affect the albacore tuna catches and the productivity of the pelagic food chain, and (2) to provide albacore fishermen with information in near realtime that could be used in scouting for fish.

The research constituted a broad and multidisciplinary program. It included four interdependent components:

### I. Remote Sensing Aircraft

NASA - Convair 240A, Lockheed P-3, RB-57  
 U.S. Coast Guard - HU-16  
 U.S. Air Force - HU-16  
 University of Michigan - C-47

### II. Oceanographic Vessels

Oregon State University - YAQUINA, CAYUSE  
 Fish Commission of Oregon - SUNRISE  
 Bureau of Commercial Fisheries - DAVID STARR JORDAN, JOHN N. COBB  
 Albacore boats with bathythermographs

### III. Commercial Albacore Boats

### IV. Albacore Advisory Service - "Albacore Central"

OSU Sea Grant's Marine Advisory Group  
 Fishery - Oceanography Center, La Jolla, California  
 U.S. Weather Service  
 Pacific Northwest Bell Telephone

Remote sensing aircraft used infrared radiometers (Barnes PRT-5) on all low level (500 or 1000 ft. altitude) flights. The calibration techniques of Saunders (1967) were used. A multispectral scanner was used on University of Michigan's C-47, a TRW Ocean Color Spectrometer and on L-band microwave radiometer on NASA's P-3, and high altitude (60,000 ft) multispectral photography from the RB-57.

Besides obtaining ground-truth for remote sensing flights, surface ships were engaged in studies on physical, chemical and biological processes and properties related to pelagic fisheries. Several commercial albacore boats were outfitted with expendable or mechanical bathythermographs (BT's) so that data on thermal structure could be obtained along with fish catch. The U.S.

Navy Fleet Numerical Weather Facility, Monterey, California provided XBT probes and Sippican Corporation loaned us two XBT launchers for this project.

Data from aircraft and vessels were communicated to "Albacore Central" on the OSU campus, combined with information from the Fishery-Oceanography Center (BCF) La Jolla and the Weather Bureau, and broadcasted twice daily by the Astoria Marine Operator (Pacific Northwest Bell) to the albacore fleet. Most of the information on sea surface temperature for these radio broadcasts were obtained from the aircraft overflights. Another Albacore Central product for the fishermen was the weekly bulletin which included a sea surface temperature chart. These were distributed to canneries and fishing ports along the coast of Oregon (Panshin, 1970).

The fishermen were important participants in the project. Besides being "consumers" of data on ocean conditions, they had a vital role in providing data on albacore catches. Over 400 albacore logbooks were distributed to fishermen from San Diego, California to Seattle, Washington. They were asked to record detailed information on catches several times a day so that catches could later be correlated with small-scale oceanographic features.

The results to date are all preliminary. The catch data from both 1969 and 1970 are still being processed. The data obtained from the multispectral scanner, the spectrometer, and microwave are on tape and also being analyzed.

#### Upwelling and Columbia River Plume

Remote sensing overflights were ideal for semi-synoptic surveys of coastal upwelling and the Columbia River plume. These two features greatly influence the pelagic environment off Oregon during the summer, and both are detectable by anomalies in sea surface temperature and water color. Sequential flights helped to reveal the dynamic nature of both of these features: patterns of sea surface temperature, for example, changed on a daily basis indicating the fluctuating nature of this region (Pearcy and Mueller, 1970).

Upwelling was evidenced by cold water (and sometimes fog) along the coast, coldest temperatures usually occurring off southern Oregon. Thermal fronts, where the temperature changed markedly, were frequently found between cold water and warmer offshore water.

The Columbia River plume was often observed as a tongue of warm water. The Columbia River is the second largest river in the United States and discharges an average of  $7300 \text{ m}^3/\text{second}$  into the Pacific Ocean. Unlike coastal streams that have peak runoff in the winter, the Columbia has a large runoff in the early summer from snow melt in the mountains. In the ocean, the

effluent responds to prevailing winds and usually flows to the southwest in the summer. Because the low salinity plume water is separated from the denser ocean water by a strong pycnocline near the surface and because of its large load of particulate matter, the plume waters are heated more rapidly than surrounding waters with a deeper mixed layer. Therefore plume waters are distinguishable by warm surface temperature early in the summer (Owen, 1968).

Changes of water color were sometimes associated with both upwelling and the plume. Multispectral scanner data and microdensitometry of high altitude Ektachrome transparencies indicated a general increase in the blue/green ratio with distance offshore. This trend could be reversed in localized regions, however, with the blue/green ratio decreasing offshore in areas of recently upwelled water along the coast.

## Sea Surface Temperatures - 1970

Some sea surface temperature maps derived from airborne infrared radiometry (Figs. 1-3) illustrate some of the important oceanographic features found off Oregon during the summer. The map for July 22 (Fig. 1) shows the influence of upwelling, with coldest surface temperatures ( $< 11^{\circ}\text{C}$ ) along the coast. Warm water ( $> 16^{\circ}\text{C}$ ) is pooled offshore and localized in a small area near the mouth of the Columbia River. For several days preceding this flight winds blew from the north at velocities greater than 10 knots. Upwelling was intense and mixing of Columbia River water with cool upwelled water destroyed the continuity of the Columbia River plume.

A week later on July 29 (Fig. 2) there is little evidence of upwelling. Surface temperatures inshore were  $> 14^{\circ}\text{C}$  and offshore were up to  $18^{\circ}\text{C}$ , both warmer than on July 22. This condition was attributable to the light winds, which were predominately from the southwest, the lack of strong upwelling, and the continued heating of surface and plume waters. Water colors visually observed from the aircraft are noted. Warmest waters, probably in the plume, were green. Blue-green water predominated offshore, and brownish water was noted near the coast. Brown water is produced when dense phytoplankton blooms occur near the surface, a condition sometimes observed in nearshore waters after northerly winds and upwelling subside. Presumably a shallow mixed layer is produced in the nutrient-rich upwelled water allowing rapid growth of phytoplankton near the surface.

On July 30, one day later, another flight was made over the same area (Fig. 3). A comparison of Figs. 2 and 3 reveals how much sea surface temperatures can change in one day. Northerly winds of 10 knots or more commenced on the afternoon of July 29 and their effect is indicated by lower inshore temperatures from upwelling ( $< 12^{\circ}\text{C}$ ). Warmest temperatures offshore are  $16.5^{\circ}\text{C}$  instead of  $18^{\circ}\text{C}$  on July 29. Note also that brown water was not seen on this flight, after the onset of strong northerly winds.

The CAYUSE made observations on temperature and salinity in the area of these overflights between July 27 and August 2. The maps of surface temperatures obtained by ship and by aircraft were similar: both showed a bilobed pattern with two regions of warm water (as in Figs. 2 and 3). The pattern of surface salinity was also bilobed, the areas of low salinity corresponding to areas of high temperature. This inverse relationship between temperature and salinity has been noted before during early summer, and Evans (unpublished M.S.) reported that the core of low salinity usually lies inshore of the core of warmest water.

## Albacore Tuna

Albacore, Thunnus alalunga, are fast swimming oceanic tuna that migrate into nearshore waters off the west coast of North America during the summer. The distribution of albacore in the northeastern Pacific is known to be influenced by sea temperatures. Clemens (1961) and Flittner (1961) reported that albacore abundance was greatest where sea surface temperatures were between 15° and 20°C in California waters. In the Pacific Northwest, where yearly fluctuations in landing are extreme, highest catch rates occurred between 14° and 17°C (Alverson, 1961; Johnson, 1962). Although sea surface temperatures are an important determinant in the migration and zoogeography of albacore, fishing within the "preferred" range does not insure good catches, or even the presence of albacore. Hence the best correlation is a negative one: low catches are found outside the preferred thermal range.

Panshin (1970; unpublished M.S.) plotted the catches of troll-caught albacore against sea surface temperature for the months of the 1969 season off Oregon. He found that the average temperature decreased from 16.9°C in July to 16.5°C in August and 15.7°C in September. Thus the average temperature was not constant but decreased by about one degree Celsius from early season to late season. We interpret this change as follows: in July as albacore migrate into Oregon waters, they are closely associated with the warmest waters available near the axis of the Columbia River plume where heating takes place rapidly. Later in the summer maximum temperatures in the region are higher and the area of warm water (14-17°C) expands. However, large catches of albacore are frequently made farther inshore, in waters adjacent to areas of upwelling. Consequently the disparity between average temperature of catches and the maximum water temperature available tends to be greater in August than July.

In 1970 most albacore troll boats that turned in log sheets moved northeast during July parallel to the axis of the Columbia River plume. High catches (averaging about 400 fish per boat per day) were recorded on July 22 and July 28, when the fleet was concentrated 90-120 miles off the mouth of the Columbia River. High catches were made along the seaward edge of the plume on July 22 (Fig. 1) and within the cooler, offshore lobe of the plume on July 28 and 29 (Fig. 2). These areas were intermediate in surface temperature, usually 15-16°C. Low catches were made in the warm (> 16°C) plume waters found close inshore (Fig. 2).

July 29 was the last day that good albacore catches were reported by troll boats off Oregon in 1970. Thereafter catches declined rapidly until the end of July, and the troll fishery off Oregon never resumed. This demise of the 1970 troll season was not related to any drastic change of ocean conditions reflected by sea surface temperatures. The surface temperatures during and after the decline were approximately the same as those in other good fishing years.

### Some Conclusions

- (1) The factors presently used by fishermen to locate albacore are surface features amenable to remote sensing. A Sea Grant questionnaire returned by 163 albacore fishermen showed that sea surface temperature, location of fleet, water color and fronts, in that order, are the most often used.

Large areas of the ocean can be surveyed by means of remote sensing. Therefore maps of sea surface temperature can be constructed. We found that our ships, on the other hand, provided too little data in a day's steaming for areal mapping.

- (2) Within the "preferred" or "optimal" temperature range of the albacore, factors other than temperature obviously affect distribution and availability. This conclusion is supported by the changing relationship between catches and sea surface temperature during the progression of the 1969 fishing season and by the collapse of the 1970 troll season in Oregon despite the presence of favorable water temperatures.

The lack of obvious correlations between absolute surface temperatures and catch rates does not necessarily mean the absence of important relationships. The pattern of surface temperatures may reflect important circulation and subsurface features. We need more information on how surface features are related to ocean processes.

- (3) Fronts are sometimes areas of high albacore and tuna catches (Hynd, 1969; Blackburn, 1964). According to Powell *et al.* (1952) good albacore water is often in the blue oceanic water bordering the cooler green coastal water. Given a suitable range of water temperatures, fronts may be areas where fish aggregate and where chances of success are increased. But as Hynd (1969) found, catches may also be high in absence of fronts. Temperature fronts off Oregon are usually near upwelling areas along the coast. Salmon are found in these frontal areas but usually temperatures are too cold for albacore, even on the oceanic side. Offshore fronts in "tuna water" may be areas of higher than average albacore abundance, perhaps because of the abundance of forage animals. We found that offshore color fronts were less common than those occurring around upwelling zones.
- (4) The instruments we used to measure the spectral quality of surface waters did not have outputs that could be interpreted in realtime, so the data were of little value in assisting the fleet in day-to-day operations. Visibility from the aircraft was also poor and continuous visual observations were difficult. A simple, rugged photometer that measures blue and green upwelled light from the sea surface and records the ratio as an output on a strip chart recorder, simultaneously with measurement of infrared temperatures, would be very useful. Such color and temperature information used in combination would enable better discrimination of water types and ocean features, and data could be made available to fishermen on a near-realtime basis.



- (5) Lastly, the distribution of albacore, or any species, is affected by a multitude of environmental factors which change in importance with season, time of day, and location, physiological state and age of fish, etc. The 1970 season was a lesson in humility for us. The drastic change in albacore availability was not predicted, nor has it been explained. The absence of obvious changes of ocean conditions that correlate with the decline of catches emphasizes how little we know about the behavior of albacore. In order to use environmental data to effectively predict distributions of migratory fishes we must also increase our understanding of their biology.

### Acknowledgments

Our multidisciplinary project on the pelagic fisheries environment off Oregon was possible only through the help and cooperation of many individuals and agencies. I thank them all. Financial support was provided by the Bureau of Commercial Fisheries (Contract No. 14-17-0002-333), the U.S. Naval Oceanographic Office (Spacecraft Oceanography, Contract No. N622306-70-C-0414) and by National Science Foundation Institutional Sea Grant (GH 45).

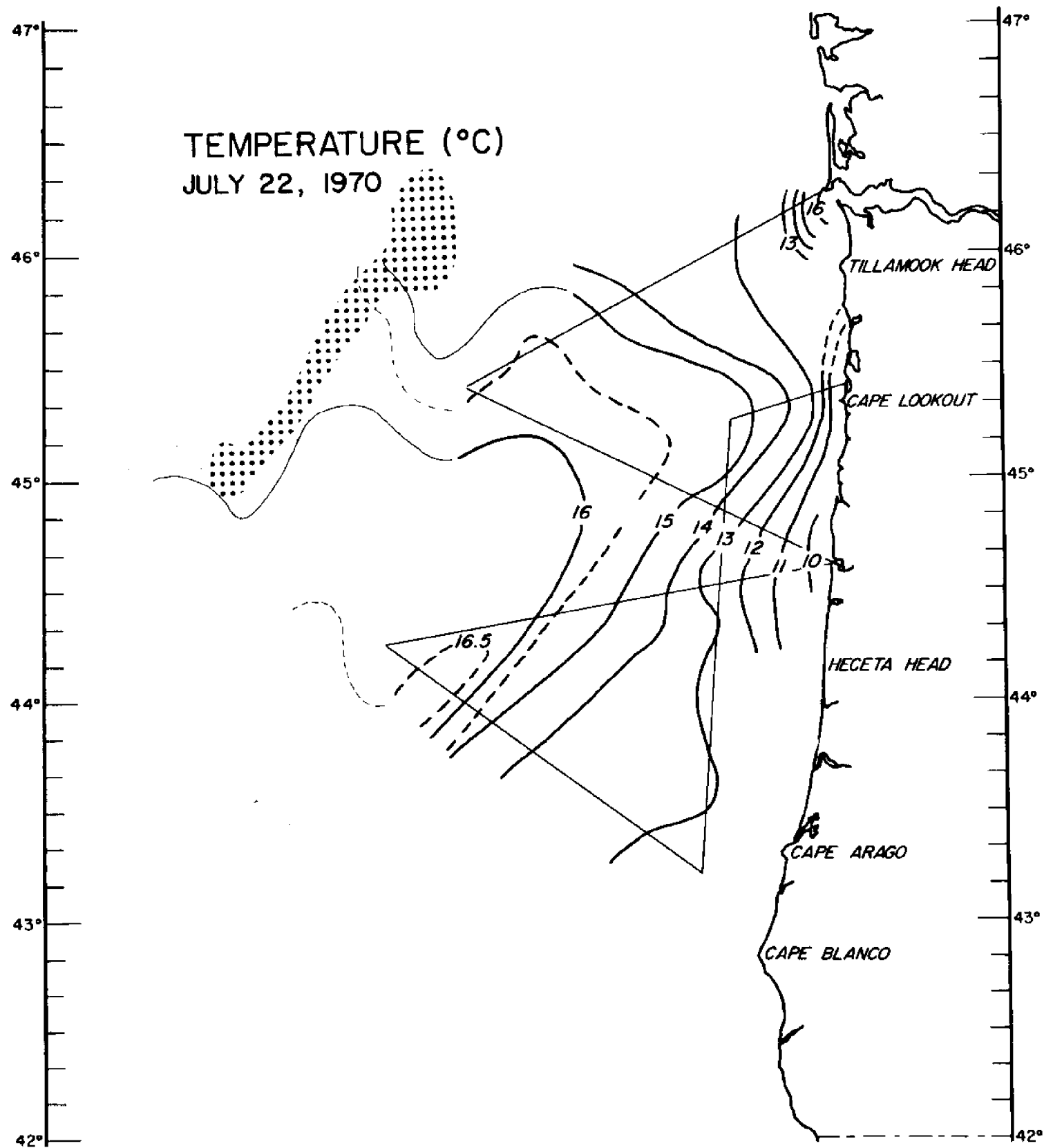
## References

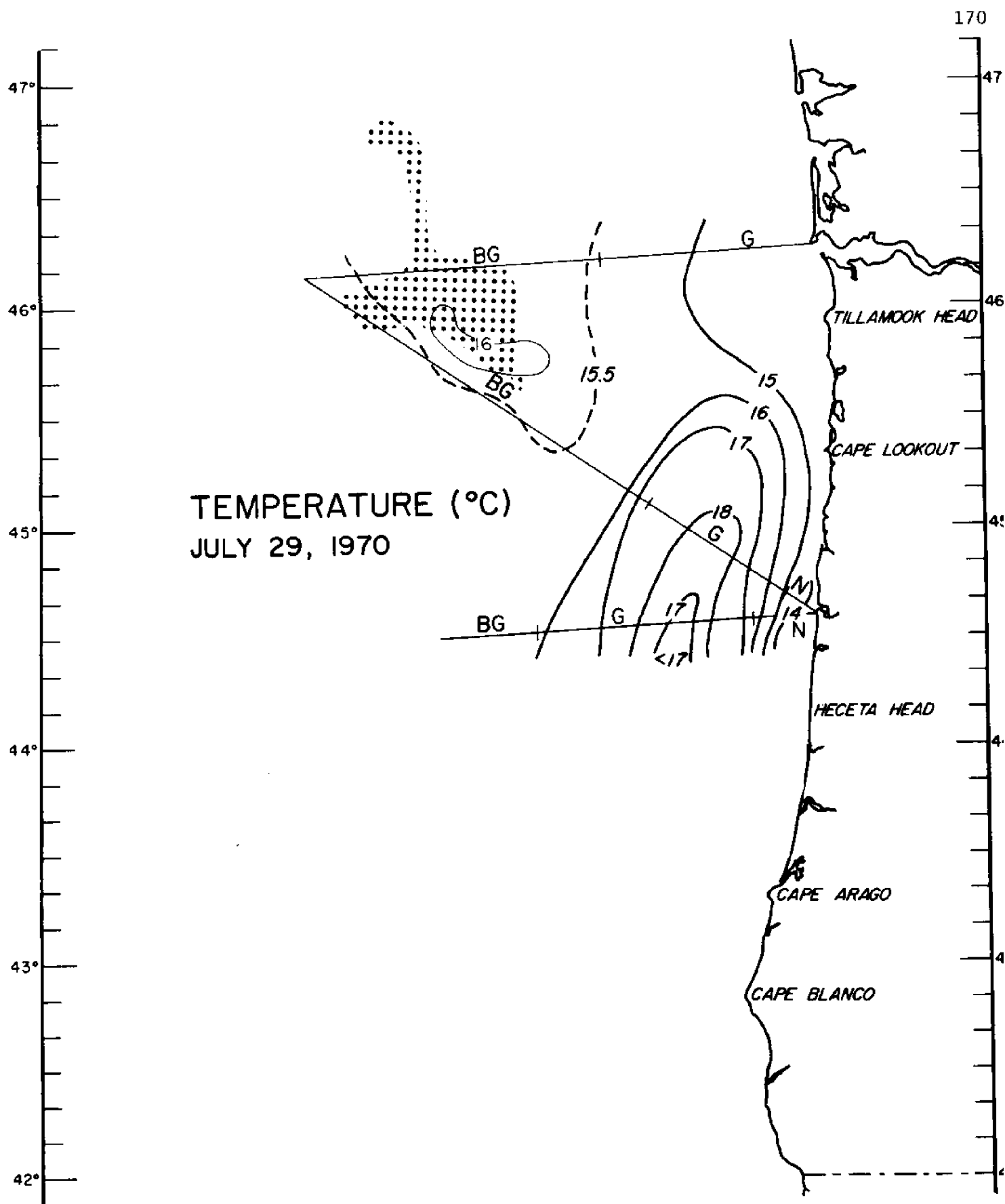
- Alverson, D. L. 1961. Ocean temperatures and their relation to albacore tuna (Thunnus germon) distribution in waters off the coast of Oregon, Washington and British Columbia. J. Fish. Res. Bd. Canada 18:1145-1152.
- Blackburn, M. 1964. Oceanography and the ecology of tunas. Oceanography and Marine Biology (H. Barnes ed.) 3:299-322.
- Clemens, H. B. 1961. The migration, age and growth of Pacific albacore (Thunnus germon). 1951-1958. California Dept. Fish and Game, Fish. Bull. No. 1159 118 p.
- Evans, Richard H. Physical parameters as tracers of Columbia River plume water. M.S. Thesis, Oregon State University, Corvallis.
- Flittner, G. A. 1961. Cooperative trolling program, 1961. Calif. Fishery Market News Monthly Summary, Dec. 1961.
- Hynd, J. S. 1969. Isotherm maps for tuna fishermen. Australian Fisheries, July 1969, 13-22.
- Johnson, J. H. 1962. Sea temperatures and the availability of albacore tuna off the coasts of Oregon and Washington. Trans. Amer. Fish. Soc. 91:269-274.
- Lane, R. K. 1965. Wind, nearshore ocean temperature and the albacore tuna catch off Oregon. Research Briefs. Fish Commission of Oregon 11:25-28.
- Owen, R. W., Jr. 1968. Oceanographic conditions in the Northeast Pacific Ocean and their relation to the albacore fishery. U.S. Fish. Wildl. Serv., Fish. Bull. 66:503-526.
- Panshin, D. A. 1970. Oregon's albacore research project. Trans. 35th No. Amer. Wildl. and Natural Res. Conf. 222-227.
- Panshin, D. A. Ocean conditions and albacore tuna catches in the northeast Pacific during the summer of 1969. unpubl. M.S.
- Pearcy, W. G. and J. L. Mueller. 1970. Upwelling, Columbia River plume and albacore tuna. Sixth Intern. Symp. Remote Sensing Environment. p. 1101-1113.
- Powell, D. E., D. L. Alverson and R. Livingstone, Jr. 1952. North Pacific albacore tuna exploration - 1950. U.S. Fish Wildl. Serv. Fishery Leaflet 402, 56 p.
- Saunders, P. M. 1967. Areal measurement of sea surface temperature in the infrared. J. Geophys. Res. 72:4109-4117.

## FIGURE CAPTIONS

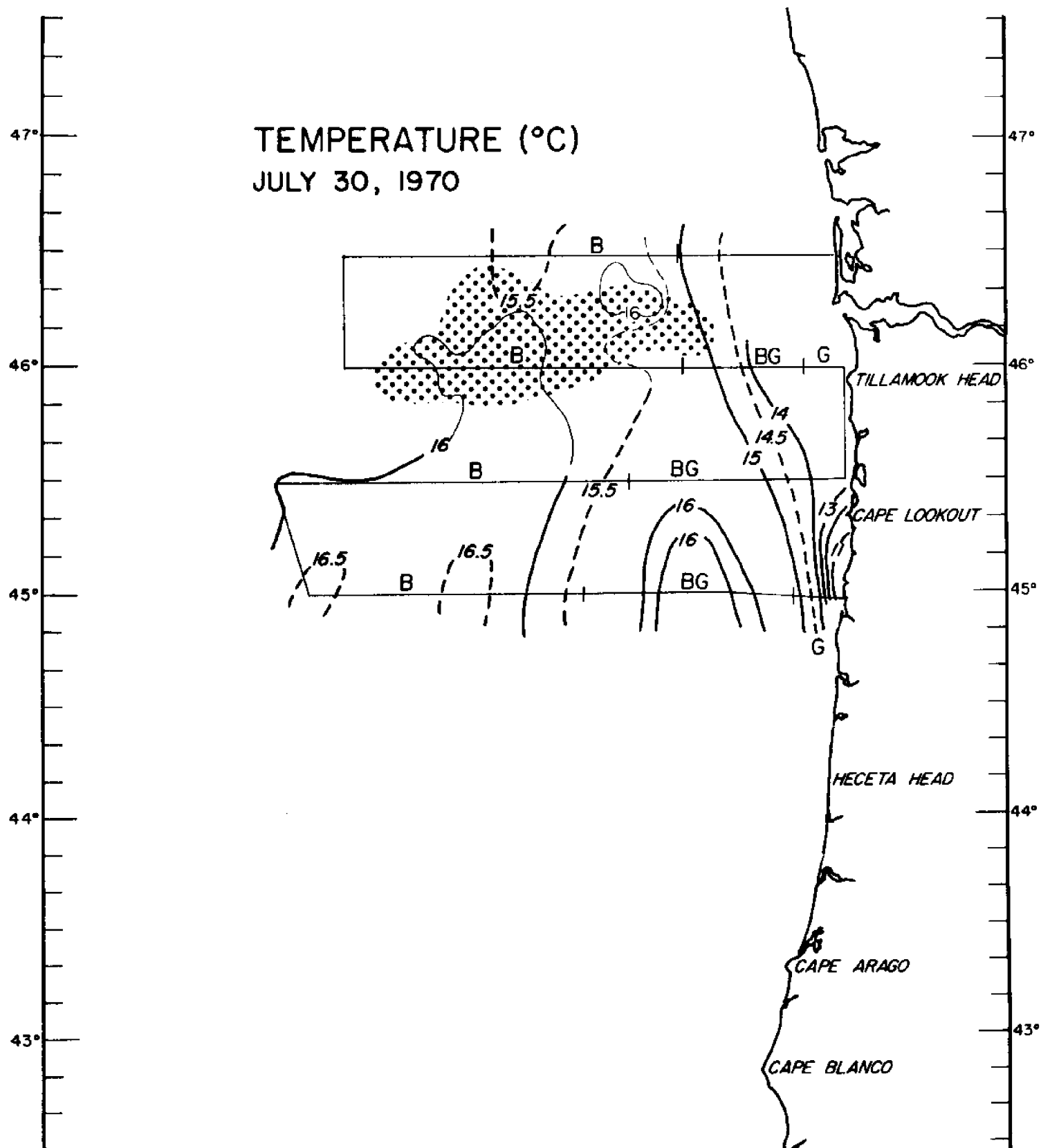
- Figure 1. Sea surface temperatures, July 22, 1970, obtained mainly by infrared radiometry. The flight lines of the U.S. Air Force's HU-16 are indicated by the straight lines. Albacore boats were located in the dotted area; surface temperatures in this area were obtained from the boats.
- Figure 2. Sea surface temperatures, July 29, 1970, obtained by infrared radiometry. The flight track of the U.S. Air Force's HU-16 is indicated by the straight lines, the location of albacore boats by the dotted area, and visual observation of water color by G (green), BG (blue-green) and N (brown).
- Figure 3. Sea surface temperatures, July 30, 1970, obtained by infrared radiometry. The flight track of the U.S. Coast Guard's HU-16 is shown by the straight lines, the location of the albacore boats by the dotted area, and visual observations of water color by G (green), BG (blue-green), and B (blue).

TEMPERATURE (°C)  
JULY 22, 1970





TEMPERATURE (°C)  
JULY 30, 1970



"Man's Effects on the Estuarine Environment"

(Abstract)\*

by

Leo F. Childs  
Code TF, NASA/MSC

The Gulf of Mexico is one of the nation's leading commercial fisheries. It is also a major sports fishery and recreation area. Shrimp and oysters account for most of the commercial fishing activities. In recent years the harvesting of menhaden and other less desirable fish for fish protein concentrates has become of considerable importance. The primary reason for the great abundance of marine life in the Gulf is the presence of an almost continuous system of estuaries ringing the Gulf from the Yucatan Peninsula to the southern tip of Florida. Texas has over 2,000 square miles of estuarine and coastal lagoons. Of equal importance is the vast marshland areas fringing the bays and lagoons.

Shrimp and other marine life, during their early life, find sanctuary in these large fertile regions where they must remain until large enough to enter the Gulf. The ecology of these areas must be preserved if the Gulf of Mexico is to remain one of the nation's most important fisheries and recreational areas.

This presentation consists of approximately 80 color slides taken over a number of years which dramatically illustrates the effects of industrialization and the encroachment of over population on the estuarine environment. Photography from the Gemini, Apollo, and aircraft program are included in the presentation.

\*The full text of Dr. Child's presentation along with NASA photographs was not available at the time of the printing of this publication. Plans are being made to issue his remarks as a special publication in the near future.



GAF COLOR FILMS FOR SPECIAL REMOTE SENSING APPLICATIONS

Ira B. Current

GAF Corporation, Binghamton, N. Y.

We have explored the land and water surfaces of the earth. The next frontier may be considered to be the depths below the water surfaces of the lakes, rivers, and oceans. Sensing systems must be capable of penetrating beneath water surfaces to as great a depth as possible, but aerial photography of surfaces near and on the waters can provide important information as to what exists beneath these surfaces.

GAF 200 Color Aerial Film<sup>®</sup> and GAF 500 Color Aerial Film<sup>®</sup>, both on polyester base, have been made available for several years as the recording element in "sensors" operating from aircraft. Now, the GAF 500 Film may be considered to be "work horse" of the GAF line of color films for aerial photography. This material is primarily a reversal film, the final product of normal processing being a positive color transparency. Yet this film can also be developed by a modified process to a color negative to fit a system based on negative "originals".

The debate as to which is the better system has not yet been resolved; i.e., is it better to start with a positive transparency, go through an intermediate color or black-and-white negative step, thence to the final positive transparencies and prints for viewing, interpretation, or measurement? Or is it better to start

with a negative from which positive transparencies or positive prints can be made? The answer may depend on the requirements of the user. An agency may wish to have wide, rapid dissemination of master negatives for printing in several locations remote from the original one, while another may want a simple system in which the required prints or transparencies can be made from the original negative carefully maintained at a laboratory in the vicinity. A third variant is to produce an original positive transparency, which may be the working record, and from which further positives are produced when required by means of a reversal color duplicating film. If the original transparencies are considered to be valuable, the working transparencies are provided by the reversal duplication process.

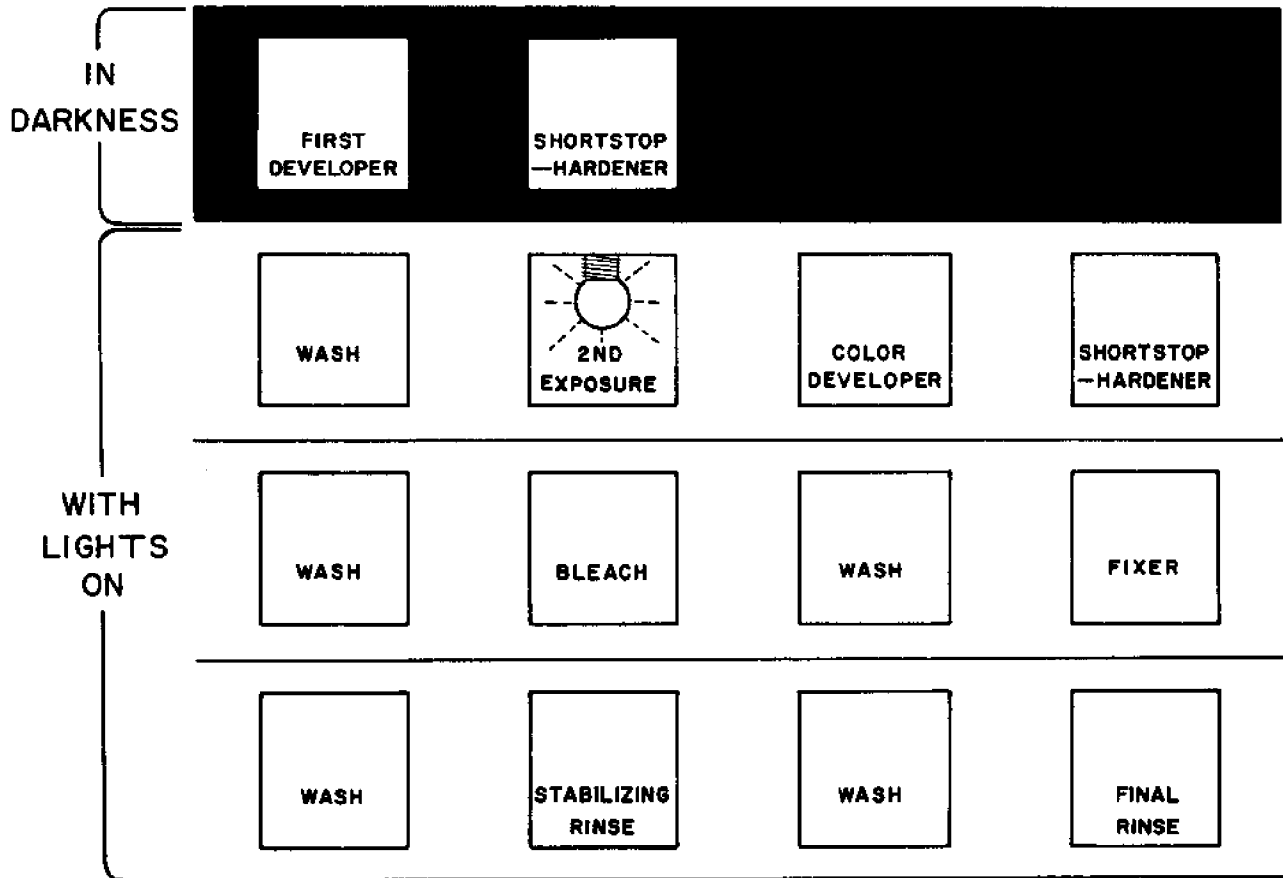
The ambidextrous nature of GAF 500 Color Aerial Film makes it possible to go either way, and in some instances it may be desirable to go both ways: start with an original negative for some projects, and start with a positive original for others.

GAF 500 Color Aerial Film is of standard tri-pack make-up with the red sensitive, cyan dye forming layer next to the anti-halation colloidal silver layer coated on the polyester base support. The green sensitive, magenta dye forming layer is separated from the bottom emulsion layer by a clear gelatin separating layer. A blue-absorbing filter layer covers the green sensitive layer, and on top of this is the blue-sensitive, yellow dye forming layer. The film has an ASA exposure index of

500, or an aerial exposure index in the vicinity of 50. Its relatively steep gradation enhances color photographs from the air. It is processed in the GAF AR-2 reversal color process in continuous machines having a "serpentine" configuration. "Field" processing may be accomplished in a modified process, AR-2c, using wind-rewind processors.

The GAF AR-2 processing procedure is relatively simple, Figure 1. A negative image is first developed in all three of the emulsion layers in total darkness, as shown in the schematic diagram. This image is made up of silver and will subsequently be removed. The second developing step during which the colored dyes are formed is carried out after the positive image in the film has been exposed to light. The other steps of the process are, in effect, auxiliaries to the basic process as just described. These include a shortstop-hardener after each of the two developer steps, a bleaching step to convert the silver from the first developer step to a silver bromide that can be removed in the fixer. The stabilizing rinse and final rinse serve to render the dye images more resistant to fading than would otherwise be the case. The other steps are washes to remove the chemicals employed in the various processing steps, prior to introduction of the film into the next step of the process.

## PROCESSING



The AR-2 chemicals form the basis for the modified procedure for obtaining a color negative with the GAF 500 Color Aerial Film. The second developer from the reversal process is modified to produce a single color-forming developer used to generate the negative image. As in the reversal process, the bleach is used to convert the silver formed at the same time as the color image, to a soluble silver halide that is removed in the fixer.

Sensitometric curves plotted from densities read through filters approximating the response of the human eye are shown in Figure 2. A curve for GAF 64 Color Slide Film, used for ordinary "ground" photography, is included on the graph for comparison. This illustrates the relative contrast characteristics of the GAF 200 and GAF 500 Color Aerial Films. The lower gradation of the GAF 200 Film, compared to the GAF 500, permits wider exposure latitude, but the contrast enhancement is not as great as that available from the GAF 500 Film.

Figure 3 shows sensitometric curves for the GAF 500 Film obtained by plotting the densities of the processed sensitometric exposures, measured through red, green and blue filters. These are the integral densities of the layers containing the cyan, magenta and yellow dyes, respectively.

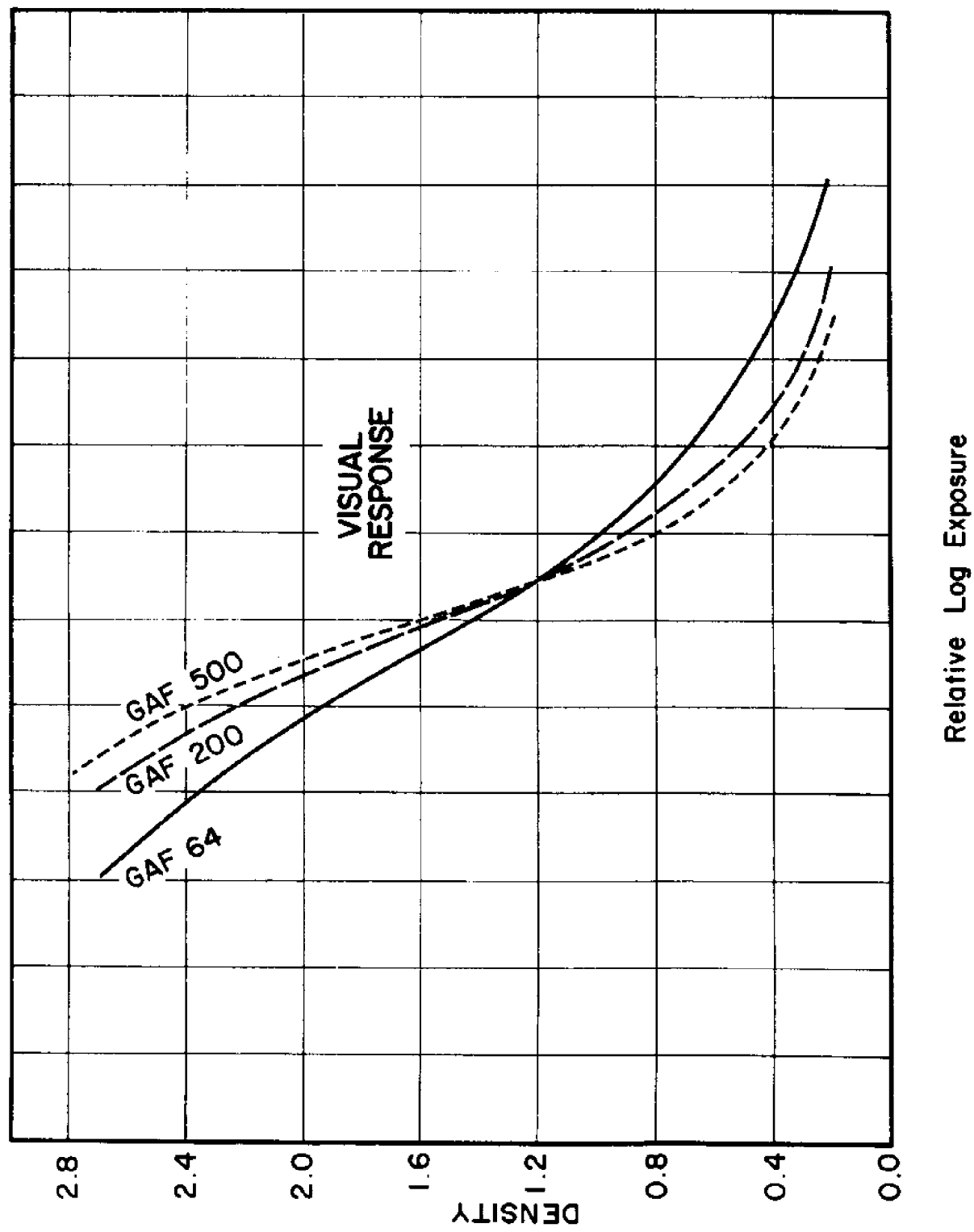


Fig.2

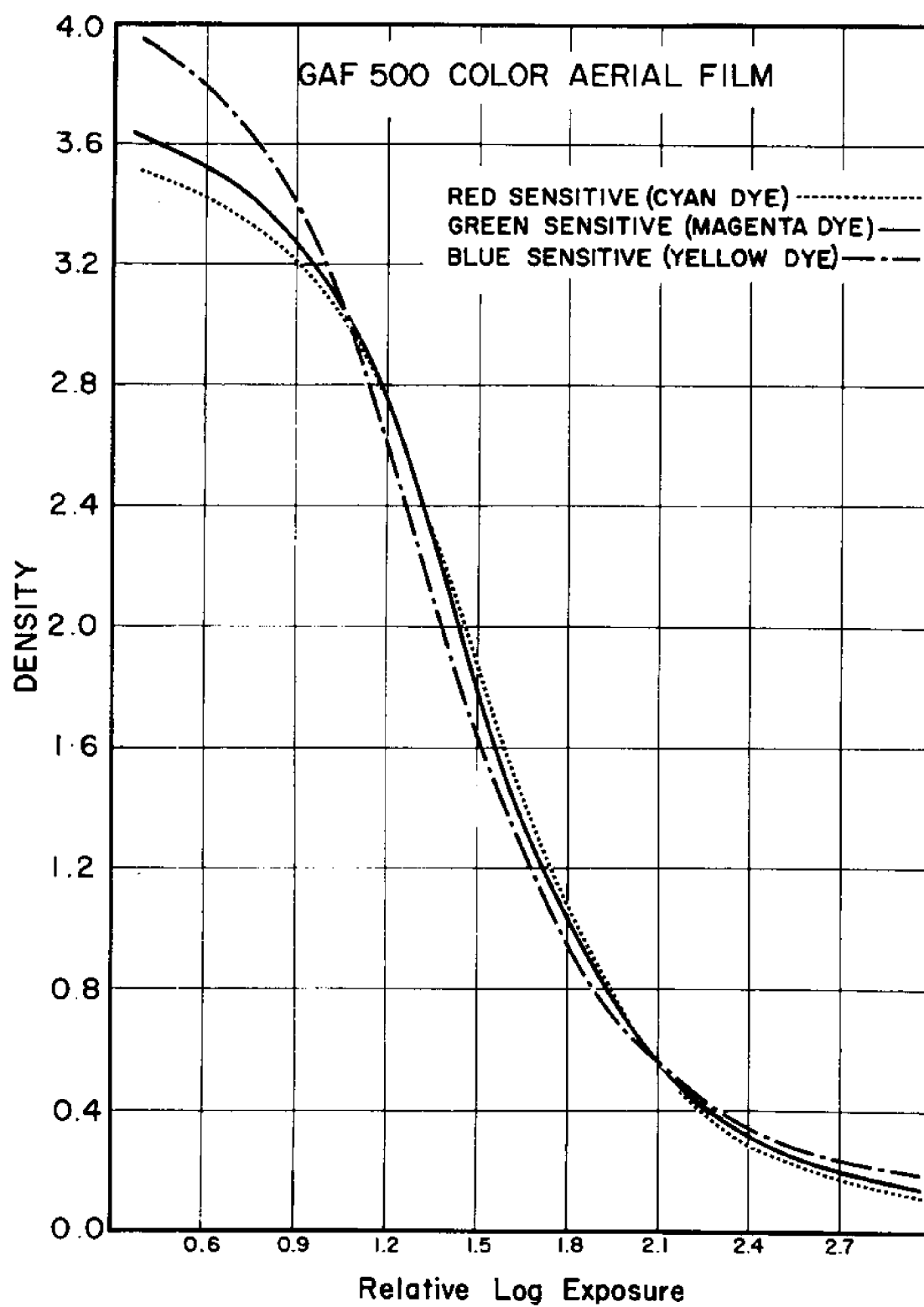


Fig.3

GAF has for many years manufactured two films designed for making reversal duplicates from aerial color positive transparencies. One of these, Type 6470, is on a 7 mil thick acetate base, and is normally for sale in sheets; although it can be made available in roll form for duplicating rolls of aerial film. Its speed is such as to facilitate making enlarged transparencies from single frames of aerial photography. The second film, Type 5470, is on a 4½ mil thick acetate "cine" base, and is sold in roll form in all widths. Processing for both of these products is identical to that for the other GAF Color Aerial Films, with the exception that they are not suitable for processing to a negative. In other words, they cannot be used as a "positive" material for printing from "negative" originals.

GAF manufactures Color Positive Paper that is ideal for printing from the color negatives obtained when the GAF 500 Color Aerial Film is processed as a negative. The processing system for the paper is not like the process for the aerial films. However, the procedure is basically similar to that used for developing the aerial films to a negative.

GAF 500 Color Aerial Film is recommended for photography over those lakes, streams, or ocean areas where there is relatively low light penetration of the surface. Highly polluted waters, or those with excess turbidity cannot be expected to be penetrated to any great depth by ordinary light recording sensors. In such instances, the water areas can be treated essentially as though



they were land areas, with only a minimum of penetration. The objective would be to obtain the best possible rendering of the subtle color differences near the surface; as, for example, the variously colored currents and pools tell their story.

However, in those water areas that are relatively clear, there is a great interest in sensing detail under water at some depths (1) from the air, and (2) from beneath the water surface itself. To serve in applications of this kind, GAF 1000 Blue Insensitive Color Aerial Film<sup>®</sup> has been provided.

When making color photographs of the ocean floor from the air with ordinary tri-pack color film such as GAF 500 Color Aerial Film, it is usually necessary to filter out practically all of the blue light reaching the top layer of the film. This is necessary because a great proportion of the light illuminating the water is "skylight illumination". Much of this light is scattered and refracted to the surface without reaching the bottom, and thus adds to the overall intensity of light at the point on the surface where the useful incident light is reflected vertically. This scattered and refracted light may be referred to as "under water haze". "Aerial haze" above the water surface is also largely made up of light in the blue region of the spectrum.

There is no need to record a blue image in this type of photography since the blue light entering the water and being radiated from the bottom back through the water is largely attenuated by this scatter and absorption. Indeed, in most cases the useful light in this kind of photography is made up of wavelengths usually in the range of 480 to 600 nanometers, and some studies have indicated that 560 nanometers represents the region of the visible spectrum that provides the maximum incident light reflected vertically from the bottom with the least interference of other light in the water. This, of course, may vary in different regions due to different proportions of materials such as plankton, minerals, etc., that exist in the water.

When the regular GAF 500 Color Aerial Film is exposed over water with a yellow filter over the camera lens and processed, it has a deep yellow color because yellow dye is formed in the unexposed top layer. In this case, the yellow serves no useful purpose, and its formation represents an inefficiency in this application of the process. The filter over the camera lens makes it necessary to give additional exposure, and thus reduces the effective speed of the film.

Experience has shown that to record details on the ocean bottom requires at least two stops more exposure than does terrain photography under similar conditions of surface illumination. The yellow filter used with ordinary three-color film has a factor of about 2, which makes it almost impossible to record detail in deep water. The GAF 1000 Blue Insensitive Color Aerial

Film, therefore, with its one stop higher speed over GAF 500 Color Aerial Film, gives a 2 stop (4X) sensitivity advantage over the GAF 500 Film with yellow filter.

In the manufacture of the new film, the yellow filter normally placed between the blue sensitive layer and the green sensitive layer has been retained, and has been more highly hardened against scratches and abrasions.

Spectral sensitivity curves for the GAF 1000 Blue Insensitive Color Aerial Film, Figure 4, are similar to those for the three-layer GAF 500 Color Aerial Film in the red and green regions, but the blue sensitivity is virtually non-existent. Superimposed on this graph are the cut-off curves for the Wratten Number 16 and Number 21 filters which under some circumstances may be of value in "balancing" red and green sensitivity in actual photography. Immediately above the spectral sensitivity curves are two attenuation curves for ocean water, one for Chesapeake Bay and the other for the Coastal Gulf Stream. Above these are curves representing the spectral distribution for a cloudy sky, and the distribution for "mean noon sunlight" at Washington, D.C. These make it possible to visualize the importance of eliminating blue light incident on the water for photography, and the coincidence of minimum attenuation for these two waters with parts of the red and green sensitization of the GAF 1000 Film.

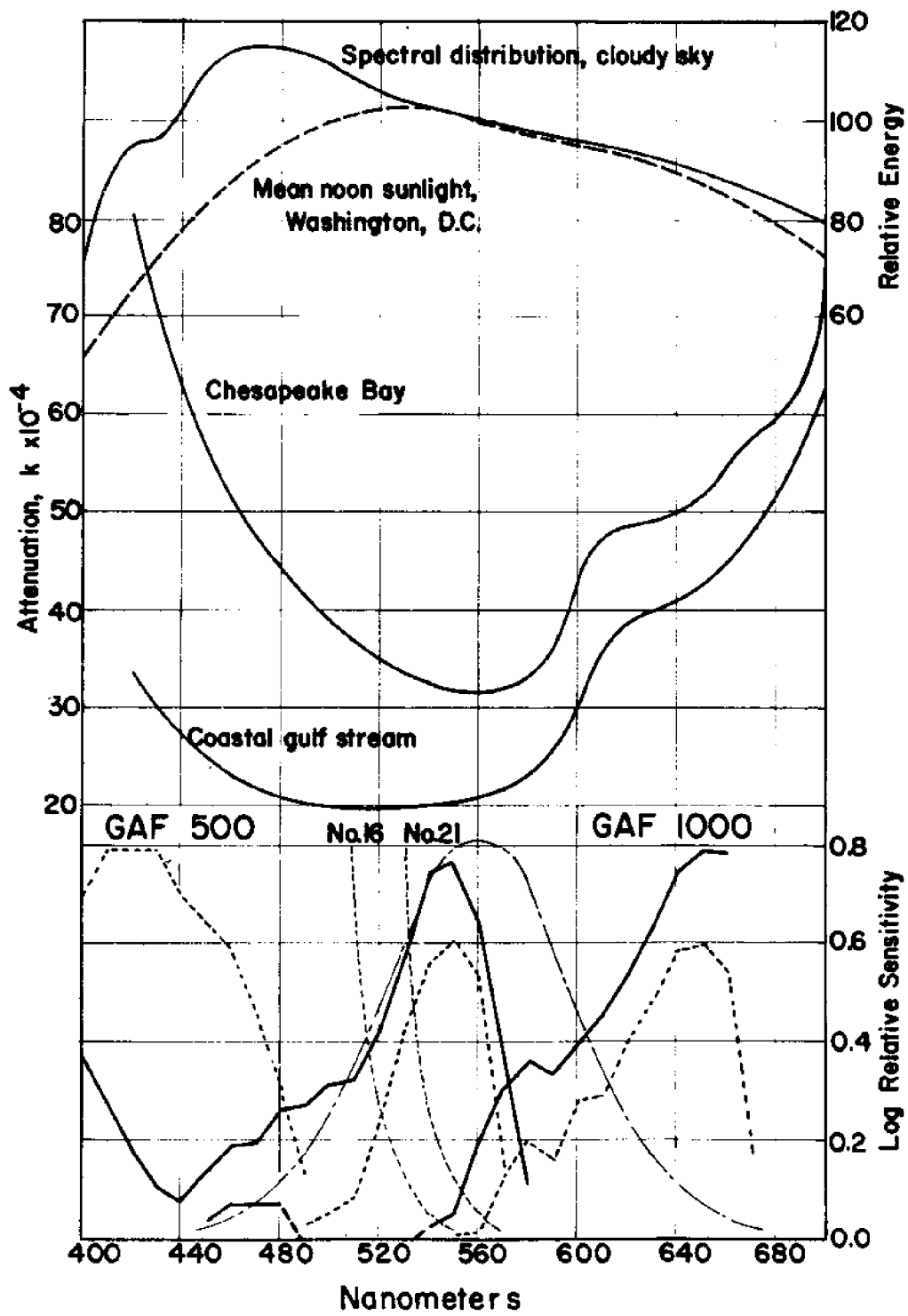


Fig. 4

Figure 5 shows integral color density curves for sensitometry of the GAF 1000 Film. Processing was accomplished in the AR-2 process. (The recommended development times for the original experimental coatings were shorter than standard. However, the production film made with a more highly hardened yellow filter layer responds well to the normal AR-2 Process.) The absence of the top layer found on the GAF 500 Film permits more rapid exchange of the processing solutions, and drying is somewhat faster, since less water load is carried out of the wash by the two layers of emulsion than would be the case when all three layers are present. The curve for blue filter densities results from blue absorptions in the cyan and magenta dyes (formed in the red and green sensitive layers).

A plot of "practical speed" versus first developing time is shown in Figure 6. These values are about equal to those that would be obtained by following the method given in American National Standards PH2.21-1961, Method for Determining Speed of Reversal Color Films for Still Photography. They can be used in conjunction with exposure meters calibrated in accordance with American National Standards, for determining the approximate exposure required for photography from the air. The Aerial Exposure Index (AEI) values to be employed with calculators for exposure in aerial photography are approximately one-tenth of these exposure index values.

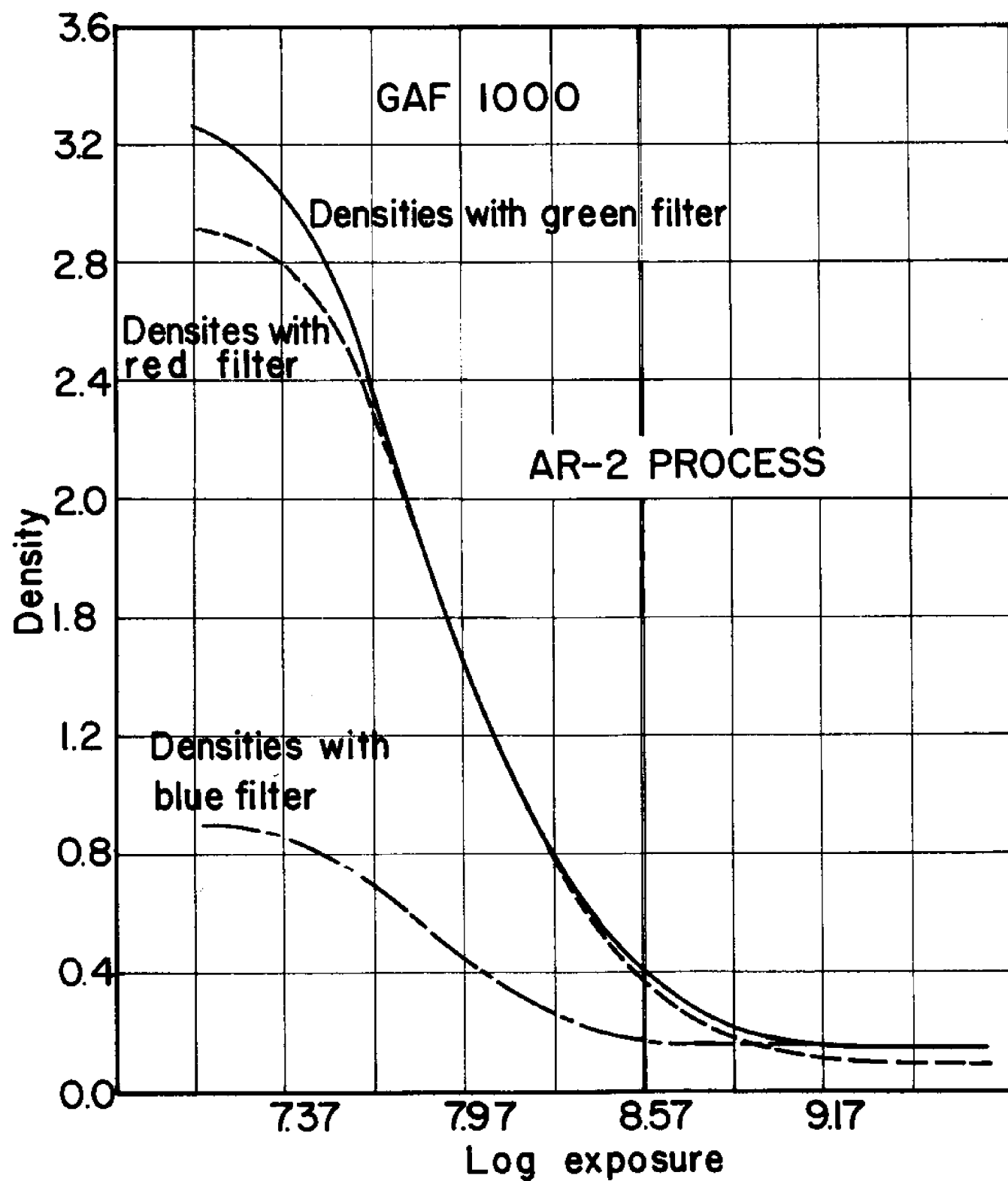


Fig.5

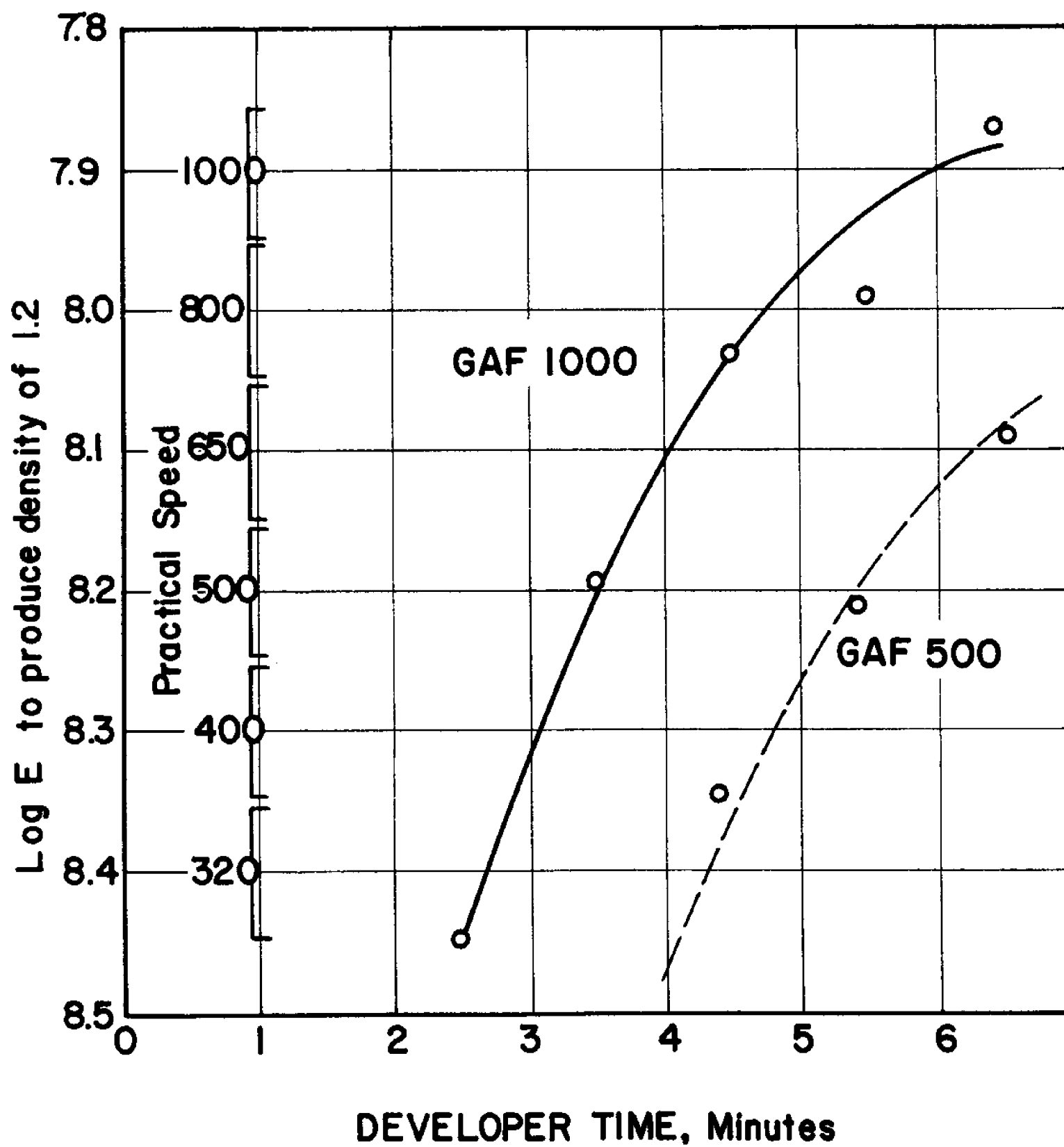


Fig.6

The determination of proper exposure for photography beneath the surface of water presents some problems, and the Exposure Index of 1000 (Aerial Exposure Index 100) should be used as a guide to establish the basic exposure for further testing. A series of tests should be flown over a given area with sensing system settings corresponding to EI 1000, and at settings that would be equivalent to an exposure one stop above and at one stop below this. Exposure meter readings, with a given meter, should be made at the time the exposures are made. Analysis of the photographs after processing in relation to the exposure meter readings can be used to establish an index value to be used with the sensing system, incorporating the GAF 1000 Film.

The visual RMS granularity (48 micrometer circular diameter scanning aperture) of the blue-insensitive film is, as would be expected, identical to that of the GAF 500 Color Aerial Film. This is illustrated in the RMS granularity vs density curves given in Figure 7. The test films were exposed with light having a "color temperature" of about 5500 K. Density measurements were made with a "visual" filter in the light path.

Resolving power of the blue-insensitive film is no higher than the maximum available from the GAF 500 Color Aerial Film, but the values for exposures other than optimum tend to be appreciably higher for the blue-insensitive film at exposure values on either side of the optimum, Figure 8. Exposures of targets were made with light having a "color temperature" about 5500 K, and the images of the targets were judged in a manner similar to that given in



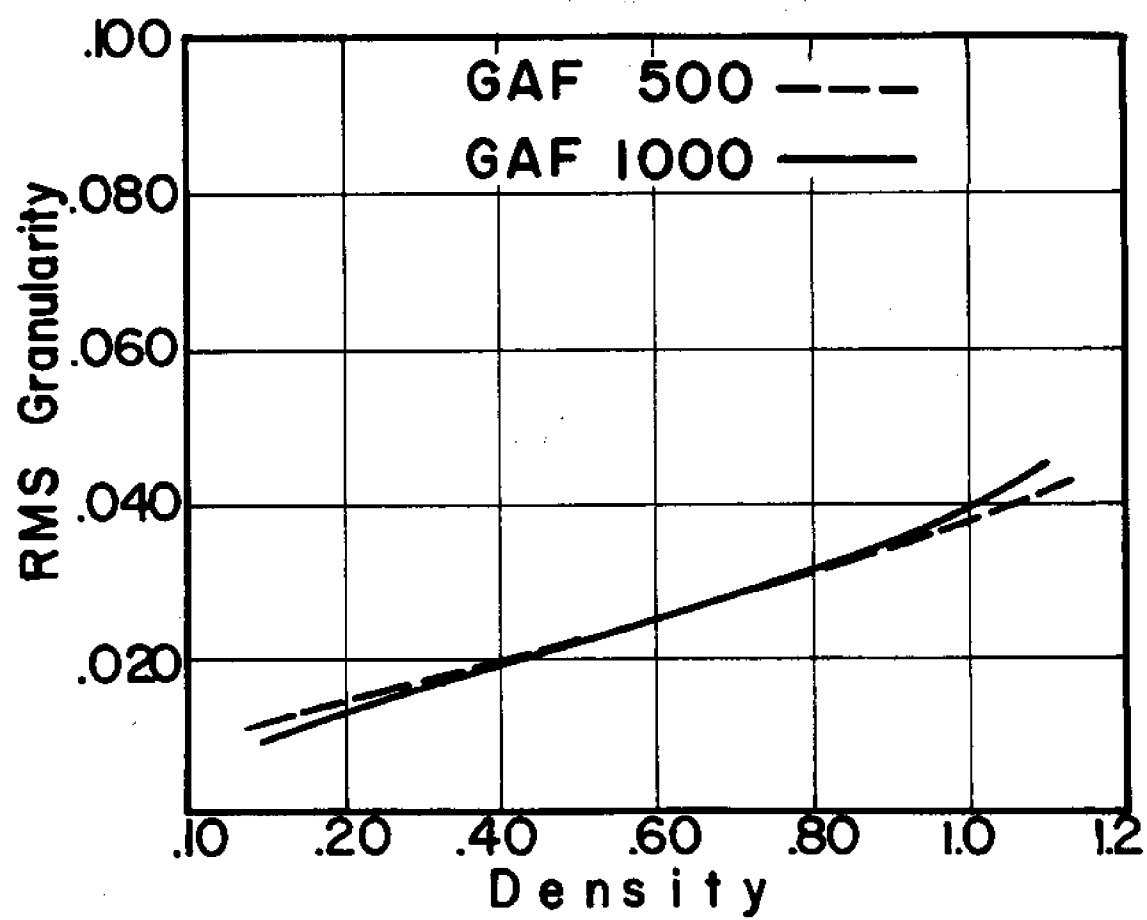


Fig.7

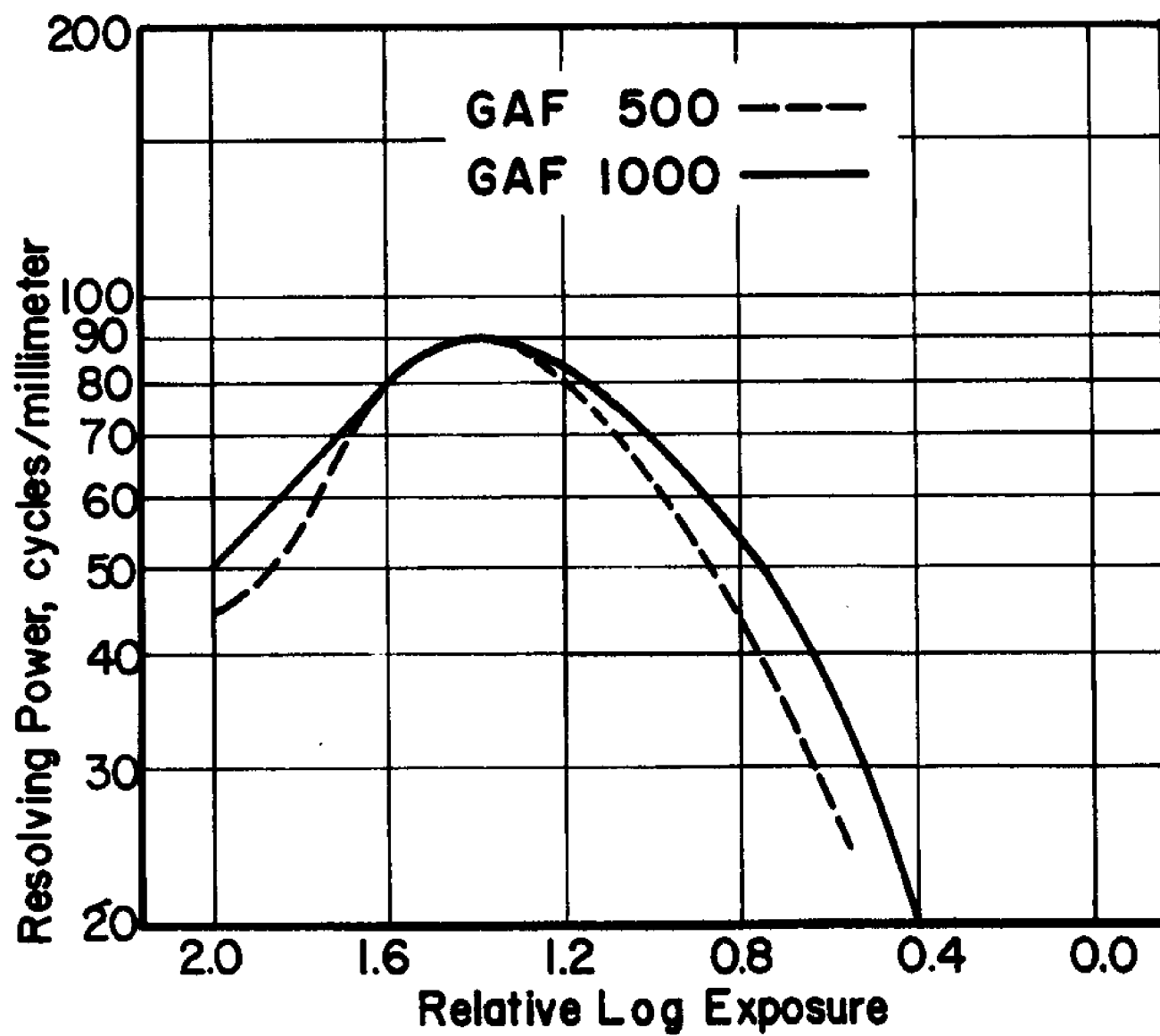


Fig. 8

ANS PH2.33-1969, Method for Determining the Resolving Power of Photographic Materials.

The GAF 1000 Blue Insensitive Color Aerial Film is also capable of being developed to a negative, just as is the GAF 500 Color Aerial Film, and a family of sensitometric curves for various color negative developments in the modified Color Developer #631 are shown in Figure 9. These are plotted from "visual" densities. Like films developed by the reversal process, these negative films, when processed, have a blue appearance.

Prints from the blue-insensitive film negatives, on color positive printing materials such as GAF Color Paper, can be balanced to have an appearance reasonably similar to those of the transparencies processed by the reversal AR-2 Process.

Contrast of films processed in the AR-2 reversal process can be increased to some extent by making reversal duplicates on GAF Color Duplicating Film Type 5470, and by proper choice of filtration when exposing the duplicates, some shift in emphasis of the details in the photographic record can be achieved.

I would like to express my appreciation to Willard Vary, John Smith (Coast & Geodetic), George Keyes, and Mel Taylor for their assistance in testing and evaluating the GAF 1000 Blue-Insensitive Color Aerial Film.

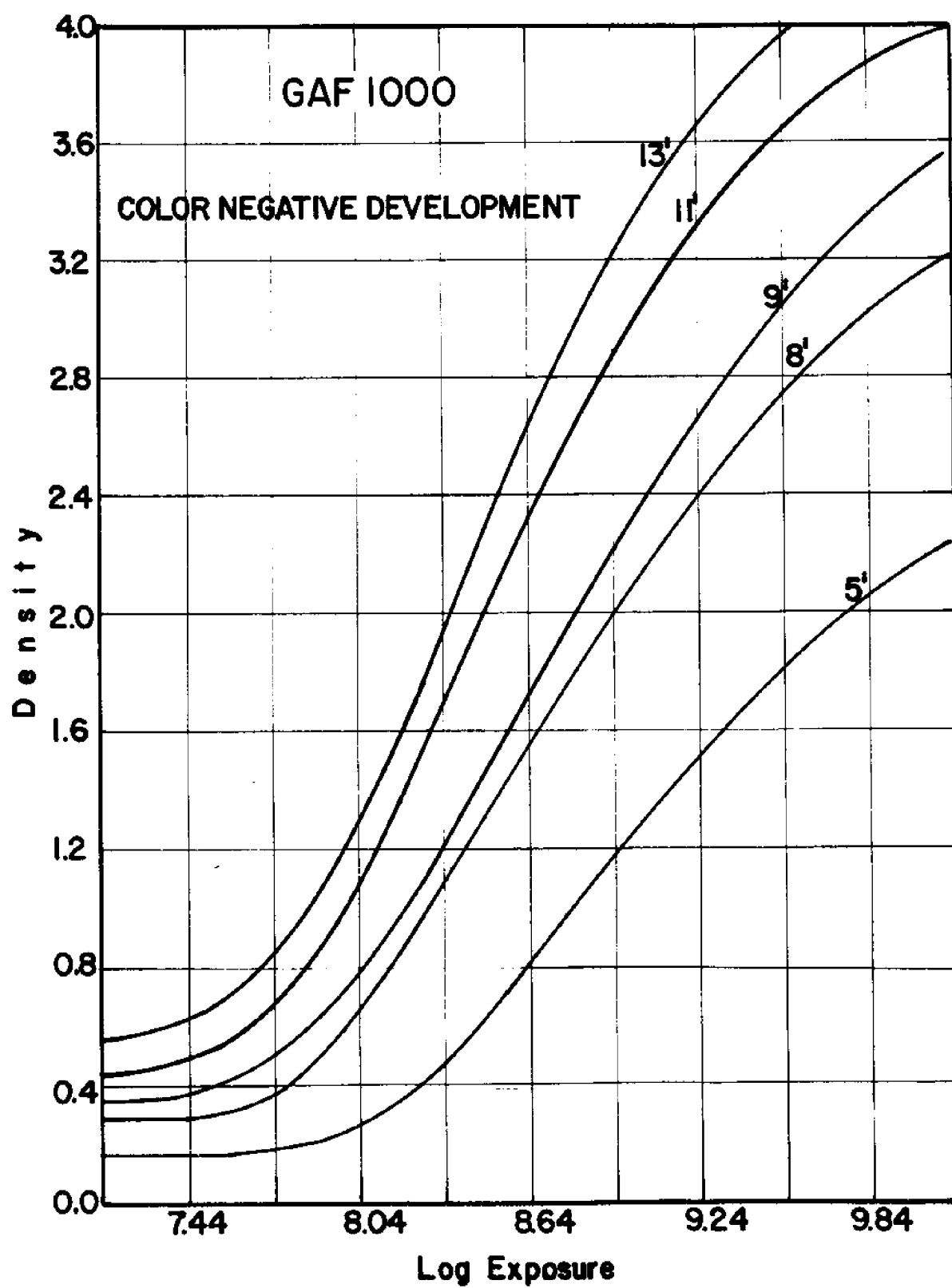


Fig. 9

BIBLIOGRAPHY

- (1) Hulburt, E. O., "Optics of Distilled and Natural Water",  
Journal of the Optical Society of America,  
Vol. 35, No. 11 (November 1945)
- (2) Current, Ira B., "Sensitometry in Color Aerial Photography",  
Photogrammetric Engineering,  
Vol. 33, No. 10 (October 1967)
- (3) Current, Ira B., "A Blue-Insensitive Anscochrome Aerial Film"  
Technical Papers from the 35th Annual Meeting,  
American Society of Photogrammetry  
(March 9-14, 1969)
- (4) Vary, Willard E., "A New Non-Blue Sensitive Aerial Color Film",  
Seminar Proceedings "New Horizons in Color  
Aerial Photography", ASP & SPSE  
(June 9-11, 1969)

## APPLICATIONS OF MULTISPECTRAL SENSING TO MARINE RESOURCES SURVEYS

By Fabian C. Polcyn  
University of Michigan

The development of the multispectral scanner (Ref. 1) has brought about a new dimension in airborne and spaceborne surveys for both marine and land resources. By utilizing the simultaneous registry of several spectral bands in the visible and in the infrared region, and storing this data on magnetic tape, electronic data processing techniques can be used to analyze large volumes of data and extract classes of features with similar spectral characteristics. Certainly the advent of satellite sensing will provide enormous quantities of data which cover large areas and will require machine methods of processing to make available this new information for the resource manager in a timely manner.

In this paper, we wish to describe examples of several applications of this new technique to various aspects of the marine environment. We shall cover (1) mapping of aquatic vegetation, (2) the feasibility of remotely measuring water depth, (3) the study of thermal effluents and associated water mass movements, and (4) the detection of industrial discharges as well as (5) the mapping of large oil slicks near shore while differentiating the oil from some of the aquatic vegetation such as kelp that occurs in certain areas.

The multispectral system used by the University of Michigan is illustrated in Figure 1. It consists of two double ended optical mechanical scanners which provide for placement of detector packages in four locations. For the visible region 0.4 to 1.0 $\mu$ m, there is a spectrometer which is used to give a simultaneous record in twelve bands for each resolution element. In

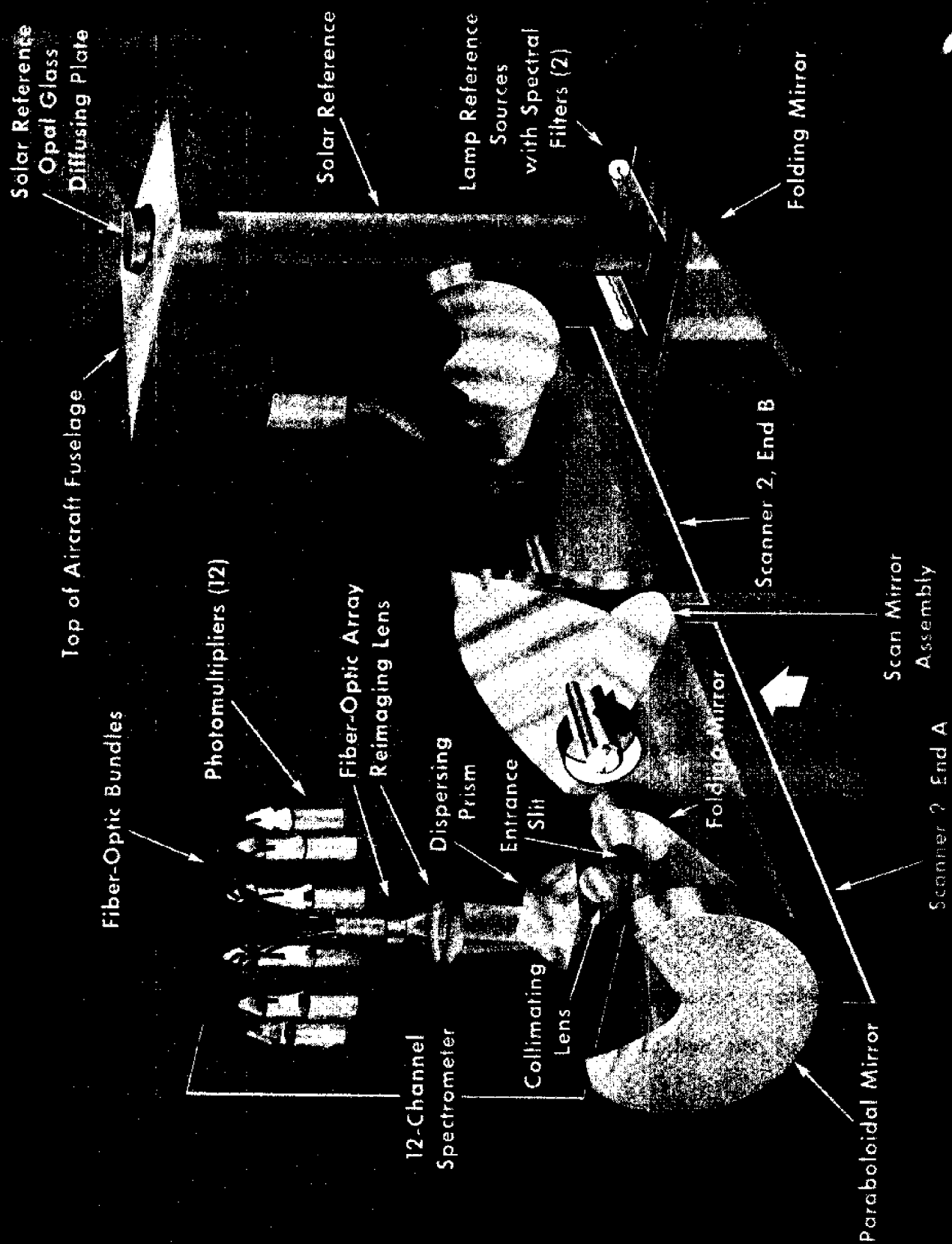
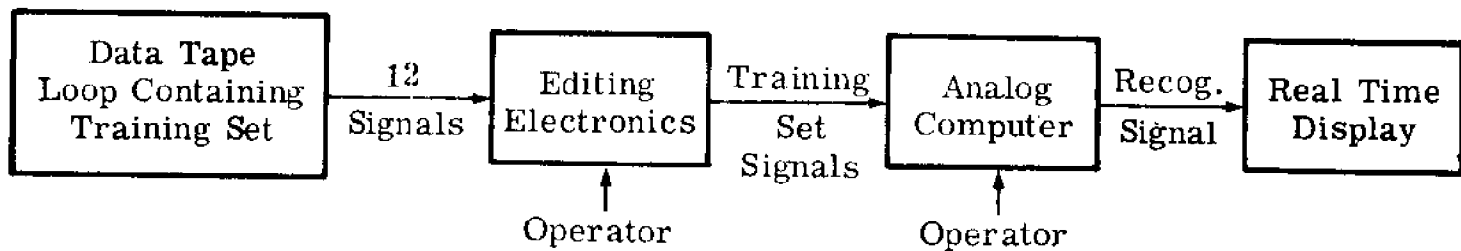


FIGURE 1. MULTISPECTRAL SCANNER

this particular system the ground resolution at 1000 ft. altitude would be equal to a 3 x 3 ft. area. In other detector positions, either single element detectors operating in the ultraviolet or thermal infrared region or a 3 element near-infrared detector is used to provide data in the 1-1.4 $\mu$ m, 1.5-1.8 and 2.0-2.6 $\mu$ m regions. Not all of these IR detectors are used in marine survey situations because of the high absorption of the infrared wavelengths by water.

Since the data is placed on magnetic tapes and has been collected through a common aperture, the format is readily usable for electronic analog and digital computer processing. This particular method of processing the data is shown in Figure 2 where we see illustrated the steps that leads to vegetation analysis of the Florida Everglades. (Ref. 2) First the operation is set up to find a training set for an object we are trying to map. The spectral characteristics are stored in the computer; the likelihood ratio is formed electronically and the data is played back in real time. Each object whose spectral characteristics matches that stored in the computer from the training set, is then printed out separately. This can be displayed as a black and white strip where white would be a positive decision that the object was indeed recognized and a black area where it is not present. These displays are normally color coded for each object and photographed as a color display and called a color coded recognition map. Since color examples were not available in this publication, only the black and white displays are shown. Other display techniques are possible, for example, digital printout sheets where symbols can be used to denote a particular material type. For some purposes, only an area count is needed and no imagery at all needs to be reconstructed. The computer can map and count each resolution





Training Mode

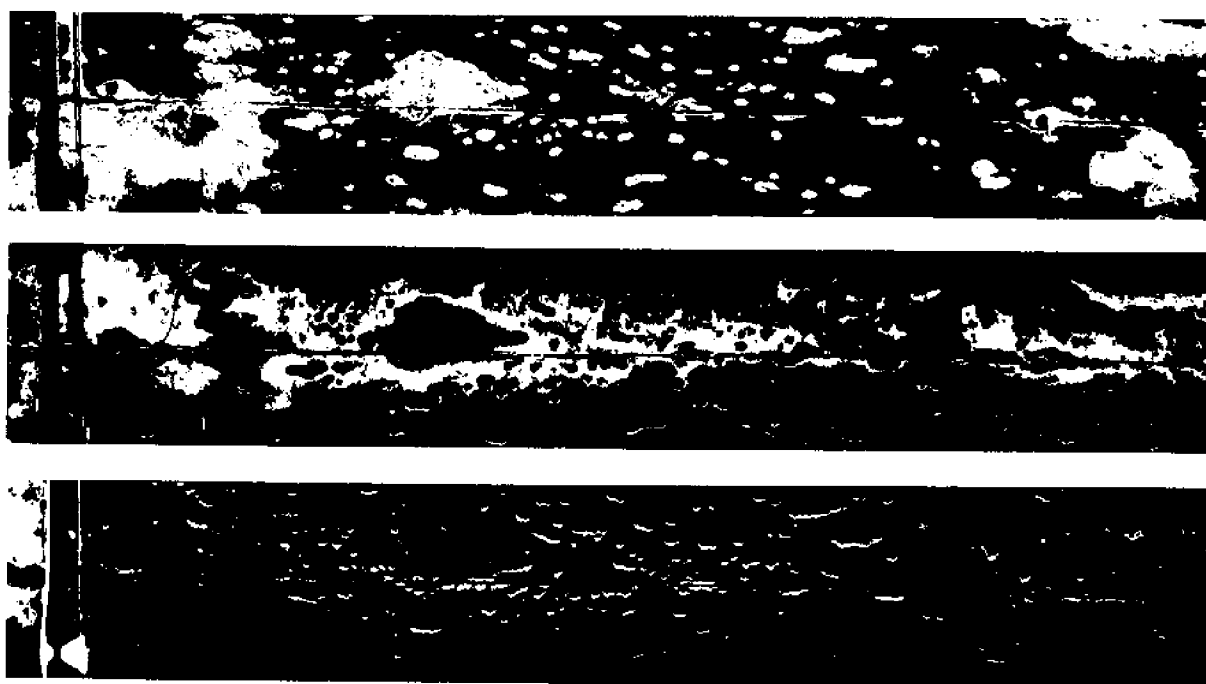
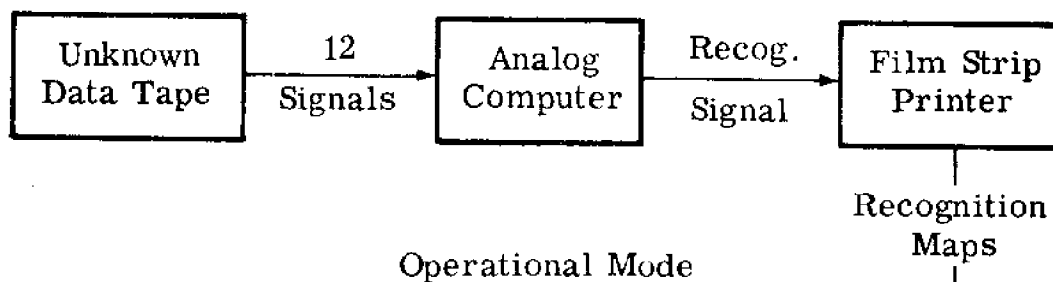


FIGURE 2. MULTISPECTRAL PROCESSING PROCEDURES AND RECOGNITION MAPS  
 Strip 1 - Tree Island  
 Strip 2 - Saw Grass  
 Strip 3 - Water

element of a given object that was recognized and provide the area numbers based on the size of the resolution element. This would be the optimum use of the machine when an inventory of the total area is desired. In some cases, the geographical distribution of a particular species is desired, so that a two dimensional format is the useful output.

Besides the demonstration of feasibility of mapping the vegetation succession in the Everglades, work has also been done to map underwater vegetation species in Biscayne Bay. This work is presently in progress and preliminary results show promise.

The area is also being used to study the potential of remotely measuring water depth. The multispectral sensing method (Ref. 3) uses ratios of signal returns in two spectral channels. In Figure 3, we see displayed five spectral channels for the area near Caesar Creek and extending out to Pacific Reef in the Florida Keys. One can note in the .4-.44 $\mu$ m channel that the light penetration is not optimum and a lower contrast image is formed. As one moves toward the bands .50-.52 and .55-.58 $\mu$ m, the underwater detail is now clearer and as one moves to the red region .62-.68 $\mu$ m, only the shallow features are displayed because of the higher absorption of the water at these wavelengths. Finally, if one looks in the .8-1.0 $\mu$ m band, only land/water boundaries are mapped.

One can see then that there is a relationship of light penetration with spectral channel and from this fact an equation was developed (shown in Figure 4) where  $z$  (representing the depth of the water being measured) is equated to certain variables which are easily measured by the scanner system itself or can be estimated a priori. The  $\alpha_1$  and  $\alpha_2$  are the extinction coefficient of water at two different wavelengths, the  $\rho_1$  and  $\rho_2$  are the

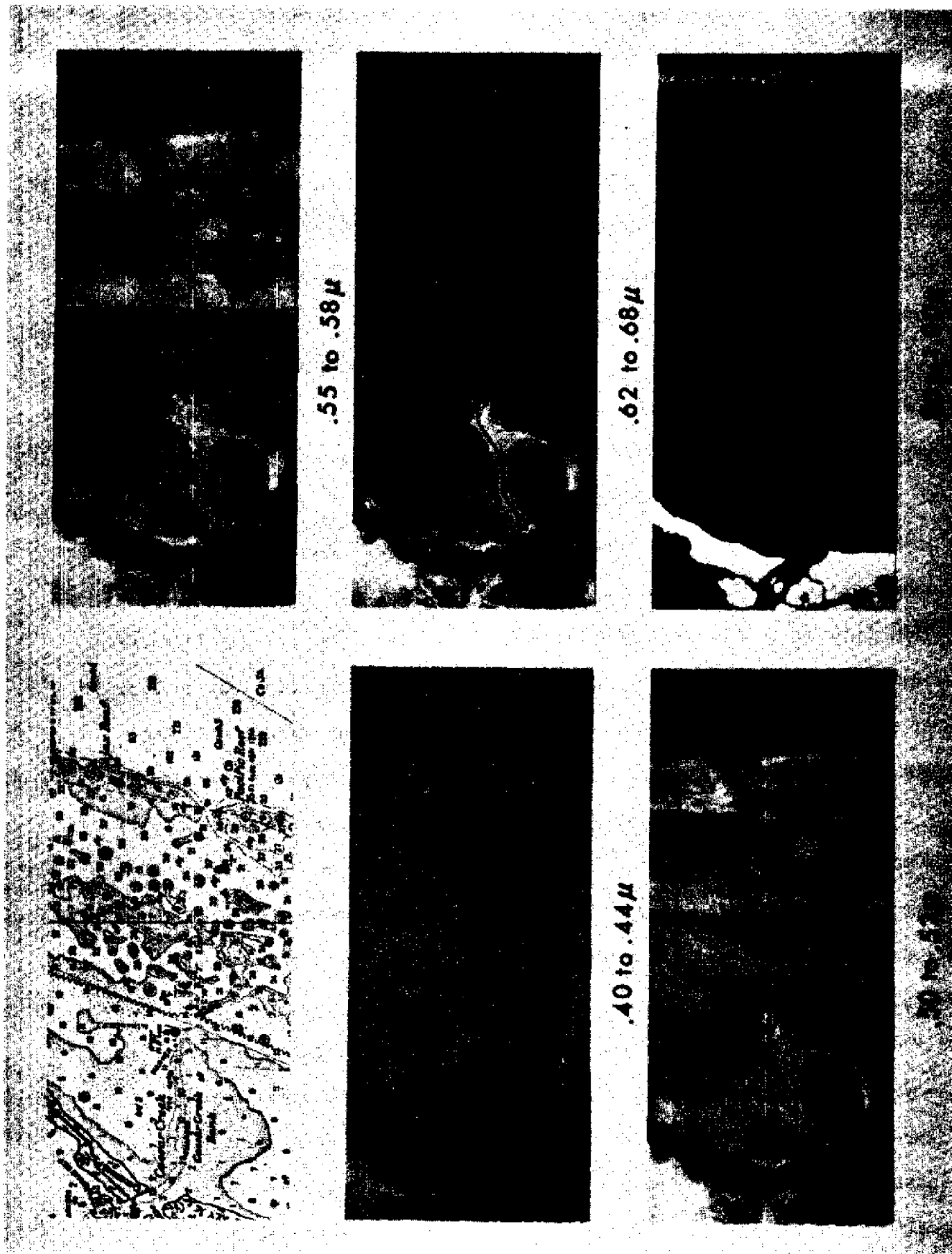


FIGURE 3. COMPARISON OF LIGHT PENETRATION IN WATER

$$V_{\lambda} = K_{\lambda} \rho_{\lambda} H_{\lambda} e^{-\alpha_{\lambda} Z (\cos^{-1} \theta + \cos^{-1} \phi)}$$

$$Z = \frac{1}{(\alpha_{\lambda_2} - \alpha_{\lambda_1}) f(\theta, \phi)} \ln \frac{V_{\lambda_1} K_{\lambda_2} \rho_{\lambda_2} H_{\lambda_2}}{V_{\lambda_2} K_{\lambda_1} \rho_{\lambda_1} H_{\lambda_1}}$$

FIGURE 4. EQUATION FOR COMPUTING WATER DEPTH

reflectances of the bottom material at different wavelengths, and the  $V$  is the voltage in the particular spectral channel, the  $E$  is the incoming sunlight in that channel, and  $K$  represent scanner constants that are known from tests of the system.

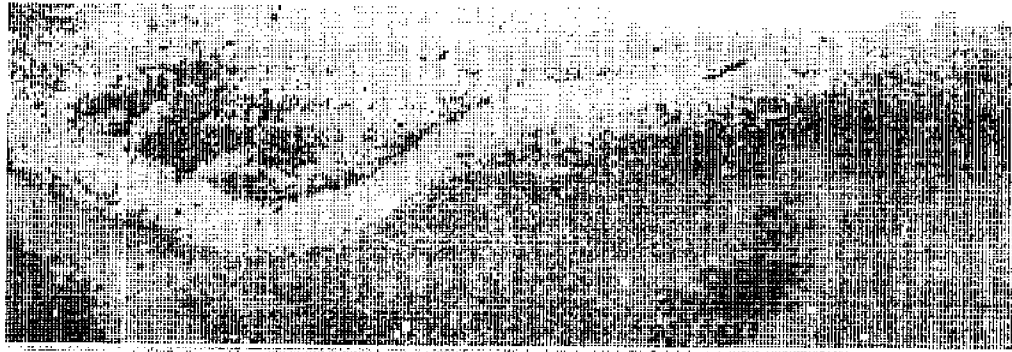
The present Michigan aircraft is equipped with a sun sensor so that for each scanline, the sensor can be referenced to both internal standard lamp, and an input that represents the illumination arriving at the top of the aircraft.

The computation using this equation is performed on a digital computer. Certain scattering and surface reflecting effects are taken out by making use of points in the scene that do not have a reflection from the shallow waters so that we separate the bottom reflection from scattering effects. The results of this processing are shown in Figure 5 where each symbol has a particular depth range as shown in Table 1. The outline of Caesar Creek can be seen in the data and for comparison, a black and white strip map of the area is shown as well.

Another application area is the study of thermal discharges from a number of power generation plants being built along the Lake Michigan shoreline (Ref. 4). Studies have been performed by the University of Michigan in the southeast corner of Lake Michigan covering areas near Michigan City, Indiana and Port Sheldon, Michigan. By using the thermal channel in the 8-14 $\mu$ m region or in some cases filtered between 10 and 12 $\mu$ m to reduce the atmospheric correction problem a map of the thermal mixing pattern can be obtained. Figure 6 shows an example of this type of survey. The original was color coded by slicing the scene at different voltages and stored on the magnetic tape and which are related to different temperatures. One can easily see the patterns of the mixing as the warm water enters into the harbor and mixes with the lake waters.

TABLE I  
DEPTH IN FEET

RANGE	SYMBOL
0	0
1	1
2	2
3	3
4	4
5	5



Infrared and  
Optics Laboratory

*Willow Run Laboratories*

THE INSTITUTE OF SCIENCE AND TECHNOLOGY  
THE UNIVERSITY OF MICHIGAN

FIGURE 5. COMPUTER GENERATED DEPTH MAP

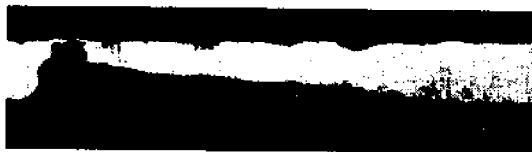


FIGURE 6

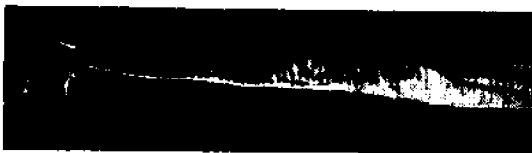
The display shown in Figure 7 is in the same area including some of the shoreline of Lake Michigan to the east of Michigan City. Each slice is shown in black and white so that the white represents all areas at the temperature indicated below each strip. As one moves up in temperature, the warmer areas are then denoted by the light tone. The point of initial discharge of the warmest water can be seen as a small white area at the left hand side of the lowest figure.

In addition the same data can be displayed in computer format (Figure 8). This is the harbor at Michigan City with symbols denoting the temperature ranges. This particular method of display is useful when corrections for atmospheric effects have to be made. This is certainly the most useful method for studying time comparisons most accurately at the same geographical points.

Besides the study of the temperature patterns in the mixing zones, one is interested in mapping the distribution of the water masses that are moved about by nearshore currents. In this case, Figure 9, (the original was in color) the zones of different water masses can be seen in different shades, in the vicinity of the harbor. These particular water masses were delineated by the multispectral processing approach in which selected areas are picked as training sets, their characteristics are stored in the computer, and the computer prints out all areas of the water that have the similar spectral characteristics. The spectral characteristics are related to the algal communities involved in the volumes of water as well as the suspended sediments, so we are seeing the distribution of a particular community as described by its color characteristics. These patterns have been observed to change from day to day because of the different winds and could be used in studying large current movements.



23.4° C and Below



23.4° C. to 23.8° C



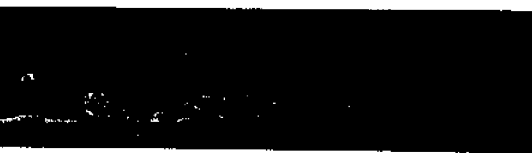
23.8° C. to 24.1° C.



24.1° C. to 24.5° C.



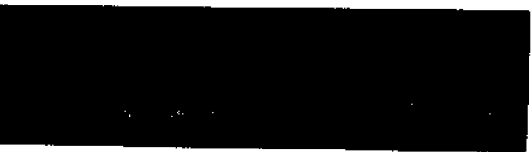
24.5° C. to 24.8° C



24.8° C. to 25.2° C.



25.2° C. to 25.6° C.

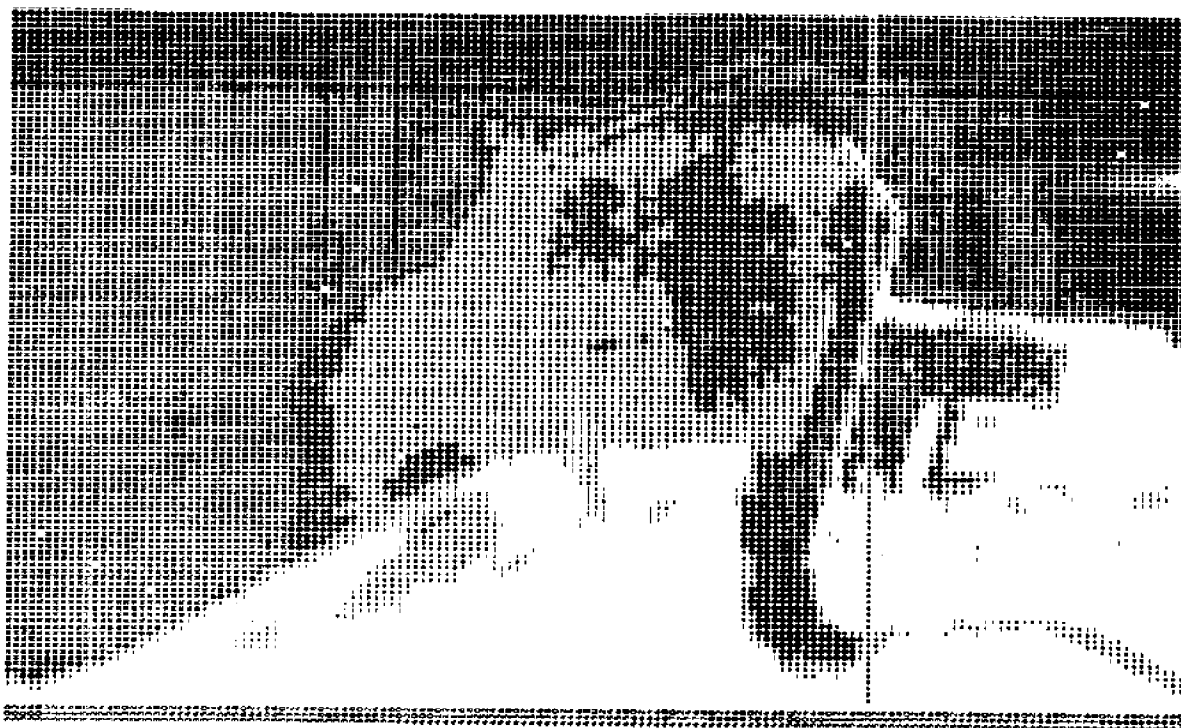


25.6° C. and Hotter

**THERMAL (8-14  $\mu$ m) CONTOUR OF MICHIGAN CITY HARBOR**  
**Data Taken: 11 August 1969**

FIGURE 7





LAKE MICHIGAN WATER POLLUTION STUDY, MICHIGAN CITY, THERMAL

RANGE	SYMBOL	TEMP [°C]
-5.0000 - .1250	-	- 23.5 C AND BELOW
.1250 .1250	-	- 23.5 C to 24.0 C
.1250 .3750	-	- 24.0 C to 24.5 C
.3750 .6250	*	- 24.5 C to 25.0 C
.6250 .8750	#	- 25.0 C to 25.5 C
.8750 1.1250	+	- 25.5 C to 26.0 C
1.1250 9.0000	K	- 26.0 C AND ABOVE

FIGURE 8



WATER MASSES AT HARBOR AT MICHIGAN CITY  
INDIANA, 11 AUGUST, 1969

WRL

FIGURE 9

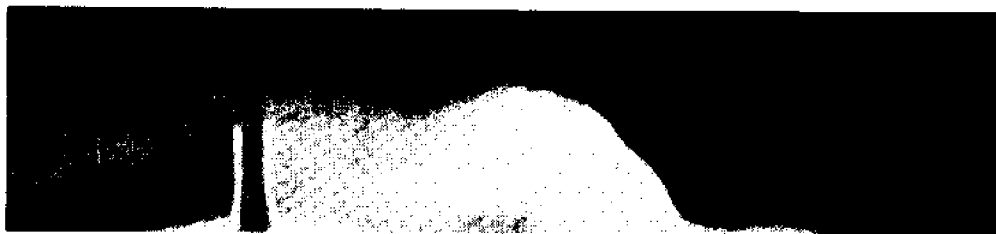
To see the way in which changes in wind direction and velocity effect the surface distribution of thermal plumes, note Figure 10 which shows a particular plume near Port Sheldon, Michigan. It was observed at the times indicated, under a variety of patterns based on both wind conditions at the time of overflight and the previous wind history of 24 to 48 hours earlier to the time of overflight. The upper strip can be seen to be produced by a wind from south, the plume is mostly northward; the second time it was observed, there was a strong wind from the northwest which produced a pattern where some of the warmer water near the surface was brought towards shore. For the last condition, (the lower strip) a case of transition was observed where a previous history of strong winds had set up a shore current moving to the left or southward. One can see the beginning of a northward movement along the lower edge to the right produced by a southeast wind which was blowing at the time the image was collected. These particular patterns are being studied in relation to the phenomena known as the thermal bar which occurs in the Great Lakes during the spring. Figure 11 shows an infrared image of the area offshore Grand Haven and Muskegon, Michigan. We are seeing a length of shoreline approximately 30 miles long, we see at the lower edge two river plumes that add their heat to the lake. The light tones are warmer than the darker tones. We also observed that at the same time there were color differences along the temperature anomalies, i.e., the lighter tones on the thermal image corresponded to lighter blue-green tones in color films. There was a 2 to 1 ratio in algal population across this temperature boundary. The multispectral technique should prove useful in mapping the distribution of these particular patterns and further studies are planned for the spring of 1971.



7 MAY, 1968, SE WIND AT



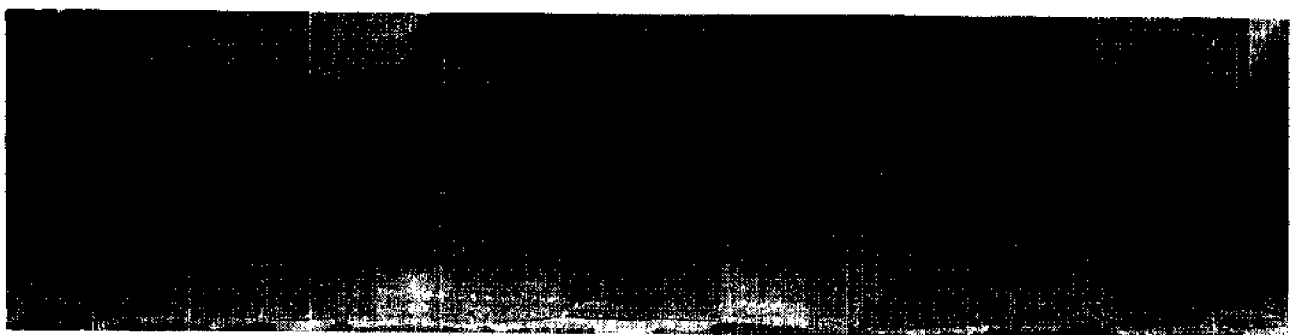
26 SEPTEMBER, 1968, NW WIND AT 10-20 KTS.



11 AUGUST, 1969, SE WIND AT 4 KTS.

## WIND EFFECTS ON DISCHARGE PLUMES

FIGURE 10



INFRARED IMAGE OF "THERMAL BAR" IN LAKE MICHIGAN

FIGURE 11

The fourth application area involves the mapping of industrial discharges by the multispectral technique (Ref. 5). Figure 12 shows four selected channels from the set of 17 that are available from the University of Michigan scanner. The upper strip is the image in the .44-.46 $\mu$ m band and shows the lighter tones due to the presence of oil films. The strip marked .58-.62 $\mu$ m tends to emphasize the steel plant discharges from a strip mill as a dark tone and the pickling liquor discharge (on the right) as a very bright tone. In the .72-.80 $\mu$ m band, the waste treatment plume outfall from the city of Detroit can be observed. Finally, in the lower strip for the 8-13 $\mu$ m band, the warm discharges from a power plant can be seen. Also, the steel plant discharge and the Rouge River entering the Detroit River come in at higher temperatures. Thus, with these four channels one can begin to see the potential capability of enhancing the contrast for different pollutant types as an aid in detection and mapping of distribution patterns. This can be seen in another way when one analyzes the data from the multispectral scanner and computes an apparent reflectance based on the data in each of the bands in the visible regions. These are displayed in Figure 13, which compares the spectra of major pollutants found along these two rivers. One can see that there are different spectral reflectance characteristics for the different manufacturing outfalls. This particular experiment also shows that two different plants using a similar manufacturing process and discharging a similar pollutant did indeed, tend to have similar spectral characteristics.

In addition, the question of mapping concentration gradients is at present, being undertaken to try to extract this particular parameter from the multispectral data.

Finally, the last application area to be discussed is the mapping of large oil slick plumes that occur offshore due to leaks from oil drilling

# DETECTION AND IDENTIFICATION OF INDUSTRIAL POLLUTANTS BY SPECTRAL ANALYSIS

MULTISPECTRAL IMAGERY OF DETROIT RIVER SHOWING SELECTIVE ENHANCEMENT OF POLLUTANTS IN VARIOUS SPECTRAL REGIONS

Oil Film

Rouge River

0.44-0.46  $\mu\text{m}$

Steel Plant  
Ship Mill Discharge

0.56-0.62  $\mu\text{m}$

City of Detroit  
Waste Treatment Plant Outfall

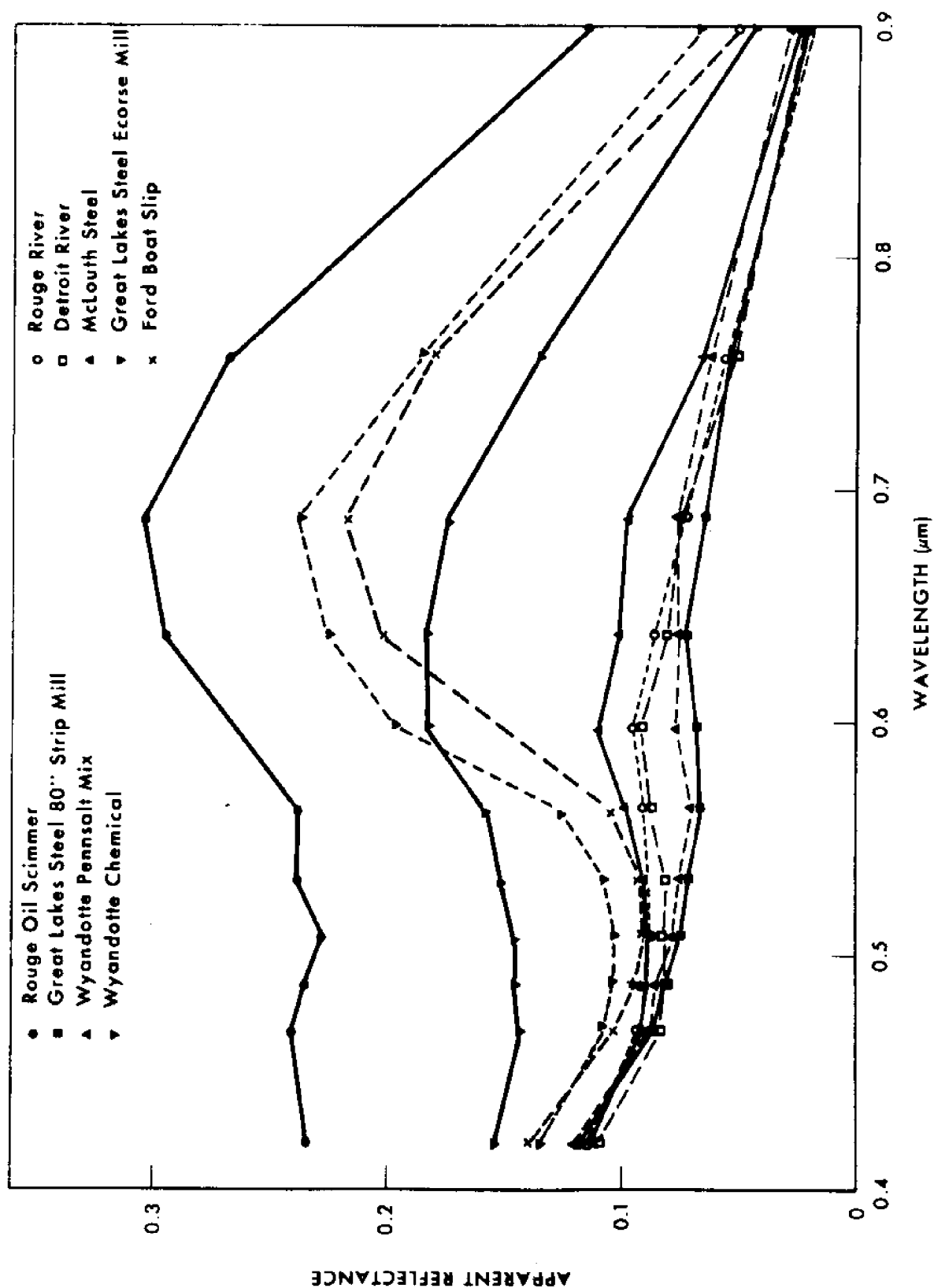
0.72-0.80  $\mu\text{m}$

Thermal Outfall  
of Power Plant

Rouge River

0.93-1.1  $\mu\text{m}$

FIGURE 12



# COMPARISON OF SPECTRA OF MAJOR POLLUTANTS IN ROUGE AND DETROIT RIVERS

Infrared and  
Optics Laboratory

*Willow Run Laboratories*

THE INSTITUTE OF SCIENCE AND TECHNOLOGY  
THE UNIVERSITY OF MICHIGAN

FIGURE 13

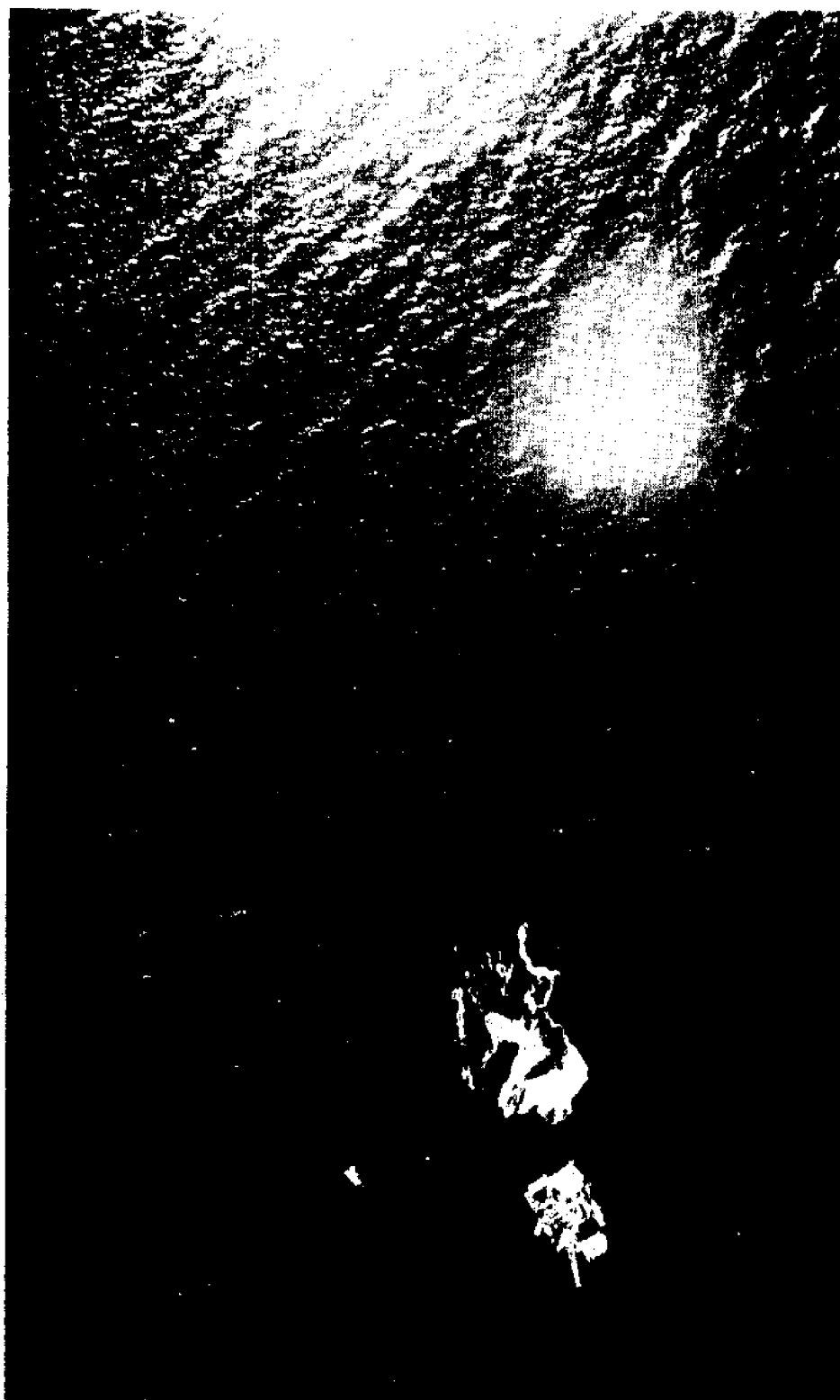
platforms or from accidental ship discharges. The Michigan aircraft was used to map the Santa Barbara oil slick in March, 1969 (Ref. 6). In Figure 14 is seen photographic data from a camera with a K-2 filter. Little evidence of the slick is seen. The drilling platform is on the lower left. The white foam near it is due to a dispersant being discharged from a boat to break up the oil film. If one looks at this plume using the several bands available in the multispectral scanner, (Figure 15) the oil slick is most readily seen with the best contrast in the ultraviolet region. As one progresses toward the red end, less contrast is observed until only the platform and dispersant is observed.

Finally, if one were to look in the thermal infrared region as shown in Figure 16, cooler portions of the slick, (dark tones) are associated with the thicker oil areas, while the ultraviolet tends to emphasize best the thin slick areas and give a better view of the total area.

Further studies have brought out the fact that different oil types tend to have better contrast in different spectral bands. For the general oil detection problem several bands are more useful but in general, the ultraviolet and the thermal infrared regions have the most consistent response, and therefore, are probably the most valuable in the detection and mapping of slicks areas.

In a particular study of the ultraviolet channel a number of voltage slices were taken and the results are shown in Figure 17. The lowest voltage slice represents the tone of the background water. The oil slick has been enhanced to appear black against the particular water background.

And then as one slices at the next higher signal level, parts of the oil film began to show. Finally, for the highest voltage slice, one does not see any return in the water, but one does see the entire slick. These



Panchromatic - K-2 Filter

## SANTA BARBARA OIL SLICK

Infrared and  
Optics Laboratory

*Willow Run Laboratories*

THE INSTITUTE OF SCIENCE AND TECHNOLOGY  
THE UNIVERSITY OF MICHIGAN

FIGURE 14



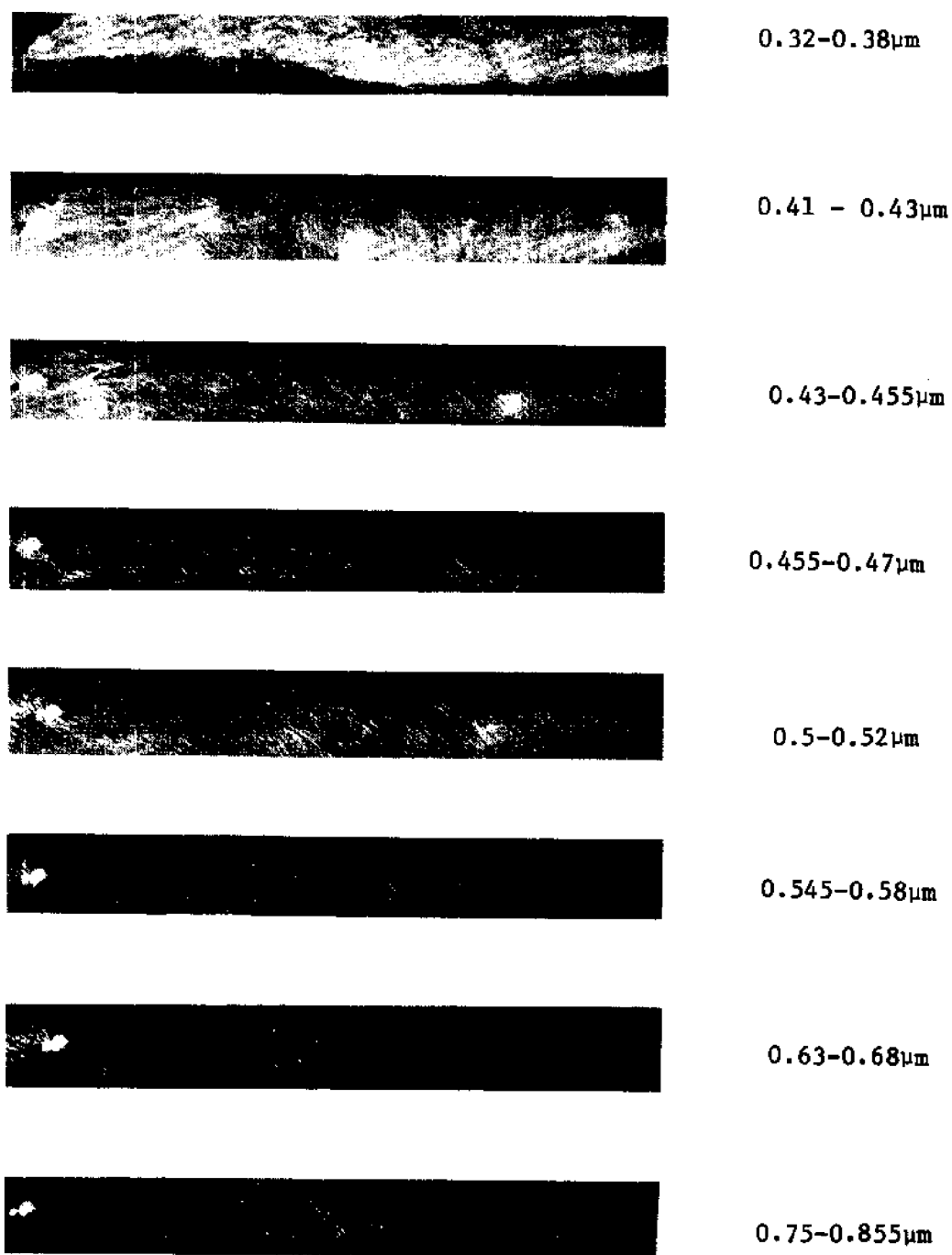


FIGURE 15. COMPARISON OF OIL SLICK CONTRAST  
IN EIGHT SPECTRAL BANDS.  
BEST DETECTION OF OIL SLICK IS  
IN THE .32 to .38 $\mu$ m BAND.



Ultraviolet -  $.32$  to  $.38\mu$



Infrared -  $8.0$  to  $13.5\mu$

## SANTA BARBARA OIL SLICK

Infrared and  
Optics Laboratory

*Willow Run Laboratories*

THE INSTITUTE OF SCIENCE AND TECHNOLOGY  
THE UNIVERSITY OF MICHIGAN

FIGURE 16



(a) Video ( $0.32$ - $0.38\mu\text{m}$ )



(b) Voltage slice



(c) Voltage slice



(d) Voltage slice

VOLTAGE SLICE OF MAIN OIL SLICK. March 7, 1969, 8:15 a.m. Altitude: 2000 ft.

FIGURE 17. ELECTRONIC LEVEL SLICING OF ULTRAVIOLET IMAGE.

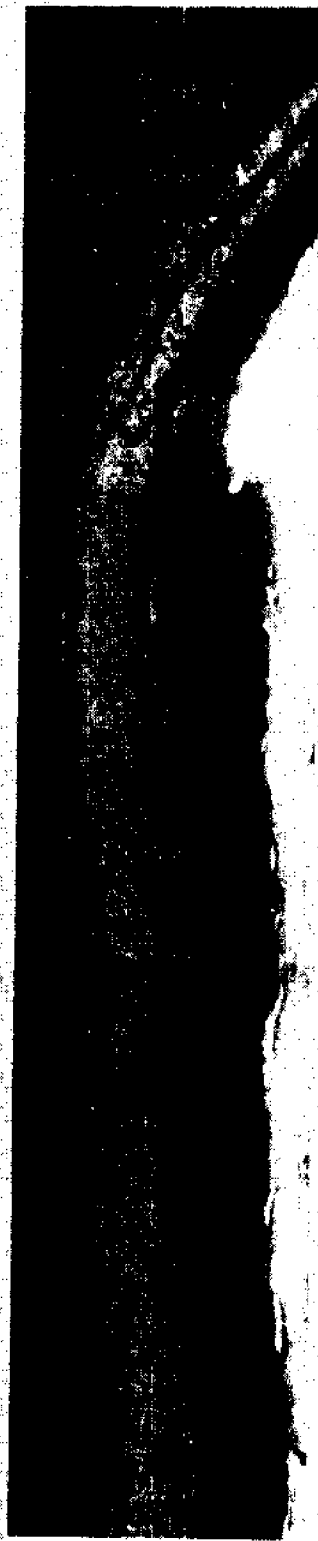
- Slice (b) - lowest signal level shows only water background
- Slice (c) - intermediate signal level shows oil only and some specular reflections from water surface
- Slice (d) - highest signal level shows areas of oil/dispersant mixture

different intensity levels in the ultraviolet channel suggest some relationship to thickness. The particular case of the Santa Barbara channel data is complicated by the presence of the chemical dispersant, but it would tend to create areas of different thicknesses depending on the effectiveness of the dispersant. Finally, during the same exercise it was desired to determine whether the multispectral scanner data could be used to differentiate oil slicks from kelp beds and whether these beds are affected by oil or not.

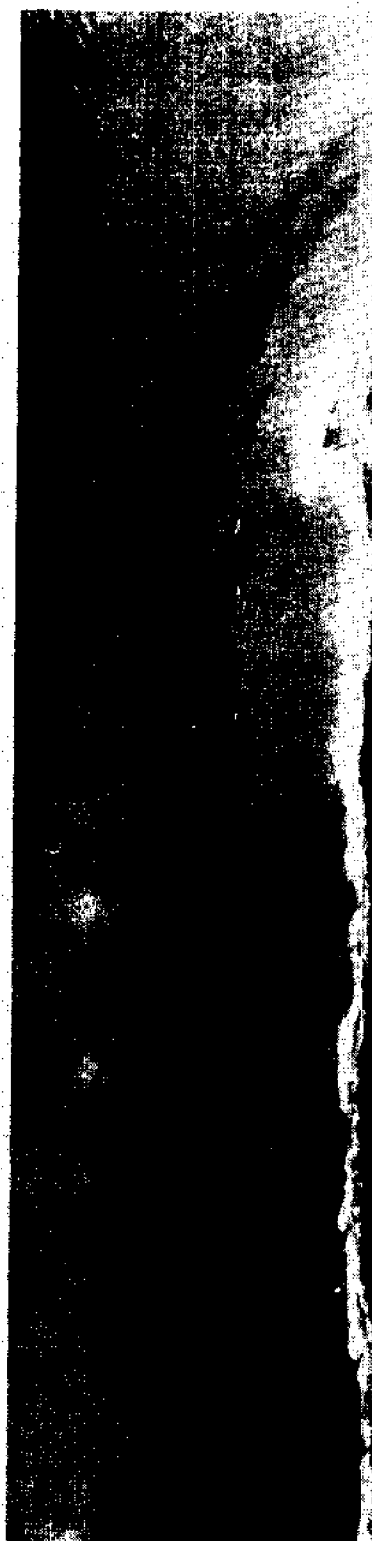
Figure 18 shows two bands, one in the ultraviolet where the kelp bed shows as a dark tone against the light water background and one in the infrared band at .8-1.0 $\mu$ m band where the contrast is reversed. In previous figures the oil slick had no response in .8-1.0 $\mu$ m band. Therefore, kelp and oil should be readily differentiable with these two bands. If oil were reaching the kelp, the lighter tones in the ultraviolet band would show the oil is present.

In summary, we have shown five examples of the use multispectral scanner data that would be useful in connection with marine environmental problems. It is suggested by these illustrations that fish oils might also be detectable in some spectral bands, that nearshore currents can be mapped, and that temperature patterns, related to certain fish species, can be obtained and become useful as an aid in their capture.

The developments of satellites such as ERTS and Skylab offer the promise that these techniques may be used on a global basis. The gulf stream and other ocean currents are already being mapped by satellite. Further research will bring about demonstration of their ultimate usefulness.



**Infrared - 0.8 to 1.0 $\mu$**



**Ultraviolet - .32 to .38 $\mu$**

**KELP**

## REFERENCES

1. Polcyn, F. C., Spansail, N. A., Malila, W.A., "How Multispectral Sensing Can Help the Ecologist", Symposium on Remote Sensing in Ecology, First AIBS Interdisciplinary Meeting on Environmental Biology, June 1968. Published in Remote Sensing in Ecology, 1969, University of Georgia Press.
2. Higer, A.L., Thomson, N. S., Thomson, F.J., and Kolipinski, M. C., (January 1970) "Applications of Multispectral Remote Sensing Techniques to Hydrobiological Investigations in Everglades National Park", Technical Report 2528-5-T, Infrared and Optics Laboratory, Willow Run Laboratories, Institute of Science and Technology, The University of Michigan, Ann Arbor, Michigan.
3. Polcyn, F. C., Brown, W.L., and Sattinger, I.J., (October 1970) "The Measurement of Water Depth By Remote Sensing Techniques", Report No. 8973-26-F, Infrared and Optics Laboratory, Willow Run Laboratories, Institute of Science and Technology, The University of Michigan, Ann Arbor, Michigan.
4. Polcyn, F. C. and Stewart, S. R., (September 1970) "Results of Remote Sensing Survey of Thermal Discharges", Four State Enforcement Workshop, Chicago, Illinois.
5. Polcyn, F. C. and Wezernak, C. T., (November-December 1970) "Pollution Surveillance and Data Acquisition Using Multispectral Remote Sensing", Water Resources Bulletin, J. A. Water Res. Assoc., Vol. 6, No. 6
6. Stewart, S., Spellicy, R., and Polcyn, F., (October 1970) "Analysis of Multispectral Data of the Santa Barbara Oil Slick", Final Report 29 September 1969 through 31 March 1970, Report No. 3340-4-F, Infrared and Optics Laboratory, Willow Run Laboratories, Institute of Science and Technology, The University of Michigan, Ann Arbor, Michigan.

## ACOUSTIC METHODS FOR ESTIMATION OF FISH ABUNDANCE

by

Lars Midttun  
Institute of Marine Research, Bergen, Norway

Short History of Development

Echo sounders were first used in fisheries research and commercial fishing in the mid 1930's. Acoustic surveys were conducted in Norwegian Waters on cod and herring in those early years and attempts were even made to estimate stock size by combining an acoustic survey technique with the catch of commercial vessels. The equipment at disposal was of rather poor quality and the results could not be expected to be accurate.

After the Second World War, equipment and technique were improved allowing higher resolution in the recordings and more sophisticated counting methods to be used. In the 1950's, acoustic surveys were carried out in several places in European Waters. Under favourable conditions, i.e. when single fish traces could be distinguished, the number of fish traces could be counted, say for every nautical mile and the number plotted along the course line. The sampling volume could be estimated by counting number of echoes within each single fish trace. It was found that this technique could not always be used with the same success due to the fish behaviour. Generally, night recordings were better than those taken during the day.

Around 1960, calibrated equipment was taken into use and target strength of individuals could be observed by means of oscilloscopes. This

gave a possibility to estimate the size of the fish and to more accurately calculate the sampling field of the echo sounder. Knowledge of the relation fish size - target strength is based on experimental work first started in USA (in 1954 by Paul F. Smith) and later continued both in Europe, USA and Japan. An example of an acoustic survey resulting in a stock size estimate is that carried out by Cushing in South African Waters several years ago.

A step forward was taken when the echo integrator was introduced and later improved so that a number of fish can be measured even when they are recorded as multiple echoes, i.e. single fish need not be distinguishable.

#### Brief Description of Method

In the following I shall give a simple description of a system now in use on board several research vessels in Europe and at many FAO projects around the World.

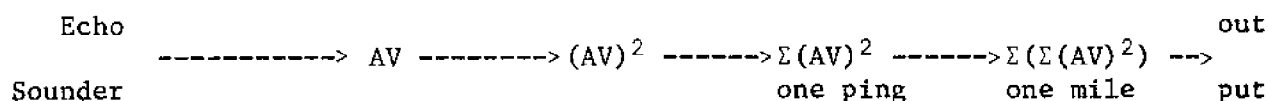
It consists of:

1. An echo sounder calibrated both for source level, receiving sensitivity and beam form; and with a time varied gain compensating for the transmission loss, either: two way geometric spreading loss and attenuation, or as another alternative: one way spreading loss and two way attenuation.
2. Attached to the sounder is an oscilloscope, whereby the signal-strength of the reflected echoes can be read. When the fish are in scattered concentrations, signal strength from individuals can be read. If a time varied gain compensating two way transmission loss is applied,

the target strength of single fish can be found by treating the signal strength values in a certain way in order to eliminate for the directivity of the transducer.(fig). The figure shows target strength composition and length composition of cod and codfish measured on their spawning grounds in Norwegian coastal waters. The target strength values are somewhat lower than should be expected and I shall return to that point later on.

3. As a third device the system have an integrator with two or more channels and paper recorders for each channel.

Signal voltage from the echo sounder is first amplified in the integrator, then squared, integrated over one ping and if desired, also over a certain distance, say one nautical mile.



By doing so one will get an output which is proportioned to the number of fish recorded regardless of whether they are observed as individuals or as multiple target. Since the volume samples by an echo sounder pulse increases in proportion to the square of the depth, one should apply a time varied gain compensating one way spreading only and two way attenuation loss. When this is done, the integrator value will be proportional to the fish density, proportional for example to the mean density over one nautical mile, provided the fish are of same size and species. In order to obtain absolute values instead of these relative ones, one has to know first the mean contributive of one fish to the integrator value. This can be found from knowledge of target strength of the individuals but the



most convenient way for calibration is simply to count numbers of fish recorded on the echo sounder paper recorder at the same time as the integrator is read. This can be done in areas of low concentration. These calibration results can be used also in the future on the same sort of fish and fish size. Secondly, it is necessary to know the sampling volume of the echo sounder beam. This can be found from knowledge of the target strength of the fish and the beam directivity pattern, but as I will show later, best by counting the average number of echoes received from individuals when passing through the beam. Again, such calibration can be used for the future.

When the integrator has now been properly calibrated, an area can be surveyed and a mapping of the fish distribution can be undertaken. A figure shows distribution of cod within a smaller area of Lofoten in Norway.

In the application of acoustic technique, one is certainly faced with several problems and limitations, for instance when fish are located too close to the bottom or in the uppermost surface layer, above the transducer level. In these cases, this method can not be applied. Abundance estimation is also difficult when the fish shoal is in too dense concentration. Then, there will be reverberation and absorption within the shoal and the integrated values are generally too low under these conditions.

On the other hand, fish generally have a behavioural pattern which gives better conditions for using acoustics during certain periods. In particular, there is very often a day and night change in shoaling

density and in vertical migration, so that the fish disperse in midwater layers during the night, at which time acoustics can be applied with the best results.

Even under favourable conditions, however, one has a strong feeling that there is often an under-estimation of fish density. This could at least partly be related to the behaviour of the fish, particularly if they are not in a horizontal position. The reflectivity pattern of sound from a fish is not a spherical one, but rather an ellipsoidal one, the head-tail aspect target strength being as much, say, as 20 db lower than the dorsal-lateral aspect target strength. (FIG.)

Even if the fish is not inclined horizontally, this directivity in reflection will reduce the detectability, especially if the ellipsoid is very slim (Table of detectability). When the fish are inclined, the detectability is even further reduced and could cause a serious under-estimation of fish density.

On the other hand, this directivity in reflection seems to be changing with regard to the fish species and could therefore, if observed, be used as an aid for identification purposes. By counting the number of echoes from single fish passing through the beam, it is possible to observe this directivity pattern and by statistical analysis, it is possible to find the composition of a directivity parameter, called (by me) the fish angle (gf).

This gives an opportunity for distinguishing cod from codfish (fig.)

There is even another parameter of interest in this connection which is also related to the target itself, viz: the extension in pulse-length

of the reflected signal as compared to the transmitted one. Indeed, there is much possible information obtainable in connection with acoustic fish detection and the statistical treatment of data, calling for the application of computers, if necessary. On the new Norwegian research-vessel, "G.O. Sars", a 16K computer has been linked to the acoustic equipment to cope with the enormous amount of data running in through the echo sounders.

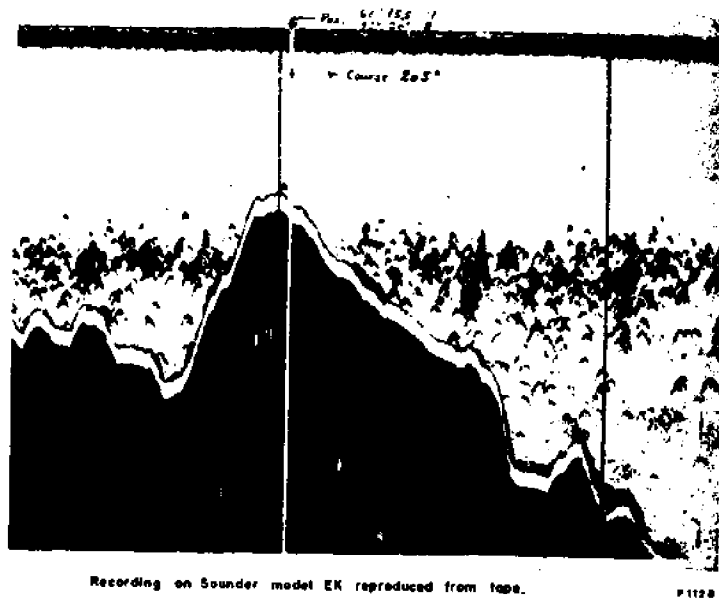
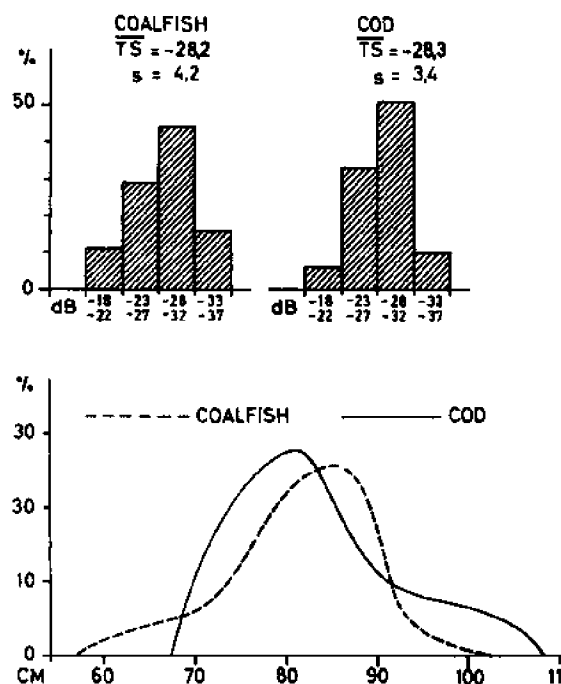


Figure 1



Distribution in per cent of target strength, TS, for observed coalfish and cod, with corresponding length distribution below.

Figure 2

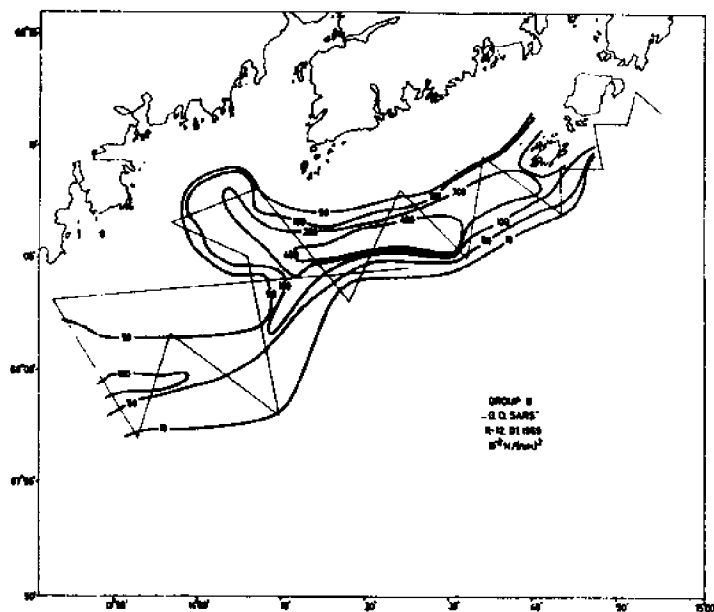
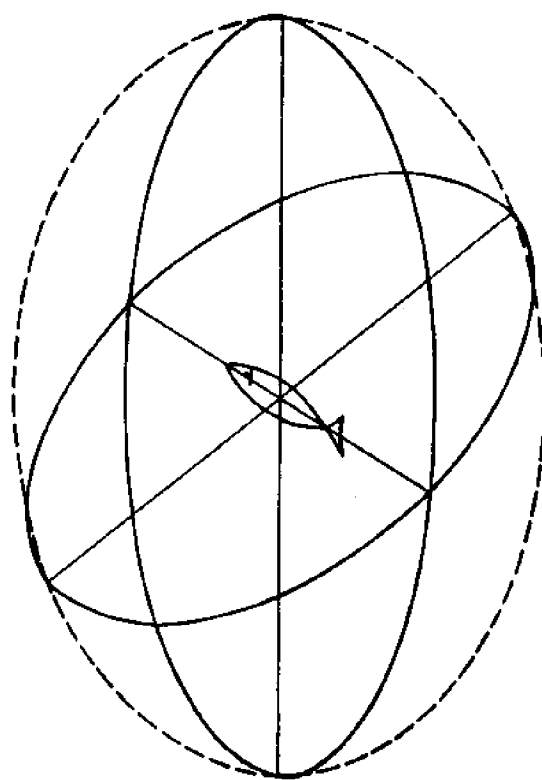


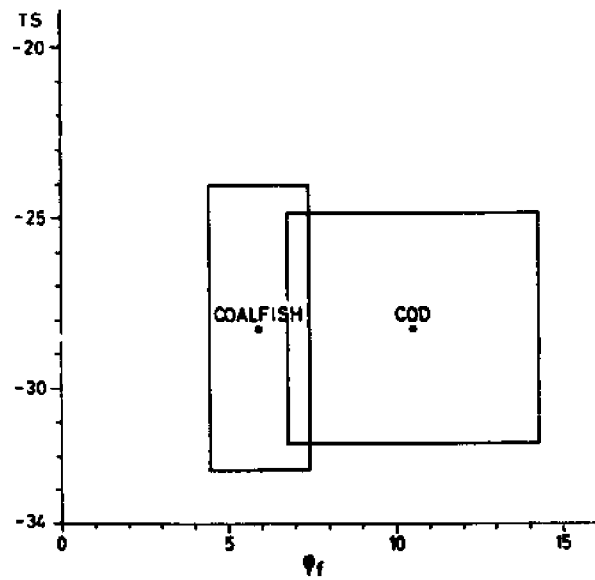
Figure 3



Schematic picture of the reflectivity pattern of an "ideal" fish target.

Figure 4

C.X. 1970/2:7



$\phi_f$  - TS diagram showing mean values (points) and standard deviations (straight lines) of observed cod and coalfish.

Figure 5

STUDIES OF BENTHIC COVER IN NEAR-SHORE TEMPERATE WATERS  
USING AERIAL PHOTOGRAPHY

by

Mahlon G. Kelly  
Dept. of Environmental Science  
University of Virginia  
Charlottesville, Virginia 22903

The work reported here was supported by NAVOCEANO contract N62306-70-A-0073-0003. Support and facilities were provided by the New York Ocean Science Laboratory. Aerial photography for the work was obtained by the NASA Earth Resources Aircraft Program. (Technical Report no. 0006 of the New York Ocean Science Lab.)

Aerial photography has been very little used by coastal marine ecologists, yet it provides a means for studying the distribution of benthic cover that is not otherwise available. Previous work (Kelly and Conrod, 1969; Kelly, 1969 a, b; Kelly, in preparation) has used aerial photography to study the distribution of shallow water benthos in clear, tropical waters, and the work reported here shows the method can be used in turbid, temperate waters as well. Biotic distributional patterns are very difficult to study from the water surface; aerial photography lets those patterns be examined with the perspective normally available in terrestrial work. Aerial photography has been used by coastal geologists, and thus the lack of its use by marine biologists is even more surprising. Much effort has been spent on inventorying coastal biota and that effort may be expected to increase as the coastal zone falls under increasing pressure from man's population and affluence. Aerial photography and other methods of remote sensing should therefore be increasingly used to help understand conditions in our coastal waters.

The objective of the work described here has been to 1) determine the feasibility of using aerial photography to study the distribution of benthic cover in turbid Long Island, 2) to find the best type of photography for that purpose, 3) to describe and map as much of the benthic cover as possible,

- 4) to examine what may be deduced from the patterns of distribution and
- 5) to compare these patterns with those previously studied in the much clearer waters of South Florida. The ultimate goal of the work is to obtain a better understanding of factors determining the distributional patterns of shallow benthic cover, but that will be discussed in future papers.

#### METHODS:

The procedure used was very simple: Aerial photography was obtained from a variety of altitudes using a variety of films, cameras and filters. Benthic cover seen in the photographs was identified on diving transects and the distributions of bottom cover were studied and mapped using the photography. These interpretations were then extrapolated to other areas. The validity of the extrapolations was spot checked in the field and many areas were examined from low flying light planes.

Photography was obtained of the entire south shore of Long Island from New York City to Montauk Point and of the north shore of the Montauk area from Gardiner's Bay to Montauk Point. Additional 18,300 m. hyperaltitude photography covered this area as well as the northern coast of New Jersey and the coast of Connecticut. Flight times and altitudes are summarized in Table I and the study area is shown in Fig. 1. The details of the photography are summarized in Table II. Color and infrared color film were used in the two metric cameras, the color film being overexposed to allow greater depth penetration. Bracketting exposures with color film were used in two of the smaller cameras to evaluate the selection of exposure for the metric camera. Another small camera used a minus-blue Ansco D-500 film especially developed for water penetration (Vary, 1969); the emulsion was designed particularly for use in clear blue waters and it was used here to evaluate its performance in more turbid, temperate waters. Wide-band multispectral photography was used with the remaining 3 cameras to roughly determine the best spectral region



for water penetration.

The object of this work was not to develop new techniques but to find the best routine, readily available methods for photographing the distribution of shallow-water benthos and to see what may be learned using such methods. Multispectral photography and scanner imagery has been studied by several workers (Yost and Wenderoth, 1970; Helgeson, 1970) and may be very valuable, but its application is limited by the specialized instrumentation needed. Routinely applicable techniques are needed that can be easily used by scientists and agencies concerned with monitoring the biota of coastal areas.

The photography was evaluated on the basis of its depth penetration and its usefulness in identifying and studying the distribution of bottom biota when used with field studies. The photography was examined extensively and compared while planning the field studies, examining the results of the field work, and mapping the distributions of benthic cover.

Field observations were concentrated along the north shore of Long Island between Gardiner's Bay and Montauk Point and in Shinnecock Bay. These areas were examined partly because of the relatively greater water clarity and partly because of the available facilities. Observations were made by towing divers along transects that had features typical of those seen in the photography. Qualitative observations were recorded continuously along the transects and more detailed observations were made at typical stations. Representative bottom plants were collected and identified. Observations in very shallow water were made by wading along the bottom at very low tide.

The transect observations were used to develop criteria for photo-interpretation and the photography was then used to identify bottom cover in other areas. That identification was field checked for accuracy and provided a test of the quality of photointerpretation. It was of course impossible to

field check all photographed areas; observations and hand-held photography from a light plane were used to check the identification of features in other areas. Those identifications must of course be tentative since field samples were not obtained. Finally the photography and field work were used to prepare maps and analyze the bottom cover.

#### PHOTOGRAPHIC TECHNIQUE - RESULTS AND DISCUSSION:

The films and filters were selected as those most likely to provide the best results without specialized cameras or instrumentation. The wide band multispectral images showed the relative importance of the spectral sensitivity of the color photography and were used to determine the best method for black and white photography. The goal was to obtain the best possible depth penetration and the least interference and contrast reduction by light back-scattered from the water, and, in the color photography, optimal color information for photointerpretation.

Depth penetration was satisfactory in all of the photography except the blue-filtered (Wratten 47) black and white material. Penetration varied from 4 m. near Montauk Point to less than 1/3 m. in Jamaica Bay. This is not surprising since temperate coastal waters are usually most transparent to longer wavelengths (green and yellow), in contrast to tropical waters where blue light penetrates most effectively. Thus while blue filtering produces best penetration in tropical waters it is nearly worthless in these temperate areas.

Best image contrast was found in the red-filtered (Wratten 25A) photography. Maximum light scatter by suspended particles is in the blue and green, and this reduced contrast in photographs using those filters. Both the minus-blue and color infrared film produced high contrast images because they were less sensitive to scattered light. While the Ektachrome film did not have as high

contrast, its blue sensitivity provided important information about bottom depth distribution. Best Ektachrome penetration was obtained with 1 f/stop more exposure than normal for over-land photography.

The Ektachrome film was therefore most satisfactory, having acceptable image contrast and good penetration as well as the most color information. The color infrared film acted simply as a minus-blue film under water, although it of course was best for marshland and coastline delineation and would be best for combined marshland and submerged vegetation studies. The minus-blue film was satisfactory for submerged objects, but was unsatisfactory for marshland or coastal work; it also was very grainy.

Optimal altitudes depended on the intended use of the material. The 18,300 m. coverage generally was only useful for seeing very widespread patterns, and lower altitude coverage was necessary for interpretation. Photography from 3,000 to 5,000 m. altitude was best, as it both provided the necessary interpretive cues and allowed major distributional patterns to be seen. Low altitude observation and hand-held photography was very useful for understanding the interpretive cues and for detailed work. General purpose satellite imagery will probably not provide sufficient resolution for work such as this.

In summary, the best photography for studying the distribution of near-shore biota may be obtained from about 4,000 m. using both infrared color and color film, the latter being overexposed 1/2 to 1 f/stop. This holds true for both tropical and temperate waters. If a choice must be made, the color infrared film is preferable because it allows study of both marshland and submerged vegetation. If black and white photography must be used, a red filter (Wratten 25A) will provide best results in turbid, temperate areas and a blue filter (Wratten 47 or 2A plus 38) will give best penetration in

clear tropical waters.

#### DISTRIBUTION OF BENTHIC COVER - RESULTS:

The types of benthic cover are much simpler in this area than in the tropical areas previously studied (Kelly and Conrod, 1969; Kelly, 1969 a, b), as would be expected from the fewer epibenthic species present. The cover may be divided into four types: eelgrass (Zostera marina) beds, mussel (Mytilus edulis) beds, masses of green algae (mainly species of Cladophora, Enteromorpha and Ulva) and mixed species of algae attached to gravel, cobbles and rocks. Each of these types of cover may be identified by photointerpretation and field checking, and maps have been made of the typical patterns of cover (Figs. 4, 6, and 8).

Eelgrass beds may be identified by their uniform dark appearance, their diffuse edges, their patchy appearance in shallow areas, and their occurrence in relatively low energy environments. They are seen to occur only in protected embayments with minimal wave-washing and away from channels with strong currents. They do not enter water shallower than about 20 cm. at low tide and occur down to about 3 m. depth, depending on the location. These distributional limitations have been described by others in a variety of environments (Burkholder and Doheny, 1968, give a good bibliography) but the photography shows the universal applicability. Figs. 4 and 6 show how the grass beds bound the deeper areas of the coastal lagoons where tidal currents are limited. The upper reaches of the beds are often broken and patchy, possibly because of wave action during storms. The absence of the beds near shallow constricted channels with high current velocities is obvious. Wave-washing and relatively coarse sediments prevent their growth along the north shore of Long Island except in a very few protected embayments. As mentioned in Burkholder and Doheny (1968), and as discussed below, the western limit of eelgrass is at the western end of

Great South Bay.

Mussel (Mytilus edulis) beds are seen only near the mouths of the coastal lagoons. Scattered clumps and individuals are found nearly everywhere, but the optimal habitat is apparently in strongly current washed locations. This holds true near all of the entrance channels along the south shore. The beds may be recognized by their very dark color, their sharp edges, the general occurrence of broken patches around the beds, and usually by the alignment of the beds with the current direction. The mussel beds may sometimes be easily confused with eelgrass beds and field checks are often necessary for definite identification. The configurations of some of the beds changed over winter between the time of the photography and the field work; apparently the beds are broken up and moved by winter storms. No previous reference has been found to either the movement of the beds or their location near current-washed channels, although these beds are of potential importance as a commercial fishery.

Although green algal debris is found many places in the south shore lagoons, it reaches its greatest development in the polluted waters west of Great South Bay. The various species grow on nearly any substrate, including on the mussel and grass beds, where they probably have a deleterious effect by shading. Only when they accumulate in large masses may they be distinguished in the photography, but it is in such masses that they cause great damage. Examples are shown in Figs. 6 and 8. These masses may be recognized by the incised or channeled appearance, the relative lack of patchiness and smooth edges, and their occurrence immediately adjacent to marshland (where Zostera usually doesn't grow). Massive green algal growth is usually symptomatic of eutrophication, and as discussed below, the photography may be very important for monitoring accumulation of the algae.

Mixed communities of algae grow attached to cobbles, gravel and boulders all along the studied portion of the wave and current-washed north shore.

These communities vary in their amount of growth and composition but that cannot be determined with the photography. All that can be distinguished is the dark-toned rocky areas and the lighter sand bodies. Most of the darker areas are less evident in winter photography, due to the seasonal variation in the growth, and they may be distinguished by that and by their occurrence in high energy locations where sand is unlikely to accumulate. Recognition of these areas may be important for locating regions of production and for monitoring the distribution of gravel and cobbles (the location varies from season to season), but they reveal little about the biology of the area.

#### DISCUSSION:

Estuaries and coastal lagoons are among the most important productive areas of the world and the submerged vegetation provides a large part of the productivity (Westlake, 1963). These areas are important for recreation and provide spawning grounds that are the basis of many sport and commercial fisheries; they are presently threatened by man's activities. Monitoring and understanding the distribution of the major bottom cover is thus very important. Aerial photography may be essential for this, because not only may the distribution of major cover be mapped and monitored but important factors determining the distribution may be inferred.

Beds of Zostera marina are a major source of energy for the detrital food chains and provide valuable protective cover for many important larval forms (Burkholder and Doheny, 1968). As described above, their distribution may be mapped and monitored using the photography. Biomass and productivity of course cannot be monitored, but the photography should greatly simplify productivity studies by helping select measurement stations. The beds are good depth indicators; in fact the paths of old lagoon entrance channels may be seen where the grass beds extend through the mud flats to the barrier islands.

As mentioned above, the western margin of eelgrass is at the end of Great South Bay. Burkholder and Doheny mentioned this, and hypothesized that the beds were increasing to the west in recovery from previous decimation by the fungal blight of the 1930's. Actually, the photography shows the grass to be even less extensive than during their study in 1966, so apparently no dispersal is occurring. Also, as discussed below, many of the suitable depths for Zostera growth are seen to be occupied by massive growths of green algae, which would very effectively shade out and kill the Zostera beds. It appears that the westward extension of Zostera may be limited by these extreme growths of green algae, and if that is the case no further extension of the grasses can be expected until the extreme nutrient concentrations in the western bays are reduced.

It is possible to monitor other changes in the eelgrass. In addition to competition with the green algae, growth may be limited by dredging or by currents associated with dredged channels. Dredging produces channels too deep and spoil banks too shallow for grass growth. This may be seen at many locations: More subtly, channel dredging may increase current flow and thus limit Zostera even in habitats of suitable depth. This probably has occurred in the area near the entrance to Shinnecock Bay shown in Fig. 4 as well as near the mouths of Moriches and Great South Bays. This in turn suggests that channels might be dredged and dredge spoil distributed in such a way as to encourage rather than discourage growth of the grass. Experiments would be needed to confirm these hypotheses, but the hypotheses point out the value of the perspective provided by the aerial photography. It would have been very time consuming to have surveyed these distributions by normal methods.

Similar observations may be made about the distribution of mussel beds (Mytilus edulis). Mussels support a small commercial fishery in the area studied, and the photography shows that the fishery could be easily

expanded. Mussels are of considerable economic importance in Europe, as indicated by their specific name edulis. Monitoring of the beds thus may be of considerable importance, especially since pump harvesting techniques would enable the beds to be wiped out very easily. The distributions of the beds in areas of current suggest that the growth might be encouraged or discouraged by the patterns of channel dredging. The most extensive beds are seen in Shinnecock Bay, where the relatively shallow channel results in dispersed, high velocity currents. They are also apparently carried by storms, as mentioned above. The bottom configuration is of course important for that transport. Again, these hypotheses must be confirmed experimentally, but the photography should be of great value in that confirmation.

The masses of green algae are of considerable importance. Cladophora, Enteromorpha, Ulva, and other greens thrive under conditions of nutrient enrichment and are thus good indicators of eutrophication. The masses also produce considerable nuisance when they develop, often clogging beaches and causing very obnoxious odors. They obviously collect in very shallow subtidal and low-intertidal areas and in protected coves and areas between marshes where their decomposition probably kills other biota. These observations could be important for controlling their distribution; again, dredge and fill operations might be designed in such a way as to minimize their accumulation. Harvesting of aquatic plants for mulch and fodder has been suggested as a means of controlling eutrophication; photographic surveys should help that work.

It is interesting to compare patterns seen here with those described in tropical areas (Kelly, 1969 a, b). The most obvious differences are the relative simplicity of types of bottom cover and the shallow depth of major plant growth in the temperate waters. It is interesting that the distribution of sediments, light and wave and current-washing provide similar controlling factors in both environments, in fact, many of the distribution patterns of



Thalassia testudinum (turtle grass) and Zostera marina are similar even though the depths involved differ by a factor of ten. The differences and similarities in distributional patterns will be discussed further in another paper.

It would seem that further use of aerial photography in studies of waters such as these should be of great value. The distributional patterns seen have obvious economic significance, and the photography should both save time and expense in monitoring the distributions and provide information that cannot be easily gained in any other way. Bottom biota is visible in aerial photography along much of the east coast, and agencies concerned with conservation of coastal lands might find these techniques very useful. As described above, some care must be taken for proper procurement of the photography, but no more instrumentation is required than is normally available in many state agencies.

Finally, it seems that perhaps the most significant products of the perspective provided by the photography are the questions and hypotheses it raises. For example: Do the massive, widespread accumulations of green algae dominate the infauna and epifauna of the bays, and do they limit the development of Zostera beds? Are eelgrass and mussel beds controlled by wave and current washing? Can these materials be controlled by proper dredge and fill operations? How do the distributions vary with time, season and eutrophication? Are the locations of the mussel and grass beds determined by current velocity? Do winter storms control the location and quantity of mussel beds? What determines the location of the algal masses? These are major, important and basic questions that must be answered if we are to make intelligent use of these coastal areas. The answers depend on understanding the distributions seen in the aerial photography.

Table I: Summary of missions flown over Long Island test site by NASA Earth Resources Aircraft Program.

NASA Mission	Aircraft	Dates	Times (Local)	Altitudes (m.)
103	RB-57	9/14/69	08:10 - 11:45	18,300
104	C-130	9/15/69	13:25 - 17:30	3,500, 3,800 7,600
121	C-130	2/20/70	09:16 - 11:40	2,900-3,800 7,600
121	C-130	2/21/70	09:08 - 09:32	2,900-3,800

Table II: Photography obtained during flights shown in table I.

Format	Camera	Film	Filter	Missions
9.5" x 9.5"	WILD RC-8	Ektachrome	haze (1)	103, 104, 121
9.5" x 9.5"	WILD RC-8	SO-117	12 (2)	103, 104, 121
9.5" x 9.5"	Zeiss, 12"	Ektachrome	haze (1)	103
70 mm.	Hasselblad	Ektachrome	haze (2)	103, 104, 121
"	"	Ektachrome	haze (3)	103, 104, 121
"	"	D-500	none (4)	103, 104, 121
"	"	pan.	25-A (1)	103, 104, 121
"	"	pan.	47 (1)	103, 104, 121
"	"	pan.	58 (1)	103, 104, 121

(1) 1 f/ stop exposure over normal.

(2) normal exposure.

(3) 2 f/ stops exposure over normal.

(4) 2 layer minus-blue Anscochrome D-500.

## BIBLIOGRAPHY:

- Anderson, R. 1969. The use of color aerial photography in marshland and estuarine studies. in: New Horizons in Color Aerial Photography. American Society of Photogrammetry, Falls Church, Va. pp. 281-288.
- Burkholder, P.R. and T.E. Doheny. 1968. The Biology of Eelgrass. Contribution No. 1227 from the Lamont Geological Observatory. pp. 1-120.
- Helgeson, G.A. 1970. Water depth and distance penetration. Phot. Eng. 36:164-172.
- Kelly, M.G. 1969a. Aerial photography for the study of near shore ocean biology. in: New Horizons in Color Aerial Photography. American Society of Photogrammetry, Falls Church, Va. pp. 347-355.
- Kelly, M.G. 1969b. Applications of remote photography to the study of coastal ecology in Biscayne Bay, Florida. Contract Report, U.S. Naval Oceanographic Office, Contract N62306-69-C-0032. 52pp.
- Kelly, M.G. and A.C. Conrod, 1969. Aerial photographic studies of shallow water benthic ecology. in: P. Johnson, ed., Remote Sensing in Ecology, Univ. of Georgia Press, pp. 173-183.
- Vary, W.E. 1969. A new non-blue-sensitive aerial color film. in: New Horizons in Color Aerial Photography. American Society of Photogrammetry, Falls Church, Va. pp. 127-130.
- Yost, E. and S. Wenderoth, 1970. Remote sensing of coastal waters using multispectral photographic techniques. Report for U.S. Naval Oceanographic Office Contract N62306-69-C-0281.
- Westlake, D.F. 1963. Comparisons of plant productivity. Biol. Rev. 38:385-425.



Fig. 1. A map of the Long Island area showing the area photographed (bracketed by the lines designated "1"), the locations mentioned in the text, and the areas mapped in

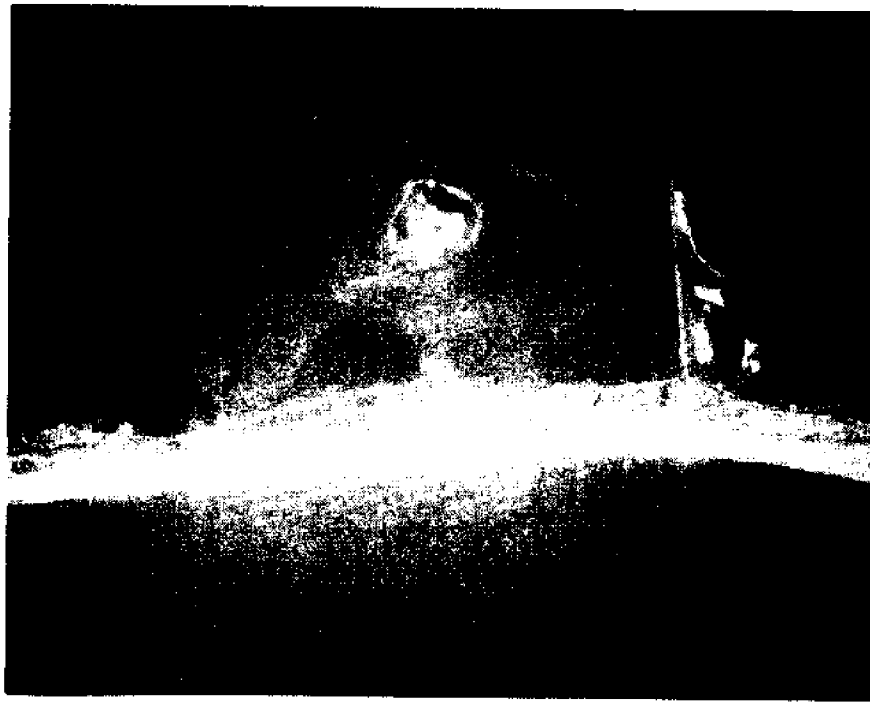


Fig. 2. a: Panchromatic photograph of part of the area shown in Fig. 4, shot through a blue (Wratten 47) filter. b: The same, shot through a red (Wratten 25A) filter. Note the increased penetration and resolution in b.



Fig. 3. Red color separation print of an Ektachrome transparency of a portion of the area shown in Fig. 4. Note the distributions of the cover shown in Fig. 4.

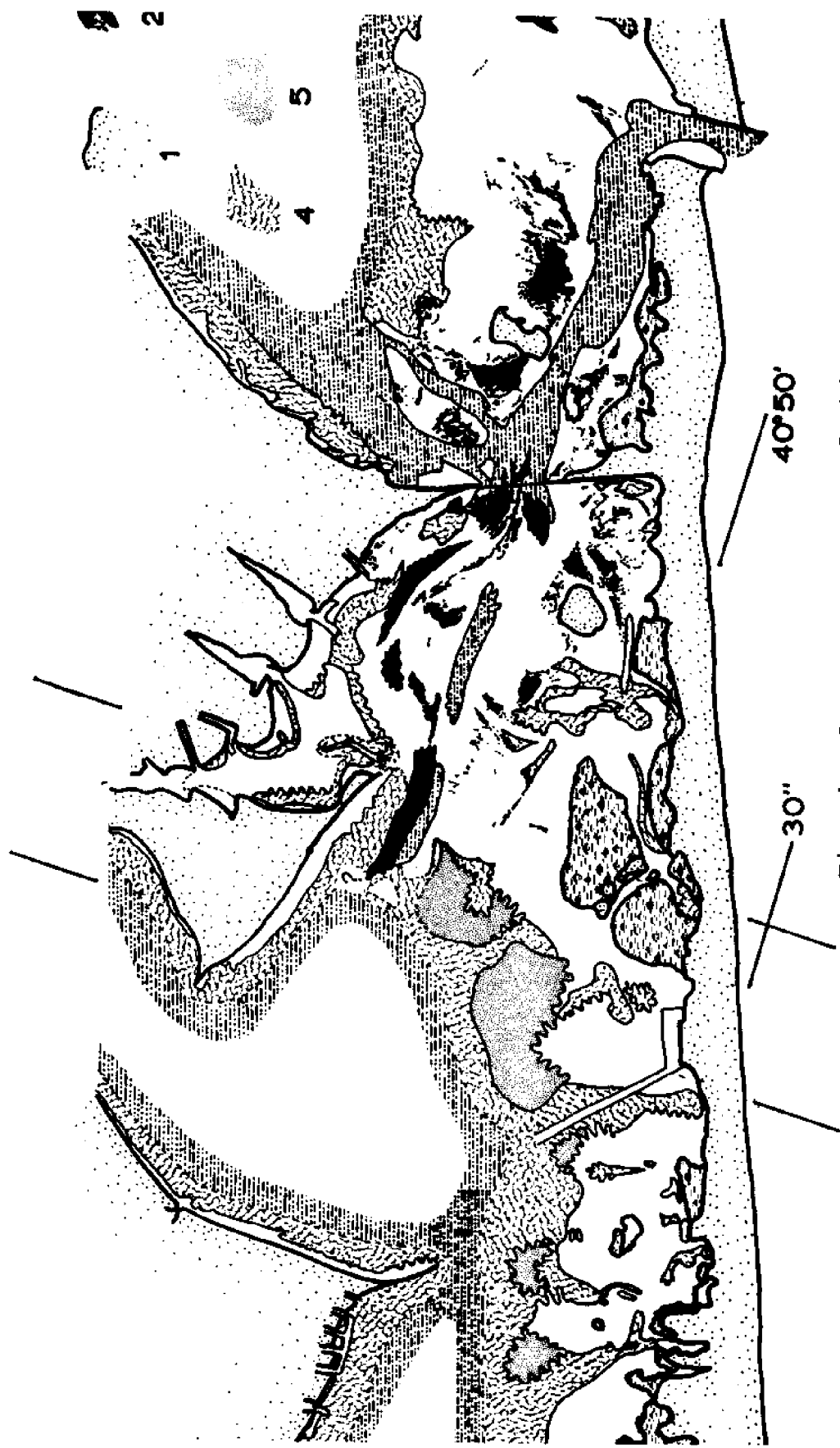


Fig. 4. Bottom cover map of Shinnecock Bay. 1. shoreline, 2. mussel beds, 3. marshland, 4. eelgrass beds, 5. patchy eelgrass beds, 6. channels and areas too deep to be interpreted, usually with dark, muddy bottom and no cover. A dashed line indicates that the boundary is uncertain and a wavy line that the boundary is diffuse.





Fig. 5. A portion of the area shown in Fig. 6. Prepared the same as Fig. 3. Note the features shown in the map of Fig. 6.



Fig. 6. The western end of Great South Bay, showing the western limit of eelgrass growth. 1. deep channels, 2. marshland, 3. patchy eelgrass, 4. eelgrass beds, 5. massive accumulations of green algae, 6. shoreline. Dashed line indicates the boundary is uncertain, wavy line that the

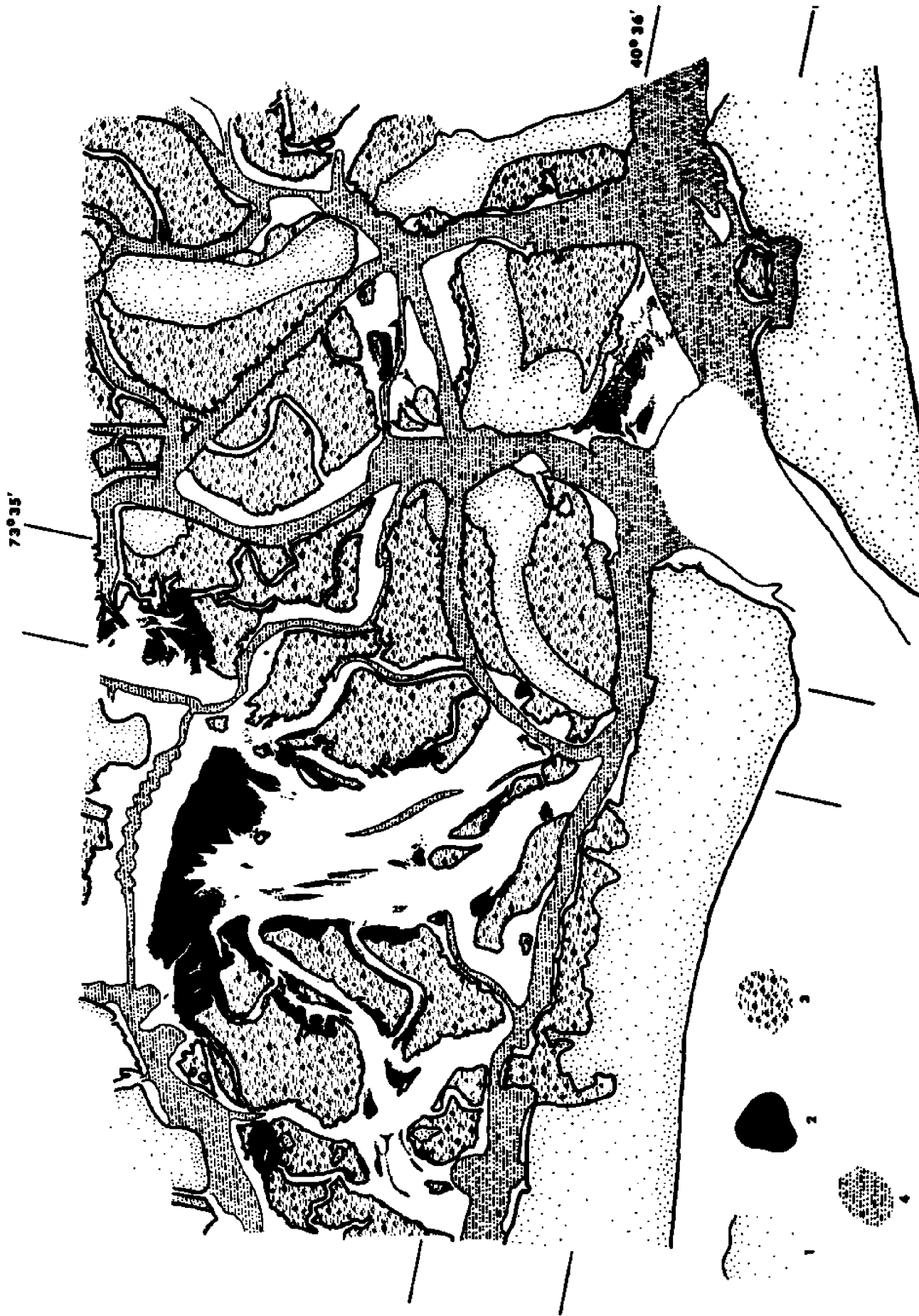


Fig. 7. A portion of the area shown in Fig. 8. Prepared the same as Fig. 3. Note the features shown in the map of



Fig. 8. A portion of Hempstead Bay near Jones Beach.  
1. shoreline, 2. massive accumulations of green algae,  
3. marshland, 4. deep channels. Wavy line indicates the  
boundary is diffuse. Mussel beds apparently occur in the area  
of algal accumulation nearest the channel entrance.

AN APPLICATION OF THE THEORY OF GAMES TOWARD IMPROVING THE  
EFFICIENCY OF CERTAIN PELAGIC FISHING OPERATIONS

Saul B. Salla  
Secretariat, Intergovernmental Oceanographic Commission,  
Paris

INTRODUCTION

One of the inefficiencies related to the harvesting of some mobile aquatic resources is the time spent in searching. Norton (1969) has demonstrated for the California (U.S.A.) based tuna purse-seine fleet that approximately three-fourths of the total time on fishing grounds is spent in search activities. This represents an estimated cost to the fleet of approximately 13 million dollars (U.S.) annually. From the above example, it seems clear that search activities, as currently conducted by some fishing fleets, represent economic waste both in terms of direct operating costs as well as social investment in capital and labor. This statement is true even if it is assumed that reduced search time does not result directly in larger quantities of fish harvested. It therefore seems appropriate to consider ways and means for improving searching efficiency. The expected economic benefits of a theoretical satellite remote sensing system that might reduce search time or increase the catch per unit of effort have already been briefly examined by Norton (1969).

The purpose of this report is to briefly consider the problem of how a fishing vessel should allocate search effort in order to make the probability of encounter and capture of a fish shoal as high as possible under specific conditions. The rational allocation of available search time as suggested in this report involved no additional expense for equipment. It merely involves some relatively simple calculations.

The importance of devising optimum searching and fishing tactics was pointed out by Beverton and Holt (1957) in their comprehensive treatment of

fish population dynamics. However, relatively little attention to these problems has been paid by fisheries scientists since then.

It seems highly desirable to consider both conceptual as well as physical schemes for increasing the efficiency of fishing operations at this time. The developing technology in remote sensing equipment, various kinds of aero-space systems (utilizing both aircraft and satellites) and improvements in communications and data processing, provide a unique opportunity for rapidly obtaining information directly or indirectly relevant to fishing operations. Maughan (1969) has already suggested some potential benefits of aerial surveillance for fish detection and other fisheries predictions. However, it remains to develop more detailed plans for utilizing this information in an effective manner.

#### THE PROBLEM

A shoal of fish, located at or near the surface of the sea, is assumed to be located in some manner by an observation vehicle, say an airplane, a satellite or even an observer on the vessel. It is assumed that the observation vehicle can accurately report the time of location and the position co-ordinates of the fish shoal to the fishing vessel or fleet of vessels located at a relatively short distance from the sighting. It is also assumed that the fishing vessel(s) are equipped with modern fish-finding equipment such as sector-scanning sonar as well as the precise navigational equipment. In other words, the fishing vessel is assumed to be able to effectively search some defined area around the vessel, and the co-ordinates of the vessel are assumed to be known precisely at the time of sighting.

If the fish shoal remains surfaced and the observation vehicle can estimate its direction of travel and its velocity within fairly narrow limits, the problem of determining a suitable course and speed for the fishing vessel in order to intercept and attempt capture of the fish shoal

is usually not difficult. The above-mentioned problem has already been treated by Saila and Flowers (1969) under the simplifying assumptions of travel in straight lines at constant velocities by both the fishing vessel and the fish shoal. If, however, the fish shoal submerges at the time of observation or its velocity and direction are unknown even if it remains at the surface, the problem of interception becomes much more difficult.

The latter problem is briefly considered in this report. That is, what is the optimum searching strategy for a fishing vessel or fleet of vessels when a fish shoal has been reported some time previously at a specified location but its speed and direction are unknown? This question will be considered conceptually only in two dimensions. That is, it is assumed the fish shoal remains at or near the surface or is within the detection limits of some electronic device which operates completely effectively within the depth range of the fish.

The fish shoal will have some maximum velocity ( $v_{\max}$ ) which is defined as the maximum sustained swimming speed of the species or higher taxonomic unit. Values for maximum sustained swimming speeds are known within reasonable limits for several important pelagic fishes. See, for example, reviews and lists of swimming speeds by Bainbridge (1958), Blaxter (1969), Nursall (1962), and Radakov (1964).

The strategy of the fish shoal, for the purposes of this model, is defined as a choice of a direction  $\theta$  from all possible directions between 0 and  $2\pi$  and a speed  $v$  such that  $0 \leq v \leq v_{\max}$ . The shoal of fish is assumed to hold to this choice of speed and direction for the duration of the search. This assumed behavior may be an over-simplification, but it is not believed to be unreasonable within a restricted time framework of a few hours. The description of the strategy of the fish shoal implies that it is chosen at the outset. That is, the strategy of the fish shoal can be conceived as

the choice of a point in a "speed circle" or radius  $v_{\max}$  as shown in Fig. 1. The concept of a "speed circle" in "speed space" is the fundamental conceptual framework within which this search problem is considered.

Consider next the strategies for the fishing vessel or vessels. It is assumed that the fishing vessel scans perfectly an area of radius  $R$  and that within the radius  $R$  detection of the fish shoal is certain and that outside the radius  $R$  detection is impossible. By an appropriate setting of the search sector controls on some operational sonars to about  $90^\circ$  port and to  $90^\circ$  starboard, an  $180^\circ$  field of search may be achieved. We assume that the fishing vessel searches at some constant speed  $s$ , which is the maximum speed before masking real echoes, and scans a distance  $R$  of  $90^\circ$  to each side of the vessel. The above are admittedly over-simplifications of how sonar works on an operational basis. For example, Jones (personal communication) has indicated that at the present stage of sonar development a target must return three echoes for a reasonable detection probability. Thus, the scanning rate apparently cannot exceed 3 degrees per second, and this implies a minimum of one minute for a  $180^\circ$  scan. In addition, it is recognized that the strength of return echoes has been found to depend upon the strength of the transmitted signal; the distance to the reflecting object; the size, shape and position of the object; and the object's reflective ability. Also, it is recognized that sonar performance is affected by both temperature and salinity stratification. However, these problems have been ignored for the purposes of initial model formulation and analysis.

It is assumed that the fishing vessel arrives in the vicinity of the reported sighting and that all searching takes place within the speed circle. The area searched by the fishing vessel is roughly approximated by a rectangle, the width of which is  $2R$  and the length of which is a product of vessel speed and search time. Thus, at the time  $t$  the fishing vessel is assumed to have



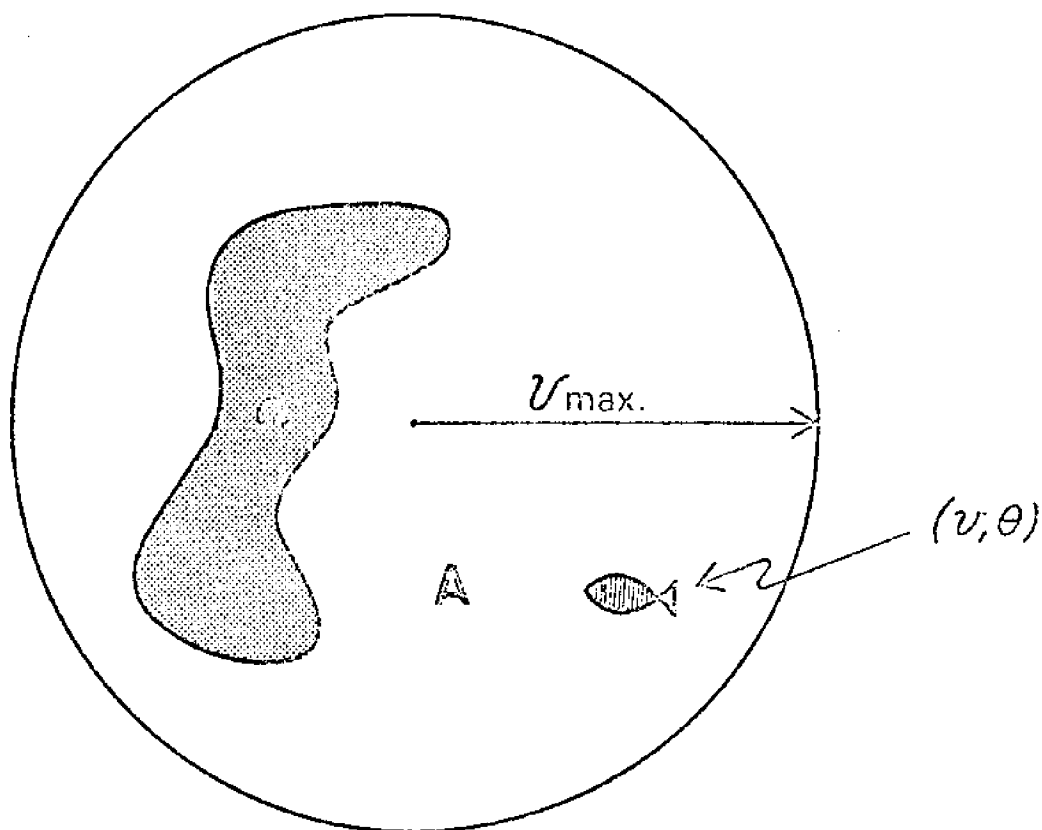


FIG. 1. An illustration of the speed circle of the fish shoal and a choice of strategy  $(v, \theta)$ . The area  $A$  illustrates a generalized searching strategy on the part of the fishing vessel. The area of the circle of radius  $v_{\max}$  is  $A$ .

scanned an area  $s(2R)t$  in real space. At the time  $t$  that the vessel has scanned an area  $s(2R)t$ , the size of the speed circle in real space is  $\pi v_{\max}^2 t^2$ . Therefore, the fishing vessel scans a proportion of the speed circle which is:

$$\frac{s(2R)t}{\pi v_{\max}^2 t^2} = \frac{s(2R)t}{A t^2}$$

where  $A = \pi v_{\max}^2$  is the area in speed space of the speed circle. We assume that the proportion searched is less than the area of the speed circle of radius  $v_{\max}$ , which implies that  $a < A$ . If more than one fishing vessel is involved in the searching activity, the numerator of the above expression is multiplied by  $F$ , the number of vessels involved in searching.

Consider an arbitrary region of speed space as shown by the shaded area of Fig. 1.

This shaded region has an area  $a$ . The solution to this search problem involves determining the optimum form of this area for the fishing vessel which is conducting the search for the fish shoal.

#### PROOF

It now seems conceptually possible to state the problem in terms of game theory. We shall consider this problem as a two-person zero-sum game. This approach has been described by Danskin (1962) and the proof of this game is entirely due to Danskin. Only the suggested application is believed to be novel.

A zero-sum, or strictly equivalent two-person game, is one in which the two players have exactly opposite preferences. The term zero-sum is used because it is possible to choose the zeros and units of the two utility functions (payoffs) so that they always sum to zero. Luce and Raiffa (1957) characterize the two-person zero-sum game and also provide a rigorous and

self-contained statement and proof of the minimax theorem, the central theorem of two-person zero-sum theory.

Denote a generalized fishing vessel strategy by  $f$ . This refers to the choice of the location of area  $a$  within the speed circle and is arbitrary. If the area  $a$  is very small relative to the speed circle, it can be shown that the probability of successful encounter with the fish shoal is also very small. From an estimate of the initial ratio of  $a$  to  $A$  it seems possible to decide whether or not it is worth while to attempt to locate the fish shoal. The fish shoal is assumed to choose its course at random and a speed  $v$  such that  $0 \leq v \leq v_{\max}$ .

Let  $P(f, v)$  be the resulting probability of detection where  $f$  is chosen to maximize and  $v$  to minimize their respective values. In terms of pure strategies, there is no solution to the game determined by  $P(f, v)$ . Given a choice of  $v$ , the fishing vessel strategy can be chosen so as to distribute the area  $a$  in an annulus covering the circle of radius  $v$  in the speed circle. Thus:

$$\begin{array}{ccc} \text{Min} & \text{Max} & P(f, v) = 1 \\ & f & \\ & v & \end{array}$$

In terms of this problem the above states that if the fishing vessel arrives at the reported location soon enough and with sufficiently good fish-finding equipment so that the vessel can effectively cover the entire area of the circle of radius  $v_{\max}$  in the speed circle, the probability of detection of the fish shoal is unity.

Similarly, given a choice of  $f$ , since  $a < A$ , the fish shoal could always avoid detection by avoiding the area:

$$\begin{array}{ccc} \text{Max} & \text{Min} & P(f, v) = 0 \\ & v & \\ & f & \end{array}$$

A real world situation such as the above might occur if it is assumed that the fish shoal could detect vessel noise and/or the searching apparatus and would then always avoid the area effectively scanned by the vessel.

For the purposes of this problem it is therefore necessary to consider mixed strategies. The fish shoal strategies  $f$  will be mixed by choosing some density function  $s(v)$  defined on the interval  $0 \leq v \leq v_{\max}$ , continuous there and satisfying:

$$s(v) \geq 0, \quad \int_0^{v_{\max}} s(v) dv = 1 \quad (1)$$

It is also possible to write:

$$\pi(f, s) = \int_0^{v_{\max}} P(f, v) s(v) dv \quad (2)$$

where  $\pi(f, s)$  is the probability of locating the fish shoal resulting from a fishing vessel strategy  $f$  for choosing the form of the area  $a$  and the fish shoal's mixed strategy  $s$ , the probability distribution from which fish shoal speed is chosen.

It is sought to determine optimal strategies,  $f_0$  and  $s_0$  in the sense of game theory. By definition,  $f_0$  and  $s_0$  will be optimal strategies if there is a number  $Y$ , which is called the value of the game with a property such that the two following conditions hold:

$$\pi(f_0, s) \geq Y \text{ for all fish shoal mixed strategies } s; \quad (3)$$

$$\pi(f, s_0) \leq Y \text{ for all fishing vessel strategies } f. \quad (4)$$

The strategies  $f_0$  and  $s_0$  will be described to demonstrate that they satisfy equations (3) and (4). The solutions to the two-person zero-sum game defined by equation 2 are the following:

- a)  $f_0$  is a wedge of area  $a$ , oriented at random. This is illustrated in Fig. 2.

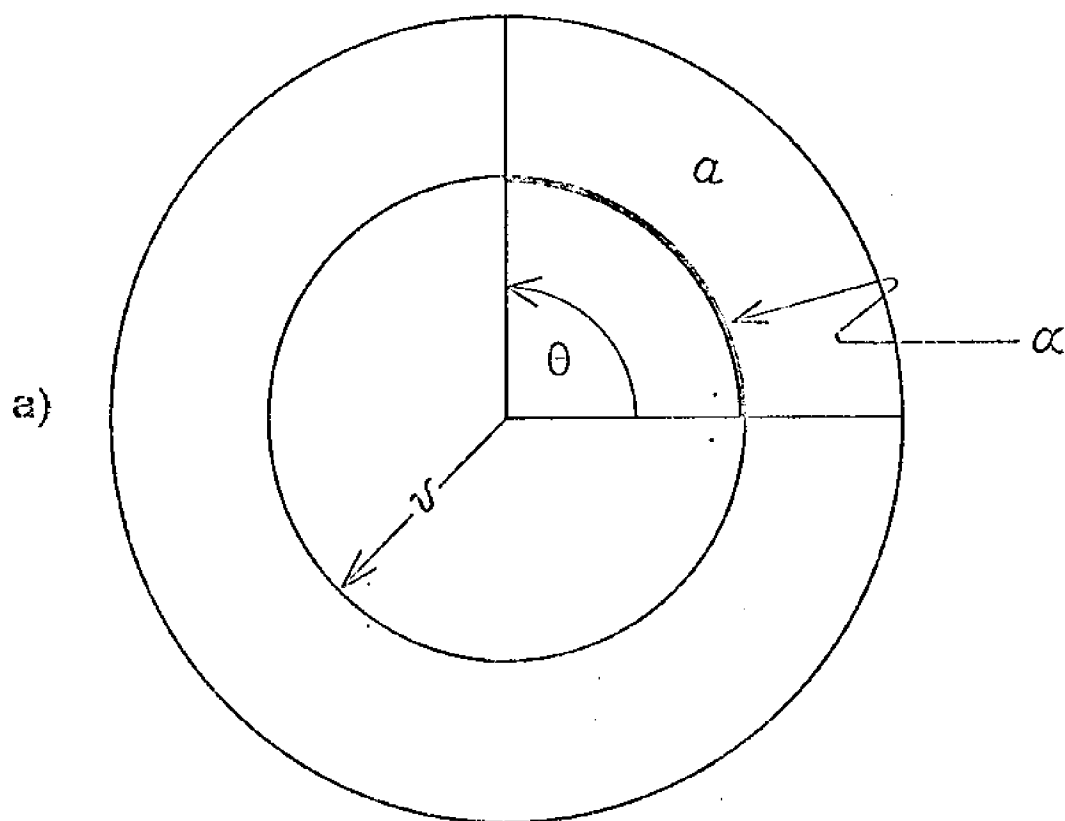


Fig. 2a. Illustration of the wedge strategy of the fishing vessel in the speed circle.

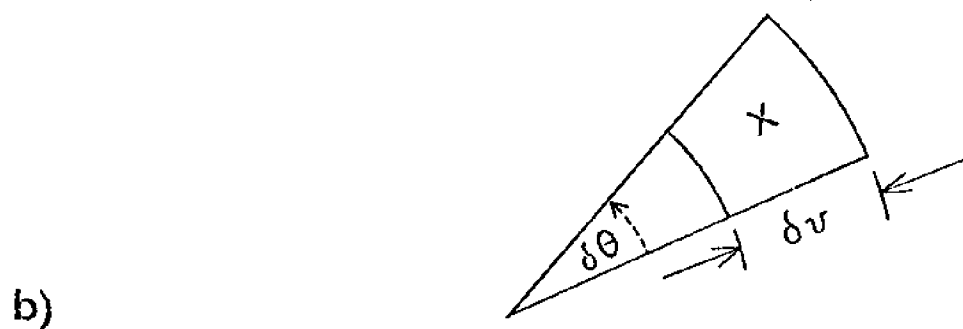


Fig. 2b. Illustration of the portion X of the speed circle lying between  $v$  and  $\delta v$  and  $\theta + \delta\theta$ .

- b)  $s_o$  is chosen so that the fish shoal is uniformly distributed in the speed circle. That is:

$$s_o(v) = \frac{2\pi v}{A}$$

- c) The value of the game is:  $Y = \frac{a}{A}$   
 d) The strategy of the fishing vessel  $f_o$  is not unique.

For proof of the above it is necessary only to prove equations (3) and (4) with  $Y = \frac{a}{A}$ . The procedure is as follows:

With reference to equation (3) consider some particular choice of speed  $v$  taken by the fish shoal. With the fishing vessel's strategy fixed as a wedge, the fish shoal's course chosen at random, the probability of locating the fish shoal is the probability that the course of the fish shoal lies in the wedge; (that is, on the arc  $\alpha$  shown in Fig. 2a). However, this is equal to  $\frac{\theta}{2\pi}$ , where  $\theta$  is the angle of the wedge measured in radians. But the area of the wedge is  $a$ , by definition. Therefore:

$$\frac{a}{A} = \frac{\theta}{2\pi}$$

Hence:

$$P(f_o, v) = \frac{\theta}{2\pi} = \frac{a}{A} \quad (6)$$

Since equation (6) holds for any  $v$  on  $0 \leq v \leq v_{\max}$  then:

$$\pi(f_o, s) = \int_0^{v_{\max}} P(f_o, v) s(v) dv = \frac{a}{A} \int_0^{v_{\max}} s(v) dv = \frac{a}{A}$$

for any mixed strategy  $s$  of the fish shoal. Hence equation (3) holds with  $Y = \frac{a}{A}$ .

With reference to equation (4), consider the portion  $X$  of the speed circle lying between  $v + \delta v$  and  $\theta + \delta \theta$ , as illustrated in Fig. 2b. If  $s_o$ , the optimal strategy for the fish shoal, is as given in equation (5), the probability that the fish shoal is in  $X$  is:

$$\frac{\delta \theta}{2\pi} \int_v^{v+\delta v} s_o(v) dv = \frac{\delta \theta}{2A} [(v+\delta v)^2 - v^2] . \quad (7)$$

But the quantity  $\frac{\delta \theta [(v+\delta v)^2 - v^2]}{2}$  is exactly the area  $a(X)$  of the portion  $X$ . Hence equation (7) may be rewritten to say that the probability that the fish shoal is in the proportion  $X$  is  $\frac{a(X)}{A}$ . That is, it is proportional to the area  $a(X)$ . The choice of  $s_o$  given by (5) assumes that the fish shoal is uniformly distributed in the speed circle. Thus, if the fish shoal stays with  $s_o$ , the probability that the fishing vessel locates the fish shoal is  $\frac{a}{A}$  no matter where the fishing vessel distributes the area  $a$ . That is:

$$\pi(f_1, s_o) = \frac{a}{A} \text{ for all } f. \quad (8)$$

Since equation (8) implies equation (4),  $f_o$  and  $s_o$  are optimal. They are obviously not unique strategies. The proof is completed for the game.

#### SUGGESTED APPLICATIONS

The wedge strategy for the fishing vessel does not seem intuitively obvious. It implies random choice of a direction of search based strictly on the assumption of no knowledge concerning speed and direction. In game theory there are subsets of the set of optimal strategies known as "good" strategies. We shall briefly consider a few as they might relate to this problem.

Before proceeding with these, however, it should be recognized that the above proof of the wedge strategy can be applied by the fishing vessel to make an initial estimate of the probability of success (hence the desirability of attempting a search) from the outset merely by calculating the ratio  $\frac{\theta}{2\pi}$  at the time the vessel would reach the perimeter of the circle of radius  $v_{\max}$ .

The wedge strategy was an optimal strategy, because when the fish shoal's course was randomized, the probability that the fish shoal was located was the

ratio of the length of the arc in Fig. 2a. to  $2\pi v$ . That is:

$$\frac{\epsilon v}{2\pi v} = \frac{a}{A}, \quad (9)$$

which is evident from equation (6). It can be shown that equation (9) holds for any  $v$  even if the initial wedge is cut along circular arcs starting from the center of the speed circle or by radii from the same origin - namely, the center of the circle. Equation (9) holds for any value of  $v$  simply because of the direct proportionality relation between the area of the wedge cut by a given angle  $\theta$  and the area of the circle of radius  $v$ . The sum of the parts of the initial wedge is equal to the whole area of the wedge.

Thus, the initial wedge of area  $\frac{a}{A}$  can be cut by arcs and radii into a number of pieces which might represent certain "good" strategies.

Fig. 3a. illustrates the initial partitioning of the wedge of Fig. 2a. into two by means of a circular arc and also by means of a radius. Fig. 3b. illustrates the fact that the initial wedge can be cut by arcs and radii in any way and the pieces can be cut and arranged to resemble in area any arbitrary pattern of search by one or more vessels. Fig. 3b. also illustrates that the inner circle of the outer ring is drawn in such a manner that the area of the piece or pieces in that ring is  $\frac{S(2R)t_1}{t_1^2}$ , and the next inner ring is chosen so that the area enclosed within it and its outer neighbor is  $\frac{S(2R)t_2}{t_2^2}$  etc.

From Fig. 3b., it is evident that if the discrete areas searched during each unit of time resembled those shown in the diagram then the optimal strategy appears to be an inward spiral. It is possible to proceed in a more practical manner by approximating equation (9) instead of the annuli of the circles. That is, we can place a continuous path in the approximate locations of the pieces of the annuli of the circles of Fig. 3b. Then, for a series of values of  $v$  circles of radius  $v$  are drawn. If we then measure at each  $v$  the



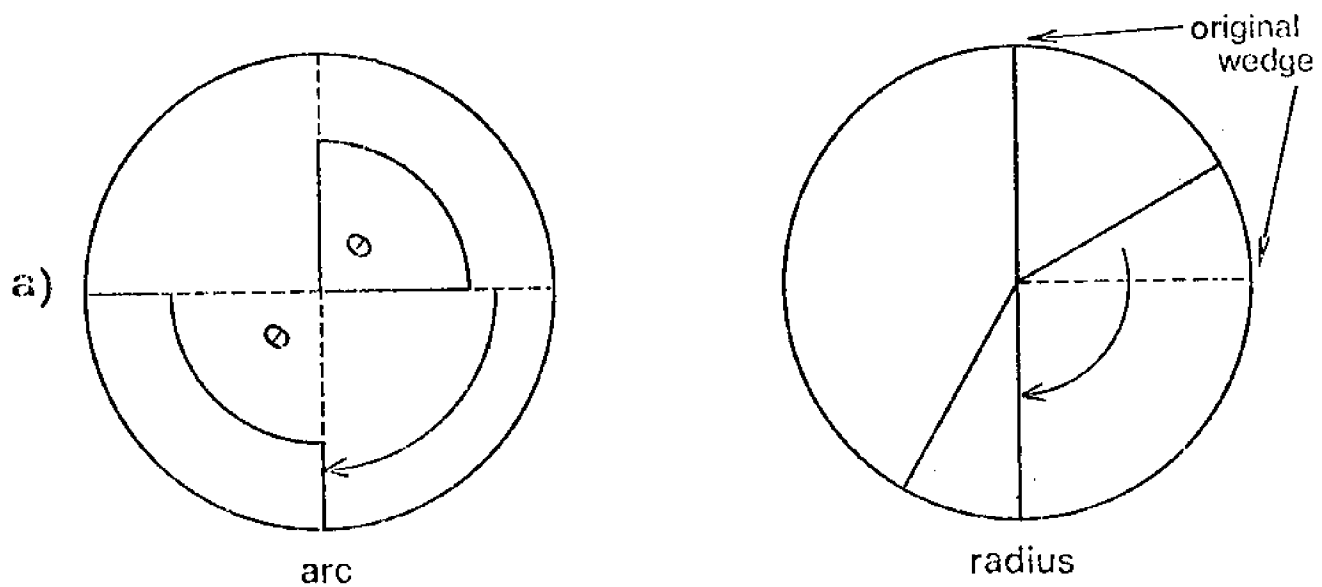


Fig. 3a. The partitioning of a circle by means of an arc and a radius.

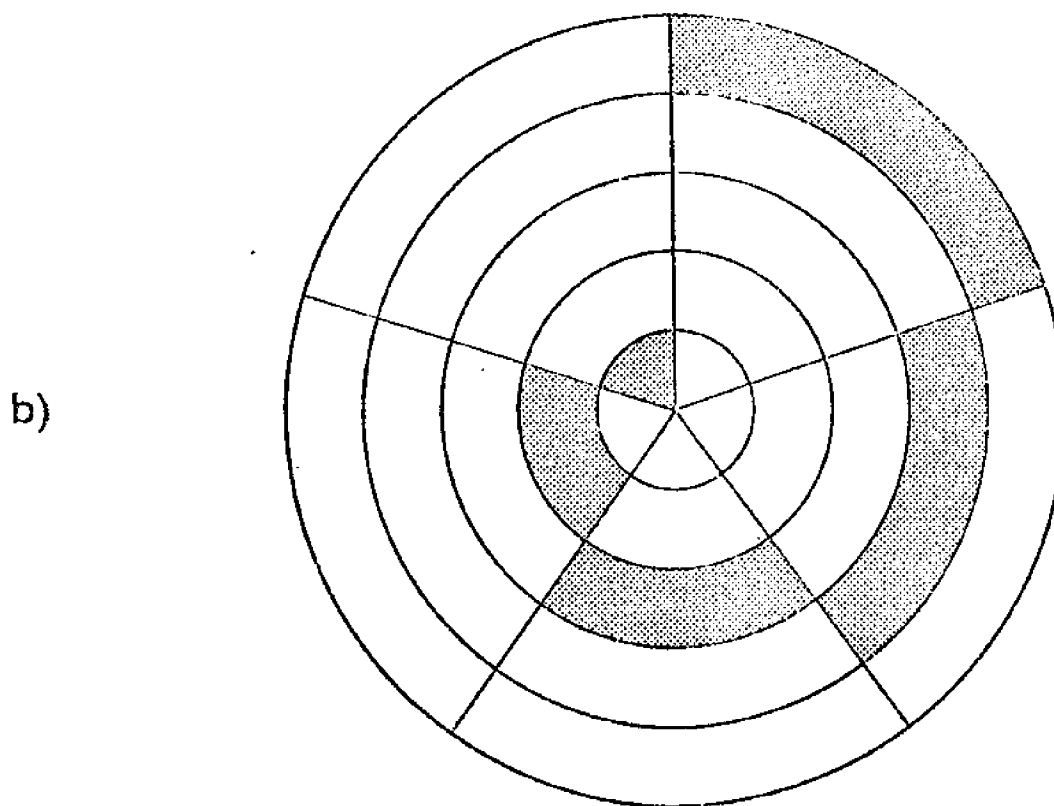


Fig. 3b. Rearrangement of pieces of annuli to resemble a search pattern.

proportion  $\frac{\theta(v)}{2\pi}$  of arc of that circle contained in a particular search configuration, a function of  $v$  is developed. This function measures the probability of successful search if the fish shoal chooses  $v$ . The degree of correspondence of the function to the probability distribution from which  $v$  was chosen roughly measures the degree of approximation of a proposed search strategy to the ideal strategy if the fishing vessel scans a search path cut out of the wedge strategy. Fig. 4a. illustrates a continuous search path. Fig. 4b. illustrates diagrammatically the probability of a successful search for circles of various radii from  $v_0$  to  $v_{\max}$  assuming a uniform fish shoal velocity distribution. Clearly there is some flexibility in the method, because various search configurations can be tested, and these may provide some useful guides to fish finding under certain limited conditions. Although the proof for the game was developed under the assumption of a uniform distribution of fish shoal speeds, it seems apparent that an increased probability of success may be achieved by concentrating the search in the vicinity of the mode of a non-uniform distribution of fish shoal velocities. Obviously, if directional information were available in addition, the search could be concentrated in the vicinity of the expected direction of travel as well as at the mode of the velocity distribution. This should further increase the probability of success.

## CONCLUSIONS

It is suggested that this exercise provides some indication of the practicability of certain remote sensing applications in fisheries as well as identifying some types of research required if we are to make additional improvements in this kind of fish-finding efficiency. Tentative conclusions include:

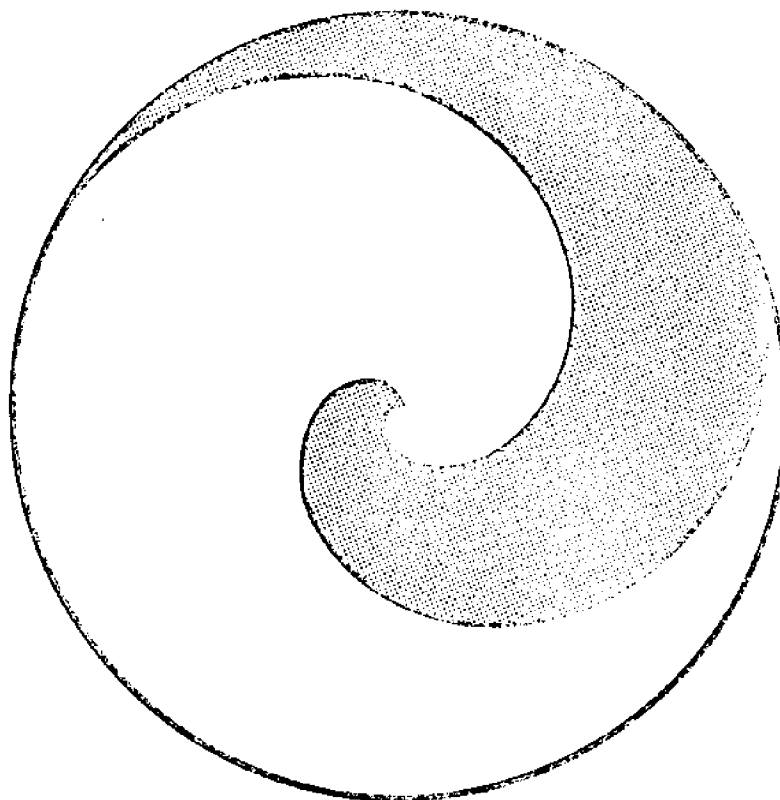


Fig. 4a. Illustration of a continuous search path as an approximation to the pieces of annuli of Fig. 3.

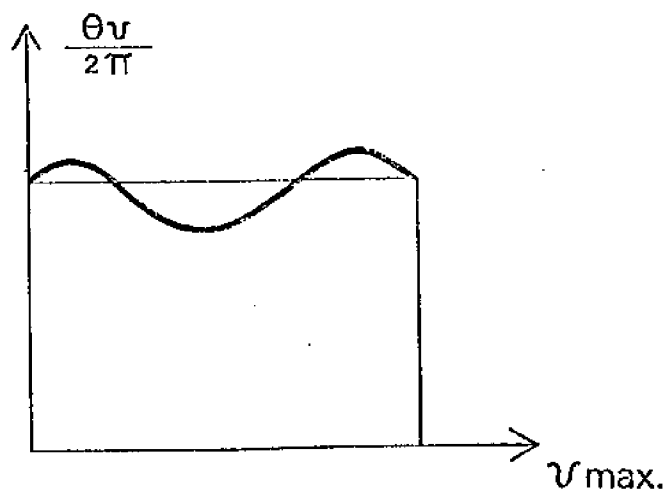


Fig. 4b. The probability of successful fish-finding as a function of a uniform fish shoal velocity distribution. The straight line refers to a uniform velocity distribution and the crossed line to the approximation derived from a given search pattern.

- 1) Under the assumptions made in this model (namely, no knowledge of the direction of the fish shoal and limited information on the range and distribution of velocities) the fishing vessel must be relatively close to the co-ordinates of the initial sighting in order to make the probability of success high enough to justify search effort.
- 2) Any additional information on the direction and/or velocity of the fish shoal reduces the difficulty of the search problem and increases the probability of success greatly. Therefore, it seems that remote sensing from aircraft or from any vehicle which can observe the fish shoal over time and thus provide this additional information is highly desirable.
- 3) If the remote sensing device can only report position co-ordinates, then further behavioral and other biological information is clearly needed. For example, frequency distributions of swimming speeds of various species under defined conditions of temperature, time of day, season, etc., would be extremely helpful in restricting the region to be searched. In addition, similar series of observations on the directional response of fish shoals to currents and other physical phenomena would also significantly add to the probability of successful searching because these data could also be used to further restrict the region to be searched and hence increase the probability of success.

### Literature Cited

- Bainbridge, R. 1958. The speed of swimming of fish as related to size and to the frequency and amplitude of tail beats. *J. exp. Biol.* 35 (1), pp. 109-133.
- Beverton, R. J. H. and S. J. Holt. 1957. On the dynamics of exploited fish populations. *Fishery Invest.*, London, 19: 533 pp.
- Blaxter, J. H. S. 1969. Swimming speeds of fish. *Proceedings of the FAO Conference on Fish Behaviour in Relation to Fishing Techniques and Tactics*. Vol. II, pp. 69-100.
- Danskin, J. M. 1962. A theory of reconnaissance: II. *Oper. Res.* 10 (3), pp. 300-309.
- Jones, F. R. H. (Personal communication dated 20 September 1970)
- Luce, R. D. and Raiffa, H. 1967. *Games and Decisions*. New York, John Wiley & Sons.
- Maughan, P. M. 1969. Remote-sensor applications in fishing research. *Marine Technology Society Journal*: 3(2), pp. 11-20.
- Norton, V. J. 1969. Some potential benefits to commercial fishing through increased search efficiency. A case study - The tuna industry. Final Report to: The Geological Survey, United States Department of the Interior: 62 pp.
- Nursall, J. R. 1962. Swimming and the origin of paired appendages. *Am. Zoologist*, 2: pp. 127-141.
- Radakov, D. V. 1964. Velocities of fish swimming. In: Pamphlet from A. N. Severtsov Institute of Animal Morphology, Moskva Nauka, pp. 4-28 (in Russian).
- Saila, S. B. and Flowers, J. M. 1969. Elementary applications of search theory to fishing tactics as related to some aspects of fish behaviour. *Proceedings of the FAO Conference on Fish Behaviour in Relation to Fishing Techniques and Tactics*, Vol. II. pp. 343-355.

## THE USE OF FISH IN BIOLOGICAL SITUATIONS

George W. Klontz, M.S., D.V.M.

Department of Veterinary Microbiology

Texas A&amp;M University

In the past decade there has been increasing interest in using fish as biological research subjects. This is evident by the large number of reports (some 8,500 in the past 12 years) appearing in the major journals. With the modern researcher expanding his horizon, various fishes have been used to great advantage in comparative studies in the fields of endocrinology, immunology, pathology, biochemistry, toxicology, physiology, and genetics (Hoar and Randall, 1969). In addition to the comparative studies, basic investigations of these animals have been useful to increase our knowledge of propagating the commercially important species. This latter consideration has become very significant in order to feed the ever-increasing population of the world.

By definition, fish are aquatic animals that embrace 42.6% of the number of living vertebrate species. Their natural environments range in depth to at least seven miles beneath the water surface, in temperature from 0°C to 28°C, and in salinity from 0.005% to 14% (Lagler et al, 1962).

Only a few primitive species of fish evolved into terrestrial forms while others have either become more specialized or have remained essentially unchanged through the centuries. Therefore a researcher can study living examples of the majority of evolutionary innovations that have occurred in this group of vertebrates over the past 200 million years. Little use, however, has been made of this potential.

The problem of which species of fish to use in a particular research situation is exceedingly complex. The investigator must be aware of the diversity of physiotypes and anatomical structures in these animals which have arisen as a result of environmental adaptations. For example, the agnatha - the hagfishes and lampreys - do not have a true stomach; the soft-rayed teleosts - trout and salmon - have a well-developed and separate pancreas whereas the spiny-rayed teleosts - the perch - have a hepatopancreas; only the teleosts have a swim bladder; the carnivorous fishes have a shorter mid-gut than do the herbivorous species. Therefore one needs to select the experimental fish in terms of the object of the research and be aware of the advantages and disadvantages of the selection. One must also be able to maintain the species selected in as near optimum environmental conditions as possible (Klontz and Smith, 1968).

Successful maintenance of fish in captivity for research depends upon the water the fish are in and the container and piping holding the water. The majority of problems arising with fish in either freshwater or sea water systems are directly attributable to not closely monitoring and controlling the following: temperature, carbonate, carbon dioxide, nitrogen - free and ammonia nitrogen, dissolved oxygen, iron, chlorine, salinity, turbidity, and biological and industrial pollutants.

Although there are no strict rules guiding the size and shape of containers to maintain fish, they should be of sufficient size to allow the fish - however many there are - to move about in their normal fashion. The materials used should not be such that they pollute the water with toxic agents. For example, there should be no zinc or copper fittings anywhere in the water supply

unless resin columns have been provided to remove the ions. Many species of fish are quite susceptible to as little as 0.04ppm copper and 0.1ppm zinc.

The importance of rigid sanitation practices cannot be too strongly emphasized. Fish, being totally and irrevocably oriented to their environment, alter the water they inhabit by their excretory products and by depleting the oxygen supply. A recent report indicates that the B.O.D. (Biological Oxygen Demand) production of 100,000 1-pound channel catfish is approximately equivalent to the B.O.D. production of 150,000 1-pound chickens.

The excretory product that usually causes the most problems in groups of fish in aquaria is ammonia-nitrogen. It attains toxic levels above 1.5ppm. At a continuous level of 0.7ppm ammonia, juvenile salmonids have gill lamellar thickening and subsequent hyperplasia, resulting in complete fusion of the lamellae. This hinders oxygen-carbon dioxide exchange to the point that the animal literally suffocates.

A final but no less important consideration in maintaining fish for biological research is nutrition. Fish normally consume an amount of feed equal to three per cent of their body weight per day. In order to maintain a good nutritional state the fish must be fed their normal diet or a nutritionally reasonable facsimile at times during the day when they usually eat.

In using fish in any of the myriad of experimental designs that have been reported over the years, the majority of the investigators neglected to take into account the large source of error occurring due to manipulative stress. In rainbow trout and coho



salmon, physical stress induces serum ascorbic acid depletion and cortisol production. If the stressor were continued, adaptation occurred as evidenced by the ascorbic acid returning to normal (Wedemeyer, 1969).

By way of example to indicate how one's data would be influenced by stressing the fish, I offer the following: We were conducting a long-term study on the primary and secondary sites of blood cell formation in young adult rainbow trout. This was a basic study - the information would be used to compare similar data obtained after the fish were exposed to various pollutants. The experimental design called for blood samples to be taken from each of 20 anesthetized fish on alternate days for nearly five months. The odd-numbered samples were obtained by one person and the even-numbered samples were obtained by another person. When the results were plotted all the even-numbered samples were on one side of the median line and the odd-numbered samples were on the other. In addition, the difference between the sample groups due to stress was considered so significant that the study was repeated in duplicate with only one person obtaining the blood samples per group of fish. The results of this study are to be published shortly.

Here at Texas A&M University, the Aquatic Animal Medicine Program, under the auspices of the Sea Grant Program, is studying the basic environmental and nutritional requirements of 10-12 species of freshwater and marine fish. The data are being incorporated into open and closed water systems to maintain these species for biological research subjects. The studies are preparatory to studying some of the basic mechanisms of the disease process in

these animals with respect to wound repair, bacterial and viral infection, external and internal parasites, and to its being altered by chemotherapeutic agents.

#### REFERENCES

- Hear, W. S. and D. J. Randall (eds.), "Fish Physiology, Volumes I, II, III" (Academic Press, New York, 1969)
- Klontz, G. W. and L. S. Smith, "Methods of Animal Experimentation, Volume III, W. I. Gay, ed. (Academic Press, New York, 1968)
- Lagler, K. F., J. E. Bardach and R. R. Miller, "Ichthyology", (John Wiley and Sons, Inc., New York, 1962)
- Hedemeyer, G. A., Comp. Biochem. Physiol. 29, 1247 (1969)

## UPWELLING STUDIES WITH SATELLITES

by

Karl-Heinz Szekiolda\*  
Goddard Space Flight Center  
Greenbelt, Maryland

## 1. INTRODUCTION

Recent studies in oceanography at Goddard Space Flight Center have investigated two different ways to obtain surface temperature structures with data from an orbiting platform.

A. Analysis of radiometric recordings during one overpass over apparently cloud-free regions has provided the surface structures of an area. This method can be used to analyze a synoptic recording and has the further advantage of noting rapid changes in the sea surface temperatures over typical scales of a few days.

B. Mapping the sea surface temperature has been accomplished through use of a multispectral method which detects cloud-free conditions and uses the radiation for the determination of the sea surface temperature. This method includes data recorded from orbiting platforms over a period of 2 to 4 weeks; therefore, short-time fluctuations are smoothed out. The method is applicable to map ocean surfaces on a global scale, (W. S. Shenk and V. V. Salomonson, 1970). Both methods were used to study areas in oceans where upwelling exists.

---

\*On leave from the Faculte des Sciences, Marseille, France, as a National Academy of Sciences-National Research Council Postdoctoral Resident Research Associate.

## 2. SOMALI COAST

Figure 1 shows the surface winds observed during the different monsoon seasons along the Northeast Coast of Africa. The left-hand illustration is based on observations made aboard the R. V. "Argo" during the 1964 Southwest Monsoon (J. Bruce, 1965); the analysis in the right-hand illustration shows the observations of wind speed and direction made during the Northeast Monsoon 1964/65 aboard R. V. "Meteor", W. Dilling, 1966). Both observations indicate high wind speeds for the different seasons, with a dominant component parallel to the coast; but their directions are opposite.

In response to the wind system over the Arabian Sea, the Somali Current changes its direction of flow from northeast to southwest along the East African Coast. The changes appear after the onsets of the Southwest Monsoon and the Northeast Monsoon, respectively.

In contrast to other western boundary currents, such as the Gulf Stream and the Kuroshio Stream, the Somali Current moves away from the coast at about 9°N during the Southwest Monsoon and turns into an anticyclonic water movement along the coast. Current measurements (Figure 2) revealed that the Somali Current is a very narrow stream and showed that current velocities up to  $350 \text{ cm}\cdot\text{s}^{-1}$  may be observed. Somewhat smaller velocities of  $200 \text{ cm}\cdot\text{s}^{-1}$  were also observed in the eastern branch of the anticyclonic eddy where the current flows in a southeasterly direction. The anticyclonic movement of the Somali Current off the coast is not limited to the upper horizons of water. Offshore water movements can still be detected at a depth of 200 m. (J. G. Bruce, 1966).

Normally, the upwelling appears near the coast at 9°N and during the fully developed Southwest Monsoon exhibits a horizontal temperature gradient of the order of  $0.05^{\circ}\text{C. km}^{-1}$ . A typical temperature distribution, obtained with the Nimbus 2 HRIR during 1966, is presented in Figure 3. Temperatures below  $23^{\circ}\text{C}$  are indicated by the gray tone in the chart. Minimum temperatures were below  $18^{\circ}\text{C}$  at 8°N. It is remarkable that the surface temperatures reflect the transportation of upwelled water; this can be seen from the  $24^{\circ}\text{C}$  isoline.

The synoptic temperature recordings with the Nimbus 2 HRIR permitted a detailed analysis of the development of the upwelling as a function of the prevailing winds as reported by ships. Normalized horizontal temperature gradients and wind amplitudes are given in Figure 4. The results can be explained in the following manner.

The similar slope of the temperature gradients and the wind amplitudes indicates a linear rather than a square-law relation. A possible interpretation (W. Düng and K.-H. Szekielda, 1970) for that relationship is the fact that upwelling stabilizes the atmosphere over the cold water, which leads to a decrease of the wind stress. A time lag of only a few days between the development of horizontal temperature gradients and the development of the wind amplitudes was found. During the formation period of the Southwest Monsoon in May and June, the horizontal temperature gradients lags 3 to 5 days behind the wind amplitudes. However, during the decay period in fall, the wind amplitudes lag 14 to 40 days behind the temperature gradients. Obviously,

the energy in the anticyclonic movement is strong enough to maintain the geostrophic slope of the isotherms after the decrease of wind stress by the Southwest Monsoon.

The temperatures in the core of upwelling indicate that the origin of the upwelled water lies at a depth of about 200 m. This water is very rich in nutrients and, even at the surface, contains phosphate concentrations on the order of  $1.4 \mu\text{g-atoms l}^{-1}$ . Figure 5 gives a horizontal distribution of reactive phosphate concentration. It is obvious that the highest phosphate concentrations were found in the core of upwelling; because the plankton needs time to grow, the highest concentrations of organic matter will not be found near the coast. Such concentrations can, however, be expected far from the coast. This can be verified when examining the vertical profile of chlorophyll concentrations observed along  $10^{\circ}\text{N}$  from the East African Coast to  $70^{\circ}\text{E}$  in August during the 1964 Southwest Monsoon (Figure 6). Near the coast where upwelling existed, very low concentrations of chlorophyll-a were detected. However, far from the core of upwelling along the thermal boundary, concentrations to  $2.5 \mu\text{g} \cdot \text{l}^{-1}$  were measured. Thus, the highest concentration of organic material is connected with the temperature gradient at  $52^{\circ}\text{E}$  to  $53^{\circ}\text{E}$  off the central upwelling area.

Since temperature and the nutrients are closely related, we can estimate the concentration of phosphate in the core of upwelling from temperatures remotely sensed by satellites.

### 3. ARABIAN COAST

Another area of strong upwelling in the northern Indian Ocean appears along the Southwest Coast of Arabia. The development of the area of cold water is also a function of the wind stress during the Southwest Monsoon period.

Temperature recordings obtained in 1970 with the THIR aboard Nimbus 4 showed a temperature decrease after the onset of the Southwest Monsoon at the end of May. On June 10, two cores with temperatures below  $23^{\circ}\text{C}$  were detected. The difference between this and the offshore water was  $4^{\circ}\text{C}$ . Four weeks later, on July 12, minimum temperatures recorded were below  $19^{\circ}\text{C}$ . A well-developed upwelling with a temperature gradient of the order of  $0.04^{\circ}\text{C km}^{-1}$  existed in the coastal waters between  $54^{\circ}\text{E}$  and  $58^{\circ}\text{E}$  (Figure 7). Because the winds were not in an offshore direction, we can assume that the cold water was predominantly generated by the geostrophic slope of the isotherms in the current. Current measurements aboard the "Discovery" detected speeds of the order of 1 knot (The Royal Society, 1963), in a northeasterly direction along the coast.

Measurements of the surface layers offshore only showed phosphate concentrations of  $0.5 \mu\text{-atoms l}^{-1}$ . However, in the upwelled water along the coast, concentrations higher than  $2 \mu\text{-atoms l}^{-1}$  appeared. The relationship between high nutrient concentrations and the low temperature of the water gives an excellent opportunity to estimate from remotely sensed temperatures the nutrient concentration available for biological depletion processes. The observed discoloration of the surface water

by a bloom of diatoms in the area of upwelling along the Arabian Coast emphasizes the possibility of determining fish population in this area by satellite measurements in the visible region of the spectrum.

Cell concentrations to  $64 \times 10^3$  per ml were found. This high concentration of organic matter gives a green or brownish discoloration to the sea water, whose dynamics can probably be investigated with the future Earth Resources Technology Satellites.

#### 4. ANTARCTIC

One of the largest areas of upwelling lies around the Antarctic, where divergent motion appears near the continent. This area is not well covered either by commercial ships or by research vessels. Therefore, satellite studies can be of considerable help in the understanding of the dynamics of the sea surface in this area. Figure 8 shows a satellite study in the southern Indian Ocean in which a multispectral method was used to eliminate the effects of moisture and cloud covers. The Agulhas Current is indicated by the isotherms, caused by the transportation of warm water along the African continent, lying almost parallel to the coast and by the upwelling area at about  $35^\circ\text{S}$ . The most striking feature in this analysis is the sharp temperature gradient starting at about  $40^\circ\text{S}$ ; it indicates the oceanic polar front between cold water from the Antarctic and the southern warmer water masses. The cold water north of the oceanic polar front has its origin at the Antarctic divergence, where the water is moving toward the Antarctic convergence zone. During the movement from the divergence to the convergence zone, a great diatom production is induced during the Antarctic spring and summer. However, the concentrations of reactive phosphate are still higher than  $0.9 \text{ ug-atoms} \cdot \text{l}^{-1}$ . This shows



that nutrients are transported to the surface faster than they are consumed by organisms. For two reasons, the Antarctic water masses are of importance in the ocean's food chain:

(1) During summertime high total phytoplankton standing crop (J. J. Walsh, 1969) enables grazing organisms to multiply to an unusually high concentration.

(2) The converging water masses at the polar front are high in organic compounds and show an active transport of these compounds to deeper horizons. This is important in relation to deeper-grazing herbivores and, ultimately, to fish production.

#### 5. NORTHWEST COAST OF AFRICA

Along the Northwest Coast of Africa, upwelling appears in connection with the Canary Current, whose intensity varies only slightly during the year. Unfortunately, only a few oceanographic stations exist in this area; thus, data on this region are not complete. The three-channel method (mentioned before) was applied to detect the Canary Current and determine its transportation of cold water along the coast; the results for a period of 6 weeks from April to May 1969 are shown in Figure 9. The current is indicated by the deformation of the isotherms in a southward direction along the coast. At about  $10^{\circ}\text{N}$ , the Canary Current leaves the coast and turns into the North Equatorial Current. This is visible from the position of the  $24^{\circ}\text{C}$  isotherm at  $10^{\circ}\text{N}$ . High temperatures were found between  $5^{\circ}\text{N}$  and  $10^{\circ}\text{N}$ , which is probably a result of the Equatorial Counter-Current. Temperatures below  $22^{\circ}\text{C}$  are caused by the Guinea Current, which is associated with a divergent motion on the left-hand side of the current. The ground resolution of the radiometer used was not high enough to separate small areas of cold water, but the position of the isotherms can be

used to determine the strength of the current and the intensity of upwelling. A comparison of the position of the 23°C isotherm during 1969 and the historical mean position, revealed no great difference between the two analyses. However, the satellite data have the advantage of wider coverage than the temperatures reported by ships. Only a few papers deal with the distribution of biological and chemical parameters in this upwelling area. Fortunately, during the Apollo 9 mission, one photograph was taken of the area near the coast where upwelling appears (Figure 10). Integrated chlorophyll-a measurements taken aboard ship showed 40 mg-m<sup>-2</sup> in the coastal area, with a decrease to the offshore water. The different colors of the water as seen in the Apollo picture can therefore be interpreted in terms of chlorophyll differences. Highest concentrations of chlorophyll, indicated by the lighter blue, can be located along the coast.

The limits between the discolored water and the blue offshore water is not parallel to the coast. Meandering and separated areas with highly discolored water are detected, which could have been produced by fluctuations in the current system itself.

A more detailed infrared analysis of recordings from the THIR aboard Nimbus 4 in this area confirmed this. Figure 11 shows an analysis of an infrared imagery obtained with the Nimbus 4 THIR over the Northwest Coast of Africa during daytime. A similar analysis of the image dissector camera system photograph taken simultaneously showed cloud-free conditions. The different colors can therefore be interpreted in terms of temperatures of the ocean surface. Cold water is shown as a blue-green color, whereas

the warmest water is displayed in red. The African continent, with high temperatures, appears black. The coldest water along the coast indicates the Canary Current, which transports water from the north and induces upwelling along the coast. After the infrared analysis the Canary Current does not appear like a broad band parallel to the coast; however, its complicated structure makes it evident that the distribution of the surface temperature is probably influenced by varying wind stress and tides.

#### 6. FINAL REMARKS

The case studies presented show the high variability of the environment in the ocean, which would be difficult to discover with conventional oceanographic methods. Therefore, remotely sensed temperatures and data in the visible spectrum obtained from orbiting platforms provide excellent information for biological and, perhaps, chemical oceanography. Recent recordings of temperature and measurements in the visible spectrum with a low-flying aircraft also show potential application to oceanography, especially in fishery research. It should be mentioned that simultaneous recordings in different regions of the electromagnetic spectrum will give much more information about the time behavior of marine populations and their response to the environment. Conventional methods which employ a research vessel in the measurement of the rate of depletion of nutrients and in the measurement of standing stock provide a basis to model the environment and the population density. However, satellite information has indicated so much heterogeneity in the surface structure of the oceans that a single ship could never map the small features and the rapid changes of oceanic fronts, for instance, along the Somali Coast and in the Gulf Stream. Since a synoptic recording of information is required, future satellites will enable us to investigate much more precisely the relation-

ship between fluctuations in temperature and biochemical processes in the sea.

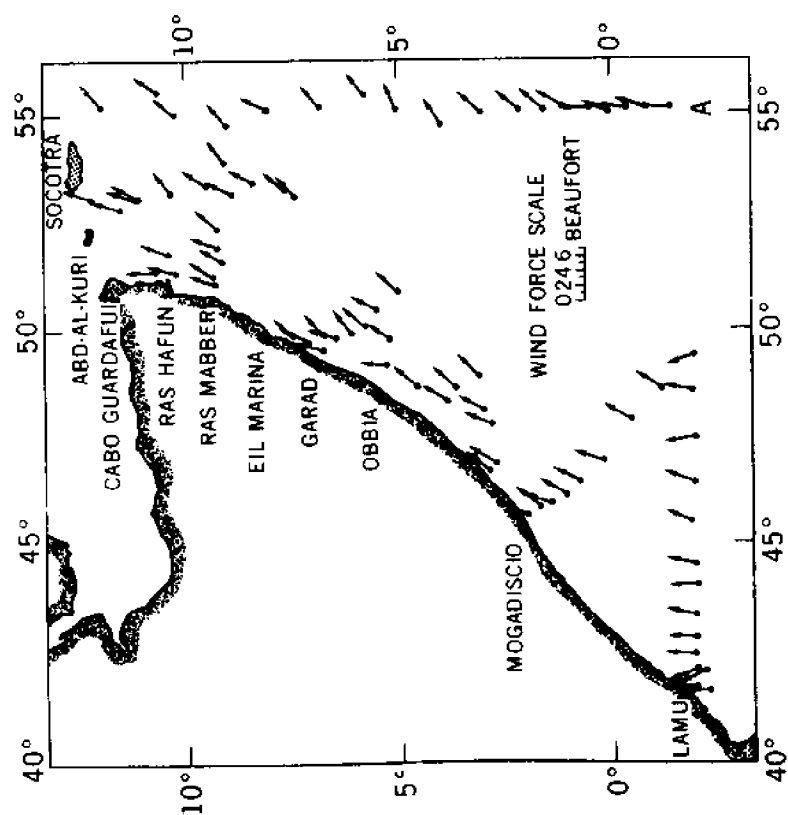
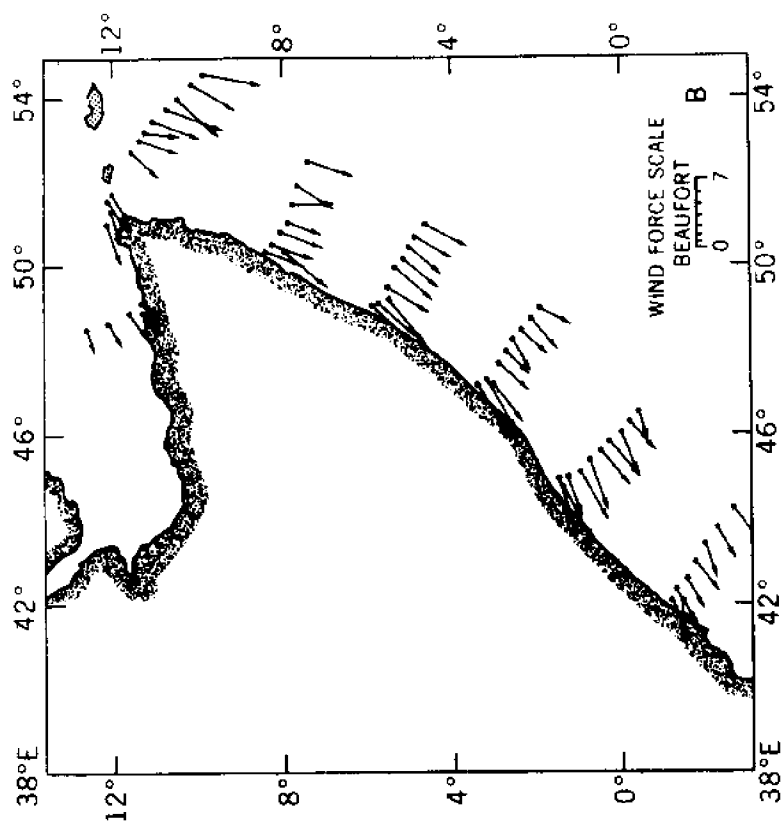
#### 7. ACKNOWLEDGEMENTS

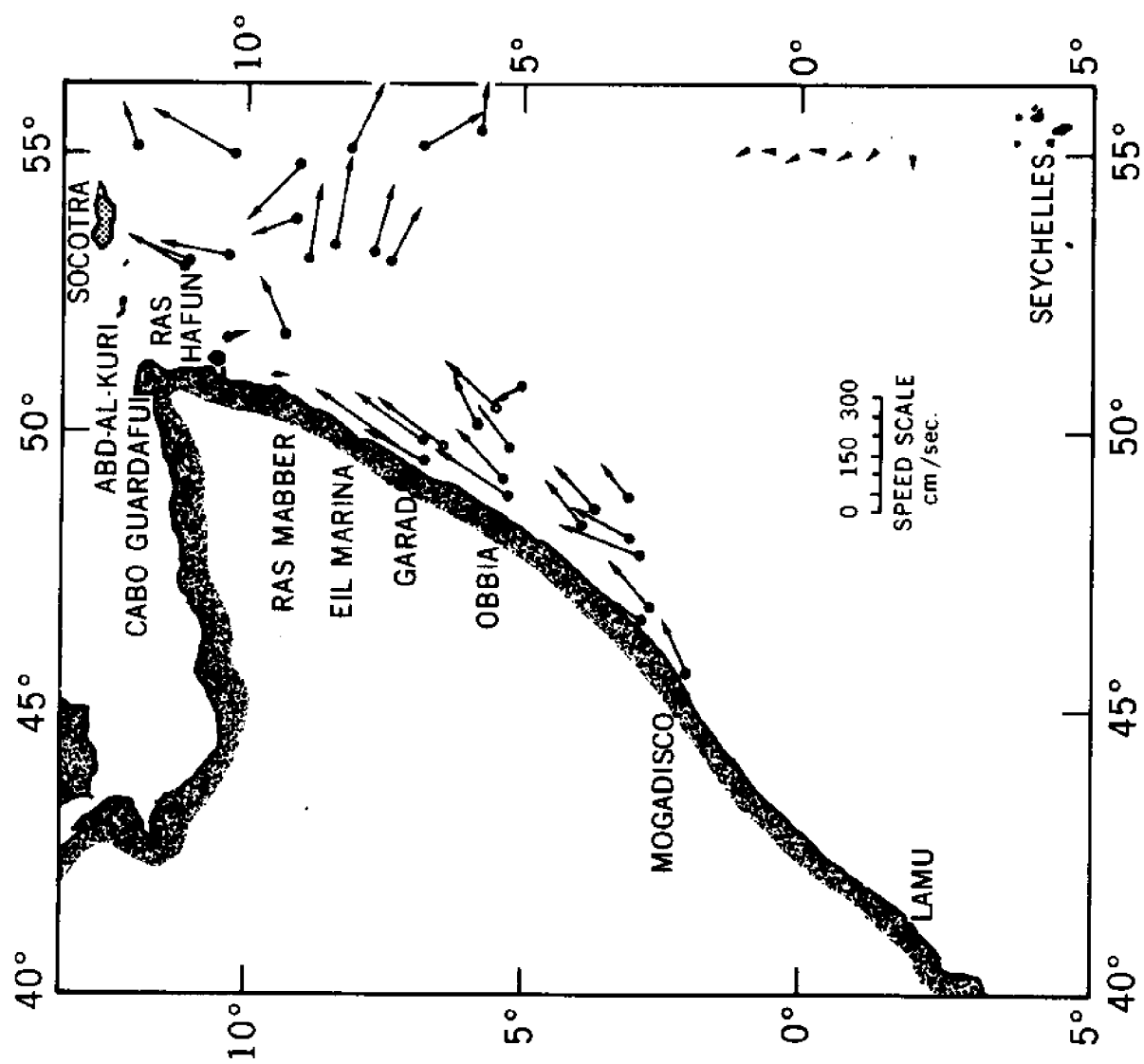
I am indebted to Drs. K. Banse, W. Düng and J. J. Walsh for helpful criticism of the manuscript.

- Figure 1 - Surface winds along the Somali Coast. Vectors represent wind speed and direction: (A) Observations during the Southwest Monsoon (J. G. Bruce, 1965), and (B) Observations during the Northwest Monsoon (W. Düing, 1966).
- Figure 2 - Current observations along the Southwest Monsoon at a depth of 10 m (J. G. Bruce, 1965).
- Figure 3 - Temperature distribution along the Somali Coast as recorded with the Nimbus 2 HRIR.
- Figure 4 - Horizontal temperature gradients obtained with Nimbus 2 HRIR and observed wind amplitudes from ship reports. All values are normalized.
- Figure 5 - Phosphate distribution at the surface during the Southwest Monsoon along the Somali Coast. Values are in microgram-atoms of phosphate per liter.
- Figure 6 - Vertical profile of chlorophyll-a distribution along 10°N from the East African Coast to 70°E, August 1964. Values in micrograms per liter, (Data according to J. Laird, B. B. Breivogel, and C. S. Yentsch 1964).
- Figure 7 - Temperature distribution along the Arabian Coast, in degrees Celsius.
- Figure 8 - Temperature distribution in the southern Indian Ocean during June and July 1966, obtained with a multispectral method using Nimbus 3 MRIR channels. Temperatures are not corrected for the atmospheric absorption; values are in degrees Kelvin (after W. E. Shenk and K.-H. Szekieda, 1971).
- Figure 9 - Temperature distribution along the Northwest Coast of Africa during April and May 1969, obtained with a multispectral method using Nimbus 3 MRIR channels. Temperatures are corrected; values are in degrees Celsius.
- Figure 10 - Color photograph of the Northwest Coast of Africa taken during the Apollo 9 flight, March 1969.
- Figure 11 - Color enhancement of a Nimbus 4 infrared imagery obtained with the THIR (11.5  $\mu$ m) during April 1970.

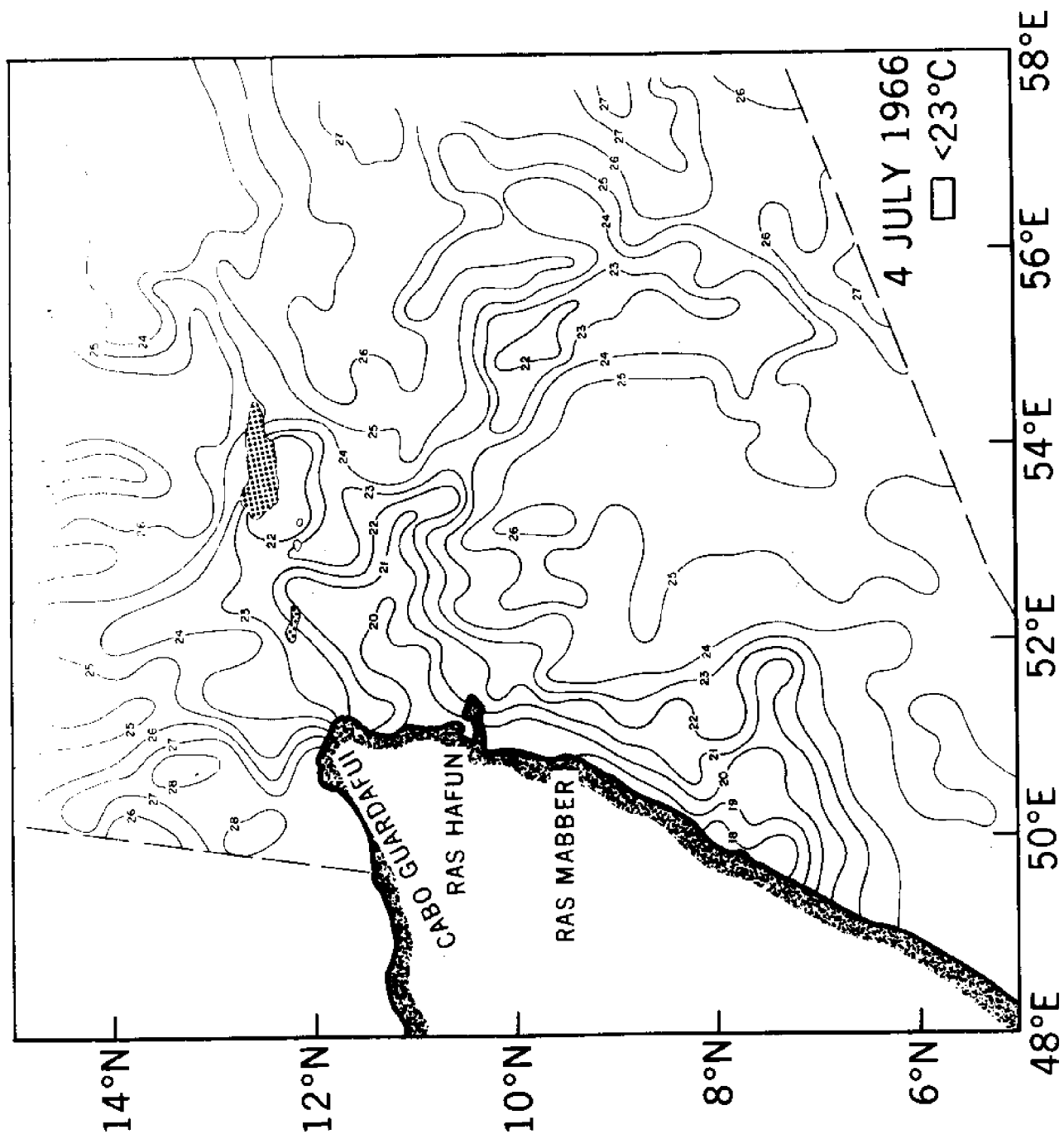
## REFERENCES

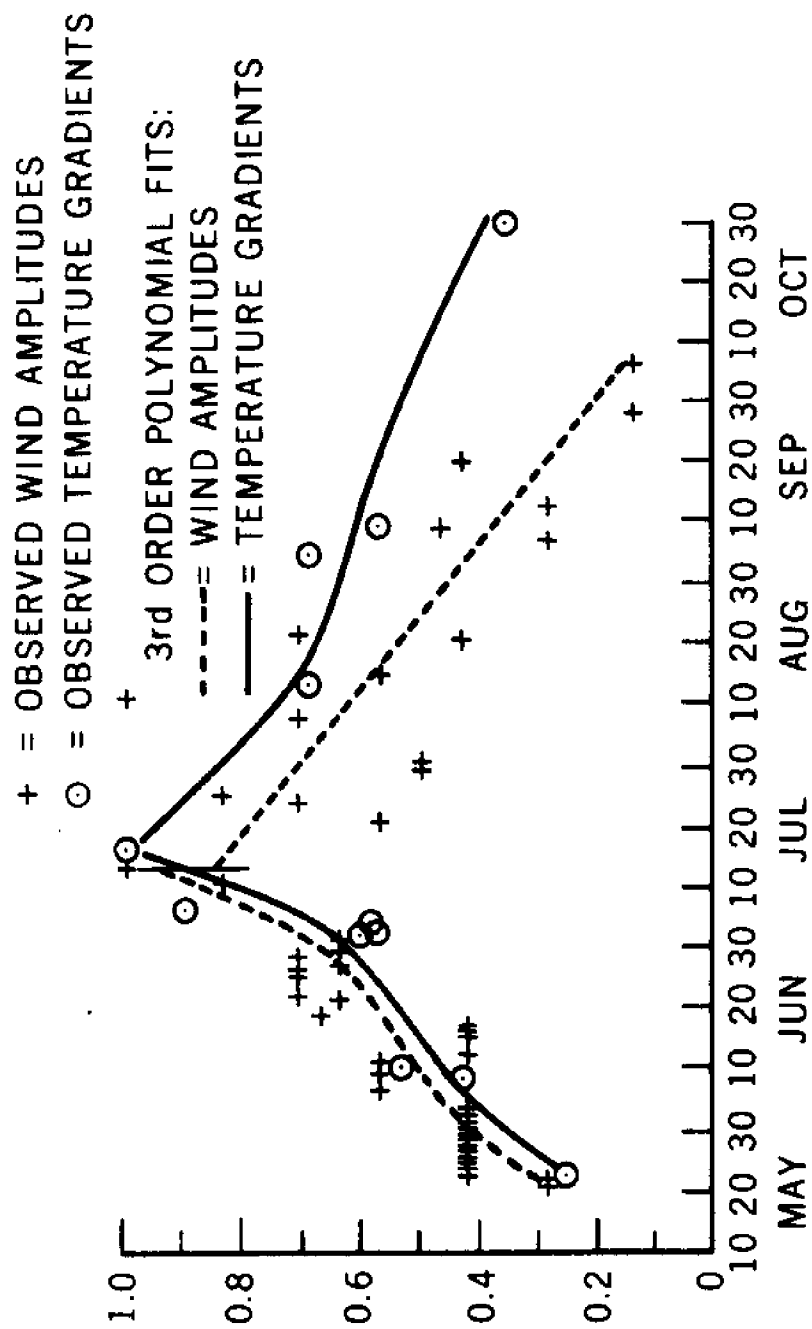
- J. G. Bruce (1965): Near Surface Currents off the Somali Coast in the Summer Monsoon, August 1964, (Unpublished manuscript).
- J. G. Bruce (1966): Near Surface Currents off the Somali Coast in the Summer Monsoon, August 1964, Part II, (Unpublished manuscript).
- W. Düng (1966): Die Vertikalzirkulation in den küstennahen Gewässern des Arabischen Meeres während der Zeit des Nordostmonsuns "Meteor" Forschungsergebnisse, Reihe A 67-83.
- W. Düng and K.-H. Szekiolda (1970): Direct Observation of Oceanic Response to Atmospheric Forcing.
- J. Laird, B. B. Breivogel, and C. S. Yentsch (1964): The Distribution of Chlorophyll in the Western Indian Ocean During the Southwest Monsoon Period July 30 - November 12, 1963. Woods Hole Oceanogr. Inst. Tech. Report No. 64-33, 1964.
- W. E. Shenk and K.-H. Szekiolda (1971): Satellite Ocean Temperature Analysis of the Indian Ocean (presented at "International Indian Ocean Expedition" Cochin, India, 1971).
- W. S. Shenk and V. V. Salomonson (1970): A Multispectral Technique to Determine Sea Surface Temperature Using Nimbus 2 Data (presented at 1970 Fall AGU Meetings in San Francisco, California).
- The Royal Society (1963): International Indian Ocean Expedition R.R.S. "Discovery" Cruise 1. South East Arabian Upwelling Region. pp 24.
- K.-H. Szekiolda (1970): The Development of Upwelling Along the Somali Coast as Detected with the Nimbus 2 and Nimbus 3 Satellites, Goddard Space Flight Center X-651-70-419, pp 52.
- J. J. Walsh (1969): Vertical Distribution of Antarctic Phytoplankton II. A Comparison of Phytoplankton Standing Crops in the Southern Ocean with that of the Florida Street. Limnology and Oceanography 14, pp 86-94.
- J. J. Walsh and R. C. Dugdale: A Simulation Model of the Nitrogen Flow in the Peruvian Upwelling System Inv. Pesqu. (in press).

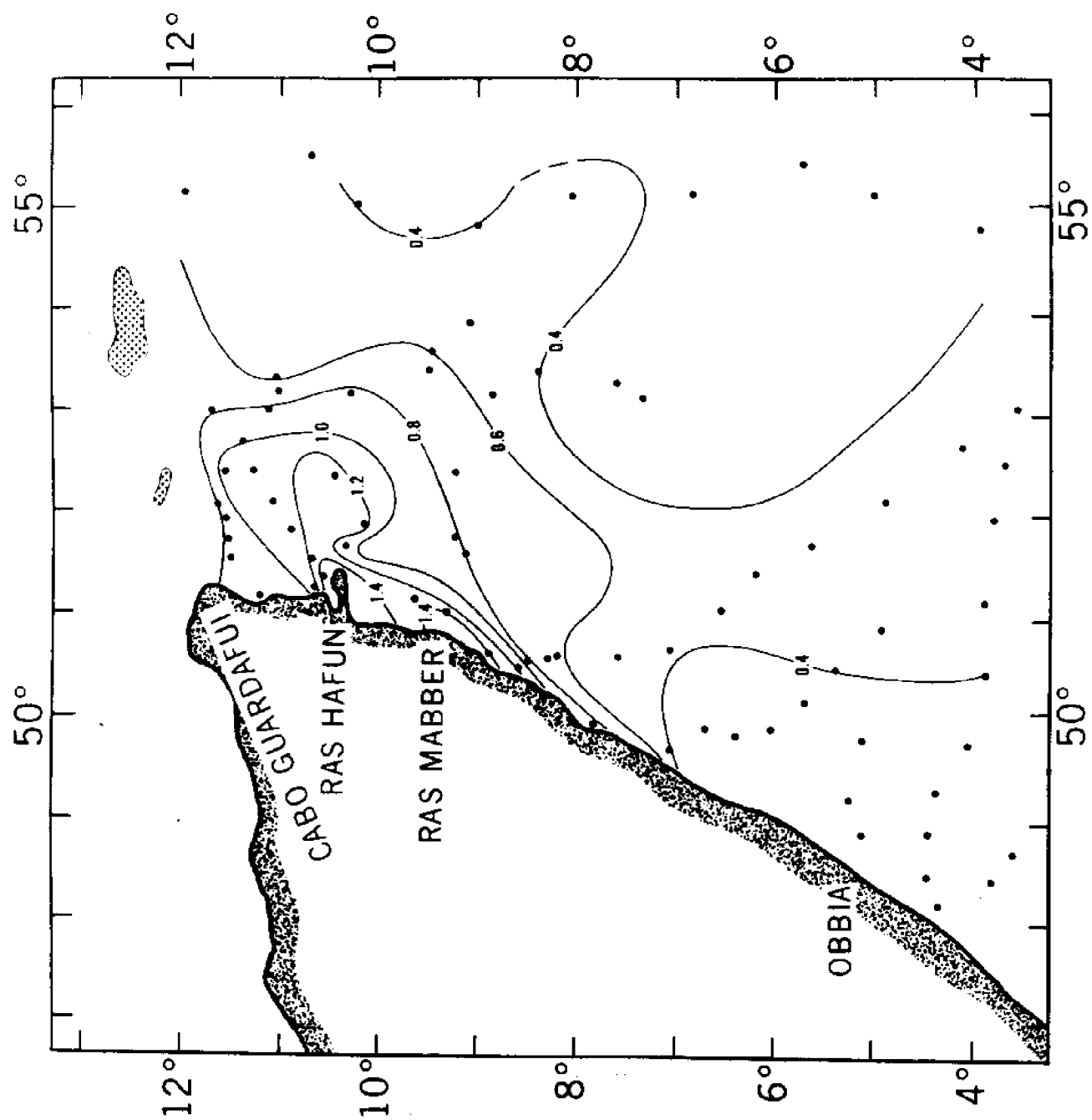


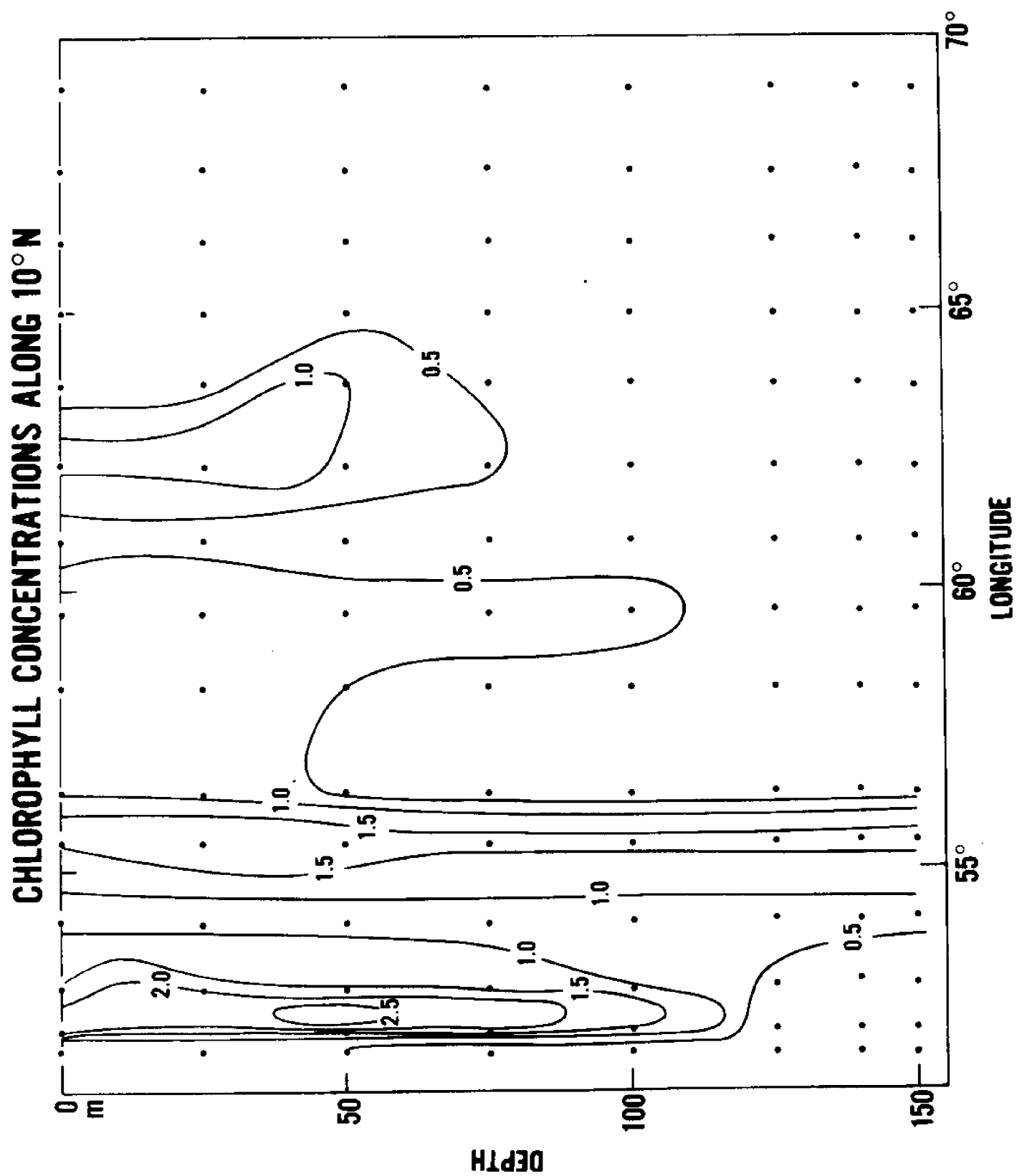


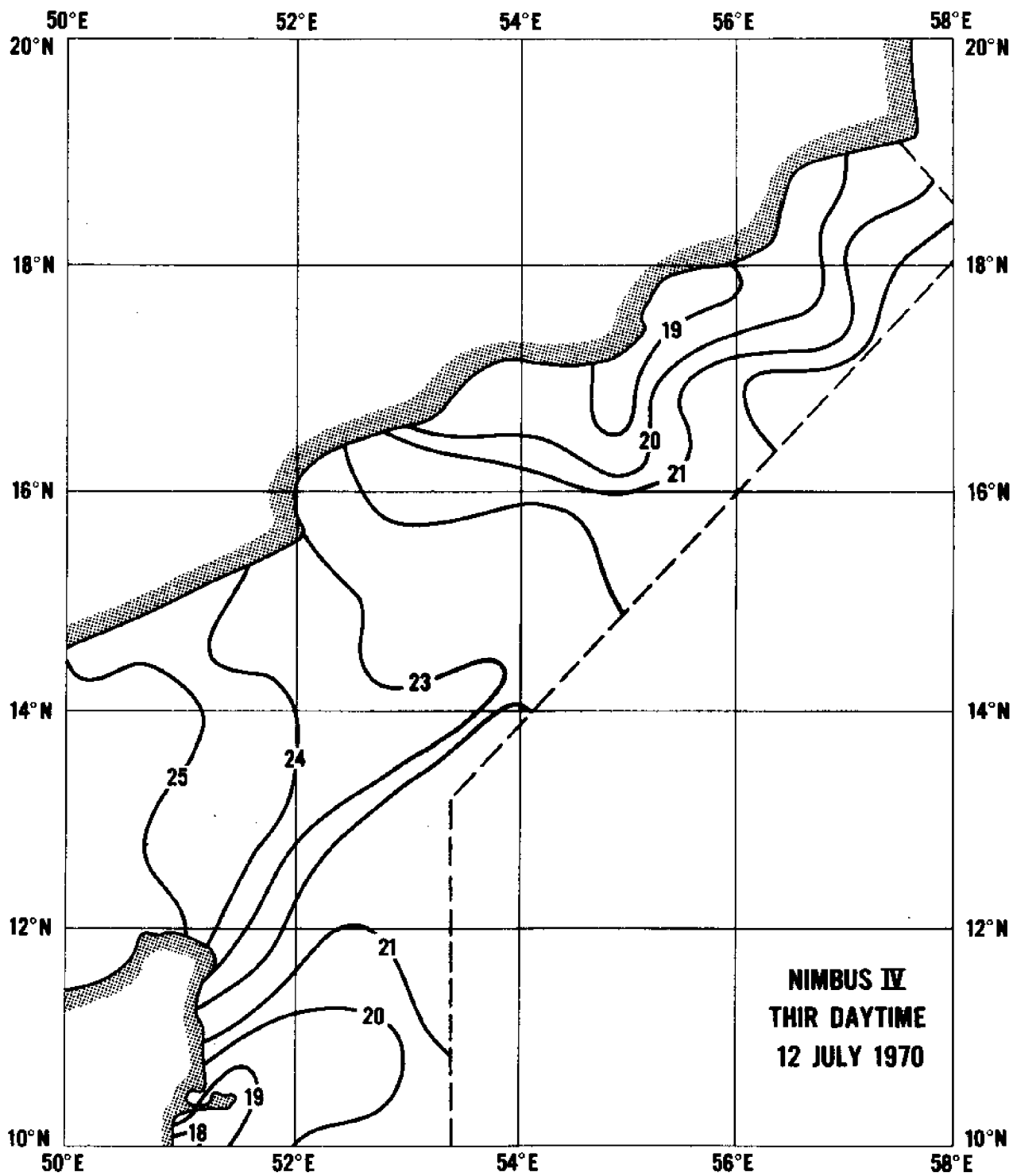


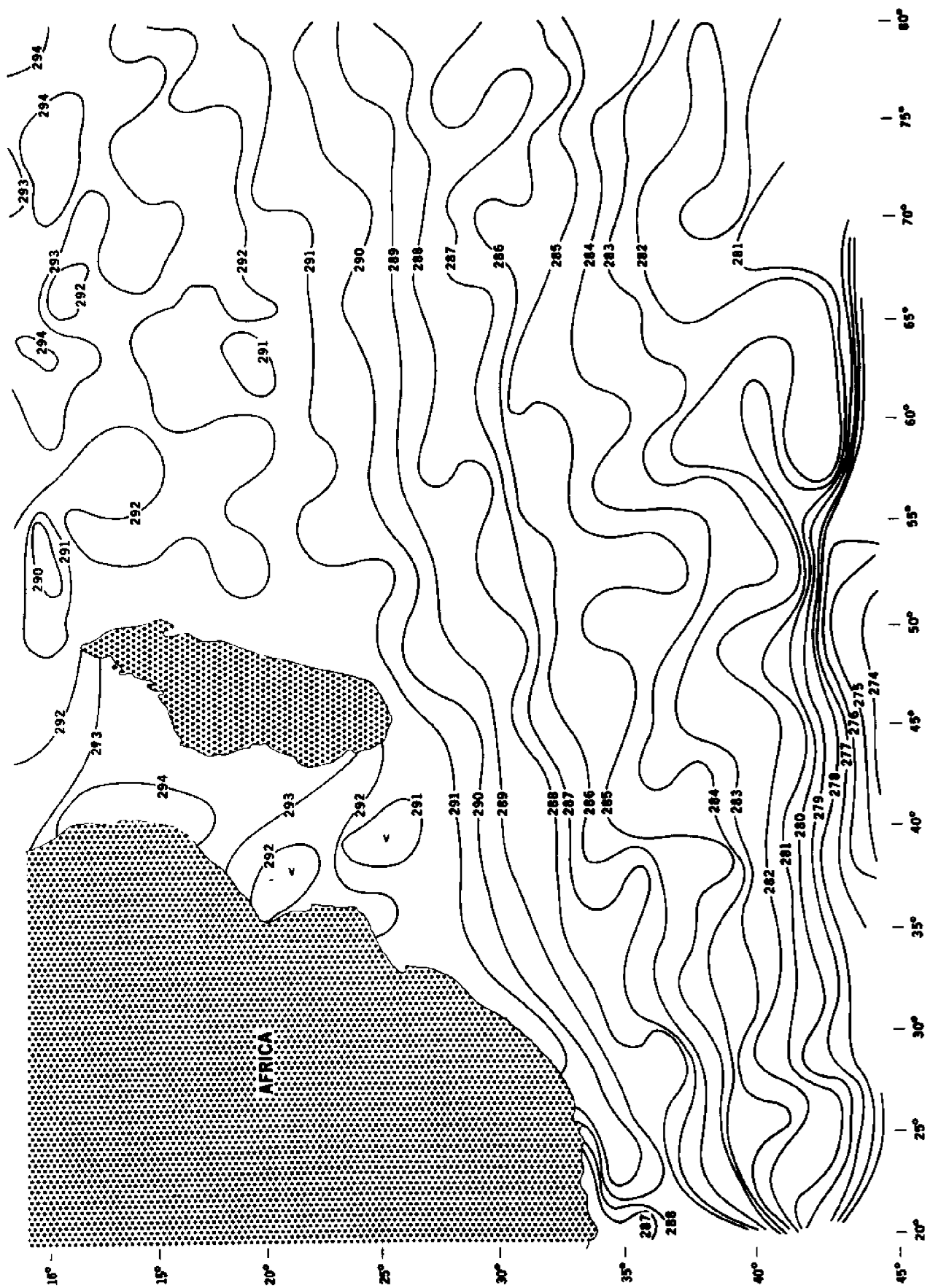


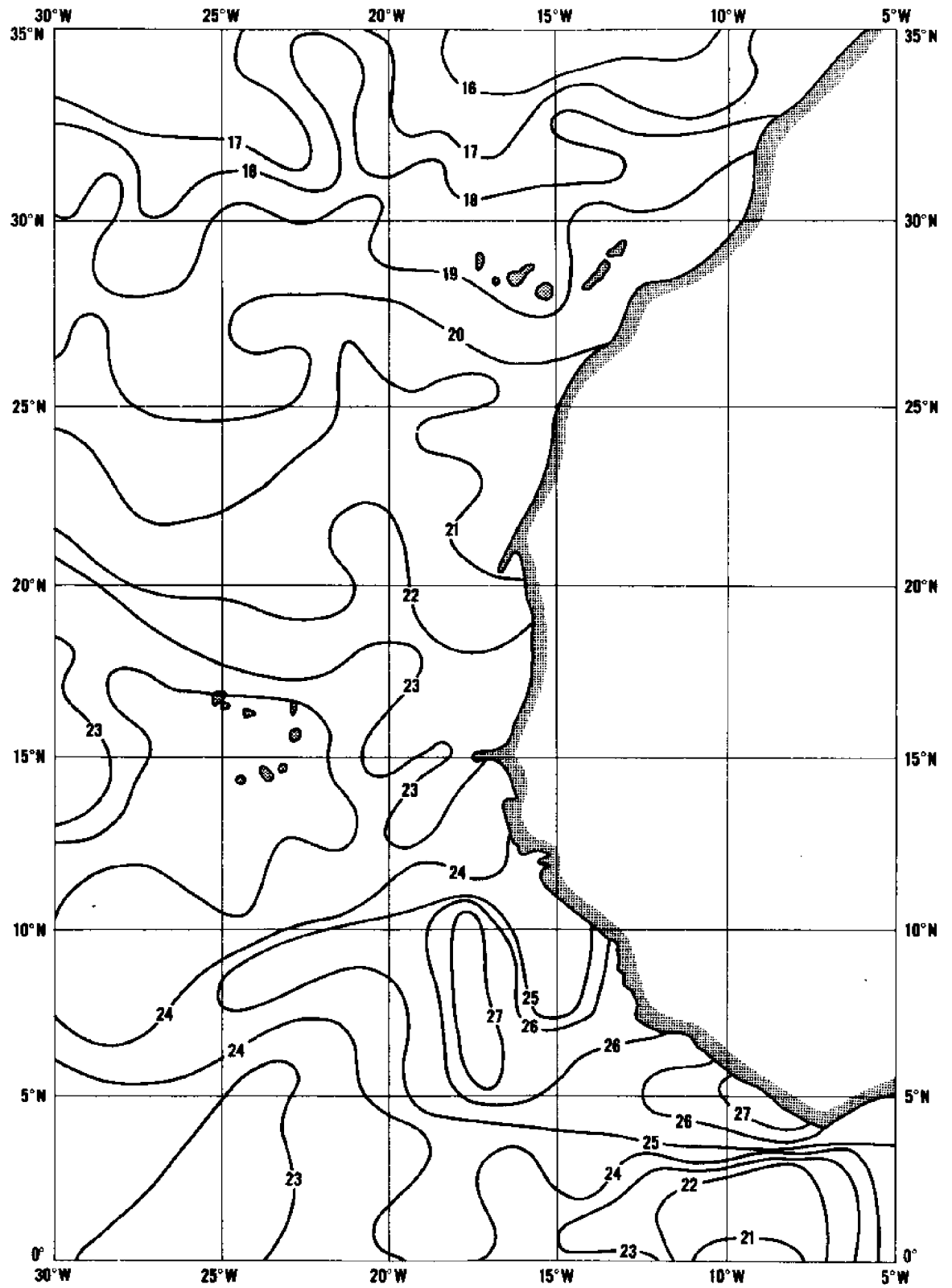






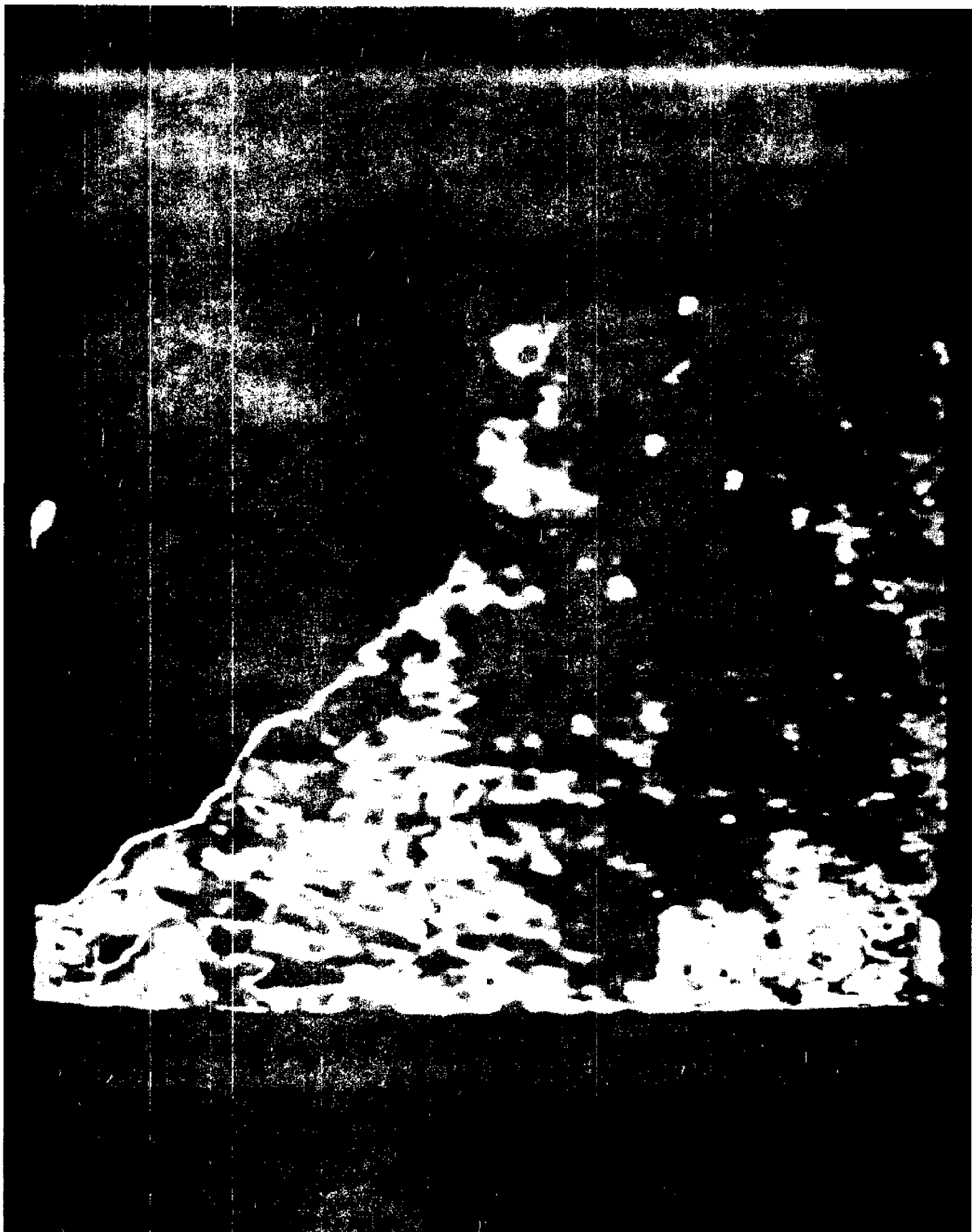












## LIST OF ATTENDEES

Howard W. Armstrong  
Graduate Teaching Assistant  
Texas A&M University  
College Station, Texas 77843

K. A. Arnold  
Assistant Professor  
Department of Wildlife Science  
Texas A&M University  
College Station, Texas 77843

Alan Aston  
Research Fellow  
Remote Sensing Center  
Texas A&M University  
College Station, Texas 77843

Leon H. Ballinger  
NASA/MSO  
NASA Road #1  
Houston, Texas 77058

Barney B. Barrett  
Geologist  
Louisiana Wildlife & Fisheries  
Commission.  
400 Royal  
New Orleans, Louisiana 70130

Brian Bedford  
Graduate Student  
Department of Biology  
Texas A&M University  
College Station, Texas 77843

C. A. Bedinger, Jr.  
NSF Trainee  
Department of Biology  
Texas A&M University  
College Station, Texas 77843

W. George Blanton  
Associate Professor  
Texas Wesleyan College  
P. O. Box 3277  
Fort Worth, Texas 76105

Fred Browand  
University of Southern California  
Department of Aerospace Engineering  
University Park, Los Angeles 90007

C. E. Bryan  
Texas Wildlife Association  
Rockport, Texas

John C. Calhoun  
Director, Sea Grant  
Dean College of Geosciences  
Texas A&M University  
College Station, Texas 77843

Luis R. A. Capurro  
Professor  
Department of Oceanography  
Texas A&M University  
College Station, Texas 77843

Michael A. Champ  
Instructor  
Department of Biology  
Texas A&M University  
College Station, Texas 77843

Ray Childress  
Biologist III  
Texas Parks & Wildlife Dept.  
P. O. Box 306  
Seadrift, Texas 77983

Leo F. Childs  
Special Assistant  
Earth Observation Division  
NASA/MSO  
Houston, Texas 77058

Bryant F. Cobb, III  
Assistant Professor  
Department of Animal Science  
Texas A&M University  
College Station, Texas 77843

Page 2  
LIST OF ATTENDEES

A. C. Conrod  
Project Engineer  
Bendix Aerospace Systems  
3300 Plymouth Road  
Ann Arbor, Michigan 48107

Earl Cook  
Associate Dean  
College of Geosciences  
Texas A&M University  
College Station, Texas 77843

George Cooper  
Professor of Botany  
USDA-ARS-SWC  
P. O. Box 267  
Weslaco, Texas 78596

Johnie H. Crance  
Area Marine Fisheries Specialist  
Texas A&M Extension Service  
Marine Lab, Building 311  
Fort Crockett  
Galveston, Texas 77550

Ira Current  
Manager  
Reversal Color Products  
Binghamton, New York

Sheila R. Davis  
Graduate Student  
Department of Biology  
Texas A&M University  
College Station, Texas 77843

Richard Defenbaugh  
Graduate Student  
Department of Biology  
Texas A&M University  
College Station, Texas 77843

Kirby L. Drennan  
Head, Zapata Remote Sensing  
Zapata Norness Company  
Pascagoula, Mississippi

Donald Durham  
Department of Oceanography  
Texas A&M University  
College Station, Texas 77843

Wayne Eaton  
NASA/MSC  
NASA Road #1  
Houston, Texas 77058

Charles Eleuterius  
Data Analyst  
Department of Oceanography  
Texas A&M University  
College Station, Texas 77843

Gifford C. Ewing  
Professor  
Woods Hole Oceanographic Institution  
Woods Hole, Massachusetts 02543

William P. Fife  
Professor  
Biology Department  
Texas A&M University  
College Station, Texas 77843

C. W. Fillman  
Engineer-Houston Requirements  
The Boeing Company  
P. O. Box 58747  
1300 Bay Area Blvd.  
Houston, Texas 77058

Norman G. Foster  
NASA/MSC  
Code TF  
1219 El Dorado  
Houston, Texas 77058

Alan Fredericks  
Texas A&M University  
College Station, Texas 77843

Larry Freeberg  
Marine Laboratory  
Galveston, Texas

Greta A. Fryxell  
Research Assistant  
Texas A&M University  
College Station, Texas 77843

Jay Gallia  
Graduate Student  
Department of Biology  
Texas A&M University  
College Station, Texas 77843

Harold W. Gausman  
USDA-ARS-SWC  
Plant Physiologist  
P. O. Box 267  
Weslaco, Texas 78596

Richard A. Geyer  
Head, Department of Oceanography  
Texas A&M University  
College Station, Texas 77843

James C. Gilmore  
Research Engineer  
Department of Oceanography  
Texas A&M University  
College Station, Texas 77843

John Goering  
Professor Marine Sciences  
University of Alaska  
College, Alaska 99701

Kirby Hanson  
NOAA  
461 South Miami Avenue  
Miami, Florida 33130

T. L. Hoffernan  
Texas Parks and Wildlife  
Rockport, Texas

John W. Highberg  
Houston Requirements Manager  
The Boeing Company  
P. O. Box 58747  
1300 Bay Area Blvd.  
Houston, Texas 77058

Arthur W. Hornig  
Director of Research  
Baird-Atomic Inc.  
125 Middlesex Turnpike  
Bedford, Massachusetts 01730

George L. Huebner, Jr.  
Associate Director  
Remote Sensing Center  
Texas A&M University  
College Station, Texas 77843

Takashi Ichiye  
Professor  
Department of Oceanography  
Texas A&M University  
College Station, Texas 77843

Douglas S. Ingram  
TRW Systems  
Space Park Drive  
Houston, Texas 77058

Harold D. Irby  
Assistant Professor  
Wildlife Science  
Texas A&M University  
College Station, Texas 77843

Eugene Jaworski  
Assistant Professor  
Department of Geography  
Texas A&M University  
College Station, Texas 77843

Harold G. Jones  
The Boeing Company  
2035 West Lake Road  
Houston, Texas 77058

Mahlon G. Kelly  
Dept. of Environmental Science  
University of Virginia  
Charlottesville, Virginia

George W. Klontz  
College of Veterinary Medicine  
Texas A&M University  
College Station, Texas 77843

Karl P. Kuchnow  
Department of Biology  
Texas A&M University  
College Station, Texas 77843

Don R. Kugle  
TRW Systems  
Space Park Drive  
Houston, Texas 77058

Carl W. Lahser  
Graduate Student  
Department of Biology  
Texas A&M University  
College Station, Texas 77843

Robert Charles Lockerman  
Oceanographic Expert  
FAO United Nations  
Hamburge 63-4° piso  
Mexico, D. F. 6

Larry D. Lusz  
Electrical Engineer  
National Marine Fisheries Service  
2725 Montlake Blvd.  
Seattle Washington 98102

Page 4  
LIST OF ATTENDEES

Allan D. Marmelstein  
Earth Satellite Corporation  
1771 N. St., N. W.  
Washington, D. C. 20036

Paul M. Maughan  
Director,  
Oceanography Applications  
Earth Satellite Corporation  
1771 N. St., N. W.  
Washington, D. C. 20036

Joe J. Mayhew  
Region II, Regional Chemist  
Texas Parks & Wildlife  
P. O. Box 7653  
Waco, Texas 77610

K. L. McCree  
Department of Biology  
Texas A&M University  
College Station, Texas 77843

Martha McCullough  
Graduate Student  
Department of Oceanography  
Texas A&M University  
College Station, Texas 77843

Bill Merrell  
Graduate Fellow  
Department of Oceanography  
Texas A&M University  
College Station, Texas 77843

E. D. Middleton, Jr.  
Director of Marine Technology  
Brazosport College  
Freeport, Texas

Lars Midttun  
Institute of Marine Research  
Bergen Norway

Daniel Mitchell  
Instructor  
College of Veterinary Medicine  
Texas A&M University  
College Station, Texas 77843

A. J. Moffat  
Barringer Research Ltd.  
304 Carlingview Drive  
Metropolitan Toronto  
Texdale, Ontario Canada

Leo Mulcahy  
Scripps Institute of Oceanography  
University of California  
San Diego, California 92037

Dean R. Norris  
NASA/MSC  
Houston, Texas 77058

Christopher T. Nosworthy  
Senior Engineer  
Lockheed Electronics  
16811 El Camino Real  
Houston, Texas 77058

Thomas Owen  
Southwest Research Institute  
8500 Culebra Road  
San Antonio, Texas 78228

Jack F. Paris  
Meteorologist  
Department of Meteorology  
Texas A&M University  
College Station, Texas 77843

Robert H. Parker  
President  
Coastal Ecosystems Management, Inc.  
3550 Hulen Street  
Fort Worth, Texas 76107

William Percy  
Professor  
Department of Oceanography  
Oregon State University  
Corvallis, Oregon 97331

Linda H. Pequegnat  
Department of Oceanography  
Texas A&M University  
College Station, Texas 77843

Willis Pequegnat  
Department of Oceanography  
Texas A&M University  
College Station, Texas 77843

William S. Perret  
Louisiana Wildlife & Fish. Comm.  
400 Royal  
New Orleans, Louisiana 70130

Sam R. Petrocelli  
Department of Biology  
Texas A&M University  
College Station, Texas 77843

Fabian Polcyn  
Willow Run Laboratories  
Ann Arbor, Michigan

Sammy M. Ray  
Galveston Marine Lab  
Texas A&M University  
Galveston, Texas

James P. Ray  
Department of Biology  
Texas A&M University  
College Station, Texas 77843

Perry E. Robinson  
U. S. Army Corps of Engineering  
819 Taylor; P. O. Box 17300  
Fort Worth, Texas 76102

Kurt A. Rottweiler  
Bendix Aerospace Div.  
3300 Plymouth Rd.  
Ann Arbor, Michigan 48107

J. W. Rouse, Jr.  
Director, Remote Sensing Center  
Texas A&M University  
College Station, Texas 77843

Saul Salla  
Assistant Secretary  
Intergovernmental Oceanographic Commission  
Place de Fontenoy  
Paris, 7 France

Sid Sers  
Remote Sensing Center  
Texas A&M University  
College Station, Texas 77843

John W. Sherman  
Spacecraft Oceanography Project  
NAVOCEANO  
Washington, D. C. 20390

Raymond F. Sis  
Department of Veterinary Anatomy  
Texas A&M University  
College Station, Texas 77843

James M. Snodgrass  
Scripps Institute of Oceanography  
University of California  
P. O. Box 109  
LaJolla, California 92037

William H. Stevenson  
National Marine Fisheries Service  
MTF  
Bay St. Louis, Mississippi 39520

John B. Suomala  
MIT  
Building E-40  
Cambridge, Massachusetts 02139

Emory Sutton  
Marine Laboratory  
Texas A&M University  
Galveston, Texas

Karl-Heinz Szekiolda  
Goddard Space Flight Center  
NAS Associate  
Greenbelt, Maryland 20771

Robert E. Taber  
University of Rhode Island  
36 Steamboat Avenue  
Wickford, Rhode Island 02851

Regis Tessier  
Esro  
114 Av. de Neuilly  
Seine, France

G. Tomczak  
FAO - Chief  
Rome, Italy

A. Venkataramaiah  
Gulf Coast Research Lab  
Ocean Springs, Mississippi 39564

Allen H. Watkins  
NASA  
Earth Orbital Mission Office  
Code TK  
Houston, Texas 77058

Melvin Weinstein  
McDonnell - Douglas Astronautics, Co.  
Mail Station 20  
5301 Bolsa Avenue  
Huntington Beach, California 92647

Robert E. Werner  
MIT  
Building E-40  
Cambridge, Massachusetts 02139

Page 6  
LIST OF ATTENDEES

Robert Whitaker  
Department of Oceanography  
Texas A&M University  
College Station, Texas 77843

Glade Woods  
National Marine Fisheries Service  
Mississippi Test Facilities  
Bay St. Louis, Mississippi

Charles S. Yentsch  
University of Massachusetts  
Marine Station  
Box 128, Lanesville Station  
Gloucester, Massachusetts 01930

James B. Zaitzeff  
NAVOCEANO  
NASA/MSC  
Code TF  
Houston, Texas 77058